The Okanogan lobe and Moses Coulee during the last glaciation

Joel H. Gombiner

A dissertation

submitted in partial fulfillment of the

requirements for the degree of

Doctor of Philosophy

University of Washington

2022

Reading Committee:

John O. Stone, Chair

Brian F. Atwater

Juliet G. Crider

Program Authorized to Offer Degree:

Earth and Space Sciences

University of Washington

Abstract

The Okanogan lobe and Moses Coulee during the last glaciation

Joel H. Gombiner

Chair of the Supervisory Committee:
John O. Stone
Earth and Space Sciences

This thesis examines last-glacial chronologies of the Okanogan lobe of the Cordilleran Ice Sheet and explores whether this glacier released floods. The findings include age ranges for ice advance and retreat across the Columbia River, and a map of a subglacial channel network tributary to Moses Coulee.

The Okanogan lobe advanced across the Columbia River between 19 and 17 ka (thousand years ago), and this piedmont glacier retreated north of the Columbia between 15 and 13.5 ka. This timing is inferred from new exposure ages that deviate somewhat from previous estimates based on varves, tephra, and radiocarbon. Independent chronologies of the same history agree broadly but differ by as much as 2,000 years for the ages of both advance and retreat.

Last-glacial floods down Moses Coulee could have come from glacial Lake Missoula, the Okanogan lobe, or both. Five such floods are known. Subglacial channels tributary to the coulee cross high divides and radiate towards the ice lobe’s margins. Subglacial drainage through these channels, if catastrophic, may thus explain the floods.

Also noted are several enigmatic features of a last-glacial flood bar, downstream from the Okanogan lobe terminus and beside a Moses Coulee scabland. These features include a basal, clast-supported, flood or alluvial gravel into which calcrete, 0.5 m thick, has formed; and an overlying, last-glacial flood gravel partly supported by a silty matrix. The calcrete, and the gravel beneath it, predate the last glaciation, but it is unclear how each of the two gravel units was deposited.

TABLE OF CONTENTS

LIST OF FIGURES

LIST OF TABLES

ACKNOWLEDGEMENTS

This study would not have been possible without a host of scientists, friends, family-members, and acquaintances. These people contributed time, physical labor, material goods, and intellectual effort to advance study of the fascinating flood and glacial geology of central Washington.

John Stone and Danielle Lemmon originated the exposure age study of the Channeled Scabland prior to my arrival at UW, and John then fostered its expansion and development with additional years of field work, and lab measurements. John personally measured all of the cathodes in this study and conducted a large proportion of the sample and chemical preparations. Were it not for John's tireless efforts in the UW Cosmo Lab, the vast majority of the exposure ages in this study would not exist.

Brian Atwater's comments and interest transformed this thesis from a collection of numbers and maps into an analysis of geologic history. Brian's consistently insightful suggestions helped me to design better figures, to write more clearly, and to see and connect salient observations that are buried in sometimes-obscure geologic literature.

Sidney Hemming inaugurated my investigations into this topic by hypothesizing that Belt-Purcell Supergroup silt and clay could serve as a tracer for the Missoula floods. Sid taught me that science is based on curiosity, experimentation, and careful measurements and were it not for her continued confidence I would have never continued to this stage.

Larry Smith shared his hard-earned knowledge about the repeated filling and lowering of glacial Lake Missoula. Andrea Balbas paved the way with her pioneering study of flood boulders. Richard Waitt laid other foundations for this work with pioneering stratigraphic

investigations, and he helped spur my curiosity through his carefully reasoned studies about Channeled Scabland flood-routing history. Nick Zentner repeatedly showed interest in my work and asked probing questions that elucidated problems and solutions. Isaac Larsen assisted with field work in Moses Coulee and participated in thought-provoking conversations about the history of the Channeled Scabland. Karen Lehnigk shared her flood model output with me, which was particularly helpful for thinking about the inundation history of Moses Coulee.

Corinna Hanson showed interest in my work and facilitated access to the Nature Conservancy Moses Coulee Preserve, a geologic wonderland containing many interesting and puzzling features. Karen Capuder shared her deep knowledge of indigenous uses of the landscape and helped with field work in Sagebrush basin, Moses Coulee.

Chris Mattinson made available the rock-crushing equipment at Central Washington University while the equipment at University of Washington was out of commission.

David McGee and Adam Jost performed the U-series analyses at MIT after COVID struck and I was unable to travel to complete the measurements, and David McGee helped with thoughtful considerations of the scattered data.

Elizabeth Horton and Nolan Conway were instrumental in collecting and processing samples from the Ephrata fan and Almira plateau. Linnea McCann and Michael Weyna helped in the lab and helped with a silt provenance project. Garrett Jones and Christopher Baird helped with sampling calcrete in Moses Coulee for U-series dating. Richard Anderson and Oliver Kou helped with measuring large boulders in Moses Coulee and other work there.

My parents, Robert Gombiner and Ester Greenfield, fostered the intellectual curiosity that allowed me to pursue a scientific study, patiently encouraged my studies, and repeatedly made available their cars for dusty field excursions into Moses Coulee.

1. INTRODUCTION

1.1 THE CORDILLERAN ICE SHEET

The Cordilleran Ice Sheet (CIS) was one of the major northern hemisphere ice sheets of the Pleistocene. At its maximum extent it covered ~2.5 million km^2 (Eyles et al., 2018) and contained 8 to 9 meters of sea level equivalent (Seguinot et al., 2016, Table 4). In some times and places, the CIS was a system of interconnected valley glaciers amidst nunataks (Jackson et al., 1991; Arnold and Hickin, 2016), and in others it was a broad, continental-scale system that overwhelmed topography (Dulfer et al., 2022, Fig. 10; Margold et al., 2013, Fig. 10) with shifting ice divides (Stumpf et al., 2000). The CIS during the last deglaciation has been proposed as an analog to the future Greenland Ice Sheet, on the basis that both were continental ice sheets in a warming climate. The last-glacial CIS had a similar ice volume to the Greenland ice sheet, and a similar bed topography consisting of an interior basin fringed with mountains (Eyles et al., 2018, Section 8, Fig. 26), though the CIS was thinner and wider than the Greenland ice sheet.

There exist numerous hypotheses about the relationships between the last-glacial CIS, climate, sea level, and other ice sheets. A thickening, late-glacial CIS may have starved the Laurentide ice sheet of moisture via orographic precipitation enhancement over the CIS, explaining out-of-phase evolution of the two ice masses (Dyck and Prest, 1987, p. 246), numerous ice streams may have simultaneously activated across the CIS at maximal glaciation and resulted in rapid deglaciation (Eyles et al., 2018, p. 110-116), rising sea level early in the last deglacial likely destabilized the western margin of the CIS (Haugerud, 2021; Hendy and Cosma, 2008), and CIS deglaciation and its separation from the Laurentide ice sheet may have

contributed to the rapid rise in global sea level during Meltwater Pulse 1A (Gomez et al., 2015; Gregoire et al., 2012). Evaluating these and other hypotheses about the CIS is helpful for understanding interactions between the cryosphere and the earth system during global warming and deglaciation. The goals of this study are to improve reconstructions of the southern margin of the CIS through landform mapping and geochronology.

1.1.1 The Okanogan lobe

The Okanogan lobe was a piedmont extension of the southern CIS that left dateable records of its existence, and well-preserved glacial landforms, affording an opportunity to reconstruct glacial processes and history. Broad swaths of drumlinization across the former bed of the Okanogan lobe suggest that it was an ice stream (Eyles et al., Fig. 12). Numerous eskers that overlie these streamlined bedforms indicate that a subglacial meltwater system existed beneath the Okanogan lobe later in its history (Kovanen and Slaymaker, 2004, p. 557). Many of these eskers terminate against recessional moraines, the distribution of which indicates brief stabilizations of the ice margin during an overall rapid retreat (Hanson, 1970, p. 91).

1.2 Connection between the Okanogan lobe and Channeled Scabland

The Okanogan lobe influenced flooding in the Channeled Scabland by re-routing water flows, both through ice damming and glacial isostatic adjustment, and by directly contributing meltwater to the Channeled Scabland. During its advance, the Okanogan lobe built an ice dam across the Columbia River, changing it into a lake that overflowed through Grand Coulee and/or Crab Creek (Bretz, 1923a, p. 602; Flint and Irwin, 1939). Glacial lake Columbia lasted for thousands of years, during which time Missoula floods from the east flowed into the lake

(Atwater, 1986). Outflows from the flood-swollen lake may have resulted in some of the largest Channeled Scabland floods, due to the Okanogan lobe's blockage of the Columbia valley flow pathway (Denlinger et al., 2021). In addition to diverting flood flows, the Okanogan lobe's glacial-isostatic effect might have tilted the hydrologic divide at the entrance to the Channeled Scabland northwestward, enhancing drainage in western tracts (Pico et al., 2022). Finally, geomorphology in British Columbia suggests that the Okanogan lobe released subglacial floods itself (Lesemann and Brennand, 2016, p. 2437), with some floods likely relating to subglacial volcanism in the ice sheet interior (Lesemann and Brennand, 2016, p. 2442). Such floods would have drained southward beneath the Okanogan lobe and into the western Channeled Scabland (Lesemann and Brennand, 2016, p. 2439).

1.2.1 Moses Coulee

Channeled Scabland canyon Moses Coulee contains unambiguous evidence that it formed in large, glacial floods, but the source(s) of the water have not been conclusively identified (Hanson, 1970, p. 60). A lack of channelized connectivity to the Columbia River distinguishes Moses Coulee from all other Channeled Scabland tracts (Bretz, 1923b, p. 619), suggesting that it might have formed in a different process than in over-spilling Missoula floods inferred to have carved much of the Channeled scabland. While some of Moses Coulee's "missing" connectivity to the Columbia River might be concealed beneath glacial sediment (Bretz et al., 1956, p. 989), glacial sediment upstream of Moses Coulee is typically thin and patchy over bedrock (Kovanen and Slaymaker, p. 562), suggesting limited likelihood of a buried surface. Plausible scenarios exist for routing Missoula floods into Moses Coulee (Denlinger et al., 2021, Scenario 3B, Hanson, 1970, Fig. 20; Waitt, 2021, p. 376), but these scenarios don't completely explain the

pattern of channelization upstream of Moses Coulee or the conspicuous differences between the headwaters of Moses Coulee and the rest of the Channeled Scabland. Other studies have proposed that supraglacial (Hanson, 1970, p. 62) or subglacial (Lesemann and Brennand, p. 2439) flooding from the Okanogan lobe might explain the differing geomorphic character of areas upstream of Moses Coulee. This study explores these hypotheses through mapping of the channels that feed Moses Coulee, and through geochronology, provenance, and sedimentology of flood deposits in Moses Coulee.

1.3 STUDY GOALS

The goals of this study are to refine the chronology of the last-glacial Okanogan lobe, and to better understand its connection to the Channeled Scabland. In the first chapter, the study employs exposure dating to refine chronologies of the last-glacial Okanogan lobe, integrates those ages with other constraints (Fig. 1-1), and uses glacial geomorphic mapping to infer ice and meltwater dynamics. In the second chapter, the study explores the history of Moses Coulee. This section evaluates two proposed hypotheses for how the Okanogan lobe influenced Moses Coulee floods: either by diverting Missoula floods into Moses Coulee, or by directly discharging subglacial floods into Moses Coulee. This chapter uses exposure dating, field observations, a catalog of flood-transported erratics, and mapping of overfit channels. These observations are compared against predictions made by the Missoula flood and Okanogan subglacial flood hypotheses.

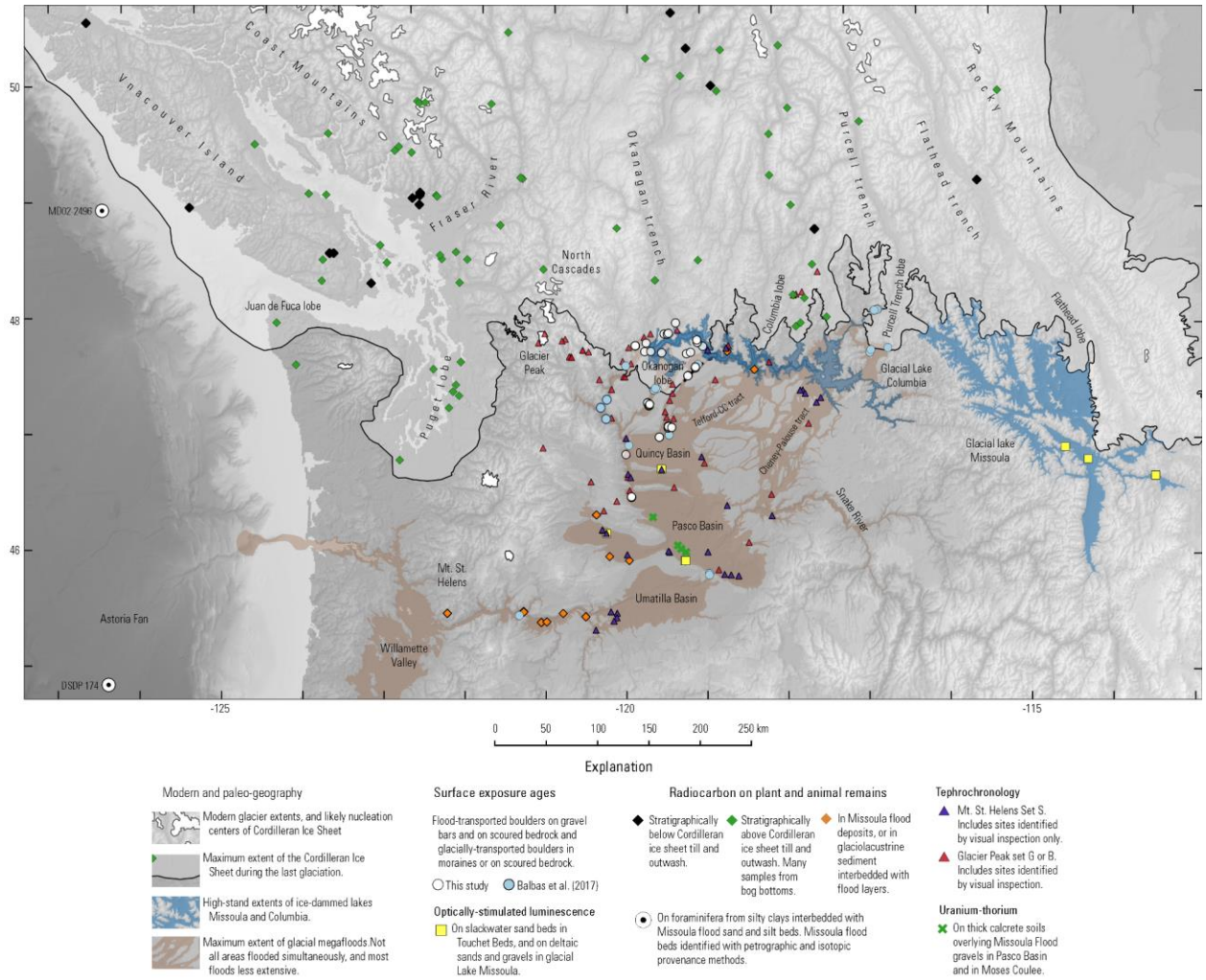

Figure 1-1: Index map of chronologic data relating to the last-glacial Cordilleran ice sheet, its proglacial lakes, and Channeled Scabland outburst floods.

2. LAST-GLACIAL CHRONOLOGIES OF THE OKANOGAN LOBE

2.1 CHAPTER SUMMARY

The Okanogan lobe of the Cordilleran ice sheet blocked the Columbia River for several thousand years during the last glaciation. Blockage began when the advancing lobe reached the Okanogan River mouth, likely between 19 ka and 17 ka. At its maximum extent, the lobe covered >3,400 km^2 of the Waterville Plateau. The retreating lobe left end moraines on the plateau. Finally, between 15 ka and 13.5 ka, deglaciation allowed the Columbia River to reestablish its former course.

This inferred history combines new exposure ages with existing age estimates, highlighting possible discrepancies and points of agreement. This study presents 16 new surface exposure ages on glacial boulders of the Okanogan lobe that directly date deglaciation, and 37 exposure ages from megaflood deposits in Missoula flood routes controlled by the Okanogan lobe.

Exposure ages in this study are calculated with production rates based on a Bonneville Flood calibration site — a wave-polished, quartzite bench first exposed during the sudden lowering of Lake Bonneville at 18.3 ± 0.3 ka (Lifton et al., 2015). Ages calculated with the commonly used production rate schemes of LSDn, Lm, and St are older by 100 to 500 years compared to those presented in this study. However, we favor the Bonneville Flood calibration site for calculating exposure ages because this proximal calibration site more directly captures the variations in cosmic ray flux that our samples experienced than do global production rate schemes.

2.1.1 Okanogan lobe advance

In this work, Okanogan lobe advance is dated in three independent ways, each of which suggests a different age of advance, but all of which require that advance occurred between 20 and 16 ka, and likely between 19 and 17 ka.

Ages of ice-rafted boulders high above Wenatchee suggest that the Okanogan lobe advanced after 17.5 to 16.5 ka. Formation of the Okanogan lobe ice dam blocked early, large Missoula floods from descending the Columbia River, so ages of earlier down-Columbia floods represented by the Wenatchee erratics must pre-date formation of the Okanogan lobe ice dam. The 17.5 to 16.5 ka exposure ages of the Wenatchee boulders (recalculated from Balbas et al. (2017) with the Bonneville flood calibration site) imply a late Okanogan lobe advance, inconsistent with some estimates for glacial Lake Columbia formation, and with some older surface exposure ages in Moses Coulee.

Ages of ice-rafted boulders in Moses Coulee suggest that the Okanogan lobe advanced before 19.5 to 17 ka. Advance of the Okanogan lobe is required to send floods into Moses Coulee. Thus, ages last-glacial Moses Coulee megafloods must post-date Okanogan lobe advance. The two oldest, last-glacial exposure ages on iceberg-transported rocks in Moses Coulee are 18.9 ± 1 ka and 17.4 ± 0.8 ka, suggesting that the Okanogan lobe advanced across the Columbia River by ~19 ka if the oldest age is accurate, and by ~17.5 ka if the younger age is accurate. However, these ages could be biased old by prior exposure.

Thirdly, estimates of glacial Lake Columbia formation from its stratigraphy suggest that the Okanogan lobe blocked the Columbia River between 20 and 16.5 ka. Advance of the Okanogan lobe across the Columbia River caused formation of glacial lake Columbia. The age

of that event can be estimated by counting the number of varves that underlie Mt. St. Helens set S tephra or that underlie a radiocarbon age on wood within the lake stratigraphy. Depending on the age of set S tephra, which remains uncertain, and on the antiquity of the wood when it was deposited in the lake sediment, this approach suggests that lake Columbia formed between 20 and 18 ka, or between 18.5 and 16.5 ka, if a younger age of set S is used in the calculation.

Resolution of these discrepancies requires that some or all of the ages are inaccurate. Sources of unaccounted error may include exhumation of the ice-rafted boulders from silty slopes above Wenatchee, resulting in apparent exposure ages that are too young, presence of inherited isotopes in Moses Coulee flood boulders, resulting in exposure ages that are too old, detrital organic material older than its enclosing sediment in glacial lake Columbia, resulting in radiocarbon ages that are too old, and/or an inaccurate age for the Mt. St. Helens set S tephra, resulting in an inaccurate pinning of the floating varve chronology in time. Overall, these age data are inconsistent about when the Okanogan lobe advanced across the Columbia River. Depending on which estimates are favored and which assumptions made, the advance may have occurred as early as ~20 ka or as late as ~16.5 ka, but likely occurred between 19 and 17 ka.

2.1.2 Okanogan lobe retreat

Multiple approaches consistently date the retreat of the Okanogan lobe to between 15 and 13.5 ka, though exposure ages tend to describe a later retreat than glacial Lake Columbia stratigraphies. Exposure ages on boulders in areas glaciated by the Okanogan lobe cluster between 15 and 14 ka, providing direct dates for deglaciation of the Okanogan lobe, though these ages are around 1,000 years younger than the age of retreat implied from set S and overlying varves.

Exposure ages suggest that the Okanogan lobe was at its maximum extent near 15 ka and that it retreated northward between 15 and 14 ka. Two ages on boulders above the east rim of Grand Coulee, likely transported by megafloods flowing alongside the Okanogan lobe when it filled upper Grand Coulee, average 14.8 ± 0.6 ka, and two on the Paynes Gulch boulder bar, deposited after the Okanogan lobe maximum in upper Grand Coulee, average 14.7 ± 0.7 ka. Together, these four ages related to upper Grand Coulee suggest that the Okanogan lobe retreated from Grand Coulee between ~15 and 14.5 ka. Further upstream, four ages on glacial boulders on the NE Waterville Plateau average 14.4 ka. A standard deviation of 160 years among these four samples suggests a high degree of precision for the implied age of site deglaciation at ~14.5 ka. These eight ages suggest that the ice margin progressively retreated over around 500 years from Grand Coulee to an intermediate position on the northern Waterville Plateau.

The exposure age data indicate that the Waterville and Omak plateaus deglaciated between 15 and 14 ka, before deglaciation of the Columbia valley near the Okanogan confluence and the Omak Lake trench between 14 and 13 ka. Four ages from glacial boulders to the north of the Columbia River, on the Omak plateau and in the Omak Lake trench, range from 15 ± 1.4 to 13.7 ± 0.5 ka, with a mean of 14.2 ka, generally consistent with progressive northward retreat of the ice margin. The oldest of these exposure ages, from a boulder on the south-central Omak plateau, may be an analytical outlier, or it may reflect early exposure of the central Omak plateau, due to a late-glacial bifurcation of the Okanogan lobe into sub-lobes in the Omak Lake trench and Okanogan valley. The youngest deglacial age of 13.7 ± 0.5 ka, from a boulder in the Omak Lake trench, confirms inferences from both distribution of Glacier Peak Set G/B tephra and from distribution and morphology of late-glacial terraces: that the last areas to become ice-

free were the low-lying valleys, including the Columbia valley, the Okanogan valley, and the Omak Lake trench.

Additionally, 23 ages from megaflood-transported boulders in or downstream from Grand Coulee, a flood route activated by Okanogan lobe glaciation, indicate that the Okanogan lobe was gone by ~14 ka, according to the youngest of the exposure ages in the Ephrata fan group. Ages for Grand Coulee floods are uniformly older than six exposure ages from a post-Okanogan lobe flood deposit in the Columbia River near Pateros that range from 13.9 to 11.6 ka, confirming that the Okanogan lobe had fully retreated from the Columbia River by ~14 ka.

The landform record of Okanogan lobe retreat on the Waterville Plateau includes thin, evenly spaced moraines, eskers, and fields of stubby, discontinuous ridges that may be crevasse-squeeze ridges. These landforms also contain information about the style and pace of Okanogan lobe deglaciation. The thinness of the recessional moraines suggests a rapid pace of retreat, and their relatively even spacing suggests periodic, but brief, stabilizations. The curvature of these moraine segments, concave towards the Okanogan valley and towards the Omak Lake trench, suggests that the Okanogan lobe bifurcated into two valley glaciers in the Okanogan mainstem and in the Omak trench, both of which briefly flowed onto the Waterville Plateau after the maximum stage of Okanogan lobe glaciation. Late-glacial, subglacial meltwater also deposited at least 485 eskers, which overlie drumlinized topography and some of which terminate on their downstream end against moraine crests.

2.2 Review of previous work on the Okanogan lobe

2.2.1 Stratigraphy and geomorphology

Initial advance of the Okanogan glacier into the Columbia valley may have first caused oscillatory damming of the Columbia River (Flint and Irwin, 1939, p. 679). Sand and gravel layers, many stratigraphically beneath Okanogan lobe till, and all low in glacial Lake Columbia fill near Grand Coulee dam, indicate that strong currents flowed along the bottom of the lake during the early, last-glacial history of lake Columbia. Most of these currents were from Missoula Flood inflows (Waitt et al., 2021, p. 274) but some currents may have been outflows from an early, unstable glacial lake Columbia that episodically flowed through an incipient Okanogan lobe ice dam (Flint and Irwin, 1939, p. 670).

Eventually, the Okanogan lobe ice dam thickened enough to completely block the flow of the Columbia River, forming a stable and deep glacial lake Columbia that overflowed through Grand Coulee (Flint and Irwin, 1939, p. 670; Bretz, 1923a, p. 592). The absence of frost-wedge casts in glacial Lake Columbia stratigraphy, which are observed widely in glacial Lake Missoula stratigraphy (Chambers, 1971, p. 50; Smith et al., 2017), suggest that the floor of glacial Lake Columbia was not exposed during the lake's existence.

After crossing the Columbia valley, the Okanogan lobe advanced onto the Waterville Plateau. At its maximum extent, the Okanogan lobe constructed a terminal moraine that is up to 30 meters tall and several km across (Bretz, 1923a, Fig. 1, Waters, 1933, p. Flint, 1935, p. 177-180). The Okanogan lobe also occupied Grand Coulee, eroding striae on its granitic floor upstream of Steamboat Rock (Bretz, 1923a, p. 604), depositing till downstream from Steamboat Rock (Atwater, 1987, p. 188), and ultimately raising the water level of glacial Lake Columbia by

several hundred meters while the low outlet through Grand Coulee was blocked (Atwater, 1986, p. 6). The ice dam in Grand Coulee, and by inference the maximum extent of Okanogan lobe glaciation, was short-lived, according to scanty and poorly developed high glacial lake Columbia shorelines at 715 m compared to well-developed shorelines at 530 m (Atwater, 1986, p. 6), and based on the small number of anomalously thin flood beds in the composite Sanpoil section that are indicative of flow attenuation in a deeper lake (Atwater, 1986, Fig. 17). Blockage of Grand Coulee during maximum Okanogan lobe glaciation re-directed Lake Columbia outflow across divides further to the east (Flint, 1935, p. 189), and/or onto the plateau to the east of Grand Coulee (Bretz, 1932, p. 38).

During its retreat, the Okanogan lobe formed moraines atop Steamboat Rock in upper Grand Coulee (Bretz, 1932, p. 35) and ~20 or so sets of thin moraine ridges on the Waterville Plateau (Hanson, 1970, p. 89, Fig. 19-2). These moraines are narrower and shorter than the Withrow moraine complex, and their regular spacing suggests a consistent, periodic process related to their formation (Hanson, 1970, p. 91). The nested, recessional moraines on the Waterville Plateau indicate that a flowing Okanogan lobe stabilized around 20 separate times during its overall retreat from the Waterville Plateau. The retreating Okanogan lobe also left behind trails of boulders on lines perpendicular to the ice margin (Flint, 1935, p. 172). Additionally, flowing subglacial meltwater during retreat deposited eskers on the Waterville Plateau (Flint, 1935, p. 180; Hanson, 1970; Kovanen and Slaymaker, 2004), the excellent preservation of which suggests that the ice stopped flowing at its bed shortly after the eskers formed (Flint, 1935, p. 180; Kovanen and Slaymaker, 2004, p. 557). Eskers on the Waterville Plateau often occur adjacent to and upstream from moraine ridges and do not typically cross

moraines (Hanson, 1970, p. 89), suggesting that the formation of some eskers is associated with ice margins delineated by the moraines that the eskers terminate against.

Retreat of the Okanogan lobe in the Columbia River west of the Waterville Plateau was accompanied by formation of terraces. Kettle-like depressions on some of the terrace surfaces suggest that they formed in ice-marginal environments (Waters, 1933, p. 791), possibly as kames adjacent to a thinning Okanogan glacier in the Columbia valley.

Table 2-1: Compilation of previous work relating to the Okanogan lobe, Missoula floods, and their chronologies in north-central Washington.

Author(s)	Year	Journal	Findings
Bretz	1923	GSA Bulletin	Describes striae on granite in upper Grand Coulee oriented NW-SE (p. 603-604), indicating that flowing ice of the Okanogan lobe filled Grand Coulee after it had formed, and possibly implying at least two episodes of Okanogan lobe glaciation, one in which the coulee formed, and another in which it was glaciated.
Waters	1933	GSA Bulletin	Composition and elevations of ice-marginal terraces and bedrock channels along the Columbia River between Chelan and Pateros. Terraces in adjacent valleys are at varying elevations and their elevations do not change in an orderly pattern, suggesting that the Great Terrace is an assemblage of kame terraces that formed in disconnected, ice-marginal environments (p. 791).
Flint	1935	GSA Bulletin	General observations of glacial features on the Waterville Plateau. Freshness of till on the Waterville Plateau indicates recent glaciation (p. 171). Flint posits multiple generations of glaciation based on the idea that the Omak Lake trench is an ancient Columbia River pathway that was diverted by a pre-last glacial Okanogan lobe to form the modern Box Canyon (p. 176). Describes glaciofluvial gravel mounds, some esker-like, and interprets them as deposits from englacial streams in the late-glacial Okanogan lobe (p. 180).

Flint, Irwin	1939	GSA Bulletin	Stratigraphies of Columbia River glacial terraces near Grand Coulee Dam, revealed by drilling and excavation for dam construction, suggest that the Okanogan lobe advance began with oscillatory damming of Columbia River before formation of a stable, deep glacial Lake Columbia that drained through Grand Coulee (p. 670). Basal sequence consisting of rhythmic repetition of gravel, massive silt, and varved silt indicates cyclic shoaling and deepening of a lake Columbia during early incursion of the Okanogan lobe into the Columbia River. Increasingly varved silts and finer sand interbeds up-section indicate a deepening and stabilization of the lake level after the Okanogan ice dam was firmly established. Distribution of the Nespelem silt terrace and kettling on its surface indicate that ice persisted in the Columbia mainstem during deglaciation downstream from Grand Coulee after areas upstream had deglaciated. Valley-train descending the Omak Lake trench indicates that a sub-lobe persisted there after deglaciation of the mainstem Columbia (p. 678).
Rubin, Alexander	1958	Science	Specifies USGS radiocarbon lab procedure of boiling samples in NaOH and HCl to remove lignins and humic acids. Notes that the procedure does not remove plant rootlets.
Fryxell	1965	Science	Identification of Glacier Peak tephra in talus and lacustrine sediment in lower Grand Coulee, indicating cessation of Grand Coulee flooding by the time of Glacier Peak eruption. Radiocarbon dating of mollusk shells in lower Grand Coulee that post-date latest Grand Coulee megafloods.
Dyck, Fyles, Blake	1965	Radiocarbon	Radiocarbon age (GSC-194) on bark and twigs below glaciolacustrine sand and silt 24.4 ± 0.4 ka. The lacustrine sand and silt are interpreted by Fulton as pre-dating last glaciation.
Lowdon, Fyles, Blake	1967	Radiocarbon	Radiocarbon age (GSC-477) of 26 ± 1.9 ka on wood fragments from borehole in silt and sand interpreted by Fulton as pre-dating last glaciation.

Lowdon, Blake	1970	Radiocarbon	Radiocarbon age (GSC-913) of 23.1 ± 0.6 ka on plant detritus and peat within silt and sand interpreted by Fulton as pre-dating last glaciation. Presence of plant rootlets on the sample could bias age young. If the procedure similar to Rubin and Alexander (1958) used, young rootlets would not have been removed before the beta counting measurement.
Hanson	1970	PhD Thesis	Detailed glacial geomorphic map of eskers, ice-flow indicators (i.e., drumlins and flutes), and recessional end moraines of the Okanogan Lobe (Fig. 19-2), indicating that ice continued flowing to the margin during the deglaciation of the Waterville Plateau. Uniformity in size and spacing of recessional moraines indicates periodic glacial phenomenon (p. 91).
Porter	1978	Quaternary Research	The northern limit of Glacier Peak set G/B tephra constrains the extent of Okanogan lobe at the time of the eruption. Glacier Peak Set G observed at site near Conconully astride lower Okanogan valley (Fig. 9). Later, more detailed observations in the area show no evidence of Glacier Peak in cores that reach glacial sediment (Mack et al., 1979).
Mullineaux, Wilcox, Ebaugh, Fryxell, and Rubin	1978	Quaternary Research	Geochemical and mineralogical correlation between tephra in Missoula flood deposits and tephra near Mt. St. Helens.
Mack, Rutter, Valastro	1979	Quaternary Research	Glacier Peak tephra on top of a terrace 4.5 km to the north of Chelan, indicating exposure of that surface and ice recession to the north of Chelan by the time of the eruption. Glacier Peak tephra not observed in cores at Mud Lake or at Bonaparte Meadows astride lower Okanogan valley, implying continued Okanogan glaciation there at the time of eruption.
Clague	1980	Quaternary Research	Compilation of radiocarbon ages from sediment that underlies Cordilleran Ice Sheet deposits, suggesting later development of Cordilleran Ice Sheet than Laurentide Ice Sheet. Site descriptions lack photographs, maps, or detailed

			notes. Each deposit dated by one age only. Radiocarbon samples likely processed using methods that don't remove plant rootlets (which were observed in some samples).
Gough	1985	Eastern Washington University Master's Thesis	Airfall deposition of Glacier Peak tephra postdates deposition of glacial outwash at Chelan Falls locality. The lowest stratigraphic occurrence of tephra is 0.8 m above glacial outwash, indicating site deglaciation before Glacier Peak set G/B eruption. Tephra occurs in ripple laminated cross-beds and laminated fine beds (p. 75).
Hibbert	1985	Office of Public Archaeology, Institute for Environmental Studies	Distribution of Lake Columbia silt and sand in Columbia River and in Omak Lake trench indicates recessional ice configuration consisting of Omak sub-lobe with a margin to the south of Goose Lake, and Okanogan sub-lobe ice filling Okanogan valley and Columbia valley downstream of Omak Lake trench. Gravel dunes (Giant Current Ripples) and fore-set, open-work cobble gravel in Omak Lake Trench indicate large, late-glacial outburst floods sourced from the retreating Omak Trench sub-glacier of the Okanogan glacier. Of five radiocarbon dates on charcoal, peat, and carbon-rich silt from various strata underlying Okanongan lobe till, three are radiocarbon-dead, and the other two are 29.9 ± 2.2 ka and 37.6 ± 4.9 ka (Table 2-1), suggesting common occurrence of re-worked detrital organic material in strata examined and/or deposition of the strata well before Okanogan lobe glaciation.
Nickmann, Leopold	1985	Office of Public Archaeology, Institute for Environmental Studies	Absence of Glacier Peak tephra in Goose Lake core within the Omak Lake trench, suggesting that the tephra was either not deposited at the site due to site glaciation at the time of the eruption, that the tephra was eroded from the site as a result of outwash from the retreating Omak Lake trench sub-lobe (p. 137), or that the core was not deep enough to encounter the tephra there. Core bottomed in gray clay beneath a calcareous gyttja dated by radiocarbon to 13.3 ± 0.2 ka, suggesting the possibility that the coring may not have penetrated deep enough to reach the stratigraphic horizon that might contain the Glacier Peak

set G or B tephra.

Pine	1985	Western Washington University Master's Thesis	Absence of Glacier Peak tephra in Sinlakehin Valley and Spectacle Lake Coulee, suggesting that the northern Okanogan valley remained glaciated at the time of Glacier Peak set G/B eruption, or that the ashfall did not extend that far north.
Waitt	1985	GSA Bulletin	Shells at Mabton in third rhythmite below set S date to 17.1 ± 1.2 ka. Stratigraphy at Rock Island Bar indicates that four separate Moses Coulee floods occurred, and that Moses Coulee floods ceased before megafloods into Quincy Basin ceased.
Baker, Bunker	1985	Quaternary Science Reviews	Shells at Mabton in third rhythmite below set S date to 16 ± 0.6 ka. Study obtained a significantly different radiocarbon age from Waitt (1985) on similar material from the same stratigraphic horizon at the same time. This suggests that one of the ages is wrong due to a laboratory error, or that the shells in the deposit do not have the same carbon isotopic composition, either because they are of mixed age or due to variable post-depositional calcite alteration.
Richmond	1986	Quaternary Science Reviews	Synthesis of Okanogan lobe history from previous work, noting presence of Glacier Peak tephra above till in (1) seasonally flooded salt flat on Omak plateau (Atwater and Rinehart, 1984), and (2) on Great Terrace (citing Mack et al., 1979).
Atwater	1986	U.S. Geological Survey Bulletin	Varve counts and estimates indicate that glacial Lake Columbia existed for at least 2,000 to 3,000 years (p. 11). A radiocarbon age on detrital wood enclosed within varves is 17.7 ± 0.8 ka, potentially pinning the stratigraphy in time, but the wood could be older than enclosing sediment by 1,000's of years (p. 29).

Moody	1987	PhD Dissertation	Microprobe and petrographic study of tephra in central Washington, including identification and characterization of Mt. St. Helens Set S tephra in (1) flood gravel at Crescent Bar (p. 88), (2) in three successive slack-water units at Wanapum Dam (p. 88), (3) and in the twelfth bed from the top of slackwater, rhythmite sections at Burlingame Canyon and at Mabton (p. 53, 278).
Atwater	1987	Quaternary Research	An outcrop to the south of Steamboat Rock in upper Grand Coulee exposes till beneath disturbed varves and flood beds. Section interpreted as evidence that a sluggish Columbia River flowed through Grand Coulee after recession of the Okanogan lobe from the coulee.
Benito and O'Connor	2003	GSA Bulletin	Radiocarbon ages on clasts in Missoula flood deposits are commonly 1,000's to 10,000's of years too old due to re-working. Stratigraphy of Missoula flood gravel deposits along the Columbia Gorge indicating <10 floods in most sections.
Lilquist	2005	Western North American Naturalist	Radiocarbon age on a mammoth tusk in the third of three Missoula Flood beds in upper Yakima basin dating to 17.7 ± 0.2 ka. Cracks and exfoliation patches on the surface of the tusk indicate exposure prior to the tusk's entrainment in a flood.
Clynne, Calvert, Wolfe, Evarts, Fleck, and Lanphere	2008	USGS professional paper	Bounding radiocarbon dates for Mt. St. Helens set S eruptions are inconsistent with each other, indicating unresolved uncertainty of around 1,000 years in dating of these eruptions. Assertion that eruption occurred "around 16 ka".
Keszthelyi, Baker, Jaeger, Gaylord, Bjornstad, Greenbaum, Self, Thordarson, Porat, Zreda	2009	GSA Field Guides	^{36}Cl surface exposure ages for morainic boulders on top of Steamboat Rock (n=3) at 16.3 ± 1, 13.2 ± 0.9, and 12.2 ± 1.1 ka, and for a flood-transported boulder in Moses Coulee (n=1) at 15.5 ± 2.9 ka.

Kuehn, Froese, Carrara, Foit, Pearce, Rotheisler	2009	Quaternary Research	Synthesis of ages for Glacier Peak Set G/B eruptions based on dozens of bounding radiocarbon dates from stratigraphies throughout the region of tephra airfall, constraining eruption to between 13.7 and 13.4 ka.
Hanson	2013	PhD Thesis	Major element analysis of tephra found within glacial Lake Columbia stratigraphy at Manila Creek section. Identified as Mt. St Helens set S tephra, possibly mixed with Mt. St. Helens set C tephra (Appendix D), potentially tying glacial Lake Columbia varve-year chronology into regional tephrochronology and providing a tie point between glacial Lake Columbia and Missoula Flood rhythmites that contain set S.
Balbas, Barth, Clark, Clark, Caffee, O'Connor, Baker, Konrad, Bjornstad	2017	Geology	Surface exposure ages on glacial and megaflood boulders constrain timing of Okanogan lobe advance and retreat. Three 10Be ages on high-level ice-rafted boulders above Wenatchee from 16.8 ± 0.6 to 17.1 ± 0.8 ka, inferred to have been deposited in a pre-Okanogan lobe Missoula Flood, suggest that the Okanogan lobe advanced across the Columbia after ~17 ka. Five 10Be ages on Withrow moraine boulders range from 26.2 ± 1.1 to 12.4 ± 0.6 indicating influence from both isotope inheritance and erosion of enclosing sediment creating both young and old biases and a challenge for determining age of initial Okanogan lobe retreat based on these ages. Three 10Be ages on boulders at Pateros Bar, formed after retreat of the Okanogan lobe from the Columbia River, range from 11.8 ± 0.6 to 14.2 ± 0.7 ka, indicating re-opening of the Columbia River due to Okanogan lobe deglaciation by 14 ka.
Smith, Sohbati, Buylaert, Lian, Murray, Jain	2018	Quaternary Science Reviews	OSL dating and stratigraphy of glacial Lake Missoula sediment at the Garden Gulch section indicating repeated lake bottom exposure. Partial re-setting of the luminescence signals prior to sand deposition may have resulted in an old bias to OSL ages, which range from 46.6 ± 3.6 to 10.6 ± 0.9 ka, with most ages between 23 and 18 ka.

Last, Rittenour	2021	Quaternary	(1) Radiocarbon ages on a collection of bones from a nearly intact mammoth skeleton indicate high-level Lake Lewis floods at 17.4 ± 0.2 ka, with supporting OSL chronology indicating similar timing of rhythmite deposition.

2.2.2 Geochronology

Many dateable deposits relate directly to the Okanogan lobe glaciation: (1) Glacial Lake Columbia deposits, which accumulated when the Okanogan lobe was across the Columbia River; (2) Missoula flood deposits in various drainages controlled by the Okanogan lobe and (3) Okanogan lobe glacial deposits.

2.2.2.1 Advance

2.2.2.1.1 Pre-glacial radiocarbon ages

The Okanogan lobe must have formed sometime after glaciation of its source areas, which likely occurred after 27.9 to 23.8 ka (Clague et al., 1980). Three radiocarbon ages from last-interglacial beds constrain the advance of the last-glacial CIS into the upper Okanogan valley. GSC-194 a sample of bark and twigs from a road cut near Shuswap Lake, British Columbia that dates to 23.8 to 24.4 ka (Dyck et al., 1965), GSC-477 is a sample of wood fragments from a borehole near Gardom Lake that dates to 27.9 to 25.1 ka (Lowdon et al., 1967, p. 172), and GSC-913 is a sample of plant detritus and peat from a stream cut on the S bank of Bessette Creek, circa 5 miles NW of Lumby, British Columbia that dates to 22.5 to 23.7 ka (Lowdon and Blake, 1970). This last, youngest age may give an age biased young by modern plant rootlets (Lowdon and Blake, 1970, p. 72).

2.2.2.1.2 Formation of glacial Lake Columbia

Following glaciation of the upper Okanogan valley, the Okanogan glacier expanded southward toward the Columbia River, eventually crossing and damming the Columbia River. Thus, the age of the oldest glacial Lake Columbia sediment dates the minimum age at which the Okanogan glacier crossed the Columbia River.

The base of the glacial Lake Columbia section can be estimated by varve counting downward from a dated horizon, using the assumptions that each varve-pair represents one year, that no varves were eroded from the composite section, and that the age of the dated horizon is accurate. Two datums exist for pinning glacial Lake Columbia stratigraphy in time: a radiocarbon age on wood enclosed within glacial Lake Columbia sediment (Atwater, 1986, Fig. 27), and an ash layer that is likely from the Mt. St. Helens set S tephra sequence (Hanson, 2013, Appendix D). These approaches indicate that glacial Lake Columbia formed sometime between 21 and 16 ka, with a higher likelihood that lake formation occurred between 19 and 17 ka than elsewhere in the range.

2.2.2.1.2.1 Set S

The set S tephra fell on glacial Lake Columbia just before its Manila Creek arm filled with sediment (Hanson, 2013, Appendix D; Waitt et al., 2021, Fig. 17). There are between 2,500 and 1,740 varves that underlie the Manila Creek tephra horizon in the composite Sanpoil section (Waitt et al., 2021, Fig. 17), indicating that glacial Lake Columbia formed at least 2,500 to 1,740 years before the eruption of set Sg, the age of which is between 17 and 15 ka (Clynne et al., 2008).

Tephra of set S erupted during the Swift Creek stage of eruptions from ~16 to ~13 ka when Mt. St. Helens unleashed pyroclastic flows into Swift Creek and erupted the set S and J tephras that were deposited regionally (Clynne et al., 2008). Set S consists of at least two tephras, So and Sg, that are interbedded in Missoula Flood rhythmites, sometimes as a couplet or triplet (Waitt, 1985; Moody, 1987), though its identification in some settings can be challenging due to geochemical similarities between set S and many other Mt. St. Helens tephras (Busacca et al., 1992).

Dating is another problem, with a likely age range for set S from 15 to 17 ka (Clynne et al., 2008). Pyroclastic flow deposits interbedded between set So and Sg tephra beds outcrop along Mt. St. Helens' Swift Creek. Three charcoal clasts from the pyroclastic flows date from 15 to 24 ka (Hyde, 1975). The old tail of ages suggests that the pyroclastic flow entrained some old charcoal that was already thousands of years old at the time of the eruption. However, the charcoal ages from the pyroclastic flow are out of stratigraphic order with radiocarbon ages on peat from overlying strata (Clynne et al., 2008, Fig. 10). One solution to this discrepancy is that the peat samples overlying set S incorporated ancient carbon at their time of formation and are thus too old. Another possibility is that some of the charcoal is too young due to contamination with modern rootlets due to a pretreatment procedure that did not fully remove plant rootlets (Table 2-1; Rubin and Alexander, 1958). However, such contamination of charcoal is typically only an issue with charcoal older than 25 to 30 ka (Higham et al., 2009). Nonetheless, the possibility of re-worked charcoal or charcoal contamination with modern rootlets adds some uncertainty to the Swift Creek ages.

Another way to date set S is via mollusk shells that underlie set S tephra in a section of Missoula flood rhythmites near Mabton. Two ages exist for the shells, obtained from the third rhythmite below the set S tephra near Mabton. An older age from Waitt (1985) is 17.1 ± 1.2 ka, while a younger age from Baker and Bunker (1985) is 16 ± 0.6 ka. The older age for shells at Mabton is in conflict with the youngest charcoal date from the pyroclastic flow at Swift Creek that implies that set S erupted after 15.4 ± 0.4 ka, while the younger age of 16 ± 0.6 ka overlaps the Swift Creek charcoal within uncertainty.

A possible solution to the shell age discrepancies is that re-mineralization of the shells altered their carbon isotopic composition, resulting in anomalously old ages through precipitation of old carbon, speculatively derived from ancient groundwater.

Set S could be as young as 14.6 to 15.4 ka, from the youngest of the charcoal ages, and as old as 15.4 to 18.3 ka, from the shell ages. Incorporating the full range of set S age and glacial Lake Columbia varve-counting uncertainty, glacial Lake Columbia might have formed as early as 20.8 ka and as late as 15.8 ka.

2.2.2.1.2.2 The wood age datum

The timing of lake formation extrapolated from the age of detrital wood in the lake stratigraphy is 19.7 to 17.7 ka. The wood, USGS-1860 (Atwater, 1986, p.1), has a radiocarbon date of 17.7 ± 0.8 ka. Between 883 and 1,171 varves underlie the wood. Assuming that the wood is not much older than the varves that contain it, the wood age combined with the varve counts indicate Lake Columbia formation at 18.7 ± 1 ka. Allowing for the possibility that the wood is reworked and much older than its enclosing varves would favor an asymmetric error with a young tail for Lake Columbia formation extrapolated from the wood age, such as 18.7 +1/-2 ka.

2.2.2.2 Retreat

The pattern of recessional moraines indicates a relatively rapid Okanogan lobe retreat punctuated by brief stabilizations. Exposure dating of the moraines is scattered, likely due to post-glacial exhumation of boulders from moraines.

Moraines atop Steamboat Rock were exposed shortly after the initial retreat of the eastern margin of the Okanogan lobe. Three ^{36}Cl ages from granite boulders atop Steamboat Rock of 12.2 ± 1.1 ka, 13.2 ± 0.9 ka, and 16.3 ± 0.1 ka. These absolute ages are not directly comparable to ^{10}Be ages because of age calibration complexity. However, the wide age range of 4,000 years with a tail of young ages, similar to the distribution observed for the Withrow moraine, indicates that exposure of morainic boulders may have continued long after deglaciation due to ground disturbance.

Recessional moraines on the Waterville Plateau are thinner and shorter than the Withrow moraine (Hanson, 1970, p. 53). Consistent spacing between moraines (Hanson, 1970, Fig. 19-2) and their similar forms suggest a periodic influence on their formation (Hanson, 1970, p. 91). Two sets of moraines radiate outward separately from the Okanogan valley and Omak lake trough (Hanson, 1970, Fig. 19-2), a pattern that indicates that the Okanogan lobe began to split into separate valley glaciers in the Omak Lake trough and Okanogan valley. The same inference is drawn from an outwash valley-train with an ice contact margin at the southern edge of Omak Lake (Flint and Irwin, 1939, p. 678), indicating a deglacial configuration in which a thinned and retreated Omak Lake Trench sub-lobe was confined to its valley (Flint and Irwin, p. 1939, p. 678).

The curvature of moraines on the NW corner of the Waterville Plateau (Hanson, 1970, Fig. 19-2) might indicate that a late-glacial version of the Okanogan lobe was topographically confined to the Okanogan valley and flowed onto the NW Waterville Plateau. Another valley glacier might have flowed down the Columbia River towards Chelan, recorded in terraced glaciofluvial deposits that line the Columbia valley upstream of Chelan. These terraces consist of fore-set gravel, bedded sand, and laminated silt and clay, indicating deposition in standing water (Waters, 1933, p. 790). Terrace surfaces are not paired in elevation nor do the elevations of terraces change in an orderly manner, suggesting that terraces formed in separate bodies of water rather than in a single lake (Waters, 1933, p. 791). Kettles on terrace surfaces (Flint, 1935, p. 186, Waters, 1933, p. 794), crenulated margins (Waters, 1933, p. 794), and the presence of erratic boulders on some terrace surfaces (Waters, 1933, p. 794) suggest that the terraces formed in ice-marginal environments, plausibly adjacent to a retreating Okanogan glacier that became increasingly confined to the Columbia valley as it thinned and retreated.

Poverty Flat terrace, located at the confluence of the Methow and Columbia rivers, consists of till, lacustrine silts and sands, and stream-bedded gravels (Waters, 1933, p. 811), and has kettles on its top that are up to 100 feet in depth (Waters, 1933, p. 816). Both the presence of till and kettles suggest that this terrace accumulated in an ice-marginal environment (Waters, 1933). Inset into the base of Poverty Flat is a boulder-studded gravel bar deposited and/or re-worked during a large, late-glacial flood down the Columbia River (Waitt et al., 2017, p. 184). The formation of this bar must post-date site deglaciation and terrace deposition, and thus the exposure ages of boulders on the surface of the bar relate to the time of reopening of the Columbia River (Balbas et al., 2017, Figure DR42). Exposure ages of three boulders on the bar

surface range from 14.3 ± 0.9 ka to 11.8 ± 0.8 ka, with a group mean of 13 ka (Balbas et al., 2017, recalculated from table DR2). The broad range of this age distribution might suggest that the ages represent several events rather than one event. The young tail of the age distribution, similar to the distribution for the Withrow moraine and for the Steamboat Rock moraines, is consistent with boulder-moving or boulder-exhuming floods across Pateros bar over thousands of years.

The next-youngest constraint on the position of the Okanogan lobe comes from the distribution of the Glacier Peak set G/B tephra. A series of sub-Plinian eruptions from Glacier Peak between 13.7 and 13.4 ka deposited sand-sized pumice grains throughout central Washington. This tephra is uniquely large, round, and phenocryst-rich in central Washington, which makes it easily identifiable in the field. Set G/B tephra is widespread throughout a cone-shaped region that radiates hundreds of miles eastward from Glacier Peak (Kuehn et al., 2009, Figure 1). Dozens of radiocarbon ages from sequences containing set G/B indicate that the eruption occurred between 13.7 and 13.4 ka (Kuehn et al., 2009, table S2).

The distribution of tephra in and above the Omak Lake trench implies that the Okanogan lobe had largely retreated from or stagnated on the Omak plateau to the west of the trench, but that the Omak Lake Trench sub-lobe occupied the trench at the time of the Glacier Peak eruption. Glacier Peak tephra overlies till in White Lake on the Omak plateau (Atwater and Rinehart, 1984), but is not present in a core of Goose Lake in the adjacent Omak Lake trench (Nickmann and Leopold, 1985, p. 137), indicating that the tephra was either not deposited at Goose Lake due to continued glaciation of the site by the Omak Lake trench sub-lobe, or that the

tephra was eroded from the site by outflow from the Omak Lake trench sub-lobe (Nickmann and Leopold, 1985, p. 137).

The distribution of Glacier Peak tephra indicates that ice had retreated to the north of the Columbia-Okanogan confluence by the time of the eruption, or that it had thinned to below the level of ice-marginal terraces. The tephra occurs on a terrace of ice-marginal sediment 4.5 km to the north of Chelan (Mack et al., 1979, p. 212) and 0.8 m above glacial outwash in a stratigraphic section near Chelan Falls (Gough, 1985, p. 75). Distribution of Glacier Peak set G/B also provides a minimum-limiting age for the end of all megafloods in Moses Coulee (this study), in Grand Coulee (Westgate and Evans, 1978), and the end of deep megafloods along the Columbia River (Waitt, 2017). Shallower Columbia River megafloods occurred after Glacier Peak Set G/B (Waitt, 2017). The Cordilleran Ice Sheet continued to shrink after set G/B (Porter, 1978).

2.3 METHODS

2.3.1 Glacial geomorphology

This study uses terrain-enhanced imagery viewed in Google Earth to trace glacial landforms of the Okanogan lobe. Google Earth's DEM (Digital Elevation Model) is more accurate and of higher resolution than the 10-m resolution NED (National Elevation Dataset) (Wang et al., 2017). Many of the satellite images that Google Earth displays capture the earth at sub-meter resolution. The ability within Google Earth to seamlessly view high-resolution satellite images of the same area captured on different dates often reveals subtle landforms that are only visible under particular combinations of sun angle, on-ground vegetation condition, and light quality. For example, the satellite images of the Waterville Plateau from 9/2011 clearly

resolve eskers, due to the late afternoon sun casting shadows that highlight low-relief landforms like eskers, and due to the late-summer vegetation condition that highlights the well-drained, gravel ridges as smooth and gray.

I visually identified glacial landforms on terrain-enhanced imagery in Google Earth, classified them into morphologic groups such as eskers and drumlins, and traced their extents as polygons (Fig. 2-1).

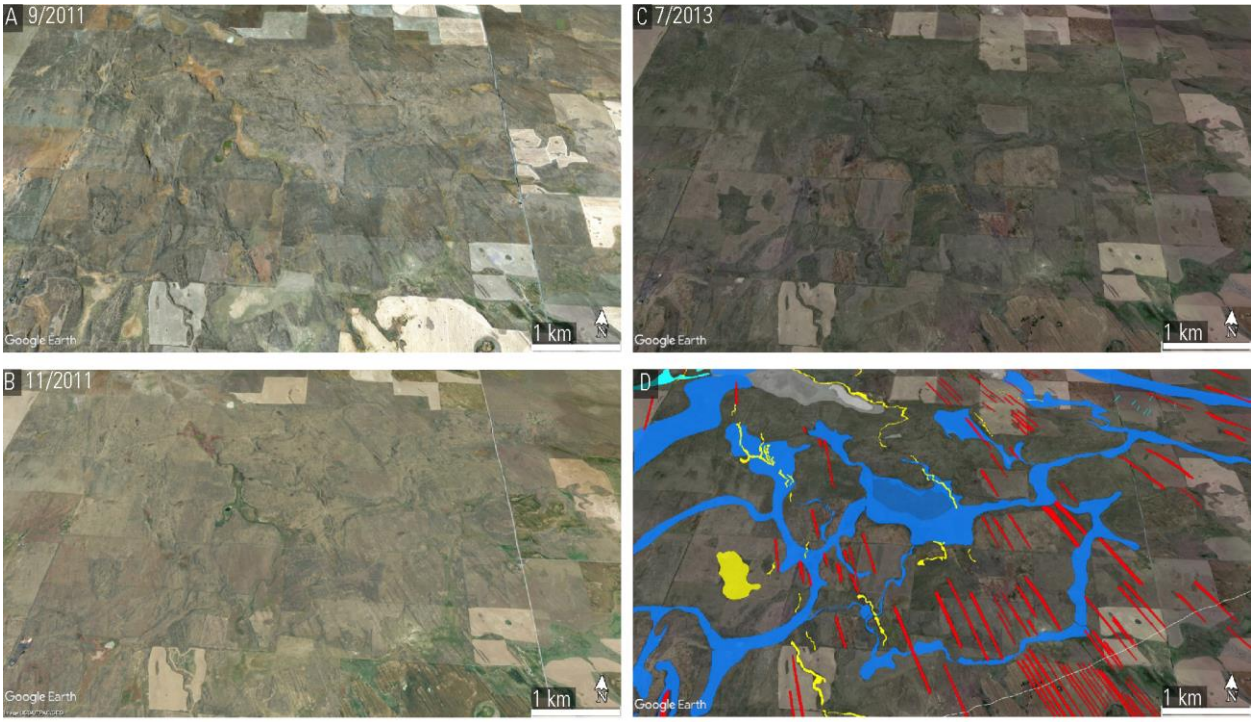

Figure 2-1: Example of glacial geomorphic mapping on terrain-enhanced satellite imagery. Three terrain-enhanced satellite images, two from 2011 and one from 2013, and glacial geomorphic mapping of the same area [47.747, -119.400]. Red represents streamlined bedforms, yellow represents eskers and esker complexes, and blue represents overfit channels.

Mapped landforms include eskers, drumlins, overfit channels, recessional moraines, and crevasse-squeeze ridges (?). Eskers are sinuous, positive-relief landforms oriented parallel or sub-parallel to paleo-ice surface slope. They may have tributaries, distributaries, connectivity to esker-fans, and smoothly convex, gray tops reflecting a paucity of vegetation due to well-

draining gravel soil. Drumlins and flutes are straight, elongated ridges of sediment or bedrock oriented parallel to paleo-ice flow and typically clustered into sets of tens to hundreds. Overfit channels are negative-relief, elongate depressions that are wider and deeper than modern drainages, often interconnected, that do not always follow surface slopes, and that often inter-weave between streamlined bedrock residuals. Recessional moraines are broadly curved and/or sinuous ridges of bouldery diamict that may define lobate curves. Crevasse-squeeze ridges are discontinuous, sub-parallel ridges that occur in sets of tens to hundreds and that may exhibit webbing/interconnectivity (Table 2-2).

Table 2-2: Criteria for identifying glacial landforms of the Okanogan lobe.

Landform	*Criteria*	*Other attributes*	*Examples of mapped forms*
Eskers	Sinuous; positive-relief; convex cross-section; parallel to paleo-ice flow	Tributaries; distributaries; braiding; connectivity to esker-fans; smooth, gray surface; Hybridization with drumlins;	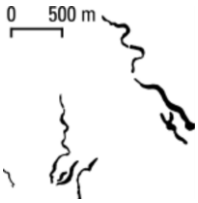
Drumlins and flutes (not distinguished)	Linear and elongate; positive-relief; convex cross-section; parallel to paleo-ice flow; clustered in sets of tens to hundreds	Smooth, gray surface	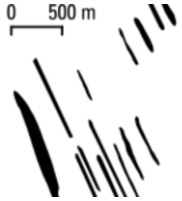
Overfit channels	Negative relief; wider and deeper than modern stream channels; U-shaped cross-sections	Interconnectivity with other channels; crossing of hydrologic divides; uphill channelization; association with streamlined bedrock residuals	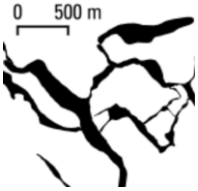
Recessional moraines	Curved to sinuous; positive-relief; perpendicular to paleo-ice flow	Regularly spaced; large boulders on surfaces	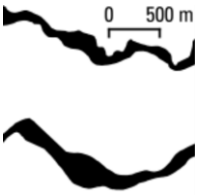
Crevasse-squeeze ridges	Low (~1 m), positive relief; discontinuous ridges; in sets of dozens to hundreds; evenly spaced; perpendicular to ice flow	Webbed interconnectivity	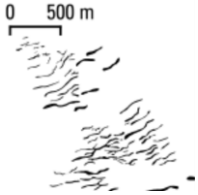

2.3.2 Surface exposure dating

2.3.2.1 Measurement details

We used a rock-hammer drill to obtain slabs of semi-uniform thickness from the surfaces of flood and glacially transported boulders in our study area. Samples were crushed and ground in the UW Rock Preparation Laboratory following rigorous between-sample cleaning using brushes, sieve picks, and compressed air. Clean quartz was obtained using sonication of crushed rock in deionized water to remove fines and organics, using surfactant separations with a lauryl amine solution to remove feldspar, and using separations in lithium metatungstate (LST) fluids to remove iron oxides and other dense minerals. We used ICP-OES to screen all quartz samples for Be, Mg, Al, Ca, Fe, and Ti < 200 PPM to minimize interferences during AMS analysis. Samples that passed chemical pre-screening were prepared for Be and Al isotope analysis using standard methods.

We measured ^{10}Be and ^{26}Al concentrations with the Accelerator Mass Spectrometer (AMS) at Lawrence-Livermore National Laboratories (LLNL) and measured ^{26}Al via AMS at Purdue Rare Isotope Measurement (PRIME) laboratory.

During ^{10}Be runs at LLNL, we monitored instrument stability using KNSTD07 ^{10}Be isotope standards prepared at UW. During a period from 2012 to 2015, we observed poor reproducibility of this standard, indicating an unusual level of instrument drift that would have also affected isotope ratio determinations of samples. For runs where KNSTD07 measurements that bracket samples are consistently offset from the standard value, we apply a correction factor based on this offset to measurements from that run and increase the analytical uncertainty on such adjusted measurements. However, in runs where the measurements of the standard varied

inconsistently, we have no way to know how instrument bias varied during sample runs, and we are therefore unable to apply a correction. We remove such uncorrectable measurements from our analysis. Exposure age data on boulders from the Rocky Ford channel of the Ephrata fan reflect the higher uncertainty and lower precision of ^{10}Be ages due to this measurement uncertainty, but the alignment of age distribution peaks between ^{10}Be and ^{26}Al ages indicates that the corrections applied were accurate (Fig. 2-19), because the ^{26}Al concentrations were measured in a different facility without the instrument drift problems.

2.3.2.2 Geologic considerations

An exposure age assumes that the sample contained zero cosmogenic nuclides when it was eroded from bedrock, that it accumulated zero nuclides during transport to its present location, and that the rock was exposed immediately after a singular event. These assumptions are commonly violated in Channeled Scabland boulder deposits to unknown degrees, creating dispersion in exposure ages that is difficult to correct. It is sometimes possible to identify the presence of an assumption violation, and in some cases to estimate its magnitude.

2.3.2.2.1 Prior exposure

The assumption that a rock sample contained no inherited cosmogenic nuclides at the time of deposition is based on a simplified model in which dated boulders derive from natural quarrying of rock by ice or water that only excavates material from several meters below the surface. In reality, rock that ultimately became a sample may have been quarried from surficial bedrock that already contained cosmogenic nuclides. Additionally, boulders quarried from depth

might have experienced thousands of years of exposure during transport before final deposition and exposure.

Field criteria for identifying and avoiding prior exposure include looking for rocks that are well-rounded and well-abraded, indicating that outer layers of rock containing inherited isotopes were removed during transport. However, it is still possible to date a pre-exposed rock that meets field criteria, and in many key study sites like Moses Coulee, perfect samples are extremely rare or non-existent.

After cosmogenic nuclide analysis it is possible to identify previously exposed rock as old age outliers in a group of samples believed to share a similar geologic history. Prior exposure manifests as anomalously old ages in a sample population. Balbas et al. (2017) identified four out of 41 rock samples that they interpreted as pre-exposed, suggesting prior exposure occurs at the ~10% level at their study sites. We analyzed some of the same sites and some different sites and observed obvious prior exposure in only one of our samples, suggesting prior exposure occurs in only ~2% of samples at our sites. It is difficult to estimate the degree that minor prior exposure, that does not obviously manifest as an outlier, contributes to an old age bias and age dispersion.

2.3.2.2.2 Reworking over multiple events

Re-working by multiple floods could create complex histories of abrasion, burial, and transport in a population of boulders, leading to age dispersion at study sites. Erosional surfaces in some gravel stratigraphies provide evidence for re-working of gravel in multiple Missoula flood events (e.g., Benito and O'Connor, 2003, Fig. 2), a process likely to cause age dispersion in exposure ages. Repeated flooding might cause each boulder to experience unique sequences of

burial, exposure, and abrasion over multiple floods, resulting in competing processes of accumulation and removal of cosmogenic nuclides across multiple floods, and ultimately creating uncorrectable dispersion in the exposure age population.

2.3.2.2.3 Incision

Progressive incision and winnowing of a diamict, as inferred for the Ephrata fan (Baker, 1973; Waitt et al., 2021, p. 295), would result in progressive exposure over time of boulders that were originally buried at various depths. As a lowering erosional surface intersected boulders, it would progressively expose them to cosmic rays. This would create dispersion in the age population of boulders now at the surface, with each exposure age dependent on the original depth of the boulder within the gravel body as well as the rate of incision.

2.3.2.2.4 Burial by loess

Shifting loess deposits could cause burial and re-exposure of study sites, though we see little evidence for this in our data. Prevailing SW winds predominantly winnow fines from Missoula Flood deposits in the Channeled Scabland. Downwind from Channeled Scabland depocenters, loess sheets are up to 100 m-thick and hundreds of thousands of years old (Sweeney et al., 2007). In contrast, loess is scattered, thin, and young (Bandow, 2001; Myers and Lillquist, 2018) in areas that were recently glaciated or swept by megaflood (Olmsted, 1963).

OSL dating of loess mound cores in and around the Channeled Scabland indicates a Holocene age of formation for some loess mounds (Bandow, 2001; Myers and Lillquist, 2018). Ages of a few thousand years for loess mound cores indicate that loess mounds are stable for long periods of time, but no not resolve whether loess mounds have been progressively forming

and stabilizing throughout the late Pleistocene and Holocene, or whether there have been post-glacial episodes of loess erosion in which post-glacial mounds were removed. Until late-Pleistocene-aged mound sediment is discovered, it is conceivable that migrating loess mounds progressively bury and expose surfaces and boulders in the Channeled Scabland.

2.3.2.2.5 Exhumation from flood sediment

Boulders now at the surface might have been originally buried in sediment and exhumed sometime after their deposition. This would result in an exposure age that reflects a period of attenuated cosmic ray flux beneath a lowering sediment shield, and then full exposure beginning once the lowering soil surface dropped below the rock sample surface.

Icebergs traveling in the Missoula floods sometimes ran aground on hillslopes, resulting in stranding of the iceberg, melting, and deposition of any debris entrained within the ice. Iceberg deposition occurred at Rattlesnake Mountain (Bjornstad, 2014), above Wenatchee (Balbas et al., 2017), throughout the Willamette Valley (Alison, 1935), and in Moses Coulee (this study). Many of the boulders deposited on hillslopes by icebergs ultimately became buried by slackwater sediment (Bjornstad, 2014).

Following the floods epoch, gravity and rainfall favored erosion of fine-grained sediment from hillslopes, resulting in progressive exhumation of boulders enclosed within the sediment. Evidence for this process is the appearance of boulders embedded within fine-grained sediments on slopes, and that typically lack the thick moss and lichen cover that is characteristic of boulders that have been continuously exposed for ~15,000 years.

Exposure dating of exhumed ice-rafted boulders on silty slopes will give ages that are younger than the depositional age of the boulder, because the sample was partially shielded from

cosmic radiation by the sediment that once buried it. The magnitude of the offset between the real depositional age of the boulder and the apparent exposure age is related to the thickness of sediment cover that has been eroded and the history of erosion.

2.3.2.2.6 Rock surface erosion

Erosion of the rock surface removes cosmogenic nuclides and results in a young age bias. Erosion rates of rock are low in the semi-arid environment of central Washington, but minor rock erosion is common. Rock erosion occurs from chemical and physical weathering and may be enhanced by acid weathering related to bird droppings (boulder tops provide perches for many birds), fire spalling, and processes related to moss and lichen cover. We visibly estimate an erosion rate for each sample based on the height difference between glacial or fluvial abrasion surfaces on the rock and the mean depth of erosion below that abrasion surface and based on an assumed sample age of 15,000 years.

2.3.2.2 Sampling strategy

We sampled felsic boulders in the western Channeled Scabland region. At every study site, we develop a geological interpretation of site history based on field-based and map-based observations of landforms and sedimentology combined with previously published interpretations of the study sites. These interpretations allow us to understand how exposure of the sample boulder relates to a geologic process such as site deglaciation or an iceberg-bearing megaflood. These interpretations are just as vital as the exposure age itself for determining the geologic history of the site.

We targeted samples that occur on the surfaces of megaflood gravels like the Ephrata fan, or that are present as lone erratics on flood or on glacially stripped basalt surfaces like the NE Waterville Plateau. We aimed to date large boulders with at least a half-meter of relief above the surface, that are in unambiguous depositional contexts, on flat surfaces away from mobile slopes, and that preserve at least some glacial-polish or fluvial abrasion surfaces on their tops. The purpose of these exhaustive sampling criteria is to avoid analyzing rocks that were exhumed or transported after their initial exposure during the event of interest.

The vast majority of glacially- and flood-transported boulders in the Channeled Scabland are basalts that cannot be accurately dated with cosmogenic nuclide methods. Of the rare felsic boulders that are present, many violate our sampling criteria. Typical problems are that the rock is embedded in erodible sediment, suggesting that it has been exhumed after the event of interest, that the top surface of the rock is rough and pitted, implying post-depositional surface erosion that is difficult to quantify, or that the rock is angular, indicating that it was not thoroughly eroded during glacial and/or megaflood transport and is likely to contain inherited isotopes from prior exposure.

Dated boulders in this study come from a variety of glacial, megaflood, and fluvial depositional environments. Some sites were affected only by glaciation or only by megaflood processes, while other sites were affected by a combination of glaciation, megaflooding, glacial outwash, and/or fluvial drainage. Understanding the geological history at every study site is critical for knowing what the exposure ages at that site represent.

Sites like Pateros bar exemplify the complexity. Pateros bar is a low-elevation site along the Great Bend of the Columbia River just downstream of the confluence of the Columbia with

the Methow and Okanogan Rivers. This site experienced Columbia River megafloods prior to the advance of the Okanogan lobe, glaciation by the Okanogan lobe, deposition of outwash of the Great Terrace during Okanogan lobe retreat, Columbia River megafloods after retreat of the Okanogan lobe, and incision of the Great Terrace by the Columbia River and the post-Okanogan lobe megafloods that coursed through it. The exposure ages of boulders now on the surface of Pateros Bar could be influenced by this entire sequence of events.

2.3.2.3 Isotope production rates from Lake Bonneville

We use a single regional calibration site from Lake Bonneville to calculate exposure ages instead of global production rate schemes. The alternative approach of calculating ages with the LSDn, Lm, or St schemes would result in ages that are systematically older by up to 500 years for all samples.

Lake Bonneville was a pluvial lake that occupied the present-day Salt Lake basin. Its sudden drainage during the over-topping of Red Rock Pass seemingly generated the perfect conditions for a cosmogenic nuclide calibration site: an event that suddenly exposed a freshly eroded, non-pre-exposed rock surface, and an event that could be precisely dated with an independent chronometer through radiocarbon and U-Th dating of high stand lake-cave tufa that were suddenly dried and fossilized in the lake drainage. Lifton et al. (2001) and Lifton et al. (2015) described the calibration site features with a careful analysis of the geologic uncertainty, noting that the wave-cut bench calibration surface is more likely to contain inherited isotopes than to have lost isotopes due to erosion. They estimate muon production beneath the pre-bench cliff at 0.5-2% level of measured isotope concentrations and estimate that water depth during bench erosion was 10 to 17 meters, the shielding effect of which would reduce spallation

production rates by 5 or 6 orders of magnitude. While Lifton et al. (2015) argued that isotope inheritance would have been negligible and did not include inherited isotopes in their calculations, it is important to recognize the asymmetry of the geological error. The field observations show that it is more likely that the estimated production rate is too high rather than too low because there are more reasonable pathways to inheritance than erosion. The total inherited isotopes in the rock could be up to 0.5-2% due to ignored muon production, and up to several percent or more due to ignored spallation production. While the muon production uncertainty is well-constrained by the geometry of the landform (Lifton et al., 2015), the water depth fluctuation uncertainty is based on the difference in elevation between the bench and local high-stand estuarine deposits which indicate that the lake level was 17 meters above the bench when the high estuarine sediments accumulated (Lifton et al., 2001). However, if Lake Bonneville water depth fluctuated during its high-stand, particularly if the water level dropped by tens of meters, or if the bench eroded while the lake was stable at the level of the bench, spallation reactions would have imparted cosmogenic nuclides into the rock prior to the Bonneville Flood. Wave-cut benches inherently form at the shoreline and thus near the water level. Additionally, it is possible that the water level fluctuated and dropped below the bench after rising above it and depositing the estuarine deposits. Lake level histories based on dated cave tufa at various elevations indicate fluctuations in Lake Bonneville water depth during the overall filling towards the Bonneville high-stand, not a monotonic increase (McGee et al., 2012). Oscillations in water depth are not surprising for a closed basin like Lake Bonneville, particularly since the regional climate is susceptible to decadal or centennial droughts. However, these lake level histories show that these fluctuations only lasted for hundreds of years, and that

the total period in which the water level was high enough that the bench could have formed is less than a few thousand years. Therefore, isotope accumulation during bench formation and possible post-bench water level fluctuations could have only added a few percent to the overall isotope totals, because these processes only could have occurred over a few thousand years, compared to the 18,000 years for which the bench has been exposed after the Bonneville Flood. If the bench contained inherited isotopes, this would have the effect of making the real production rate lower, which in turn would make all of our ages older. This asymmetric error would only have the ability to shift ages older by a few hundred years to a thousand years at most, because that is maximum-allowable time from lake level histories in which the bench formed, was inundated with water, and was exposed in the Bonneville Flood.

The second major uncertainty about the Promontory Point calibration site is the assumed age of the Bonneville Flood. In the early 2010's, a new set of radiocarbon and U-Th ages from dating of cave tufa and shells led to a reassessment of the age of the Bonneville Flood, indicating that the event was about 1,000 years older than previously accepted. The potential problem with the reassessment is that shells and tufa from similar settings often contain old calcite or form from groundwater or old lake-water, and thus give ages that are older than their age of precipitation. McGee et al. (2012) made compelling arguments that the textures of the Lake Bonneville tufa, and its uranium isotope composition characteristic of freshwater sources, indicate that Bonneville-stage tufa formed from lake carbon with a reservoir age of only a few hundred years. Nonetheless, the geologic error for the radiocarbon age of the Bonneville Flood is likely also asymmetric, more likely too old than too young. If the real age for the Bonneville Flood were 1,000 years younger, this would shift all of our ages younger by 1,000 years as well.

The second benefit of the Lake Bonneville calibration site is its stratigraphic relationship to the Missoula floods. Bonneville Flood gravel underlies Missoula flood rhythmites at Lewiston, ID (Waitt, 1985, Fig. 15). The 21 post-Bonneville flood rhythmites at Lewiston were not necessarily deposited by the same individual floods that emplaced the boulders in our study sites, but they do relate to the same family of events that deposited boulders in the western Channeled Scabland. The stratigraphic relationship between the Bonneville Flood gravel and the flood rhythmites at Lewiston pins the age of the Promontory Point calibration site to before the time period in which most of our samples were exposed. This relationship ensures that the calibration site captures the regional cosmic ray flux that the Channeled Scabland experienced.

To calibrate production rates at our sample sites, we use UW measurements of ^{10}Be and ^{26}Al in the Promontory Point quartzite from the wave-cut bench exposed in the Bonneville Flood. Using the complete CRONUS dataset from all labs results in systematic offsets between ^{26}Al and ^{10}Be ages for the same rock, a result of anomalously low ^{26}Al measurements from some labs. We calculate ages using the CRONUS v3 calculator, inputting an age of 18,300 ± 300 years for the Bonneville Flood (Lifton et al., 2015). We present ages scaled between Promontory Point and our study sties with the LSDn scheme (Lifton et al., 2014).

2.3.2.4 Age calculations

Inputs to exposure age calculations include the thickness of the rock sample, the density of the rock sample, an estimate of the erosion rate of the rock surface since exposure, the isotope concentration of ^{10}Be or ^{26}Al in clean quartz from the sample, and the production rate of the relevant isotope at the sample site over the period of sample exposure.

We estimated sample thickness both during sample collection and during our sample preparation process at UW. We measured the density of a chip from each sample using the buoyancy method with a wet balance. We estimate the post-depositional surface erosion rate based on the extent and depth of surface erosion to primary abrasion surfaces on the surface of each rock.

We measured ^{10}Be in all samples, and ^{26}Al in some samples. In cases where we measured both ^{10}Be and ^{26}Al isotopes on a single rock sample, we calculate a weighted-mean age that incorporates both isotope measurements. The degree to which each exposure age contributes to the combined age is inversely proportional to the analytical error of each measurement. Measurements that are more uncertain contribute less to the final age. In most cases, the ^{26}Al measurement has a greater analytical error, and therefore contributes less to the final age. However, in cases where the ^{10}Be measurement had to be corrected for instrument bias and its uncertainty increased, the ^{26}Al measurement contributes more to the final age.

We measured ^{10}Be concentrations of 15 glacially transported boulders and ^{26}Al concentrations on seven of those boulders. For the seven boulders where we measured both isotopes, we calculate three separate exposure ages: a ^{10}Be age, an ^{26}Al age, and a combined age based on the weighted mean of the ^{10}Be and the ^{26}Al age, with weights inversely proportional to analytical error. Within this group of seven boulders, the standard deviation of combined exposure ages is smaller than that for ^{10}Be or ^{26}Al exposure ages alone, suggesting that the combined ages are more accurate. For samples where we measured only one isotope, we calculate a standard exposure age for the rock based on that isotope concentration.

2.4 GLACIAL GEOMORPHOLOGY

Glacial landforms dominate the geomorphic character of the northern half of the Waterville Plateau. Well-preserved drumlins, flutes, eskers, moraines, crevasse-squeeze ridges, and meltwater channels exist throughout the area glaciated by the Okanogan lobe. These glacial landforms are organized into an overarching system with a radial geometry that reflects the ice surface slope of the lobe-shaped, piedmont glacier that once existed on the plateau.

The ubiquity of fluting, drumlinization, and eskers, combined with the presence of crevasse-squeeze ridges, suggest that the Okanogan lobe might have been a surge-type glacier with high basal water pressure. The diversity and complexity of the landform record is partly presented, but not fully explained in this study. Thin, short, and numerous recessional moraines indicate that the Okanogan lobe retreated rapidly, with brief stabilizations at ~20 separate positions. The curvature of those moraines suggests that ice flow during retreat became increasingly concentrated into the Okanogan valley and Omak Lake trench.

2.4.1 Bedrock erosion

Basal sliding by the Okanogan lobe abraded and striated some surfaces of the Waterville Plateau (Fig. 2-2). A fragmented but smoothly convex surface bearing striations occurs on the upstream side of a drumlin near 48.063, -119.092 (Fig. 2-2A/B).

Non-striated, smoothed bedrock surfaces in an area of anabranching bedrock channels near [47.758, -119.363] could have formed from direct effects of glacial erosion or from abrasion in subglacial meltwater flows (Fig. 2-2D).

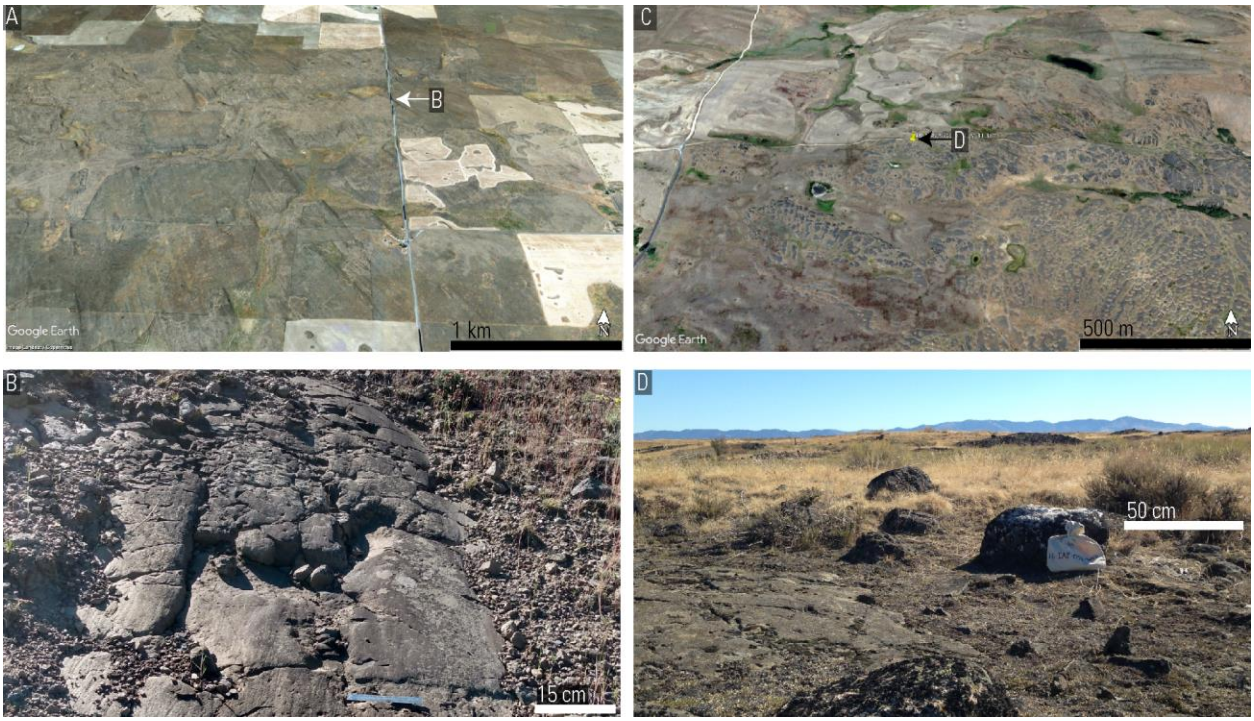

Figure 2-2: Glacially eroded basalt on the Waterville Plateau. (A, B): Drumlinized topography with polished, striated surface [B, 48.063, -119.092], (C,D) Anabranching channels in bedrock and smooth, bedrock surface with basalt and granite erratics [D, 47.758, -119.363].

2.4.2 Meltwater channels

Most of the land area that was beneath the former Okanogan lobe is incised with overfit channels. With the exception of Foster Coulee, which likely formed under westward surface drainage, most of the channels appear to have formed from southward flow of subglacial meltwater beneath the Okanogan lobe and/or from proglacial meltwater at intermediate stages of glaciation. The channels in different areas of the Waterville Plateau have differing geomorphic character. The channels on the NE Waterville Plateau near Steamboat and Wilson Buttes are generally narrower, shallower, and more numerous than the wider and deeper channels on the northern and central plateau, near Mansfield and Moses Coulee.

Channels on the NE Waterville Plateau near Steamboat and Wilson Buttes form an anabranching, SE-trending network cut into basalt. Individual channels are typically around 10-30 meters deep, and around 50-200 meters across (Fig. 2-3A/B). Channel bottoms typically contain numerous closed basins elongated parallel to channel flow direction. The anabranching geometry of this NE plateau channel network, its orientation parallel to drumlins and flutes, and its breaching of divides well above the highest, flood-swollen stage of glacial Lake Columbia suggest that it formed in a subglacial environment (see sections 3.5.2 and 3.5.3).

Channels near Mansfield, on the northern edge of the Waterville Plateau near Pearl Hill, and north of Moses Coulee are larger, wider, and less numerous than the NE plateau system, but similarly linked into an interconnected network. A prominent channel of the Mansfield system has an apparent depth of 30 meters, though this is a minimum because it is partly filled with sediment. At around 500 meters wide, it is around 5 times broader than typical channels of the NE system (Fig. 2-3E). Bedrock terraces on its western wall and its U-shaped cross profile (Fig. 2-3E), are reminiscent of Scabland-style coulees and indicative of fluvial rather than direct glacial erosion as the channel-carving process.

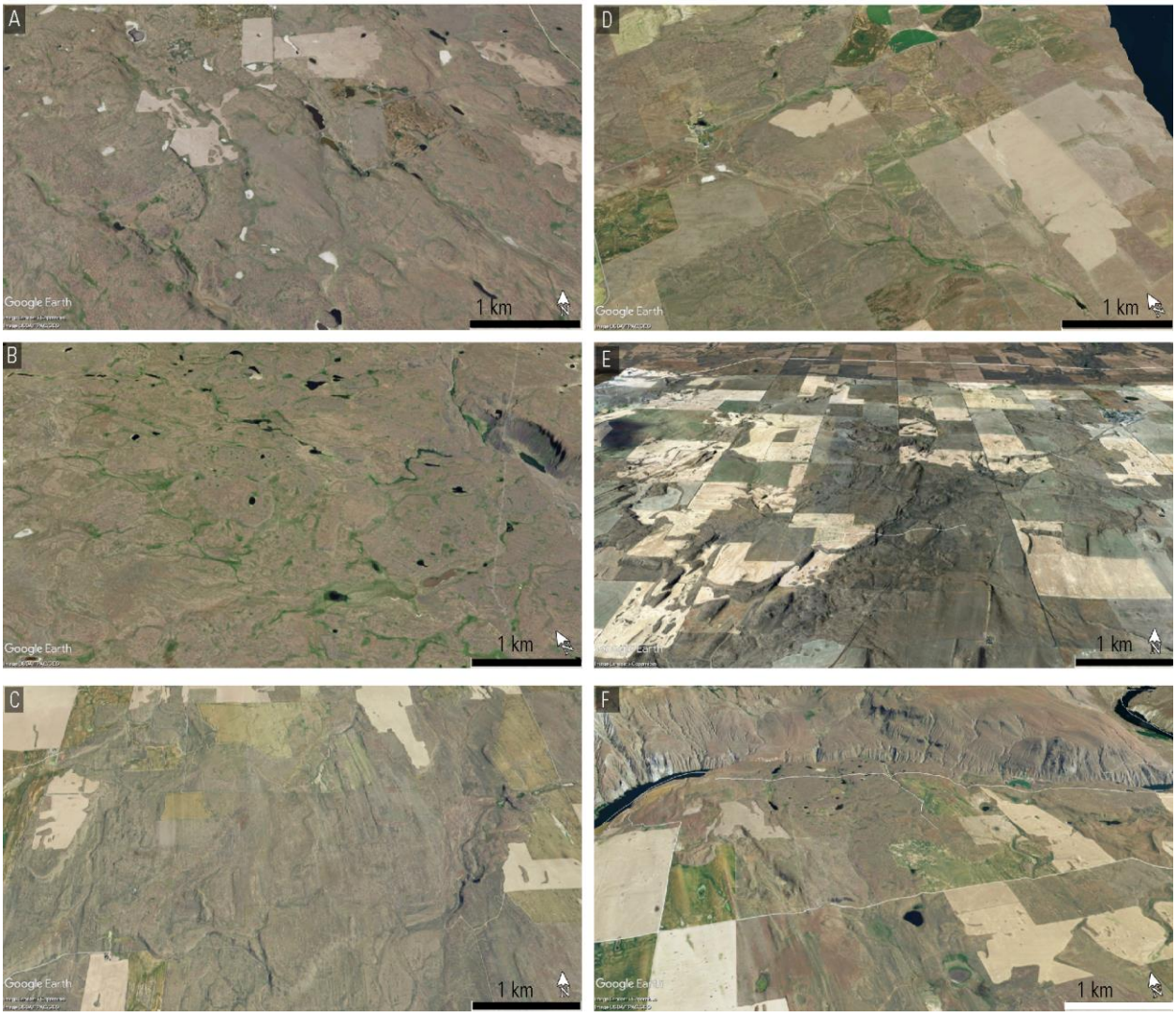

Figure 2-3: Terrain-enhanced imagery examples of overfit channels on the Waterville Plateau. (A) Steamboat Butte channels above Strahl Canyon [47.9722, -119.2144], (B) Steamboat Butte channels above Barker Canyon [47.9464, -119.2007], (C) Channels to north of Moses Coulee [47.7915, -119.5506], (D) Channels above west rim of Grand Coulee [47.7944, -119.2982], (E) Channels to SW of Mansfield [47.7712, -119.7055], (F) Channels near Pearl Hill [48.0446, -119.4568]

The channels can be viewed as several separate systems, each with a unique geomorphic character. At the same time, the channels can be seen as an integrated subglacial drainage network (Fig. 2-4).

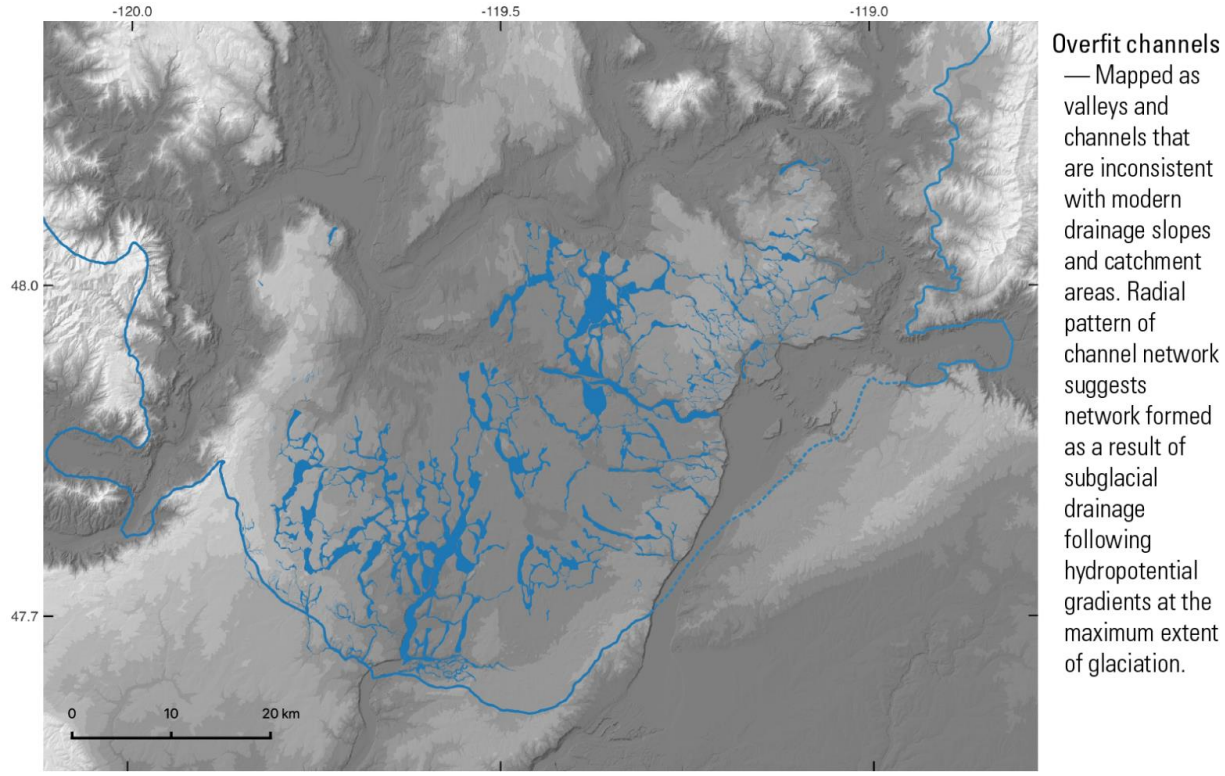

Figure 2-4: Extents of overfit channels on the Waterville Plateau, interpreted as a subglacial drainage system.

2.4.3 Flutes and drumlins

Streamlined glacial bedforms are common across the Waterville Plateau (Fig. 2-5). These highly elongated landforms are 100's to 1,000's of meters long, typically 10's or fewer meters wide, and typically a few meters tall. They are composed of sediment in some places, and bedrock in others (Fig. 2-2B).

Figure 2-5: Streamlined topography on the Waterville Plateau on terrain-enhanced imagery. (A) Drumlinized surface cut by channel [47.78, -119.71]; (B) Detail of A showing drumlins on and below higher surface [47.786, -119.704]; (C) Detail of A showing superposed drumlinization at multiple scales [47.791, -119.712]; (D) Fluting east of Grimes Lake [47.70, -119.53]; (E) Detail of D showing channel cutting across flutes [47.698, -119.553]; (F) Detail of D showing pervasive fluting [47.697, -119.528].

One drumlin at 47.759, -119.692 consists of angular clasts of basaltic cobble gravel with a silt and sand matrix (Fig. 2-6C/D). The angularity of the gravel and its dominantly basaltic composition indicate that the gravel was likely sourced from local bedrock and that the clasts did not travel for a long period of time in the subglacial sedimentary system.

Figure 2-6: Drumlinized topography on the Waterville Plateau — terrain-enhanced imagery and field photographs. (A) Drumlinized topography above lower Foster Creek [47.968, -119.697]; (B-D) Drumlin composed of angular, cobble gravel [47.759, -119.692].

This study does not distinguish mega-scale glacial lineations, drumlins, or flutes, but groups all of these streamlined bedforms together and uses them as indicators of ice flow direction of the Okanogan lobe. This study did not observe any cross-cutting relationships between streamlined bedforms. The overall pattern of streamlined bedforms is that they radiate outwards towards the glacial maximum marked by the Withrow moraine (Fig. 2-7).

A comparison of the orientations of streamlined bedforms north and south of Foster Coulee suggests a pattern of topographically controlled ice flow emanating from the Okanogan valley. On the Omak plateau and north-central Waterville Plateau north of Foster Coulee, streamlined bedforms are oriented N-S. However, south of Foster Coulee on the Waterville Plateau, they are oriented NW-SE near 47.75 N, and then smoothly curve to follow a N-S

orientation towards 47.7 N. The NW-trending streamlined bedforms south of Foster Coulee point towards the Okanogan valley, rather than towards the Omak plateau, suggesting that the ice that formed them flowed SE-ward out of the Okanogan valley and onto the Waterville Plateau, rather than southward from the Omak plateau and onto the Waterville Plateau. The pattern of drumlinization appears consistent with an ice flow pattern that was controlled by valley topography.

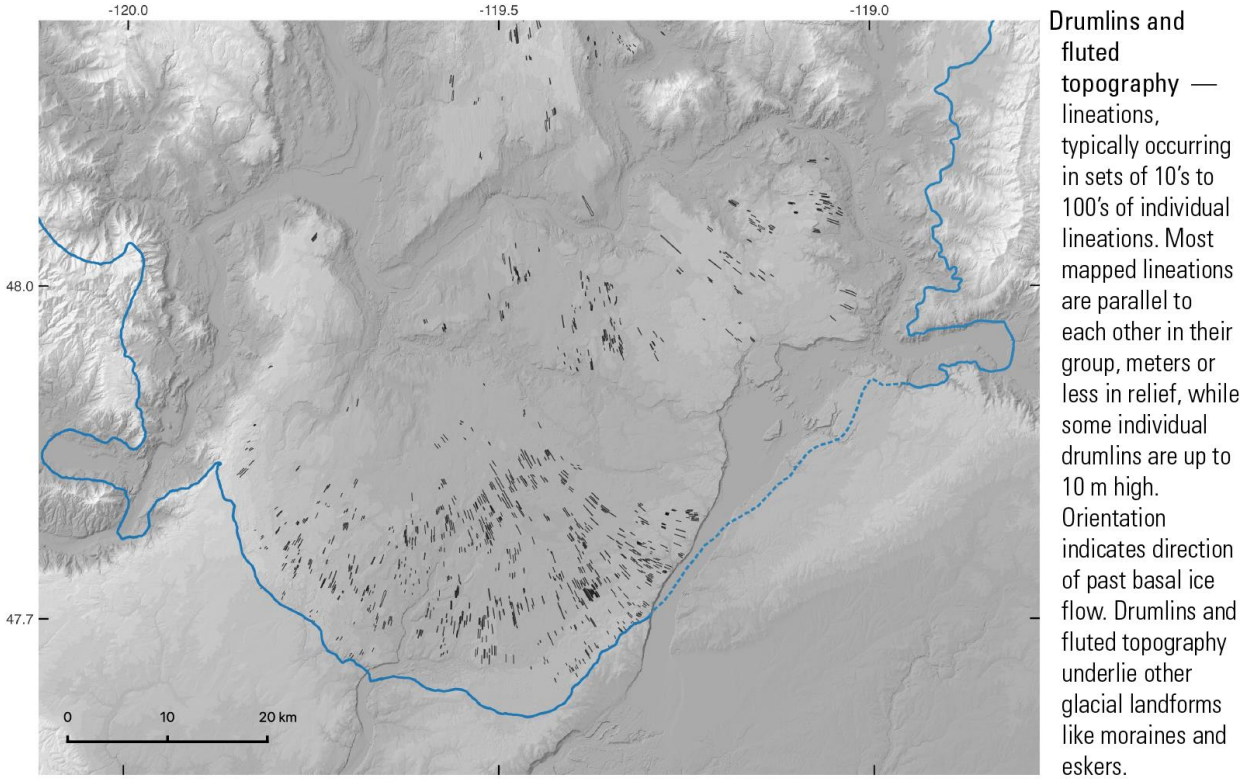

Figure 2-7: Map of drumlins and fluting on the Waterville Plateau, interpreted as indicators of past direction of basal ice flow of the Okanogan lobe.

2.4.4 Eskers

Eskers of the Okanogan lobe are sinuous ridges, at least some of which are composed of sandy cobble gravel. This study identified 485 eskers on the Waterville and Omak plateaus from terrain-enhanced imagery. Exposures at roadcuts and gravel pits suggest that a typical esker

consists of sub-rounded, basaltic cobbles and pebbles with an open-work texture or a silty sand matrix. Of three exposures analyzed, two consist of an equal mixture of a silty sand and gravel (Fig. 2-8A/B), while one consists of 90% gravel and only 10% sand matrix (Fig 2-8C/D; Table 2-3). This variability indicates a variety of flow and sediment transport conditions in subglacial meltwater streams beneath the Okanogan lobe. The high degree of rounding and sorting suggests significant transport distances of clasts and suggests stable and interconnected subglacial hydrologic systems that were able to round, sort, and transport clasts up to large cobbles.

Table 2-3: Grain-size distribution of three samples of Okanogan lobe eskers.

				Mass percentage in each grain-size bin (μm)						Sample mass (g)
Figure	Description	Lat.	Long.	<63	63-125	125-250	250-500	500-850	>850	
8A/B	Gravel near top of esker-fan; just east of Sims Corner	47.8153	-119.3267	11%	6%	6%	13%	12%	52%	343.7
9A/B	Pebble-cobble gravel near top of esker; near Pot Hills	47.8164	-119.4133	18%	13%	8%	5%	3%	53%	397.4
8C/D	Cobble-pebble gravel near top of esker; Mansfield channels	47.7719	-119.7282	1%	1%	2%	3%	5%	89%	954.1

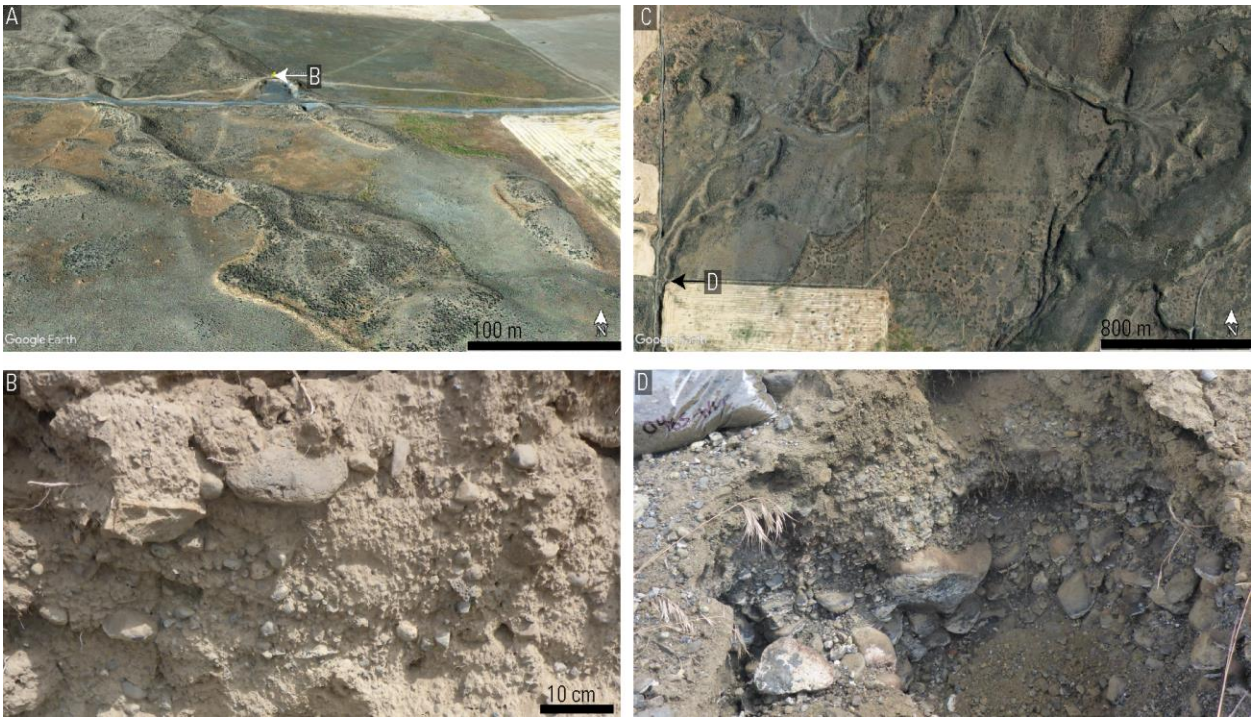

Figure 2-8: Exposures of gravel in two eskers. (A/B) Pair of eskers; western one terminating in fan and eastern one exposed in gravel pit [47.8153, -119.3267]: (C/D) Esker near Mansfield channels, with exposure showing open-work cobble gravel [47.7719, -119.7282]

Eskers are often located amidst fields of drumlins (Fig. 2-9). One landform in a field of drumlins near 47.796, -119.496 appears to alternate between sections that are esker-like and sections that are drumlin-like (Fig 2-9C/D). One explanation for this glacio-fluvial landform is that it was deposited in an R-type channel (a subglacial channel eroded upwards into the basal ice) that had both straight and sinuous segments. This would imply that some drumlins on the Waterville Plateau could be glaciofluvial if they were deposited in similarly straight subglacial tunnels. Another explanation for the hybrid drumlin-esker landform is that the Okanogan lobe began to flow again after depositing this esker, resulting in partial remolding of the esker into a drumlin-like form. The repeated alternation between straight and sinuous segments in the

landform (Fig. 2-9D; white arrows) would imply that basal ice flow during this hypothetical episode occurred in patches of flowing ice separated by zones of ice that were not flowing.

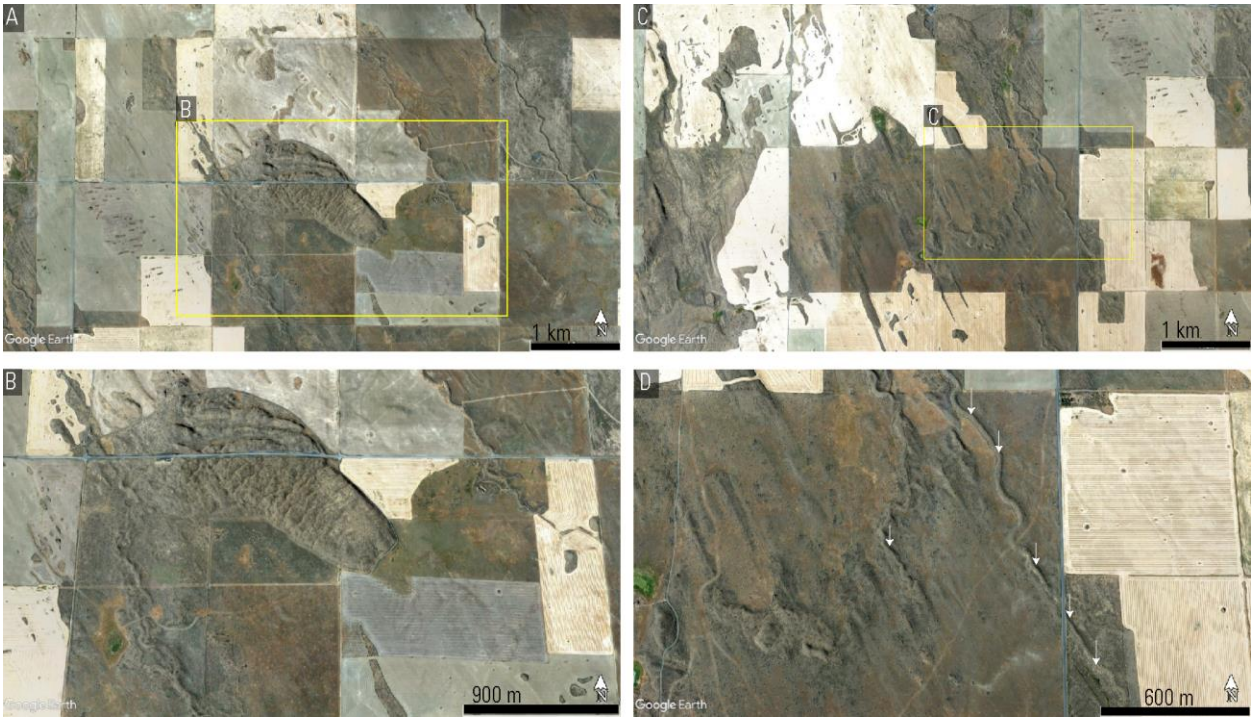

Figure 2-9: Eskers and other gravelly, glaciogenic landforms on the Waterville Plateau. (A, B) Eskers, drumlins, and crevasse-squeeze ridges of Pot Hills [47.869, -119.445], (C, D) Partly drumlinized eskers [47.796, -119.496], white arrows in panel D highlight transition points between straight and sinuous segments of the landform.

Some eskers terminate on their downstream ends in lobate deposits, interpreted here as esker-fans. Some of these esker-fans are topped with esker-like ridges (Fig. 2-10A), suggesting that a single esker branched into distributaries on top of the esker-fan and that the fan formed under the ice. Other esker-fans are incised with distributary channels (Fig. 2-10B), suggesting that subglacial meltwater became downwardly erosive across the esker-fan surface, or that the form formed in a proglacial environment.

Some eskers are braided (Fig. 2-10C/D), indicating that the subglacial tunnels in which the eskers formed also had interwoven geometries.

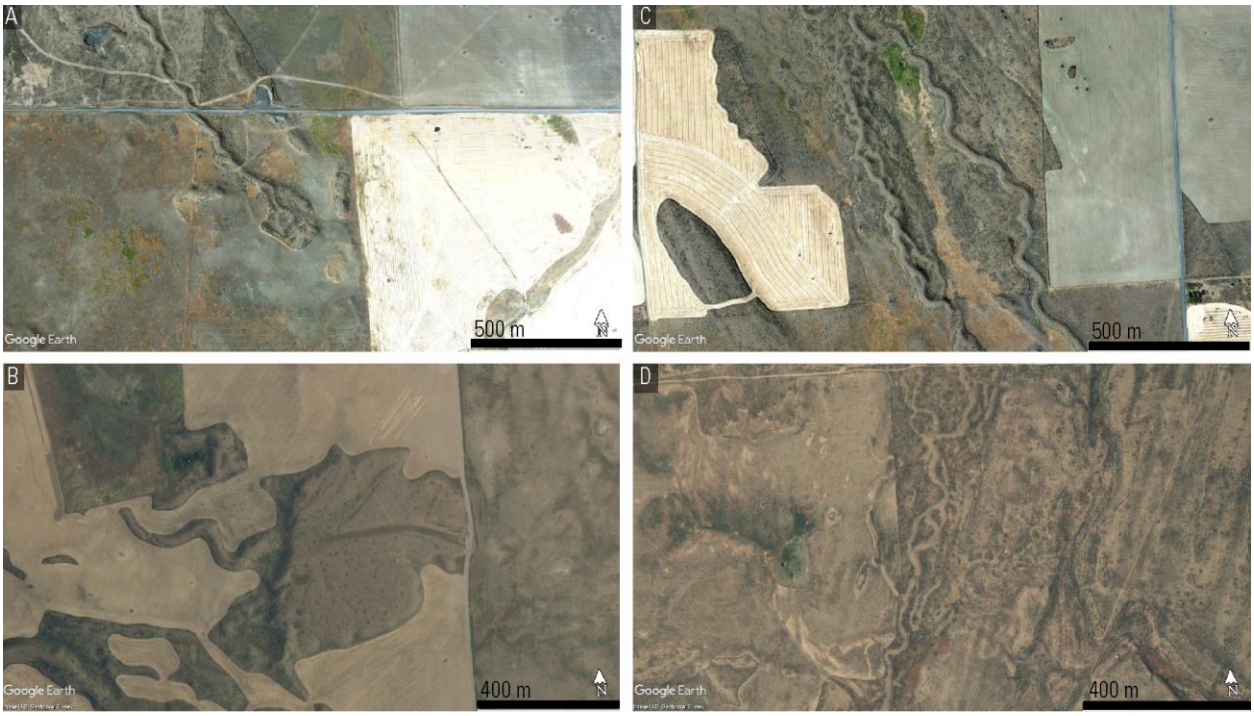

Figure 2-10: Eskers, esker-fans, braided eskers, and esker tributaries on terrain-enhanced imagery. (A) Esker feeding proportional, lobate esker-fan *topped* with distributary/anabranching eskers [47.812, 119.412], (B) Esker feeding outsized, lobate esker-fan *incised* with splaying distributaries [47.810, -119.324], (C) Braided eskers [47.805, -119.503], (D) Braided and tributary eskers [47.784, -119.716].

Eskers are present across most of the area glaciated by the Okanogan lobe (Fig. 2-11). The highest concentration of eskers exists in the shallow basin in the SE sector of the glaciated Waterville Plateau (Kovanen and Slaymaker, p. 557; Fig. 2-11). Eskers there are typically longer and larger than those elsewhere on the Waterville Plateau. Overall, the orientations of eskers are similar to those of drumlins, splaying outward towards the former ice margin of the Okanogan lobe. However, there is more variability in the orientations of eskers. Deviations from the overarching pattern appear related to bed topography, such as the system of eskers near 48.12, -119.43 that trend SW (Fig. 2-12), rotated around 45° from the N-S orientation of drumlins and other eskers there. The tendency for eskers to follow a combination of surface topography and

paleo-ice surface slope indicates that both factors were relevant for the direction of subglacial meltwater flow.

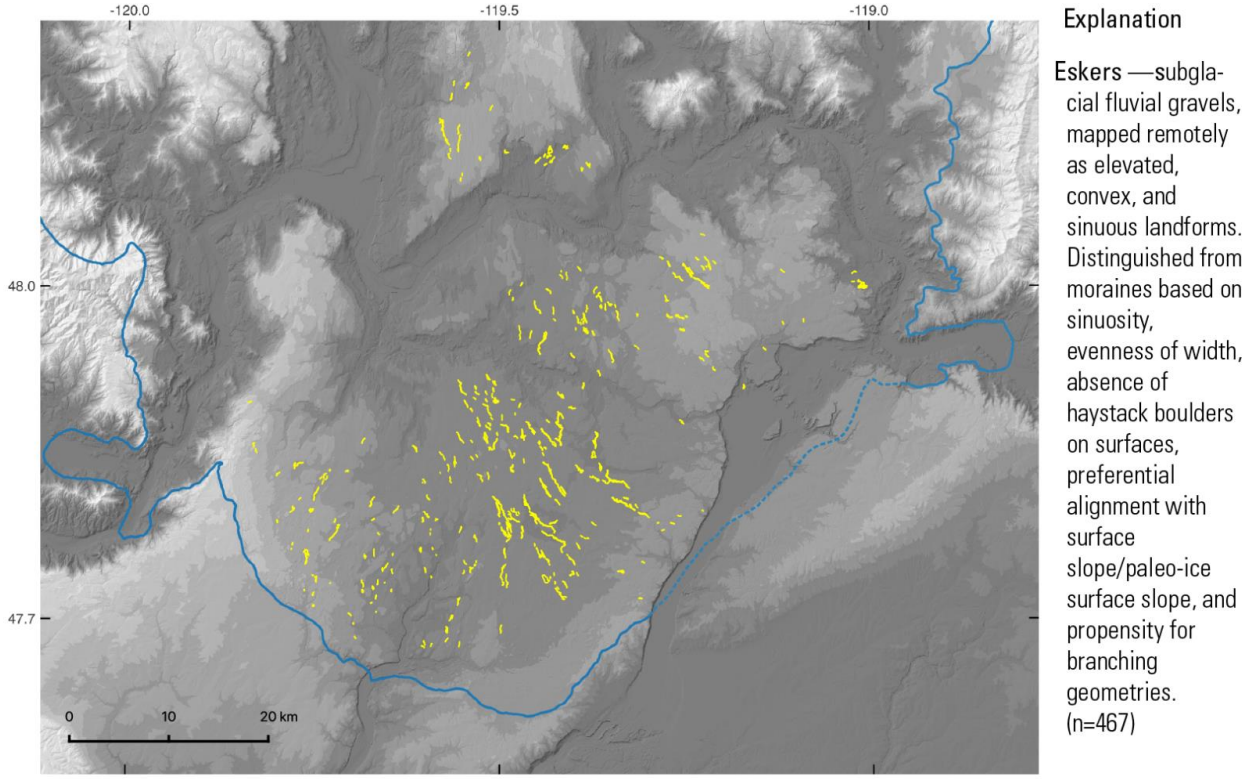

Figure 2-11: Distribution of eskers on the Waterville Plateau. Thickness enhanced to highlight at this map scale.

2.4.5 Recessional moraines

Recessional moraines of the Okanogan lobe are curved to straight ridges of sediment that are often studded with large basaltic boulders visible on satellite imagery. Moraines often occur in sets in which the individual ridges are separated by 100's of meters (Fig. 2-12). Recessional moraines of the Okanogan lobe are much smaller (10's of meters across and a few meters in height) compared to the Withrow moraine complex (several kilometers across and around 100 meters in height).

Nested recessional moraines indicate that the Okanogan lobe progressively diminished in size as its ice margin retreated north, while their small size indicates only brief stabilizations during retreat. Moraines delineate stable ice margins during glacier retreat. The size of a moraine is related to sediment supply, velocity of the glacier at the time of moraine formation, and the duration of ice margin stabilization. While thinner moraines could be explained by a diminished sediment supply, a thinning Cordilleran ice sheet would have increasingly exposed and destabilized valley walls and lateral moraines on its margins, increasing sediment supply during deglaciation. Therefore, the thin recessional moraines are likely related to the short durations of recessional ice margin stabilization.

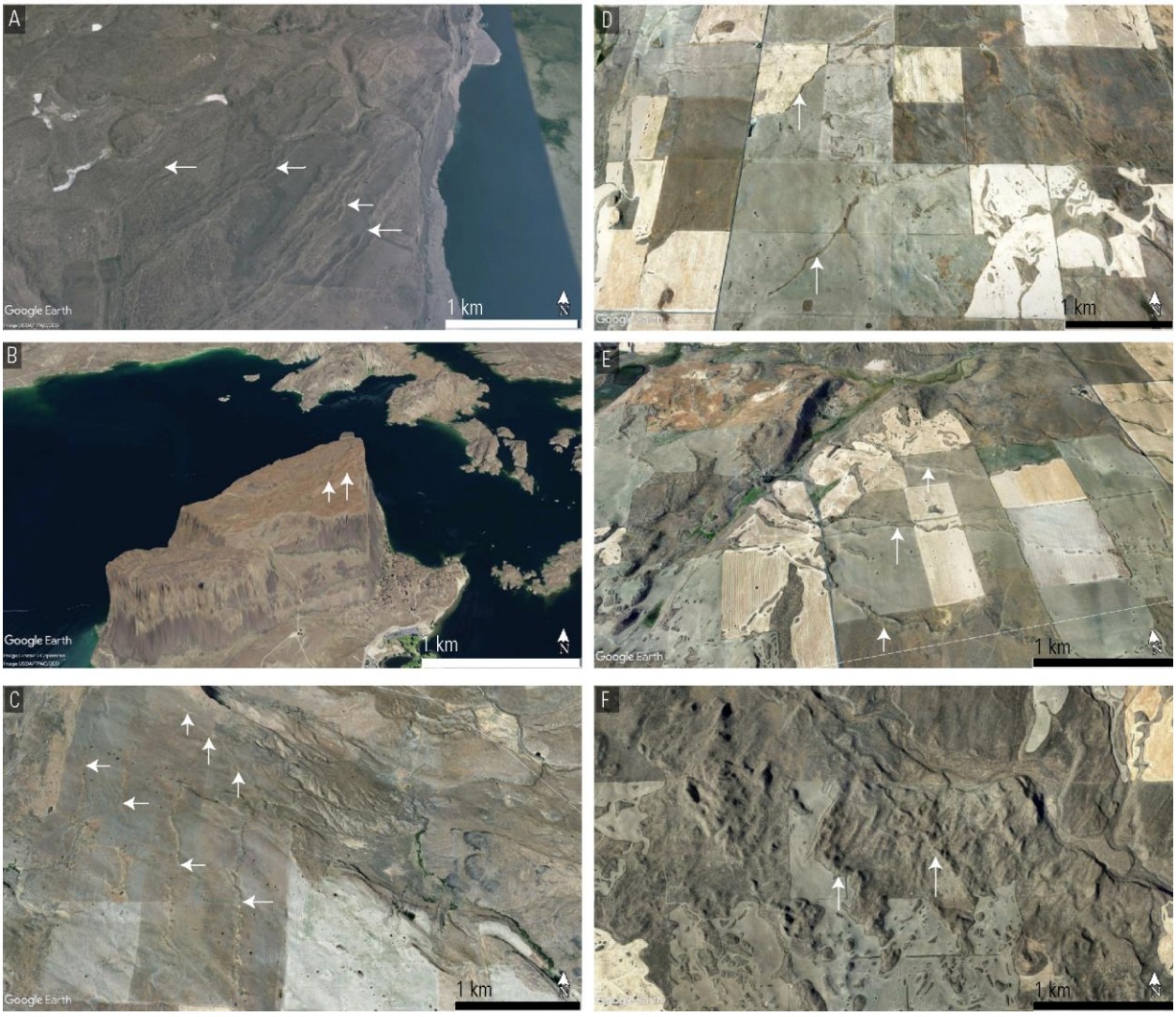

Figure 2-12: Recessional moraines on the Waterville Plateau and on Steamboat Rock. White arrows identify moraines and point in the direction of ice recession. (A) 47.8185, -119.2168, (B) 47.8716, -119.1258, (C) 48.0638, -119.2668, (D) 47.8608, -119.5695, (E) 47.8601, -119.7505, (F) 47.6933, -119.7122

2.4.6 Crevasse-squeeze ridges

Several sets of short (10's of meters), low (<1 meter), sub-parallel, and discontinuous ridges occur on the glaciated Waterville Plateau (Fig. 2-13 A, B, D, E). The surfaces of these ridges are studded with cobbles and boulders of both basalt and granite, suggesting that they are

composed of till (Fig. 2-13 C/F). No exposures were available, and no excavations were attempted. The ridges typically overlie fluted topography and often occur adjacent to eskers.

These landforms are similar in appearance to features that formed near the former margins of the Laurentide and Fennoscandian ice sheets that have been interpreted as crevasse-squeeze ridges (e.g., Evans et al., 2016; Lamsters et al., 2021), the formation of which is associated with surge-type glaciers and pressurized subglacial water (Rea and Evans, 2011). The possible presence of crevasse-squeeze ridges on the Waterville Plateau, previously considered absent from the area (Kovanen and Slaymaker, 2004, p. 562), suggests that the late-glacial Okanogan lobe may have been a surge-type glacier with high subglacial water pressure.

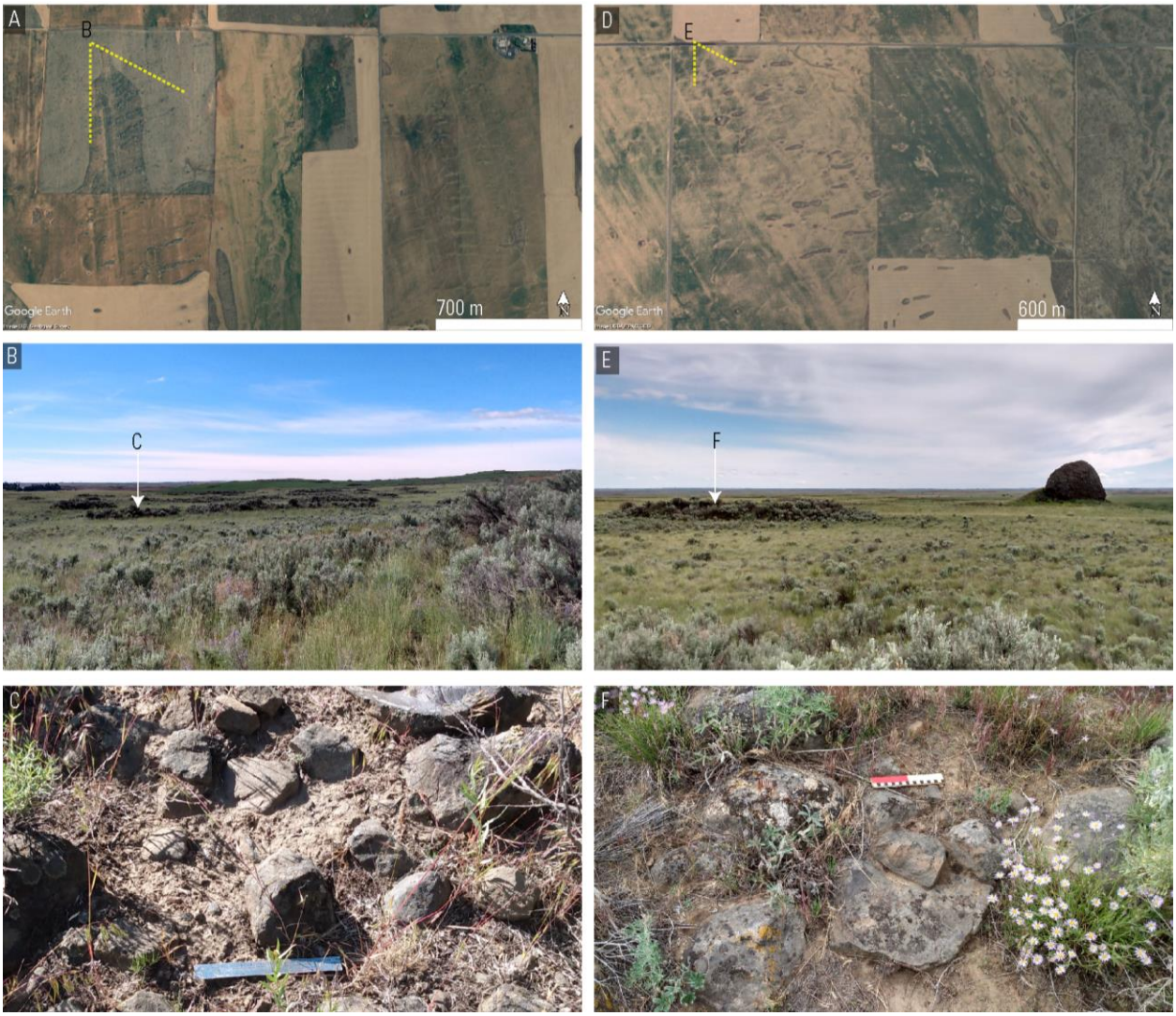

Figure 2-13: Possible crevasse-squeeze ridges on the Waterville Plateau. (A-C) Crevasse-squeeze ridges and eskers overlying fluted topography [47.6988, -119.5092], (D-F) Crevasse-squeeze ridges overlying fluted topography [47.8145, -119.4885].

2.4.7 Cross-cutting relationships

Recessional moraines on the Waterville Plateau typically overlie other glaciogenic landforms like drumlins (Fig. 2-14A) and channels (Fig. 2-14C), consistent with the interpretation that recessional moraines were the last glacial landforms to form.

Cross-cutting relationships involving channels are varied. Some smaller channels cut other features, like drumlins (Fig. 2-6E, 2-14B). However, eskers and drumlins often exist within larger channels (Fig. 2-14D), suggesting that the largest channels may pre-date formation of eskers, drumlins, and moraines. The variation in cross-cutting relationships involving the channel systems may indicate that the channels are a palimpsest that progressively formed during earlier glaciations, and during multiple episodes of both pro- and sub-glacial meltwater flow during the last glaciation.

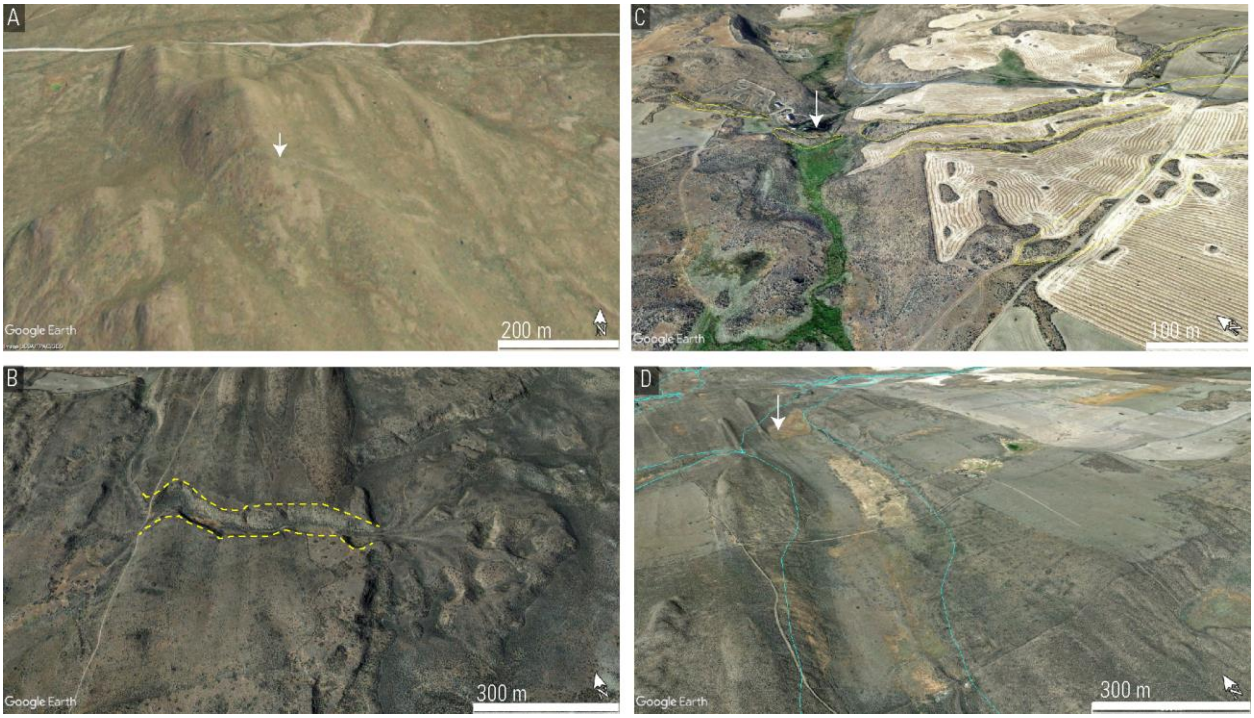

Figure 2-14: Cross-cutting relationships between glacial landforms (A) Recessional moraine overlying drumlins [47.999, -119.532], (B) Bedrock channel and its esker-fan (?), cross-cutting drumlins [47.779, -119.708], (C) Recessional moraine within overfit channel [47.867, -119.755], (D) Drumlins in overfit channel [47.689, -119.552].

2.5 Exposure ages

This study uses two groups of samples to date the advance and retreat of the Okanogan lobe. Exposure ages of boulders within the area once glaciated by the Okanogan lobe directly

date the timing of ice retreat. Additionally, exposure ages of boulders deposited by the Missoula floods in specific channels date the timing of Okanogan lobe diversions of the Columbia River. Exposure ages on flood-transported boulders from the mainstem Columbia, from Moses Coulee, and from Grand Coulee all help to constrain the timing of Okanogan lobe advance and retreat.

The natural drainage route for the Missoula floods was through the Columbia River. However, when the Okanogan lobe blocked the Columbia River, this diverted flows from the Columbia River into Moses Coulee, Grand Coulee, and/or the Telford-Crab Creek tract, flow pathways that would have been mostly or entirely inaccessible without Okanogan lobe impoundment (Denlinger et al., 2021, Fig. 7). The implication for dating the Okanogan lobe is that the ages of floods in Moses Coulee, Grand Coulee, and Telford-Crab Creek tracts all date times when the Okanogan lobe was across the Columbia River. The correlative is that the exposure ages on flood-transported boulders in the Columbia River downstream from the Okanogan lobe date when the Okanogan lobe was not across the Columbia River.

2.5.1 Glacially transported boulders

2.5.1.2 Withrow moraine

Ages from the Withrow moraine are scattered and do not provide a strong constraint on the time of deglaciation. The Withrow moraine complex marks the maximum extent of the Okanogan lobe and its exposure thus relates to early stages of ice margin retreat. Exposure ages from the moraine range from 12.4 ± 0.8 ka to 26.2 ± 1.1 ka, dating onset of Okanogan lobe deglaciation (Table 2-4). However, an old outlier at 26.2 ± 1.1 ka and a young outlier at 12.4 ± 0.8 ka indicate that the age population is influenced by biases that pull ages in both directions.

The young bias can be explained by post-glacial slope failures that exhumed boulders from the moraine and/or by erosion of boulder surfaces, while the old bias can be explained by the Okanogan lobe's quarrying of pre-exposed rocks.

Excluding the two outliers, the remaining four exposure ages range from 15.8 ± 1 ka to 14.3 ± 1 ka. The two ages of 14.3 ± 1 ka are similar to ages on glacial boulders upstream on the Waterville Plateau, while the two ages of 15.8 ± 1 ka (Balbas et al., 2017, WIT-13) and 15.1 ± 0.8 (069-MOS) are older than most ages upstream. If the latter two ages, between 15 and 16 ka, accurately date deglaciation of the Withrow moraine, this would indicate that the Withrow moraine likely deglaciated 500 to 1,000 years before deglaciation upstream on the Waterville Plateau and would imply a slower, progressive retreat of the Okanogan lobe. If, instead, those ages are biased old by pre-exposure and the 14.3 ± 1 ka ages are accurate, this would suggest that the entire Waterville Plateau deglaciated rapidly, likely within ~500 years, at around 14.5 ka.

Table 2-4: Surface exposure ages of Withrow moraine boulders, in or near upper Moses Coulee. All ages recalculated from Balbas et al. (2017) except 18–IAF-069-MOS, from this study.

Sample Lab ID	Latitude DD	Longitude DD	Altitude MASL	Substrate	^{10}Be age ka	Err. (2σ int.)
WIT-15	47.6500	-119.6500	615	Till	12.41	0.83
WIT-12	47.6600	-119.6130	636	Till	14.31	0.98
WIT-18	47.6650	-119.6340	635	Till	14.32	0.88
069-MOS	47.6517	-119.6673	573	Till	15.10	0.75
WIT-13	47.6490	-119.6570	655	Till	15.77	0.97
WIT-19	47.6650	-119.6340	633	Till	26.20	1.10

2.5.1.3 Waterville Plateau, Omak plateau, and Omak Lake trench

Exposure ages on isolated glacial erratics perched on bedrock of the Waterville Plateau date the northward retreat of the Okanogan lobe to between 15 and 14 ka. ^{10}Be ages of glacially transported boulders on the Waterville Plateau upstream from the Withrow moraine are all

between ~16 and ~13.5 ka, with most of the ages between ~15 and ~14 ka (Table 2-5). The high density of ages between 15 and 14 ka suggests that this is when the main deglaciation of the Okanogan lobe occurred. Young outliers in the population at 13.8 and 14 ka might be explained by exhumation of the dated samples from till. One older outlier near 16 ka might be explained by an early thinning of the Okanogan lobe, or by prior exposure.

The most robust deglaciation ages come from four boulders on the NE Waterville Plateau that give similar ages and for which we measured both ^{10}Be and ^{26}Al concentrations. The ^{10}Be ages for these four range from 14.1 to 14.9 ka, a range of 800 years, while the ^{26}Al ages range from 14.2 to 14.7, a range of 500 years. However, the combined exposure ages incorporating both isotope measurements and their uncertainties range from 14.3 to 14.6, a span of only 300 years (Table 2-5). The smaller range of the combined exposure ages in a situation where the ages are expected to match supports the idea that these combined ages provide a better estimate of the true exposure age than an age calculated from one isotope alone.

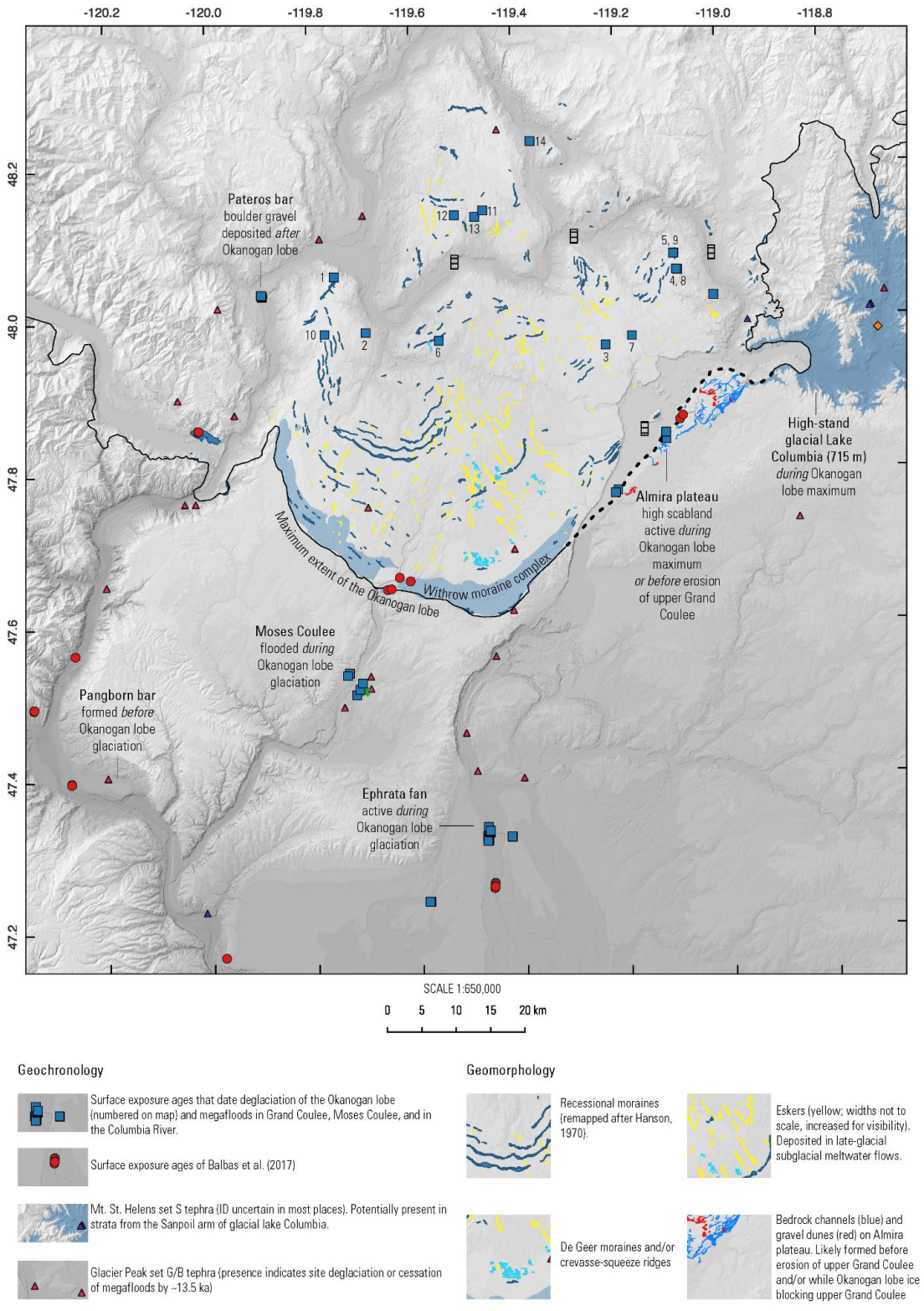

Figure 2-15: Index map of geochronology and geomorphology of the Okanogan lobe.

Table 2-5: Surface exposure ages of boulders glacially transported by the Okanogan lobe. Numbers correspond to those in Fig. 2-15.

Sample	Latitude	Longitude	Altitude	Substrate	^{10}Be age	Err.	^{26}Al age	Err.	Combo age
Map ID Lab ID	DD	DD	MASL		ka	(2σ ext.)	ka	(2σ ext.)	Wtd. mean
Waterville Plateau									
1 18-IAF-081-WVP	48.0599	-119.7527	865	Till	13.84	0.45			
2 18-IAF-082-WVP	47.9864	-119.6923	688	Till	14.05	0.46			
3 13-IAF-013-WVP	47.9651	-119.2253	781	Bedrock	14.07	0.53	14.71	0.78	14.28
4 16-IAF-055-WVP	48.0621	-119.0821	795	Bedrock	14.39	0.58	14.16	0.81	14.32
5 18-IAF-073-WVP	48.0841	-119.0886	792	Till (thin)	14.41	0.96			
6 14-IAF-035-WVP	47.9769	-119.1737	735	Till	14.53	0.38	14.26	1.04	14.50
7 18-IAF-072-WVP	47.9745	-119.5499	714	Till (thin)	14.79	0.43			
8 16-IAF-057-WVP	48.0628	-119.0844	798	Bedrock	14.86	0.56	14.22	0.67	14.61
9 18-IAF-074-WVP	48.0835	-119.0898	785	Bedrock	15.44	0.43			
10 18-IAF-080-WVP	47.9848	-119.7722	892	Bedrock	15.81	0.59			
Omak plateau									
11 17-IAF-066-CMLK	48.1444	-119.4605	744	Bedrock	13.98	0.74			
12 14-IAF-026-CMLK	48.1388	-119.5155	762	Till	14.39	0.85	13.81	0.79	14.09
13 17-IAF-065-CMLK	48.1362	-119.4761	725	Bedrock	15.03	1.27			
Omak trench									
14 14-IAF-027-OMK	48.2341	-119.3653	425	Till	13.68	0.41	13.88	0.98	13.71

Figure 2-16: Photographs of glacially transported boulders on the Waterville Plateau. (ND (Not Dated), and (4) and on the NE Waterville Plateau. Boulders (10) and (1) on NW Waterville Plateau. See Fig 2-15 for locations.

2.5.2 Flood-transported boulders

2.5.2.1 Moses Coulee

Exposure ages for flood-transported boulders in Moses Coulee are scattered and do not provide a strong constraint. If two of the older ages accurately represent flood events, they suggest an early advance of the Okanogan lobe between 19 and 17 ka.

Moses Coulee depended on the existence of the Okanogan lobe for receiving floods. Floods into Moses Coulee either required an Okanogan lobe blocking the Columbia River, to

route Missoula floods into Moses Coulee, or a near-maximally advanced Okanogan lobe, to route subglacial floods directly from the Okanogan lobe into Moses Coulee (see Ch. 3 for more detail). Though the source and pathways of Moses Coulee floods remain uncertain, all plausible options for Moses Coulee floods require an Okanogan glacier that has dammed the Columbia or an Okanogan lobe that is even more extensive on the Waterville Plateau.

Ages on iceberg-rafted erratics in Moses Coulee range from 13.76 ± 0.53 to 28.1 ± 1.21 ka (n=7) indicative of last-glacial megafloods in Moses Coulee. The anomalously old age is likely pre-exposed (and notably similar to the 26.2 ± 1.1 ka age on WIT-19 from the Withrow moraine), while the anomalously young age is from a low-relief boulder that was likely exhumed from flood-deposited sand and silt. The remaining ages range from 15.52 ± 0.69 to 18.85 ± 0.83 ka (n=5).

These remaining Moses Coulee ages are older than all but the highest-elevation glacial sample from the Waterville Plateau, suggesting that Moses Coulee floods pre-dated Okanogan lobe retreat. The overlap between the younger ages from Moses Coulee and the oldest, high-elevation age from the Waterville Plateau suggests that Moses Coulee floods could have occurred after the Okanogan lobe had begun to thin.

In the scenario in which Moses Coulee floods were from lake Missoula, the end of Missoula floods prior to retreat of the Okanogan lobe (Atwater, 1987) would explain why Moses Coulee floods do not overlap in time with Okanogan lobe retreat. By the time the Okanogan lobe had retreated enough to re-open a flood path for Missoula floods into Moses Coulee, the Missoula floods were likely small or non-existent. If, however, Moses Coulee floods came directly from the Okanogan lobe, a change in subglacial water routing during the onset of

deglaciation could have re-directed flows away from Moses Coulee. Deglaciation of the Columbia River sub-lobe near Chelan would have re-routed subglacial meltwater from Moses Coulee to the Columbia River by creating a path of lower subglacial hydro-potential along the Okanogan valley into the Columbia valley. See section 3.3.4.2 for a more detailed discussion of these ages.

Table 2-6: Surface exposure ages of flood-transported boulders and cobbles in Moses Coulee

Sample	Latitude	Longitude	Altitude (m)	Sample substrate	Exposure age (ka)	Error (2σ)
1 095-MOS	47.52711	-119.7088	557	Erratic- rich silty sand, flat.	13.8	0.7
2 090-MOS	47.54043	-119.73371	565	Erratic- rich silty sand, slope.	15.5	0.8
3 104-MOS	47.48475	-119.77719	511	Erratic-rich pavement over silty sand, flat.	16.1	0.8
4 092-MOS	47.51173	-119.72022	530	Erratic-rich silty sand, flat.	16.3	0.7
5 094-MOS	47.51891	-119.71362	543	Erratic-rich pavement over silty sand, flat	17.4	0.8
6 091-MOS	47.53722	-119.73732	570	Embedded in erratic-bearing gravel, flat.	18.8	1
7 093-MOS	47.51891	-119.71362	543	Erratic-rich pavement over silty sand, flat	28.1	1.4

2.5.2.2 Grand Coulee

Like Moses Coulee, Grand Coulee needed Okanogan lobe diversion to receive flow and megafloods from the Columbia River. Exposure ages from the Ephrata fan, a bouldery gravel deposit at the outlet of Grand Coulee, thus date the timing of Grand Coulee floods and constrain the timing of Okanogan lobe glaciation. These ages range from 12.05 ± 0.6 to 18.44 ± 1.15 ka (n=20), with the bulk of the ages between 13.98 and 16.14 ka (n=18). These ages significantly overlap with glacially transported boulders on the Waterville Plateau, although the ages from the Ephrata fan are slightly older. The age overlap suggests that floods through Grand Coulee continued during deglaciation of the Waterville Plateau between 15 and 14 ka.

The mean age of the non-outliers from Moses Coulee is 16.8 ka (n=5), while the mean for Ephrata fan boulders is 15 ka (n=20), suggesting that flooding in Moses Coulee generally pre-dated flooding on the Ephrata fan, and matching an inference about the sequence of flood routes

from the gravel fan below Moses Coulee (Waitt, 1985, p. 1276). However, there is some overlap between individual ages from Moses Coulee and the Ephrata fan, with seven boulders from the Ephrata fan dating to 15.58 to 15.94 ka, between two of the younger ages from Moses Coulee at 15.52 and 16.1 ka. Though this age overlap could be seen to imply simultaneous flooding through Grand Coulee and Moses Coulee, it is also plausible that the overlap is an accident of analytical error or geologic error, especially given the lack of stratigraphic evidence for simultaneous flooding of Grand Coulee and Moses Coulee in the Rock Island fan.

Table 2-7: Surface exposure ages of Ephrata fan flood-transported boulders.

Sample	Latitude	Longitude	Altitude	Substrate	^{10}Be age	Err.	^{26}Al age	Err.	Combo age
Lab ID	DD	DD	MASL		ka	(2σ ext.)	ka	(2σ ext.)	Wtd. mean
Rocky Ford channel									
13-IAF-009-EPH-262	47.3189	-119.4708	362	Gravel	13.92	0.64	14.1	0.91	**13.98**
15-IAF-036-EPH	47.3288	-119.4676	358	Gravel	14.26	0.67	14.46	1.23	**14.31**
17-IAF-063-EPH	47.3313	-119.4675	359	Gravel	14.39	0.58	14.23	1.09	**14.35**
17-IAF-061-EPH	47.3365	-119.4713	359	Gravel	14.31	0.51	14.65	1	**14.39**
13-IAF-009-EPH	47.3189	-119.4708	362	Bedrock	13.58	1.53	15.09	0.92	**14.75**
13-IAF-010-EPH	47.3181	-119.472	364	Bedrock	13.88	1.41	15.19	0.89	**14.86**
15-IAF-037-EPH	47.3288	-119.4677	358	Gravel	14.98	0.46	15.28	1.2	**15.02**
13-IAF-008-EPH	47.322	-119.471	361	Bedrock	14.93	1.44	15.19	0.88	**15.12**
13-IAF-008-EPH-254	47.322	-119.471	361	Bedrock	15.58	0.93	14.69	0.86	**15.13**
15-IAF-038-EPH	47.3296	-119.4674	359	Gravel	15.19	0.57	14.76	1.49	**15.14**
12-IAF-001-EPH	47.3237	-119.4718	364	Gravel	15.7	2.51	15.15	0.75	**15.2**
12-IAF-003-EPH-254	47.3241	-119.4725	364	Gravel	15.9	0.95	15.13	0.9	**15.52**
12-IAF-002-EPH	47.3239	-119.4731	364	Gravel	15.83	2.66	15.72	1	**15.74**
15-IAF-039-EPH	47.3301	-119.4681	358	Gravel	15.85	0.5	15.53	1.19	**15.8**
12-IAF-003-EPH	47.3241	-119.4725	364	Gravel	15.63	2.58	16.2	0.93	**16.14**
15-IAF-040-EPH	47.3311	-119.4675	359	Gravel	18.11	0.73	19.76	1.58	**18.44**
High fan terraces									
18-IAF-079-EPH	47.2395	-119.5856	372	Gravel	12.05	0.6			
19-IAF-088-EPH	47.3234	-119.426	376	Gravel	14.97	0.78			
19-IAF-087-EPH	47.3229	-119.4253	376	Gravel	15.29	0.8			
18-IAF-078-EPH	47.2394	-119.5839	374	Gravel	15.94	0.63			

2.5.2.2.1 The Ephrata fan

The final incision of ~1400 km^2 of channelized flood gravel at the outlet of Grand Coulee occurred between 16 and 14 ka, according to exposure ages there. The exposure age data do not resolve whether the flood-rinsed boulder gravel of the Ephrata fan formed in a two-stage process of early, large, depositional floods and later, winnowing floods (Waitt et al., 2021, p. 295), or, whether it formed in a single flood that both deposited and winnowed (Baker, 1973, p. 41-42).

2.5.2.2.1.1 Morphology

Floods expanding out of lower Grand Coulee into Quincy Basin deposited bouldery gravel that fines downstream over tens of kilometers to cobbles, pebbles, and sand. Tens of meters of winnowing and channelization (Baker, 1973, p. 41-42) of primary debris-flow like diamict (Waitt et al., 2021, p. 294) occurred under flows that inundated much of the 1400 km^2 fan surface (Bretz et al., 1956, p. 974).

Three channel systems radiate outward from the outlet of Grand Coulee into Quincy Basin. The westernmost system, known as the Ephrata Channel System, is distinct from the other two channel systems of the Ephrata Fan. Its upstream drainage divide between Grand Coulee is significantly higher than divides into the central Rocky Ford Channel and higher than the divide into the easternmost Willow Springs Channel System. A smaller flood would inundate these systems, while leaving the Ephrata Channel System dry. The Ephrata Channel System terminates in a shallow basin that appears to have been backfilled with sediment from the Rocky Ford Channel System. In contrast, the Willow Springs Channel System and the Ephrata Channel System reconnect at their downstream ends, before draining into the Drumheller Channels at the outlet of Quincy Basin. These topographic observations suggest that flooding on the Ephrata

Channel System ended before flooding on the Rocky Ford and Willow Springs Channel Systems (Bretz et al., 1956, p. 974).

The bed-slope of the channel at the upstream end of the fan suggests that the final events to affect the fan were large, depositional floods. The Ephrata fan extends from the outlet of Grand Coulee southward to the Drumheller Channels. At its upstream end near Soap Lake, the surface of the Ephrata Fan has a reverse slope (Bretz et al., 1956, p. 969). If a normal stream were to flow through this area, it would quickly erode a channel that sloped downstream. While the Columbia River likely did flow across this surface during the last glaciation, the reverse slope at the upstream end of the Ephrata Fan suggests that the last events to shape this surface were large floods that buried any downstream-sloping channel that the Columbia River had eroded.

Upstanding remnants separate the three channel systems. These residual landforms are elongated in the direction of flow, have tear-dropped shaping on both their upstream and downstream ends, and slope gently downstream. The remnants are notched on their downstream sides with northward-tapering grooves, indicating the beginning of headward erosion under a flood that covered the entire fan surface (Bretz et al., 1956, p. 974).

2.5.2.2.1.2 Exposure ages

Exposure ages on high surfaces of the Ephrata Fan are slightly older (mean 15.4 ka, n=3) than ages in the most-incised zone in the Rocky Ford channel (mean 15 ka, n=16). The similarity in mean age, and the relatively small number of ages from higher surfaces, suggests that the difference is not significant enough to strongly reject the hypothesis that all boulders in the Ephrata fan were exposed in a single event. However, the pattern of older exposure ages on higher surfaces of the Ephrata fan is also consistent with a two-stage fan formation consisting of

deposition of the fan gravel, and later incision and winnowing of that gravel (Waitt et al., 2021, p. 51). The 400-year magnitude of the age offset between the high elevation samples and the low elevation samples matches the hundreds of years of time during which small, later Missoula floods occurred (Waitt et al., 2021, Fig. 17) and when these floods may have winnowed, and progressively exposed boulders previously buried in the Ephrata fan.

Exposure ages (n=16) on boulders in the Rocky Ford channel form a normal distribution, consistent with exposure in a single event with exposure ages broadened by normally distributed age errors (Fig. 2-17). ^{26}Al ages on the low-elevation Rocky Ford samples cluster more tightly together than their ^{10}Be ages, a result of higher analytical errors during a period of problematic beryllium isotope determination at LLNL. The ^{26}Al ages, and the error-weighted mean combo ages that are strongly weighted towards the ^{26}Al ages, both apparently form normal distributions. This normal age distribution is centered at about 15 ka and extends ~1 ka on both sides of the peak, similar to 2-sigma analytical errors for the individual samples. The similarity in analytical error of individual samples to the width of the age probability distribution suggests that the spread of ages could be entirely due to analytical error. This is consistent with the hypothesis that the boulders were deposited and/or exposed in a single event, with the distribution of apparent ages broadened by analytical error only. If, however, the boulders in Rocky Ford channel were progressively exhumed over multiple events, the expected effect would be to broaden the age distribution and to reduce the density of ages near the peak of the distribution. The higher density of ages towards the peak of the age probability distribution suggests that the boulders in Rocky Ford channel were not progressively exhumed over 1,000's of years. The distribution could be

consistent with a winnowing or exhumation process that was most active around 15 ka, but relatively short, or with a single deposition or exposure event at 15 ka.

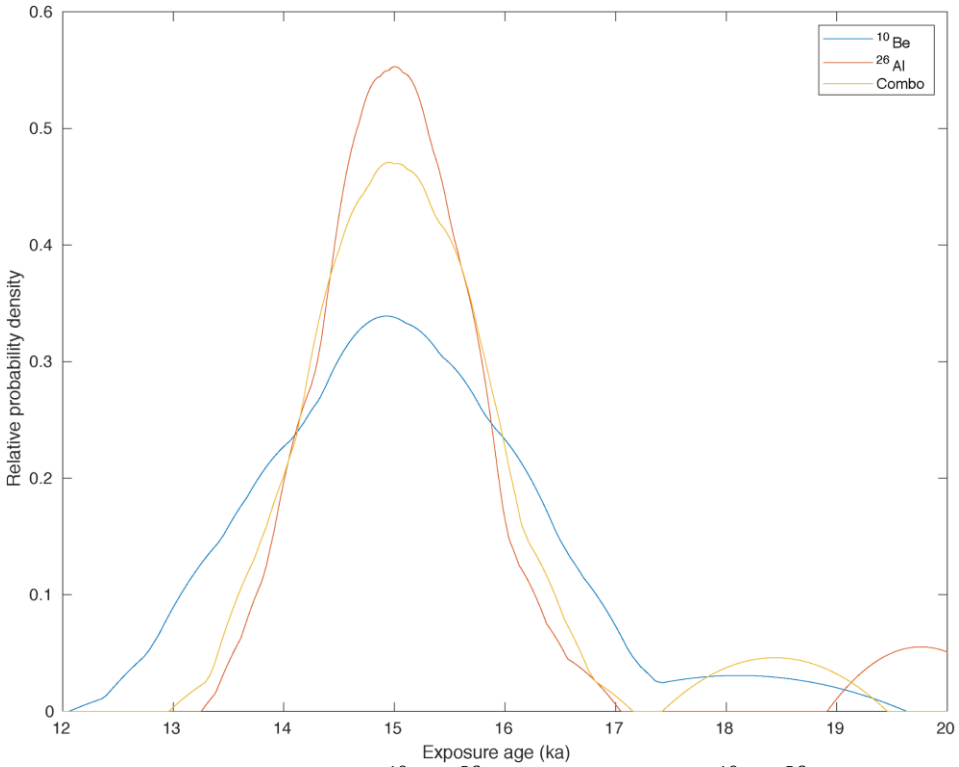

Figure 2-17: Probability distributions of ^{10}Be, ^{26}Al, and combined ^{10}Be-^{26}Al ages for 16 flood-transported boulders in the Rocky Ford channel of the Ephrata fan.

2.5.2.2.2 Upper Grand Coulee

Ages of boulders on the plateau above the east rim of Grand Coulee and boulder ages on a flood bar within upper Grand Coulee both suggest initial Okanogan lobe retreat from Grand Coulee between ~15 and 14.5 ka. Granite boulders on the flood-scoured plateau above the east rim of upper Grand Coulee (Almira plateau) likely relate to Missoula floods synchronous with the Okanogan lobe maximum or to Missoula floods that pre-date final incision of upper Grand Coulee. Two boulders on the Almira plateau date to 14.83 ± 0.48 and 14.85 ± 0.63 ka (n=2). The Paynes Gulch bar in upper Grand Coulee is a flood bar that formed in Missoula floods after the

Okanogan lobe maximum (Atwater, 1987, p. 193). Two boulders from the Paynes Gulch bar date to between 14.5 to 14.9 ka (n=2). Together, the two sites suggest onset of Okanogan lobe retreat between 15 and 14.5 ka.

2.5.2.2.2.1 Almira plateau

Granite boulders on the Almira plateau above Whitney Canyon and near Steamboat Rock might have been deposited directly by ice, if ice crossed Grand Coulee and flowed onto its eastern rim, or they may have been deposited by a megaflood flowing alongside the Okanogan lobe when it occupied upper Grand Coulee. Flood-scoured bedrock and gravel dunes on the Almira plateau provide unambiguous evidence for large floods, but no moraines, striations, or glacial till has yet been identified to suggest that the Okanogan lobe ever advanced onto the Almira plateau. The evidence for large-scale flooding and the absence of evidence for plateau glaciation suggests that the erratic boulders on the Almira plateau were deposited in floods synchronous with Okanogan lobe glaciation of upper Grand Coulee.

Two ages of 14.85 ± 0.63 and 14.83 ± 0.48 ka on Almira plateau boulders fit well with other constraints, while an outlier of 12.3 ± 0.6 is likely a result of post-glacial erosion. These ages suggest that either the Okanogan lobe occupied upper Grand Coulee until around 14.8 ka, or that upper Grand Coulee remained blocked by rock through this time. The two ages on the Almira plateau (mean of 14.84 ka) are ~500 years older than the mean of four ages on glacial boulders that are located around 15 km to the NW on the Waterville plateau (14.34 ka). This pattern suggests that the Okanogan lobe margin retreated northwestward from Grand Coulee towards the northern edge of the Waterville Plateau between ~14.84 and ~14.34 ka, or that late glacial megafloods carved upper Grand Coulee after 14.84 ka.

Table 2-8: Exposure ages relating to upper Grand Coulee floods.

Sample Lab ID	Latitude DD	Longitude DD	Altitude MASL	Substrate	^{10}Be age ka	Err. (2σ ext.)	^{26}Al age ka	Err. (2σ ext.)	Combo age Wtd. mean
Paynes Gulch bar									
16-IAF-050-EBK	47.7715	-119.2121	493	Gravel	14.63	0.6	14.24	0.8	14.5
16-IAF-046-EBK	47.7752	-119.207	497	Gravel	14.7	0.57	15.24	0.82	14.89
Almira plateau									
20-IAF-100-WHI-306	47.8493	-119.1112	695	Bedrock	12.3	0.61			
19-IAF-085-WHI	47.8402	-119.1113	694	Bedrock	14.83	0.48			
19-IAF-084-WHI	47.8403	-119.1125	693	Bedrock	14.85	0.63			

2.5.2.3 Columbia River at Pateros

The boulder gravel of Pateros bar formed after the Okanogan lobe had retreated from the site. Six boulders from Pateros bar range from 11.59 ± 0.71 to 13.85 ± 0.99, younger than ages on Grand Coulee and Moses Coulee floods, consistent with the stratigraphic interpretation that late-glacial megafloods down the Columbia River occurred after floods through Grand and Moses Coulee had ended (Waitt, 1985, p. 1276).

Table 2-9: Surface exposure ages of boulders on Pateros bar, a megaflood-constructed gravel bar inset against the Great Terrace and post-dating deglaciation of the Okanogan lobe.

Sample Lab ID	Latitude DD	Longitude DD	Altitude MASL	Substrate	^{10}Be age ka	Err. (2σ ext.)	^{26}Al age ka	Err. (2σ ext.)	Combo age Wtd. mean
14-IAF-020-PAT	48.0351	-119.8932	272	Gravel	11.59	0.71			
14-IAF-024-PAT	48.0368	-119.8946	274	Gravel	11.97	0.73			
14-IAF-021-PAT	48.0354	-119.8938	275	Gravel	12.35	0.85			
14-IAF-022-PAT-259	48.0358	-119.8940	274	Gravel	13.18	0.57	13.26	0.90	13.46
14-IAF-022-PAT	48.0358	-119.8940	274	Gravel	13.32	1.13			
14-IAF-023-PAT	48.0367	-119.8949	277	Gravel	13.85	0.99			

The boulders of Pateros bar are on a sediment terrace that is the second lowest in a flight of nine terrace levels that span hundreds of feet above the Columbia River. The uppermost terrace level, known as Poverty Flat, is kettled, intermediate levels are not, and the surface of Pateros bar that hosts the boulders also contains an apparent kettle depression. Presence of

kettles on some terrace surfaces suggests that the terraces formed astride a thinning glacier in the Columbia valley that shed ice blocks into ice-marginal lakes or streams to form the kettled surfaces (Waters, 1933, p. 811). This history implies that the low, boulder-dotted terrace level formed after ice had thinned below the level of 900 to 1000 feet. Additionally, the presence of gravel dunes on this terrace suggests that outburst floods either formed or re-worked the deposit (Fig. 2-18). The correspondence between the oldest exposure ages on Pateros bar and the youngest exposure ages on glacial boulders on the NW Waterville Plateau suggests that floods across Pateros bar may have occurred shortly after or during deglaciation of the NW Waterville Plateau (Fig. 2-19).

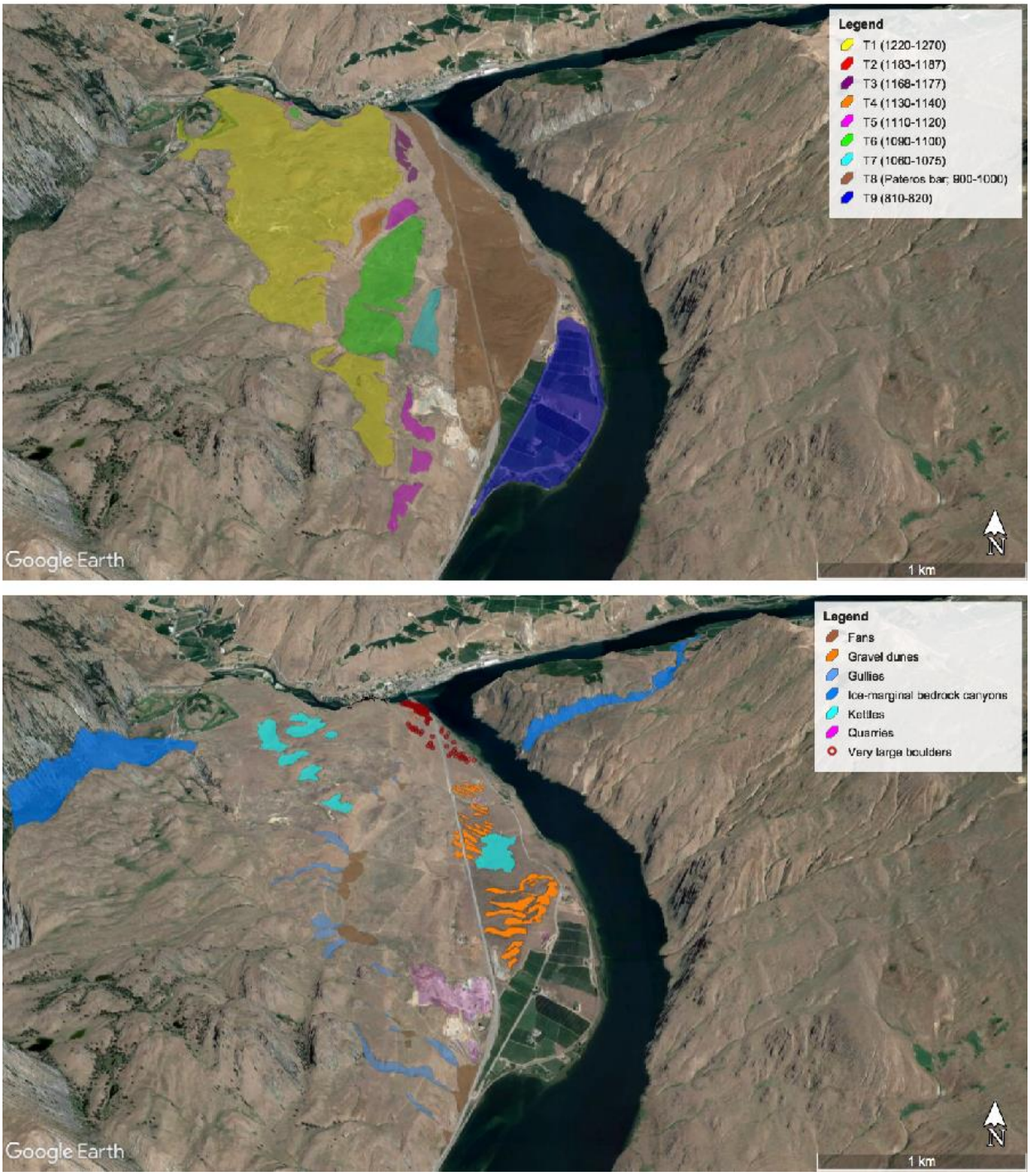

Figure 2-18: Geomorphic map of terrace complex at Columbia-Methow confluence. Oblique aerial view of the terrace complex that includes Pateros bar. Terrain enhanced 3x to highlight geomorphology. Top panel shows nine terrace levels (and their elevations in feet) while bottom panel shows some surficial geomorphology of the terrace complex including dated low-level boulder gravel decorated with gravel dunes.

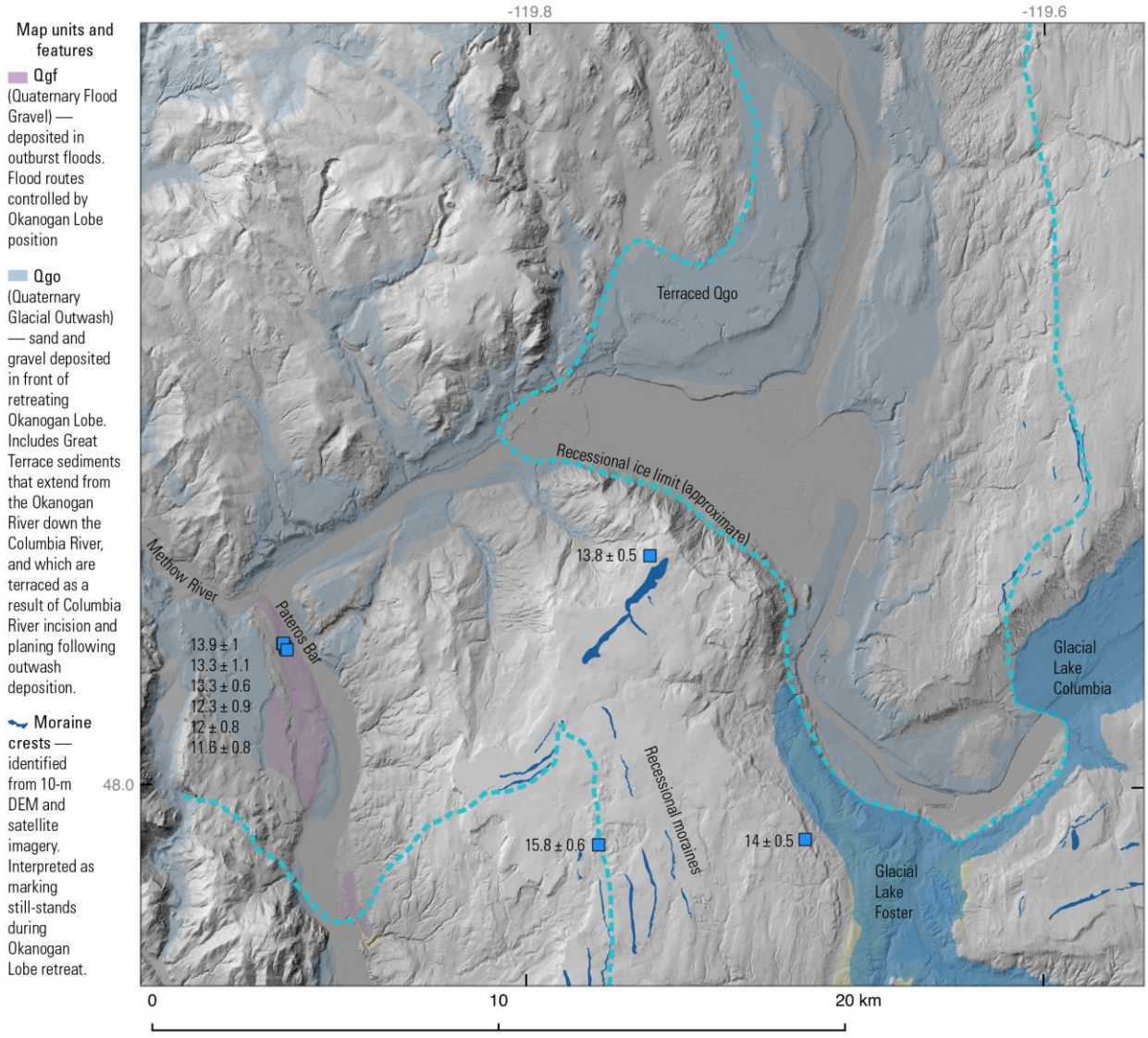

Figure 2-19: Map of deglacial geochronology of floods and glacial retreat at the Okanogan-Columbia confluence, highlighting the correspondence between the oldest exposure ages for Pateros Bar boulders (13.9 ± 1.1 ka and 13.3 ± 1.1 ka) and the deglaciation ages for some boulders on the NW Waterville Plateau (14 ± 0.5 ka and 13.8 ± 0.5 ka).

2.5.3 Inter-laboratory comparison with Balbas et al. (2017)

Balbas et al. (2017) reported surface exposure ages from four of the same sites we studied: the Withrow moraine, Ephrata fan, Pateros bar, and Mattawa fan. This presents the opportunity for an inter-laboratory comparison to see how different field sampling criteria,

laboratory methods, and age-calculation parameters affect exposure age data. Overall, there is good agreement between our exposure ages and those from Balbas et al. (2017).

To compare our ages with those of Balbas et al. (2017), I recalculated their exposure ages using their published isotope concentrations and sample characteristics with the Promontory Point, UW calibration data and LSD scaling calculated through CRONUS v3. Ages are plotted below with 2-sigma internal errors, appropriate for inter-comparison between cosmogenic nuclide ages.

For the Withrow moraine, Balbas obtained one clearly pre-exposed age of 26.2 ± 1.1 ka and four last glacial ages from 12.4 ± 0.8 ka to 15.8 ± 1 ka, overlapping our age of 15.1 ± 0.8 ka.

Balbas et al. (2017) and we both sampled from near the base of the Rocky Ford channel of the Ephrata Fan. Balbas et al. (2017) mainly sampled at a site that is about 10 km downstream and about 15 meters lower than our primary sample site (Fig. 2-20). Balbas dated seven boulders with ages from 13.9 ± 1 to 15 ± 1 ka, whereas we dated 16 boulders with ages from 14 ± 1.2 ka to 18.4 ± 1.6 ka. The mean of our 16 ages is 15.2 ka, or 15 ka ignoring the old outlier at 18.4 ka. The mean of Balbas's seven ages is 14.5 ka. Though our surface exposure ages overlap within error, Balbas trends a little younger, with the mean of Balbas's ages about 500 years younger than the mean of our ages. This offset could be a matter of random chance. A geologic interpretation for the younger ages relates the discrepancy to progressive incision of the Ephrata Fan. Perhaps the lower-elevation samples that Balbas dated at ~345 meters were exposed at a later time than the samples we dated at ~360 meters.

At Pateros Bar, we obtained six ages from 13.9 ± 1 ka to 11.6 ± 0.7 ka, with a group mean of 12.7 ka, while Balbas obtained three ages from 14.3 ± 0.9 ka to 11.8 ± 0.8 ka, with a

group mean of 13 ka. We both sampled this site in the same location. It is notable that we both obtained a wide range of exposure ages for this site, and that ranges span about the same time interval from 14 to 12 ka. Our ages for this site agree within error.

At Mattawa fan, we obtained five ages from 14.6 ± 0.9 ka to 13.5 ± 0.8 ka with a group mean of 14 ka, while Balbas obtained two ages of 13.6 ± 1 ka and 13.3 ± 0.7 ka, with a group mean of 13.5 ka. We both sampled the Mattawa fan in the same area. While we measured three ages that are significantly older than those measured by Balbas, we measured two ages that are almost identical to the ages from Balbas. The spread of over 1,000 years in our ages suggests that the small range of only 300 years between the two ages measured by Balbas under-estimates the true exposure age range of this deposit.

While there are some subtle offsets between the two labs, ages from the same sites overlap with analytical error. For these sites, one or two samples is not enough to capture the geologic complexity in exposure age populations.

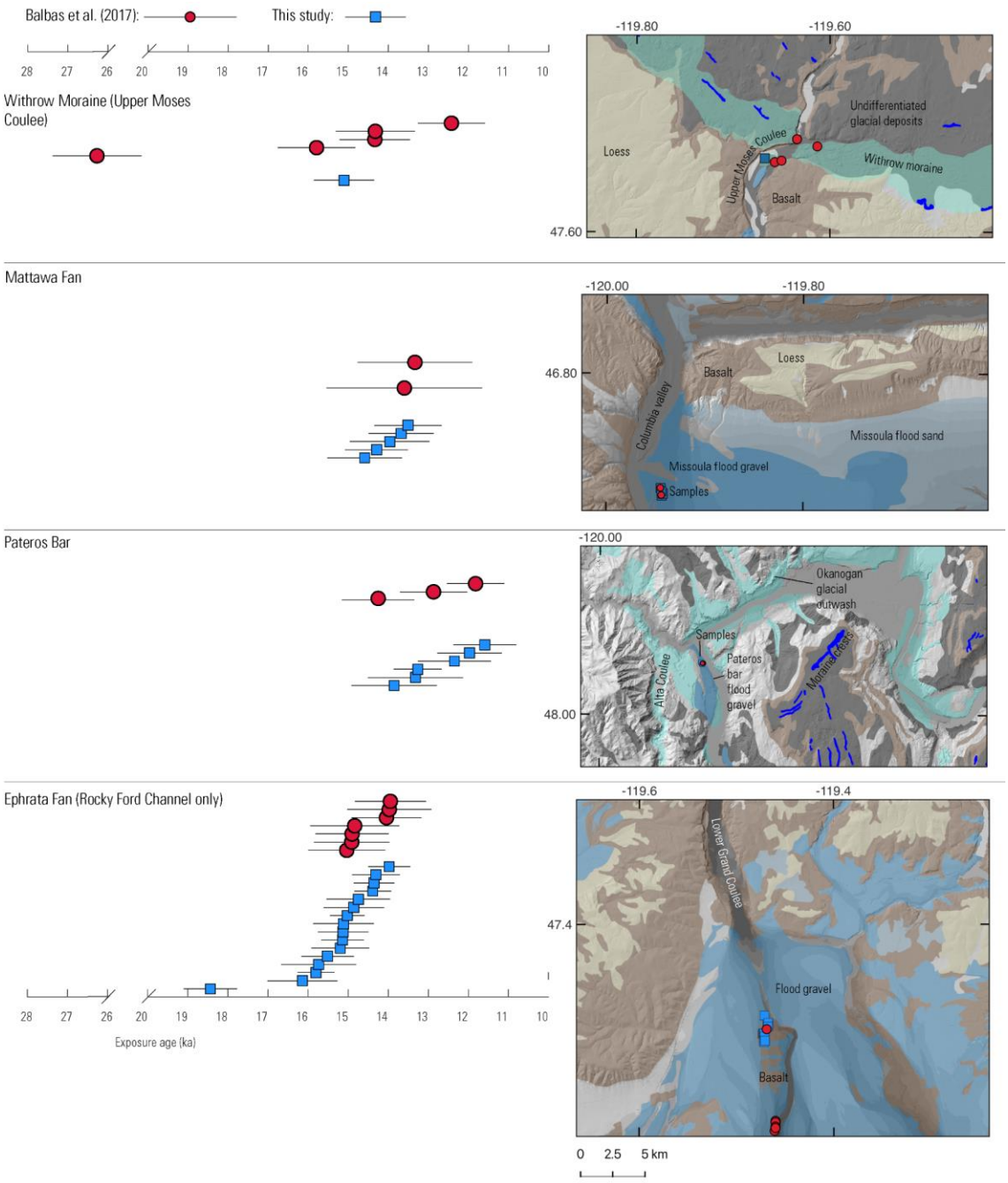

Figure 2-20: Comparison of exposure ages between Balbas et al. (2017) and this study. Vertical axis in the age plot is the relative rank of the age in its group.

2.6 GEOCHRONOLOGY SYNTHESIS

A synthesis of these exposure ages with interlocking time constraints from glacial Lake Columbia stratigraphy, tephrochronology, and other ages highlights points of agreement and discrepancies between time records of the same Okanogan lobe history. The exposure ages suggest Okanogan lobe glaciation might have begun as early as 19 ka, as inferred from only two old ages in Moses Coulee. The exposure ages strongly suggest that Okanogan lobe glaciation ended at around 14 ka, based on internally consistent ages from multiple sites. This 19 to 14 ka history would imply a longer, ~5,000-year duration of Okanogan lobe glaciation than inferred from the <3,000 varves in glacial Lake Columbia. However, this exposure age-inferred duration is potentially an artifact of prior exposure of samples in Moses Coulee, resulting in old age biases. Most exposure ages of floods in routes that were activated by Okanogan lobe glaciation and of Okanogan lobe deglaciation itself group between 16 and 14 ka, consistent with a duration of Okanogan lobe glaciation similar to that recorded in varves.

The exposure ages are internally consistent about the timing of Columbia River re-opening at about 14 ka, but imply a younger re-opening date than the 16 to 15 ka age implied by Mt. St. Helens set S in late glacial Lake Columbia stratigraphy. The set S and Glacial Lake Columbia chronostratigraphy suggests an earlier re-opening of the Columbia River between 16 and 15 ka. One possible resolution to this discrepancy is that the exposure ages are uniformly young, a result that would imply that assumed production rates are too high by ~5%. Another possible resolution to the apparent discrepancy is that inferred correlations between Glacial Lake Columbia strata and our study sites are not accurate.

2.6.1 Advance across the Columbia River

2.6.1.1 Inception of Glacial Lake Columbia

Once the ice margin reached the confluence of the Okanogan Columbia Rivers, an ice-dammed, proglacial lake formed in the Columbia River valley. Formation of glacial lake Columbia occurred between 21 and 16 ka, and likely between 19 and 17 ka (see section 2.2.2.1.2 for complete discussion of chronology).

Interpolation between preglacial radiocarbon dates (Clague et al., 1980) and the formation of glacial Lake Columbia roughly suggests that the ice margin advanced 250 km between ~25 ka, when the upper Okanagan Valley near Shuswap Lake was still ice free, and 19 to 17 ka, when glacial Lake Columbia formed, an advance rate of the ice margin in the Okanogan Valley of 30 to 40 meters per year.

2.6.1.2 Onset of Moses Coulee flooding

It is impossible for Columbia River megafloods to reach Moses Coulee without Okanogan lobe ice blocking the Columbia. Whether the scenario is a Missoula Flood traversing the Waterville Plateau or a subglacial Okanogan lobe flood directly entering Moses Coulee, Okanogan lobe ice must be advanced across the Columbia River for megafloods to enter Moses Coulee. The oldest ages for Moses Coulee floods therefore constrain Okanogan lobe advance. The oldest believable age in our dataset is at 18.8 ± 1 ka (an age at 28 ka is interpreted as pre-exposed and discounted as inconsistent with regional ice age history), suggesting Okanogan lobe formation by this time. However, the presence of prior exposure in the dataset suggests that this older, last-glacial age could be influenced by prior exposure as well.

2.6.1.3 Ice-rafted erratics above Wenatchee

A discrepancy exists between the older of these estimates for Okanogan lobe advance and the inferred age of glacial Lake Columbia formation from a set of ice-rafted erratics above Wenatchee. Here, three erratics embedded in silt on the south slopes of the lower Wenatchee River date from 16.8 ± 0.6 to 17.1 ± 0.8 ka. Note that the absolute ages considered here are about 1,400 years younger than the ages calculated in Balbas et al. (2017), which uses a global production rate calibration and the SA scaling scheme of Lifton et al. (2014). While this difference affects comparisons with radiocarbon ages, it has little effect on relative differences between TCN ages. Regardless of production rate scheme, the apparent ages of the Wenatchee erratics are younger than the ages of two of the Moses Coulee erratics. The Wenatchee erratics are well above the level of downstream sediment dams that impounded lakes at levels up to 275 m. The high elevation of these erratics well above the levels of sediment-dammed lakes in the Columbia valley, and their position well downstream of glaciation in the upper Wenatchee Valley, suggests that the boulders instead arrived in a Missoula Flood that inundated the Columbia River near Wenatchee to a height of at least 440 meters. This depth of flooding is most conceivable before the Okanogan lobe is blocking the Columbia River. When the Okanogan lobe is not across the Columbia River, Missoula Floods drain through only the Cheney-Palouse Tract and the Columbia River. This set of drainage pathways, combined with the largest possible Lake Missoula outburst, is the most favorable way to achieve water inundation up to 440 meters near Wenatchee. When the Okanogan lobe is across the Columbia River, water is blocked from draining through the Great Bend of the Columbia River, and instead flows through the Cheney-Palouse, Telford-Crab Creek, and Grand Coulee tracts. Though this water does eventually re-

coalesce in the Columbia River, water enters the Columbia River well downstream of the Wenatchee Valley, resulting in much lower inundation depths near Wenatchee. Therefore, previous authors have interpreted that high erratics near Wenatchee were deposited in a pre-Okanogan lobe Missoula Flood down the Columbia River (Balbas et al., 2017, p. 584)

2.6.1.4 Discrepancy between Wenatchee and Moses Coulee erratics

Three ages for the high Wenatchee erratics range from 16.8 ± 0.6 to 17.1 ± 0.8 ka, younger than two ages on ice-rafted erratics in Moses Coulee at 18.8 ± 1 ka and 17.4 ± 0.8 ka. The Moses Coulee erratics should be younger than the Wenatchee erratics, because floods can only enter Moses Coulee after the Okanogan lobe has crossed the Columbia River, while floods can only inundate Wenatchee to 440 meters depth before the Okanogan lobe has crossed the Columbia River. The exposure ages are in the opposite of their expected order.

Three remedies for this discrepancy are: (1) the Wenatchee erratics are too young due to exhumation, (2) the Moses Coulee erratics are too old due to pre-exposure, (3) assumptions about flood routing and inundation depths are wrong.

I favor explanation (1) due to the position of the Wenatchee erratics on an erodible silty slope and the visual appearance of the rock surfaces of the Wenatchee erratics compared to the Moses Coulee erratics. The Wenatchee erratics are embedded in a silty slope (Fig. 2-21). Gullies on the slope indicate episodic fluvial erosion has occurred since emplacement of the glacial flood slope cover (Fig. 2-21). Though the erratics are not in the gullies themselves, slopewash across the broad surface in which the erratics are embedded could have eroded the meter or so of silt necessary to exhume the boulders. Consistent with this interpretation, the surfaces of the Wenatchee erratics lack significant lichen or moss, surface coatings that do not grow beneath soil

(Fig. 2-21). Thick lichen cover is a common surface feature of boulders that have been consistently exposed since the last glaciation throughout the Columbia Basin. In contrast, the Moses Coulee erratics are perched on rocky pavements on flat surfaces. On these flat surfaces there is no gravitational potential or water catchment area to generate significant erosion. In addition, there is no evidence of remnant silt deposits in which the boulders could have once been buried. The mossy, lichen-covered surfaces of the Moses Coulee erratics (Fig. 2-21) are consistent with the interpretation that they have been consistently exposed on rocky surfaces since deposition.

However, explanation (2), that the Moses Coulee ages are wrong due to pre-exposure, is also possible. Out of seven ice-rafted erratics dated in Moses Coulee, one is clearly an old outlier whose age of 28.1 ± 1.4 ka is only explainable as a result of pre-exposure. The presence of this pre-exposed rock in the Moses Coulee age population indicates that any rock in Moses Coulee could be affected by isotope inheritance. Nonetheless, it is notable that the pre-exposed rock is an angular quartzite, while the six rocks that give plausible last-glacial ages are all granitic, and the oldest ages come from sub-rounded to rounded granite boulders and cobbles that appear to have been thoroughly shaped by glaciation prior to transport and deposition. Quartzite is more resistant to weathering, more likely to survive multiple generations of glaciation, and thus more likely to contain inherited cosmogenic isotopes. The two granites with ages of 18.8 ± 1 and 17.4 ± 0.8 ka are less likely to suffer from pre-exposure than quartzite.

Explanation (3) for the discrepancy, that assumptions about flood routing and inundation depth are wrong, is also possible. Assumptions behind the interpretation of the Wenatchee erratics as a pre-Okanogan lobe down-Columbia flood are (1) Last glacial lakes in the

Wenatchee Valley, impounded by landslides or megaflood sediment deposits, reached a maximum height of 275 meters, much lower than the elevation of ice-rafted erratics in the Wenatchee Valley. Therefore, the high Wenatchee erratics could not have been emplaced as a result of boulder-bearing icebergs floating to the sample sites in a landslide-dammed lake. (2) Missoula Flood inundation depth near Wenatchee can only reach the heights of 420 to 440 meters when the Great Bend of the Columbia River is open. Therefore, the Wenatchee erratics could not have been emplaced when the Columbia River was blocked by the Okanogan lobe, a scenario in which flow-splitting into multiple Scabland tracts that drain into the Columbia downstream of Wenatchee results in lower inundation depths near Wenatchee. (3) Columbia River megafloods after the Okanogan lobe had retreated from the Columbia River were much smaller than early glacial floods, and too small to create a stage height at Wenatchee to 440 meters. Assumption (1) is supported by the present-day surface elevations of remnants of landforms that blocked the Columbia River downstream of Wenatchee. While it is possible that much higher river-blocking landforms existed during the last glaciation, and that they either have not been recognized or that they have been eroded, there is no evidence for this. Assumption (2) is supported by flood modeling of Denlinger et al. (2021), which achieves the highest flood stages near Wenatchee with an open Columbia River. While the modeled stage height of 455 m in Denlinger et al.'s scenario 2b is above the highest of the dated erratics, it is 35 m lower than the highest observed erratic in Wenatchee Valley at 490 m. This discrepancy led Denlinger et al. (2021) to propose that water from glacial Lake Columbia, if added to a Missoula Flood, might be sufficient to make up the 35 m difference for Wenatchee, though they did not model this scenario. A Missoula Flood augmented with water from glacial Lake Columbia is conceivable

early in the advance of the Okanogan lobe. During the early phase of advance, the height of the Okanogan lobe in the Columbia River would have been lower than the spillway elevation through Grand Coulee. This configuration would allow glacial Lake Columbia to float its ice dam, a drainage option that became impossible once the height of the Okanogan lobe rose above 10/9 the height of the Grand Coulee spillway.

Both the model-field discrepancies of stage heights near Wenatchee, and the geochronology discrepancy between Moses Coulee and Wenatchee erratics, could be resolved if the Wenatchee erratics are not from a pre-Okanogan lobe advance flood, but from an early Okanogan lobe advance Missoula Flood, augmented with water from glacial Lake Columbia, which drained through an incipient Okanogan lobe that was not thick enough to block drainage through the Great Bend of the Columbia River. Given this possibility for the interpretation of the Wenatchee erratics, as well as the potential issue with exhumation resulting in ages that are too young, I do not favor the Wenatchee erratics as a strong constraint on the time of Okanogan lobe advance across the Columbia River.

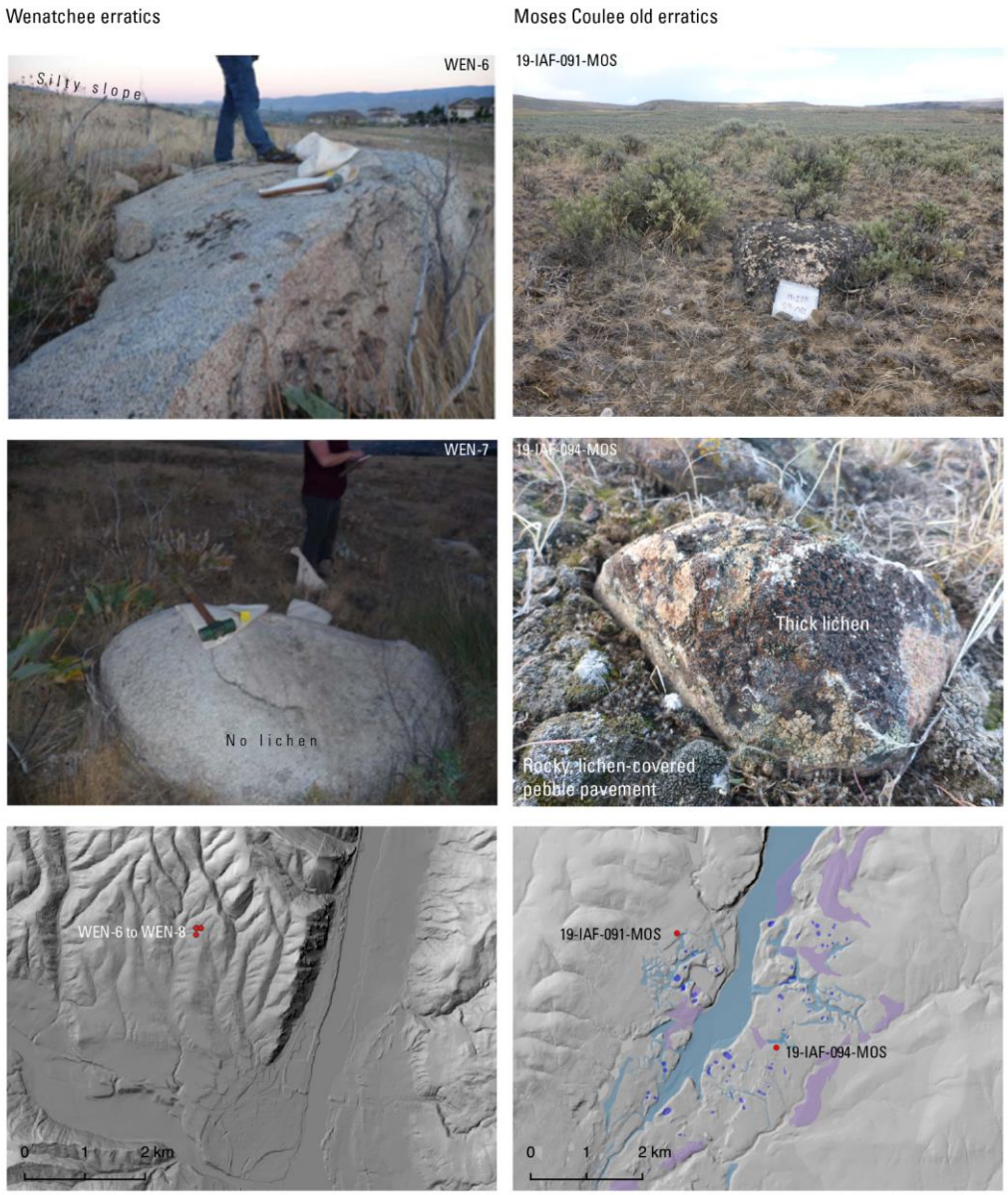

Figure 2-21: Comparison of ice-rafted erratics above Wenatchee with ice-rafted erratics in Moses Coulee. Map panels at bottom show locations of samples on shaded relief maps. Moses Coulee map includes geologic mapping of gravel deposits (lavender), flood-eroded potholes (dark blue), and bedrock channels (light blue).

2.6.1.5 Advance at ~18.5 ka or ~16.5 ka?

Synthesis of relevant geochronology (Fig. 2-22) suggests Okanogan lobe advance across the Columbia River likely between 19 and 17 ka. Advance at about 18.5 ka is consistent with

pre-glacial radiocarbon ages compiled by Clague (1980), with the age earliest age of 18.8 ± 1 ka for Moses Coulee flooding, and with the two older estimates of glacial Lake Columbia formation pinned to set S dated by Mabton shells or to the radiocarbon age on detrital wood, interpreted as fresh wood (Fig 2-23). However, advance at ~18.5 ka is inconsistent with the age of glacial Lake Columbia formation dated from the younger set S age that relies on charcoal ages at Swift Creek, which implies lake formation around 18 ka (Fig. 2-23). The older ~18.5 ka age for Okanogan lobe advance is also inconsistent with a pre-Okanogan lobe flood at ~16.5 ka, as interpreted from apparent exposure ages of Wenatchee erratics (Fig. 2-23).

An advance and formation of glacial Lake Columbia at ~16.5 ka is consistent with the Wenatchee erratics and with the younger age of glacial Lake Columbia formation inferred from the set S ash dated by Swift Creek charcoal, but inconsistent with the oldest geologically plausible age for a Moses Coulee erratic, and with the age of glacial Lake Columbia formation from set S dated by shells at Mabton or detrital wood in glacial Lake Columbia. If the Okanogan lobe did advance across the Columbia River at 16.5 ka, it would imply that the detrital wood was around 1,000 years old when it was deposited in glacial Lake Columbia, that the shells at Mabton are too old by about 700 years, perhaps due to precipitation of calcite from groundwater containing ancient carbon, and that the longest-exposed boulder in Moses Coulee contains inherited isotopes and doesn't accurately represent the time of a megaflood in Moses Coulee.

On the other hand, an advance at 18.5 ka would imply that the boulders above Wenatchee are too young due to the effect of exhumation, or that they represent a post-Okanogan lobe advance flood. An advance at 18.5 ka would also imply that the age of set S determined from

charcoal at Swift Creek is too young and/or that hundreds of varve-years are missing from the composite varve count between the set S ash and the base of the glacial Lake Columbia section.

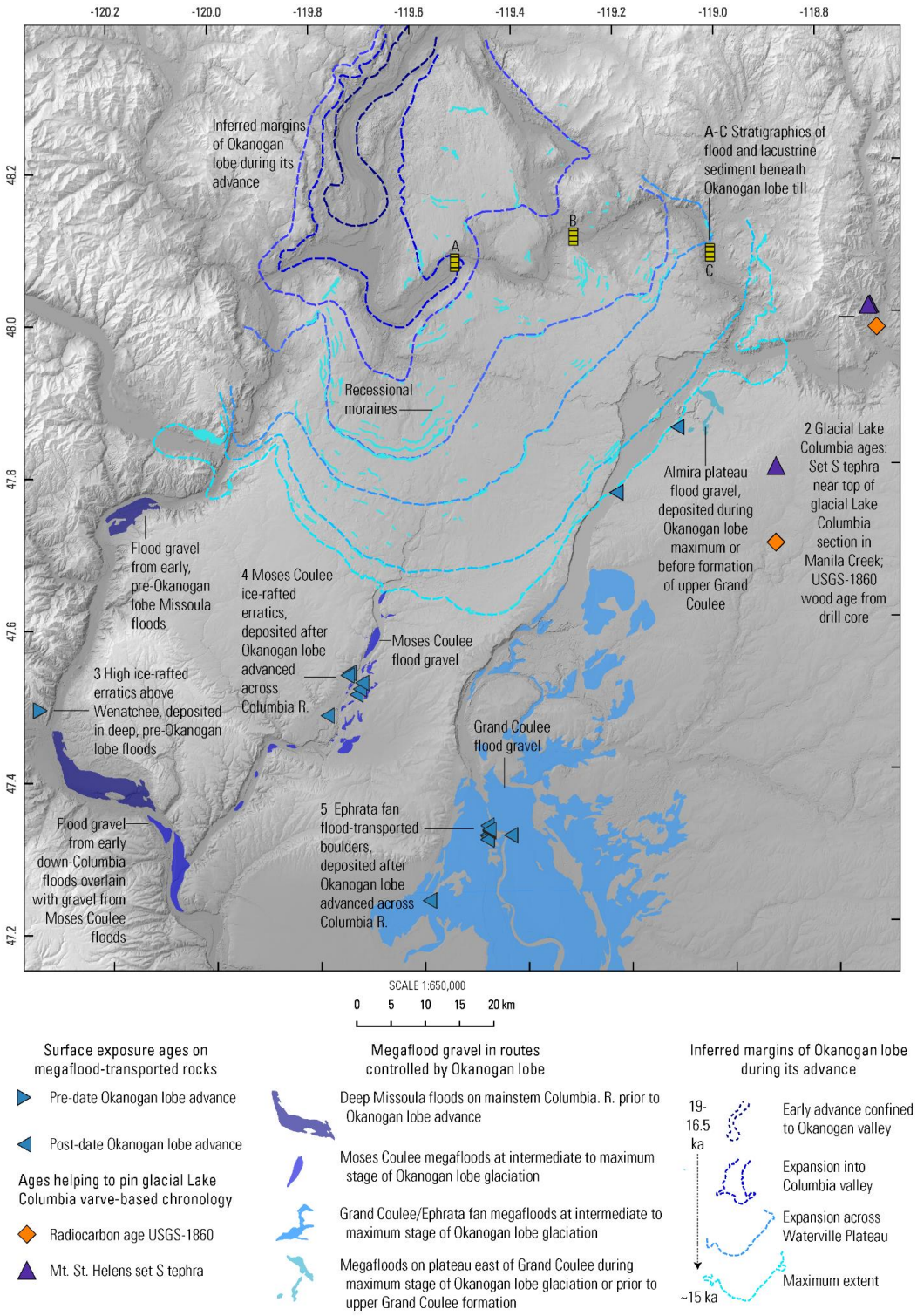

Figure 2-22: Locations of samples used to infer the age of the Okanogan lobe advance across the Columbia River. Numbers on map correspond to numbers on Fig. 2-23.

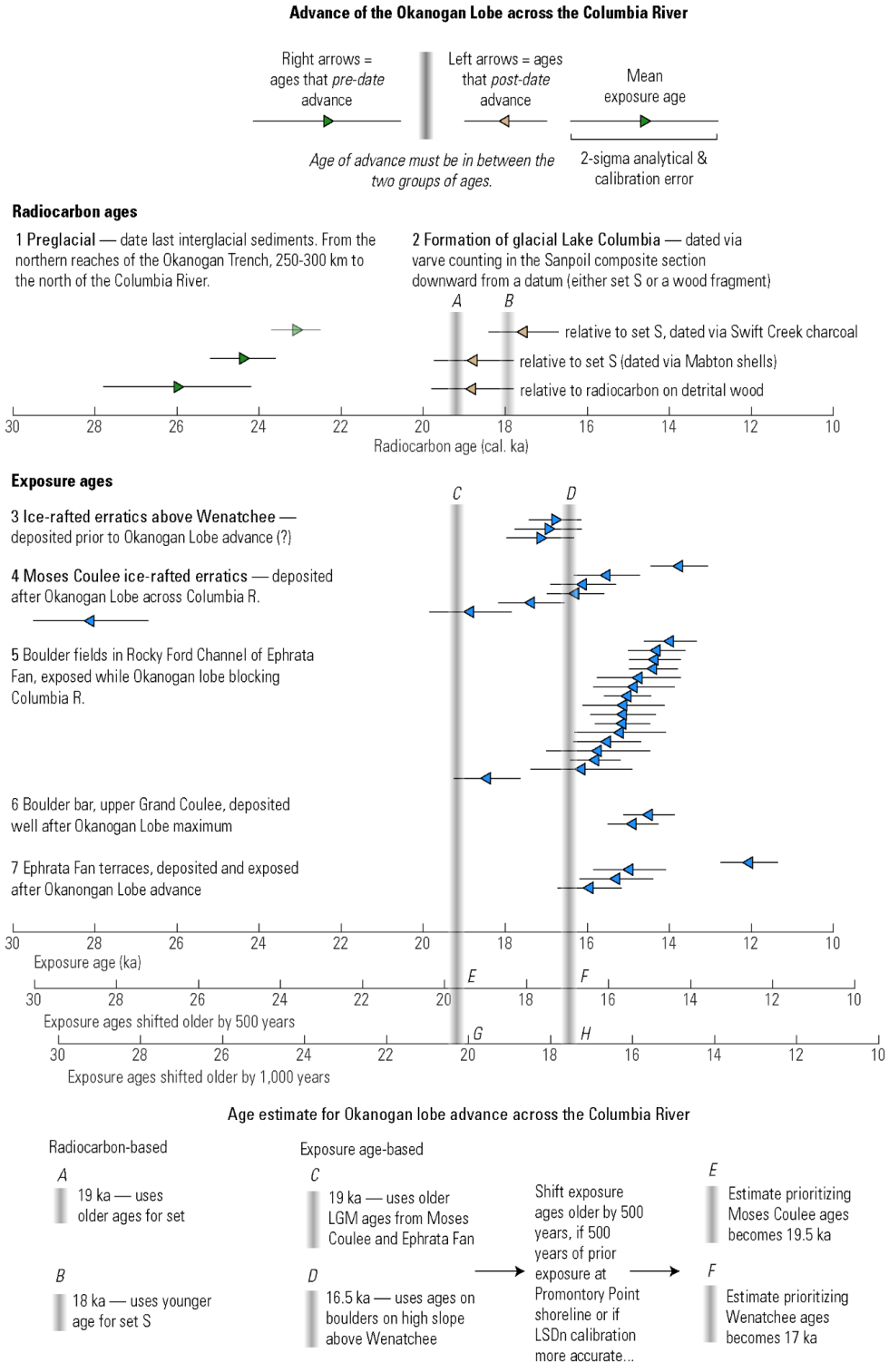

Figure 2-23: Synthesis of relevant geochronology for advance of the Okanogan lobe across the Columbia River.

2.6.2 Maximum extent of Okanogan lobe around 15 to 16 ka

At its maximum extent, the Okanogan lobe reached a latitude of 47.5 °N, extending further south than any lobe of the Cordilleran Ice Sheet other than the Puget lobe, which reached ~46.5 °N. Much of the ice flowing out of the Okanogan Valley spread across the Waterville Plateau forming a lobate, piedmont glacier that would have had a low surface slope (Kovanen and Slaymaker, 2004). To the east of the Waterville Plateau, a small lobe of ice flowed eastward up the Columbia River past Grand Coulee Dam. To the west of the Waterville Plateau, ice flowed down the Columbia River reaching the Chelan valley. Here ice may have merged with Cordilleran ice flowing down the Methow valley and/or the Chelan valley. Glacial trimlines and lateral moraines visible on the south wall of the Chelan valley dip up-valley with a gradient of around 60 m/km, indicating that Okanogan glacial ice, perhaps augmented with ice from the Methow valley, flowed westwards up the Chelan valley. Okanogan ice flowed southward down the Columbia River to a point several kilometers past the mouth of the Chelan valley.

2.6.2.1 Glacial maximum in Grand Coulee

Fluted topography extends to the eastern rim of the Waterville Plateau above Grand Coulee at ~47.8° N (Fig. 2-7) indicating that fast-flowing, wet-based ice reached the edge of the plateau surface above Grand Coulee and implying that ice would have continued flowing off of the plateau and into Grand Coulee. Near this zone of fluting, recessional moraine crests demarcate several ice limits near the eastern edge of the Waterville Plateau above Grand Coulee (Fig. 2-24). These moraine crests are approximately parallel to moraine crests on the summit of Steamboat Rock (Fig. 2-24), suggesting that, during recession, an ice limit extended from the surface of the Waterville Plateau, across Grand Coulee, and across the summit of Steamboat

Rock. It is not clear if these moraines formed at a time when Grand Coulee was eroded to its modern extent, or if they formed on a relatively flat Waterville Plateau surface when Steamboat Rock was contiguous with the Waterville Plateau. These are the easternmost moraine crests of the Okanogan lobe. There are no moraine crests on the Almira plateau, likely because ice-marginal megafloods swept this area clean after or during the time when moraines could have formed there or because moraines never formed there.

Glacial till, and polished, striated bedrock on the floor of Grand Coulee indicate that grounded, Okanogan lobe ice occupied Grand Coulee (Bretz, 1923, p. 603-604). These sites are no further east than Steamboat Rock, so they don't provide any additional information about the extent of glaciation beyond that provided by the moraine crests on Steamboat Rock.

With an ice margin on the surface of Steamboat Rock, ice would have reached the base of the east wall of Grand Coulee. Did the ice completely fill Grand Coulee and advance onto the Almira plateau above the east coulee wall? Evidence for a temporary lake level in glacial Lake Columbia at ~715 m requires that the Grand Coulee outlet of glacial Lake Columbia was completely filled with ice but does not inform on the extent of this high ice level. An apparent ice-marginal channel carved into bedrock at the NW tip of the Almira Plateau at 47.9° N suggests that an ice configuration existed where only the upper few km's of Grand Coulee was completely filled with ice to the top of its eastern wall, diverting outflow from glacial Lake Columbia across the Almira Plateau to form the bedrock channel. At the time this channel formed, the ice surface at the channel outlet must have been lower than the Almira plateau to allow outflow through the bedrock channel.

It is, however, uncertain whether the Okanogan lobe filled Grand Coulee completely and advanced onto the Almira plateau to the east of Grand Coulee, and if so, how far east the ice limit extended.

The Almira plateau is a west-dipping surface above the east rim of Grand Coulee. This surface was once part of the Waterville Plateau but was isolated when Grand Coulee cut through the plateau. The Almira plateau rises from an elevation of 670 meters above Grand Coulee to an elevation of around 800 meters on an unnamed N-S trending ridge. The western edge of the Almira Plateau above Grand Coulee has been stripped of loess cover, leaving a bare basalt surface dotted with mounds of loess. The boundary between bare basalt and loess-covered basalt is clearly visible on satellite imagery as a contact between a dark brown zone and a light-colored patchwork of wheatfields. The elevation of this stripped basaltic surface descends from 750 meters at the north end of the Almira plateau to around 650 meters at the southern end of the Plateau.

It is not clear whether the stripped basalt on the west edge of the Almira plateau formed as a result of megafloods, glaciation, or both. Bretz (1932) contrasted features of the Almira Plateau with those of the Waterville Plateau, noting a lower concentration of erratics, an absence of striated surfaces, an absence of till, and the presence of "more nearly vertical walls of buttes, basins, and channels" on the plateau above the east rim of Grand Coulee. He used the geomorphic contrast between the Almira plateau and the Waterville Plateau to argue that glacial ice of the Okanogan lobe never advanced onto the Almira plateau, and that the stripped basalt surface there formed as a result of megaflood erosion.

Waitt and Thorson (1983) describe the Almira plateau as an "unglaciated eastern upland at the head of the [Grand] coulee" but draw the ice limit across the Almira plateau. Stoffel et al. (1991) also draw an ice limit on the Almira plateau but use a dashed line to express their uncertainty about its location there. Both studies draw the ice limit very close to the rim of Grand Coulee.

During field investigations on the Almira Plateau, we observed clusters of granitic boulders and cobbles that are resting directly on basalt. The clustering of erratics is characteristic of bergmounds, suggesting that megafloods or glacial Lake Columbia overflow brought icebergs across the plateau. However, another possibility for the clusters of granitic boulders and cobbles is direct deposition from glacial ice that occupied the plateau surface for a period of time that was too short to build significant moraines, but long enough to deposit a few erratics and some small piles of glacial sediment.

The geomorphic character of the stripped basalt surfaces on the Almira Plateau indicate that high-energy floodwaters transited the Almira Plateau. For floods to transit this surface, Grand Coulee must be filled with glacial ice or rock. If open, Grand Coulee is able to drain even the largest Missoula Flood (Denlinger et al., 2021) and little to no water flows across the Almira plateau. If Grand Coulee is blocked with ice, water would flow southward across the Almira plateau until reaching the southern limit of ice in Grand Coulee, at which point water would pour off of the plateau and into Grand Coulee.

Ice must have filled Grand Coulee to near or above the height of the east rim everywhere that evidence for megafloods is present on the Almira plateau, or those flood-erosional features must pre-date formation of upper Grand Coulee. The southernmost limit of megaflood evidence

on the Almira plateau occurs at around 47.8° N, directly adjacent to a large boulder bar on the floor of Grand Coulee. Here, the stripped basalt surface is pockmarked with circular potholes, evidence of erosive floodwaters. To the east of these potholes, a series of evenly spaced ridges of sediment are several meters in height, around 80 meters apart, and 100's of meters in length. These ridges are similar in appearance to the mega ripples seen in other Channeled Scabland settings. South of this site, the bare basalt surface extends southward for several miles, but the surface lacks any diagnostic megaflood features.

These observations imply that Grand Coulee was filled with ice up to its east rim from its head at the confluence with the Columbia River, to about 47.8° N near the large boulder bar. This ice configuration is needed to explain the megaflood features on the Almira plateau.

2.6.3 Deglaciation between 16 and 13.5 ka

Numerous exposure ages indicate that Okanogan lobe deglaciation occurred between 16 and 13.5 ka, with most areas on the plateaus becoming ice-free between 15 and 14 ka. This may be somewhat younger than the age for the same history implied from Glacial Lake Columbia stratigraphy and set S.

Exposure ages of glacially transported boulders exposed by the retreating Okanogan lobe, exposure ages of flood-transported boulders in drainages only active during Okanogan lobe glaciation, distribution of Glacier Peak set G/B tephra, and post-glacial radiocarbon ages from bogs in areas upstream of the Okanogan lobe all suggest re-opening of the Columbia River at about 14 ka (Fig. 2-24, 2-26). The large number of recessional moraines on the Waterville Plateau indicate that ice continued flowing to the margin during retreat (Fig. 2-24, 2-12), but their small size compared to the much taller and broader Withrow moraine complex suggests that

deglacial stabilizations of the ice margin were brief. These landforms imply a relatively rapid withdrawal of ice from the Waterville Plateau. This geomorphic interpretation is matched by exposure ages of glacially transported boulders on the Waterville Plateau and on the Omak plateau, which range from 16 to 13.5 ka, cluster between 14.5 and 13.5 ka (Fig. 2-27, Table 2-5), and which exhibit a correlation between age and distance northward along flowlines from the maximum ice margin (Fig. 2-27).

2.6.3.1 Re-opening of the Columbia River

The Okanogan lobe must have retreated to the north of the Columbia River *after* deposition and/or fluvial incision of flood-transported boulders in Moses Coulee, on the Almira plateau, in upper Grand Coulee, and in the Ephrata fan, all sites that require Okanogan lobe damming of the Columbia River to receive appreciable water discharges needed to move or exhume boulders. Exposure ages from these sites range from ~19 to ~12 ka, with the bulk of the ages between 16 and 14 ka (Fig. 2-26). Three outliers younger than 14 ka, one from the Almira plateau, one from a high terrace of the Ephrata fan, and one from Moses Coulee, are all on rocks embedded in sand and silt, consistent with the interpretation that their ages are too young due to exhumation.

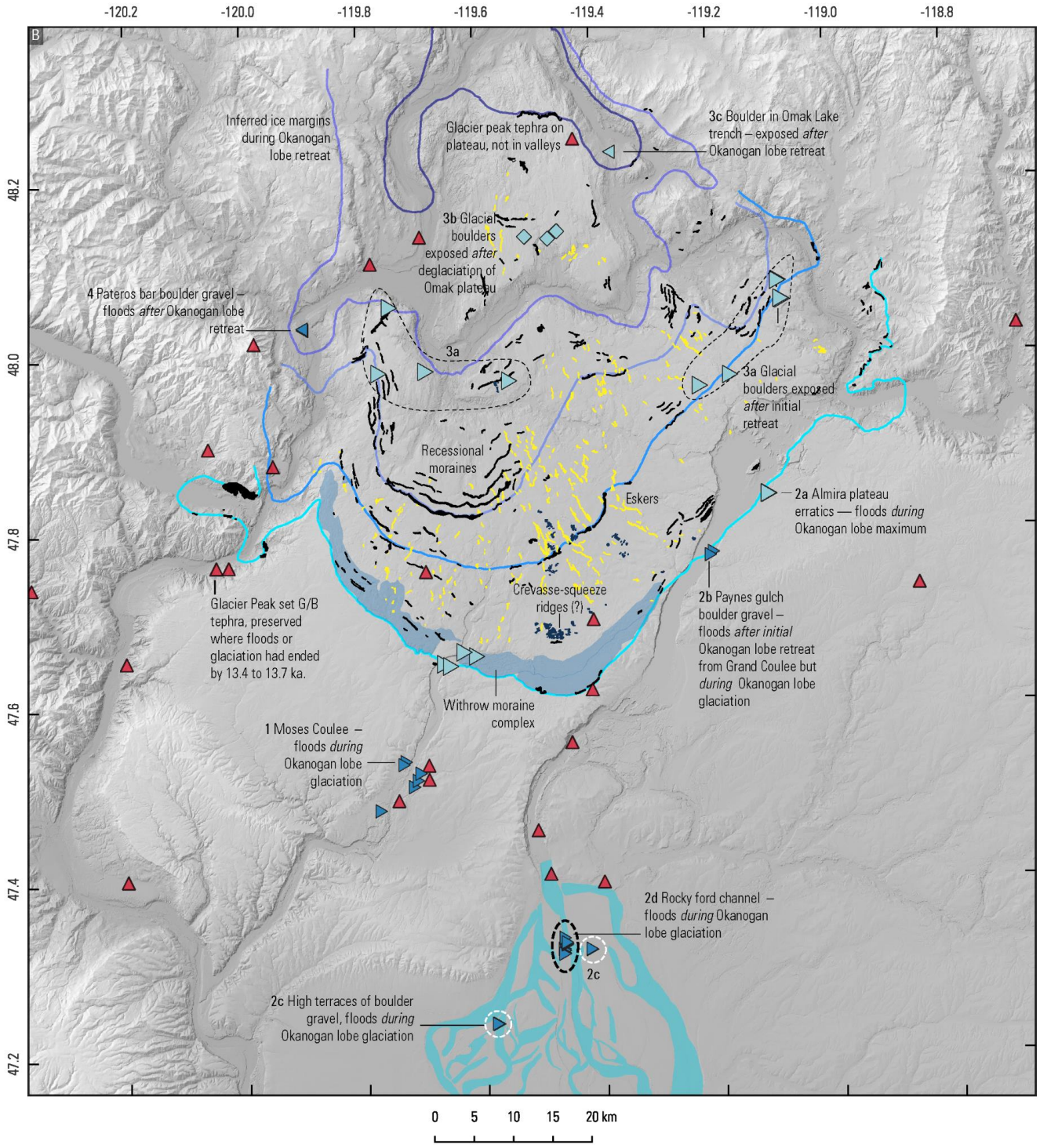

Figure 2-24: Map synthesis of geochronology and geomorphology of Okanogan lobe retreat. Numbers on map correspond to numbers on Fig. 2-26.

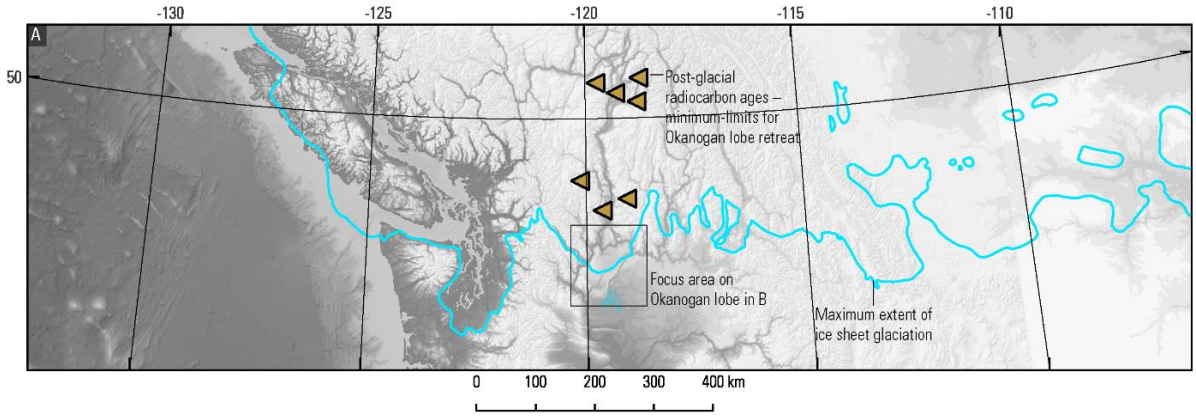

Figure 2-25: Locations of post-glacial radiocarbon ages along the Okanogan valley.

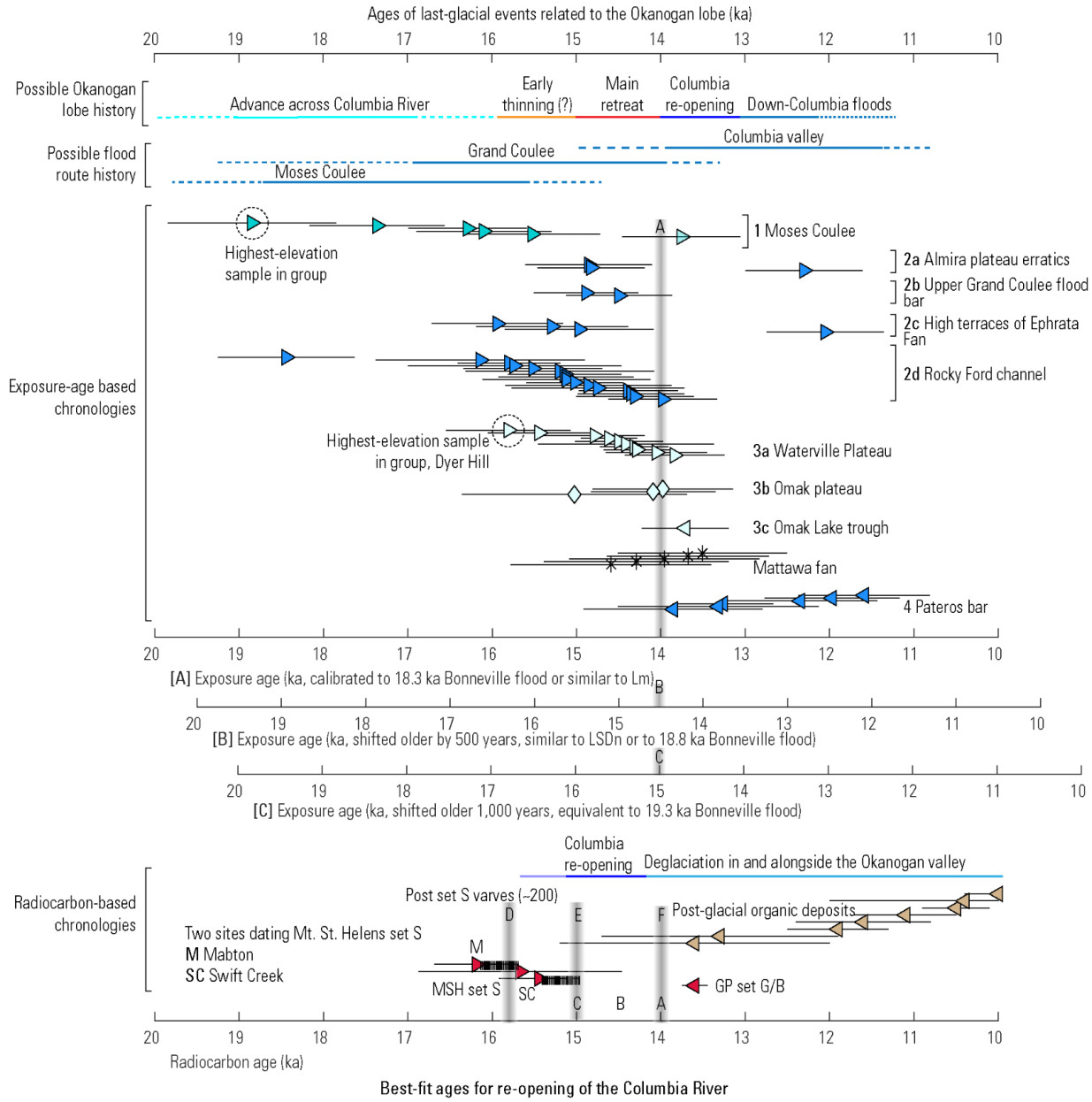

Best-fit ages for re-opening of the Columbia River

A-C [*14 to 15 ka, 14 or 14.5 ka most likely*] – Age scale for A corresponds to our preferred calibration to the 18.3 ka Bonneville Flood and is similar to the Lm global production scheme. Age scale B uniformly shifted older by 500 years, implying an older Bonneville Flood at 18.8 ka or pre-exposure of the wave-cut bench calibration surface for 500 years. Ages similar to ages using the LSDn global production scheme. Age scale for C shifted older by 1,000 years, implying an even older Bonneville Flood at 19.3 ka or 1,000 years of prior exposure of the calibration surface. Age scale C older than commonly-used global production rate schemes.

D-E [*15 to 16 ka*] Draining of glacial Lake Columbia — if GLC outlasted glacial Lake Missoual by several centuries. History based on observations of several hundred GLC varves lacking flood interbeds, inferred to post-date Mt. St. Helens set S (17 to 15 ka)

F [*14 ka*] Inferred from post-glacial radiocarbon ages and distribution of Glacier Peak set G/B (13.4 to 13.7 ka). GP set G/B distribution indicates that the Columbia had re-opened by 13.7 to 13.4 ka, but absence of tephra in lower Okanogan valley and central Omak Lake trench suggests ice margins of Okanogan valley and Omak Lake trench glaciers were 10's of km north of the Columbia at the time of set G/B eruption.

Figure 2-26: Synthesis of Okanogan lobe retreat geochronology and age of re-opening of the Columbia River.

2.6.3.2 Northward propagation of ice margin

Exposure ages on glacial boulders suggest that the Okanogan lobe ice margin progressively retreated northward between 15 and 13.5 ka (Fig. 2-27). Exposure ages in figure 2-27 are plotted against relative distance from the north tip of the Omak plateau to the glacial maximum along a glacial flowline inferred from the mapping of streamlined bedforms to have passed through the sample site (Appendix 1-1A). This framework links the exposure ages to a variable that is likely to explain their pattern.

The exposure ages generally young upstream, consistent with the progressive deglaciation inferred from recessional moraines. Scatter from the trend may be partly explained by isotope inheritance or exhumation and is also related to sample elevations.

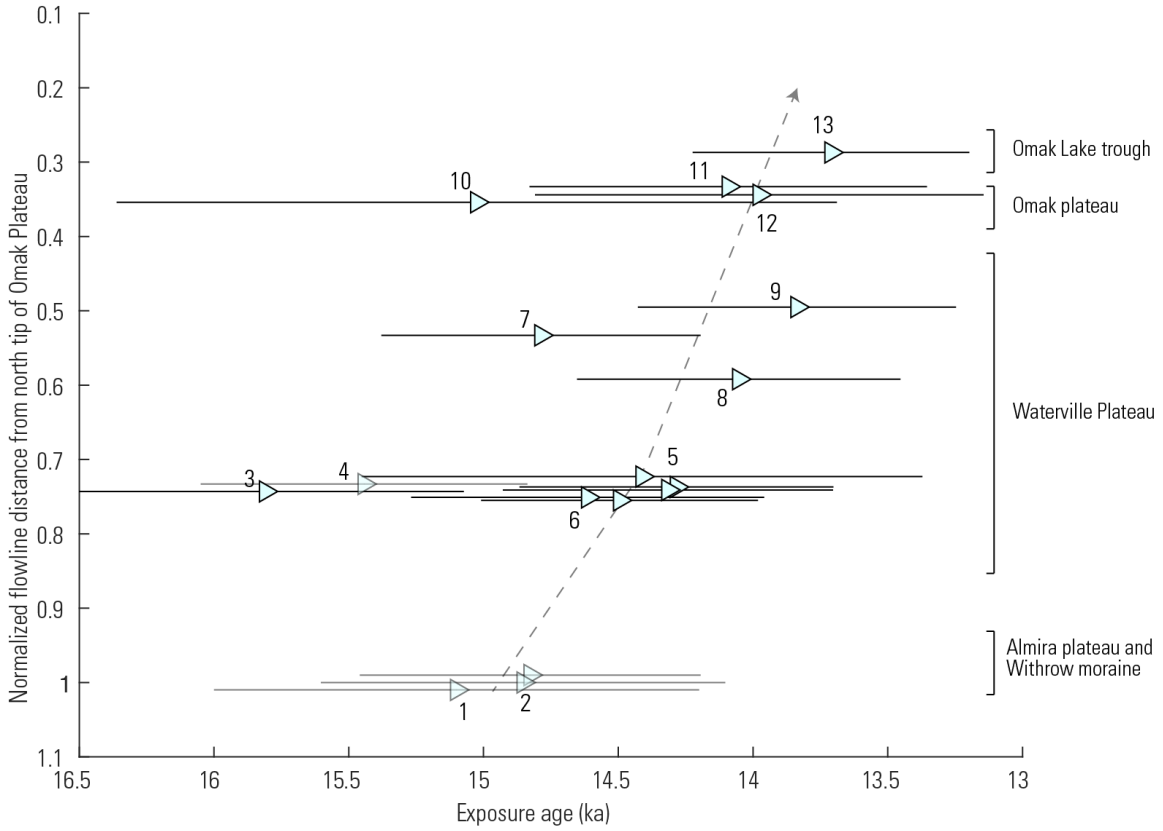

Figure 2-27: Northward retreat of the Okanogan lobe. Exposure ages for boulders exposed by the retreating Okanogan lobe plotted against normalized flowline distance.

2.6.3.3 Thinning history

In addition to implying a northward retreat, the exposure age data suggest that the Okanogan lobe thinned over time between 16 and 14 ka (Fig. 2-28). There is limited topographic relief on the Waterville Plateau, so it is difficult to reconstruct the thickness history of the Okanogan lobe. Exposure ages over the 200-meter range of elevations on the plateau hint at a thinning trend over time. The oldest age on a glacially transported rock within this study comes from the sample from the highest elevation (Fig. 2-16-10), a possible coincidence, or a hint that the ice thinned below 900 m ~16 ka, and possibly prior to reaching its maximum extent. This inference is not robust because it is based on a single sample. However, the possible thinning pattern matches inferences from the distribution of Glacier Peak Set G/B tephra, present on the Waterville and Omak plateaus (Richmond, 1986), but likely absent from the Okanogan (Porter, 1978) and Omak Lake valleys (Nickmann and Leopold, 1985, p. 137). Early thinning at a time of ice margin stability or advance, implied by comparison of the 15.81 ± 0.59 ka age for the highest-elevation, glacially-transported sample in this study (from 892 m at Dyer hill; Fig. 2-16-10) with other ages in the study, is consistent with inferences from other geochronology and geomorphology in other sectors that the CIS may have thinned as ice margins stabilized or advanced (Eyles et al., 2018, p. 110-116, Darvill et al., 2022, p. 7).

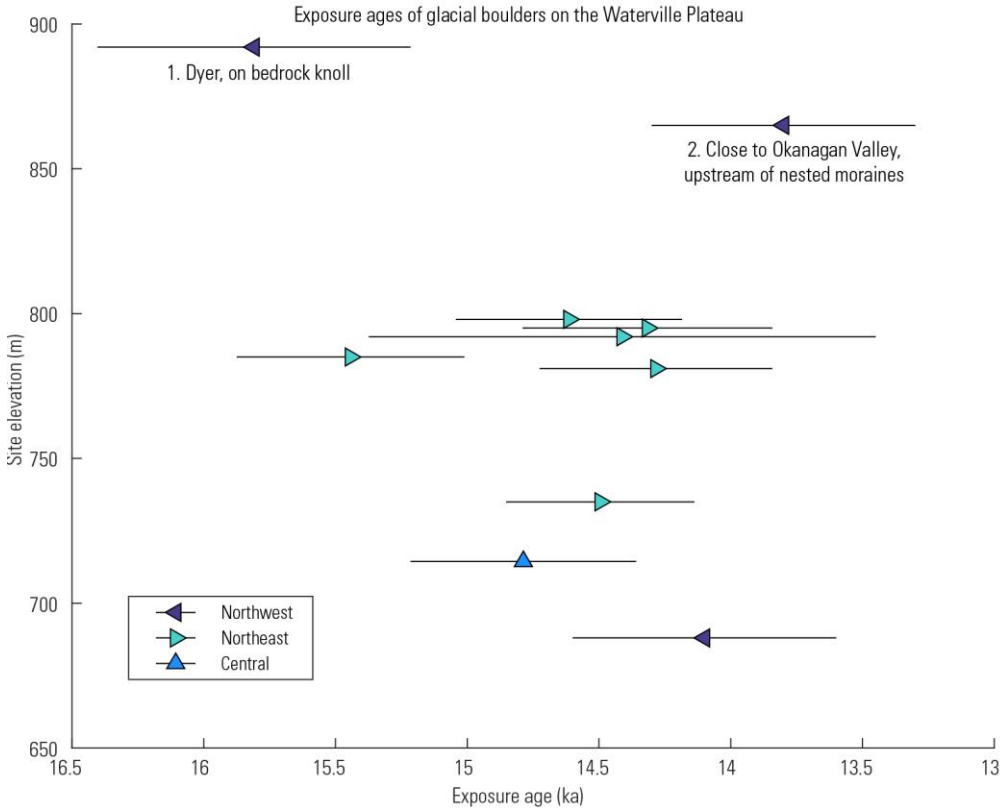

Figure 2-28: Age-elevation pattern of surface-exposure ages of glacially transported rocks on the Waterville and Omak plateaus indicating a weak correlation between higher elevation and older exposure age, potentially indicative of an Okanogan lobe glacier that thinned between 16 and 14 ka.

2.6.4 Discrepancies and similarities between exposure and radiocarbon ages

Individual exposure ages in this study appear discrepant by up to 2,000 years with radiocarbon-pinned chronologies of glacial Lake Columbia. The exposure age data appear to indicate later deglaciation and a later end to the Missoula floods than the stratigraphy of glacial Lake Columbia. The sources of these discrepancies are not clear, and it is also unclear if the discrepancies themselves are statistically significant. The apparent age discrepancies could relate to erroneous correlations between deposits, or to the causes of exposure age dispersion at study sites.

One discrepancy relates to the implied age of Okanogan lobe deglaciation and re-opening of the Columbia River. Glacial Lake Columbia stratigraphies, pinned to dated horizons, imply that the lake disappeared by around 16 to 15 ka, while exposure ages suggest that the Okanogan lobe continued to cover the Waterville Plateau through 14.5 ka and that Pateros bar was not exposed until 14 ka (Fig. 2-29). These exposure age estimates imply a later existence of glacial Lake Columbia than its own stratigraphy. Possible analytical remedies to this discrepancy include shifting exposure ages older, which might imply 500 years of prior exposure on the Promontory Point calibration surface (Fig. 2-29), or an error in scaling the Promontory Point-derived production rate to the Channeled Scabland that resulted in an overestimate of the production rate.

The discrepancies may relate to statistical interpretation. If exposure ages at the Ephrata fan and Pateros bar boulder gravel sites reflect the age of one event, with ages scattered due to random error, then the mean age of the population is the best estimate of that single event. However, if exposure age distributions reflect re-working or incision of boulder gravel in multiple events, then a population mean elides information in the data about multiple events, and the range of ages indicates the duration over which the flood gravel was active.

In the case of the Ephrata fan, there are a significant number of exposure ages younger than 14.5 ka (Table 2-7; Fig. 2-26), a possible discrepancy with the age of the last Missoula flood recorded in glacial Lake Columbia stratigraphy. However, whether this is a discrepancy hinges on both the correlation between the Ephrata fan and floods beds in glacial Lake Columbia and on the reasons for scatter in the Ephrata fan exposure age data. The young exposure ages that appear discrepant comprise the young shoulder of an age distribution that is close to normal (Fig. 2-17),

and that is consistent with a single event that exposed all boulders in the group at 15 ka, with the age dispersion the result of randomly distributed prior exposure, exhumation, and erosion. If this is an accurate explanation of the data, the implication would be that the last boulder-moving flood crossed the Ephrata fan at about 15 ka. This age is nearly consistent with the age for the last Missoula floods in Glacial Lake Columbia, pinned to set S dated via Swift Creek charcoal. If, however, the boulders in the Ephrata fan were moved over many floods that progressively abraded and exposed surfaces, a process implied by stratigraphic evidence for repeating Missoula floods, then the youngest ages in the population might relate to a younger set of boulder-moving events, rather than to random errors in a single-event distribution. In this case, remedying the discrepancy might require shifting exposure ages older via adjustment to production rate calculations, or inferring that exposure of the Ephrata fan boulders is not coincident with the latest Missoula floods.

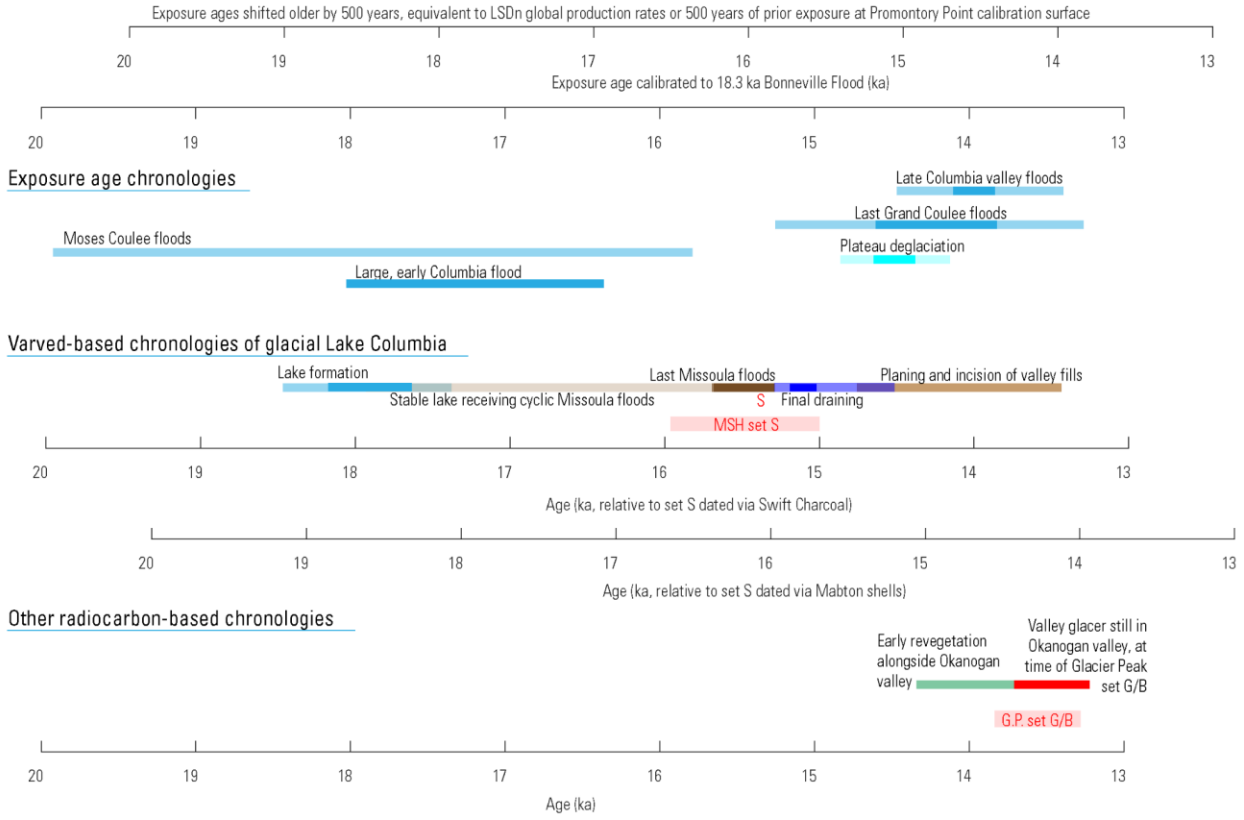

Figure 2-29: Possible chronologies of the Okanogan lobe and glacial Lake Columbia implied from exposure age chronologies, and from glacial Lake Columbia chronostratigraphy and other radiocarbon-based chronologies.

2.7 CONCLUSION

Histories of Okanogan lobe glaciation and Channeled Scabland flooding inferred from exposure ages, radiocarbon ages, and varves differ by several thousand years, beyond the range of analytic uncertainties on age determinations. Discrepancies might be resolved via a better age for the set S marker ash, greater certainty in cosmogenic nuclide production rates in the region, and improved understanding of the relationships between disparate lacustrine, flood, and glacial deposits from throughout the system. A generalized chronology that honors most of the available

geochronology is Okanogan lobe advance around 19 to 17 ka, maximum between 17 and 15 ka, and retreat between 15 and 13 ka.

2.8 References

Arnold, H., and Hickin, A.S., 2016, Using derived-stereo imagery to map macroscale ice-flow features: Geological Fieldwork, p. 2017–1.

Atwater, B.F., 1986, Pleistocene glacial-lake deposits of the Sanpoil River valley, northeastern Washington: U.S. Geological Survey Bulletin 1661, 39 p., doi:10.3133/b1661.

Atwater, B.F., 1987, Status of glacial Lake Columbia during the last floods from glacial Lake Missoula: Quaternary Research, v. 27, p. 182–201, doi:10.1016/0033-5894(87)90076-7.

Baker, V.R., 1973, Paleohydrology and Sedimentology of Lake Missoula Flooding in Eastern Washington:, doi:10.1130/SPE144.

Baker, V.R., and Bunker, R.C., 1985, Cataclysmic late Pleistocene flooding from glacial Lake Missoula: A review: Quaternary Science Reviews, v. 4, p. 1–41, doi:10.1016/0277-3791(85)90027-7.

Balbas, A.M., Barth, A.M., Clark, P.U., Clark, J., Caffee, M., O'Connor, J., Baker, V.R., Konrad, K., and Bjornstad, B., 2017, 10Be dating of late Pleistocene megafloods and Cordilleran Ice Sheet retreat in the northwestern United States: Geology, v. 45, p. 583–586, doi:10.1130/G38956.1.

Bandow, J., 2001, Possible limiting age for soil mounds in the Kittitas Valley, Washington [Undergraduate Thesis]: Central Washington University, https://www.cwu.edu/geography/sites/cts.cwu.edu.geography/files/limiting%20age%20soil%20mounds001.pdf.

Benito, G., and O'Connor, J.E., 2003, Number and size of last-glacial Missoula floods in the Columbia River valley between the Pasco Basin, Washington, and Portland,

Oregon: GSA Bulletin, v. 115, p. 624–638, doi:10.1130/0016-7606(2003)115<0624:NASOLM>2.0.CO;2.

Bjornstad, B.N., 2014, Ice-rafted erratics and bergmounds from Pleistocene outburst floods, Rattlesnake Mountain, Washington, USA: E&G Quaternary Science Journal, v. 63, p. 44–59, doi:10.3285/eg.63.1.03.

Booth, D.B., Troost, K.G., Clague, J.J., and Waitt, R.B., 2003, The Cordilleran ice sheet: Developments in Quaternary Sciences, v. 1, p. 17–43, doi:10.1016/S1571-0866(03)01002-9.

Bretz, J.H., 1923a, Glacial drainage on the Columbia Plateau: Bulletin of the Geological Society of America, v. 34, p. 573–608, doi:10.1130/GSAB-34-573.

Bretz, J.H., 1923b, The channeled scablands of the Columbia Plateau: Journal of Geology, v. 31, p. 617–649, doi:10.1086/623053.

Bretz, J.H., 1932, The Grand Coulee: American Geographical Society Special Publication 15, 89 p., https://hdl.handle.net/2027/mdp.39015035583924.

Bretz, J.H., Smith, H.T.U., and Neff, G.E., 1956, Channeled Scabland of Washington: new data and interpretations: GSA Bulletin, v. 67, p. 957–1049, doi:10.1130/0016-7606(1956)67[957:CSOWND]2.0.CO;2.

Brock, F., and Higham, T., 2009, AMS radiocarbon dating of Paleolithic-aged charcoal from Europe and the Mediterranean Rim using ABOx-SC: Radiocarbon, v. 51, p. 839–846, doi:10.1017/S0033822200056149.

Chambers, R.L., 1971, Sedimentation in glacial lake Missoula [Master's Thesis], https://scholarworks.umt.edu/cgi/viewcontent.cgi?article=8126&context=etd.

Clague, J.J., Armstrong, J.E., and Mathews, W.H., 1980, Advance of the late Wisconsin Cordilleran Ice Sheet in southern British Columbia since 22,000 yr BP: Quaternary Research, v. 13, p. 322–326, doi:10.1016/0033-5894(80)90060-5.

Clynne, M.A., Calvert, A.T., Wolfe, E.W., Evarts, R.C., Fleck, R.J., and Lanphere, M.A., 2008, The Pleistocene eruptive history of Mount St. Helens, Washington, from

300,000 to 12,800 years before present, *in* Sherrod, D.R., Scott, W.E., and Stauffer, P.H. eds., A volcano rekindled: The renewed eruption of Mount St. Helens, 2004–2006, Reston, VA, v. U.S. Geological Survey Professional Paper 1750, p. 593–627, doi:10.3133/pp175028.

Denlinger, R.P., George, D.L., Cannon, C.M., O'Connor, J.E., and Waitt, R.B., 2021, Diverse cataclysmic floods from Pleistocene glacial Lake Missoula, *in* Waitt, R.B., Thackray, G.D., and Gillespie, A.R. eds., Untangling the Quaternary Period—A legacy of Stephen C. Porter, Geological Society of America Special Paper 548, doi:10.1130/2021.2548(17).

Dulfer, H.E., Margold, M., Darvill, C.M., and Stroeven, A.P., 2022, Reconstructing the advance and retreat dynamics of the central sector of the last Cordilleran Ice Sheet: Quaternary Science Reviews, v. 284, p. 107465, doi:10.1016/j.quascirev.2022.107465.

Dyck, W., Fyles, J.G., and Blake, W., 1965, Geological Survey of Canada Radiocarbon Dates IV: Radiocarbon, v. 7, p. 24–46, doi:10.1017/S0033822200037061.

Dyke, A., and Prest, V., 1987, Late Wisconsinan and Holocene history of the Laurentide ice sheet: Géographie physique et Quaternaire, v. 41, p. 237–263, doi:10.7202/032681ar.

Evans, D.J., Storrar, R.D., and Rea, B.R., 2016, Crevasse-squeeze ridge corridors: diagnostic features of late-stage palaeo-ice stream activity: Geomorphology, v. 258, p. 40–50, doi:10.1016/j.geomorph.2016.01.017.

Eyles, N., Moreno, L.A., and Sookhan, S., 2018, Ice streams of the late Wisconsin Cordilleran ice sheet in western North America: Quaternary Science Reviews, v. 179, p. 87–122, doi:10.1016/j.quascirev.2017.10.027.

Flint, R.F., 1935, Glacial features of the southern Okanogan region: Geological Society of America Bulletin, v. 46, p. 169–194, doi:10.1130/GSAB-46-169.

Flint, R.F., and Irwin, W.H., 1939, Glacial geology of Grand Coulee Dam, Washington: Geological Society of America Bulletin, v. 50, p. 661–680, doi:10.1130/GSAB-50-661.

Fryxell, R., 1965, Mazama and Glacier Peak volcanic ash layers - relative ages: Science, v. 147, p. 1288-, doi:10.1126/science.147.3663.1288.

Gomez, N., Gregoire, L.J., Mitrovica, J.X., and Payne, A.J., 2015, Laurentide-Cordilleran Ice Sheet saddle collapse as a contribution to meltwater pulse 1A: Geophysical Research Letters, v. 42, p. 3954–3962, doi:10.1002/2015GL063960.

Gough, Stan., 1995, Description and interpretation of late quaternary sediments in the Rocky Reach of the Columbia River Valley, Douglas County, Washington: Eastern Washington University.

Gregoire, L.J., Payne, A.J., and Valdes, P.J., 2012, Deglacial rapid sea level rises caused by ice-sheet saddle collapses: Nature, v. 487, p. 219–222, doi:10.1038/nature11257.

Hanson, M.A., 2013, Sedimentological and paleomagnetic study of glacial Lake Missoula lacustrine and flood sediment: Simon Fraser University, 217 p., http://summit.sfu.ca/item/12949.

Hanson, L.G., 1970, The origin and development of Moses Coulee and other scabland features on the Waterville Plateau, Washington: University of Washington, https://www.proquest.com/openview/d1f4ec1ed1e7958503c42e788b365f59/1?pq-origsite=gscholar&cbl=18750&diss=y.

Haugerud, R.A., 2021, Deglaciation of the Puget Lowland, Washington:, doi:10.1130/2020.2548(14).

Hendy, I.L., and Cosma, T., 2008, Vulnerability of the Cordilleran Ice Sheet to iceberg calving during late Quaternary rapid climate change events: Paleoceanography, v. 23, doi:10.1029/2008PA001606.

Hibbert, D.M., 1985, Quaternary geology and the history of the landscape along the Columbia between Chief Joseph and Grand Coulee dams, *in* Campbell, S.K. ed., Summary of Results, Chief Joseph Dam Cultural Resources Project, Washington, Office of Public Archaeology, Institute for Environmental Studies, University of Washington, p. 85–111, https://apps.dtic.mil/sti/pdfs/ADA166700.pdf.

Hyde, J.H., 1975, Upper Pleistocene pyroclastic-flow deposits and lahars south of Mount St. Helens Volcano, Washington: U.S. Geological Survey Bulletin 1383-B, 20 p., doi:10.3133/b1383B.

Jackson, L., Ward, B., Duk-Rodkin, A., and Hughes, O., 1991, The last Cordilleran ice sheet in southern Yukon Territory: Géographie physique et Quaternaire, v. 45, p. 341–354, doi:10.7202/032880ar.

Keszthelyi, L.P., Baker, V.R., Jaeger, W.L., Gaylord, D.R., Bjornstad, B.N., Greenbaum, N., Self, S., Thordarson, T., Porat, N., and Zreda, M.G., 2009, Floods of water and lava in the Columbia River Basin: Analogs for Mars: Field Guides, v. 15, p. 845–874, doi:10.1130/2009.fld015(34).

Kovanen, D.J., and Slaymaker, O., 2004, Glacial imprints of the Okanogan Lobe, southern margin of the Cordilleran Ice Sheet: Journal of Quaternary Science, v. 19, p. 547–565, doi:10.1002/jqs.855.

Kuehn, S.C., Froese, D.G., Carrara, P.E., Foit, F.F., Jr., Pearce, N.J.G., and Rotheisler, P., 2009, Major- and trace-element characterization, expanded distribution, and a new chronology for the latest Pleistocene Glacier Peak tephras in western North America: Quaternary Research, v. 71, p. 201–216, doi:10.1016/j.yqres.2008.11.003.

Lamsters, K., Vītola, Z., Karušs, J., and Džeriņš, P., 2021, Evidence of ice streaming and ice tongue shutdown in western Latvia: revealed from the mapping of crevasse-squeeze ridges.: Baltica, v. 33.

Last, G.V., and Rittenour, T.M., 2021, Chronology of Missoula Flood Deposits at the Coyote Canyon Mammoth Site, Washington State, USA: Quaternary, v. 4, p. 20, doi:10.3390/quat4030020.

Lifton, N., Caffee, M., Finkel, R., Marrero, S., Nishiizumi, K., Phillips, F.M., Goehring, B., Gosse, J., Stone, J., and Schaefer, J., 2015, In situ cosmogenic nuclide production rate calibration for the CRONUS-Earth project from Lake Bonneville, Utah, shoreline features: Quaternary Geochronology, v. 26, p. 56–69, doi:10.1016/j.quageo.2014.11.002.

Lifton, N.A., Jull, A.T., and Quade, J., 2001, A new extraction technique and production rate estimate for in situ cosmogenic 14C in quartz: Geochimica et Cosmochimica Acta, v. 65, p. 1953–1969, doi:10.1016/S0016-7037(01)00566-X.

Lifton, N., Sato, T., and Dunai, T.J., 2014, Scaling in situ cosmogenic nuclide production rates using analytical approximations to atmospheric cosmic-ray fluxes: Earth and Planetary Science Letters, v. 386, p. 149–160, doi:10.1016/j.epsl.2013.10.052.

Lillquist, K., Lundblad, S., and Barton, B.R., 2005, The Moxee City (Washington) mammoth: morphostratigraphic, taphonomic, and taxonomic considerations: Western North American Naturalist, v. 65, p. 417–428.

Lowdon, J., and Blake, W., 1970, Geological Survey of Canada radiocarbon dates IX: Radiocarbon, v. 12, p. 46–86, doi:10.1017/S0033822200036213.

Lowdon, J., Fyles, J.G., and Blake, W., 1967, Geological Survey of Canada radiocarbon dates VI: Radiocarbon, v. 9, p. 156–197, doi:10.1017/S0033822200000503.

Mack, R.N., Rutter, N., and Valastro, S., 1979, Holocene vegetation history of the Okanogan Valley, Washington: Quaternary Research, v. 12, p. 212–225, doi:10.1016/0033-5894(79)90058-9.

Margold, M., Jansson, K.N., Kleman, J., Stroeven, A.P., and Clague, J.J., 2013, Retreat pattern of the Cordilleran Ice Sheet in central British Columbia at the end of the last glaciation reconstructed from glacial meltwater landforms: Boreas, v. 42, p. 830–847, doi:10.1111/bor.12007.

McGee, D., Quade, J., Edwards, R.L., Broecker, W.S., Cheng, H., Reiners, P.W., and Evenson, N., 2012, Lacustrine cave carbonates: Novel archives of paleohydrologic change in the Bonneville Basin (Utah, USA): Earth and Planetary Science Letters, v. 351, p. 182–194, doi:10.1016/j.epsl.2012.07.019.

Moody, U.L., 1987, Late Quaternary stratigraphy of the Channeled Scabland and adjacent areas: University of Idaho, 419 p., https://www.proquest.com/dissertations-theses/late-quaternary-stratigraphy-channeled-scabland/docview/303588763/se-2.

Mullineaux, D.R., Wilcox, R.E., Ebaugh, W.F., Fryxell, R., and Rubin, M., 1978, Age of the last major scabland flood of the Columbia Plateau in eastern Washington: Quaternary Research, v. 10, p. 171–180, doi:10.1016/0033-5894(78)90099-6.

Myers, E., and Lillquist, K., 2018, The Age and Origin of Soil Mounds on Manastash Ridge in Kittitas County, Washington, https://www.cwu.edu/geography/sites/cts.cwu.edu.geography/files/documents/Myers.%202019.%20The%20age%20and%20origin%20of%20Soil%20Mounds%20on%20Manastash%20Ridge%20Final.pdf.

Nickmann, R., Leopold, E., and Campbell, S., 1985, A postglacial pollen record from Goose Lake, Okanogan County, Washington: evidence for an early Holocene cooling, *in* Summary of results, Chief Joseph Dam Cultural Resources Project. Edited by SK Campbell. University of Washington, Office of Public Archaeology, Institute for Environmental Studies and US Army Corps of Engineers, Seattle District, Seattle, Wash, p. 131–147, https://apps.dtic.mil/sti/pdfs/ADA166700.pdf.

Olmsted, R.K., 1963, Silt mounds of Missoula flood surfaces: Geological Society of America Bulletin, v. 74, p. 47–54, doi:10.1130/0016-7606(1963)74%5B47:SMOMFS%5D2.0.CO;2.

Phillips, F.M. et al., 2016, The CRONUS-Earth project: a synthesis: Quaternary Geochronology, v. 31, p. 119–154, doi:10.1016/j.quageo.2015.09.006.

Pico, T., David, S.R., Larsen, I.J., Mix, A.C., Lehnigk, K., and Lamb, M.P., 2022, Glacial isostatic adjustment directed incision of the Channeled Scabland by Ice Age megafloods: Proceedings of the National Academy of Sciences, v. 119, p. e2109502119, doi:10.1073/pnas.2109502119.

Pine, K.A., 1985, Glacial geology of the Tonasket - Spectacle Lake area, Okanogan County, Washington: [Western Washington University], https://cedar.wwu.edu/wwuet/836/.

Porter, S.C., 1978, Glacier Peak tephra in the North Cascade Range, Washington: stratigraphy, distribution, and relationship to late-glacial events: Quaternary Research, v. 10, p. 30–41, doi:10.1016/0033-5894(78)90011-X.

Rea, B.R., and Evans, D.J., 2011, An assessment of surge-induced crevassing and the formation of crevasse squeeze ridges: Journal of Geophysical Research: Earth Surface, v. 116, doi:10.1029/2011JF001970.

Richmond, G.M., 1986, Tentative correlation of deposits of the Cordilleran ice-sheet in the northern Rocky Mountains: Quaternary science reviews, v. 5, p. 129–144, doi:10.1016/0277-3791(86)90179-4.

Roed, M.A. et al., 2014, Evidence for an Early Pleistocene glaciation in the Okanagan Valley, southern British Columbia: Canadian Journal of Earth Sciences, v. 51, p. 125–141, doi:10.1139/cjes-2013-0106.

Rubin, M., and Alexander, C., 1958, United States Geological Survey Radiocarbon Dates IV: Science, v. 127, p. 1476–1487, doi:10.1126/science.127.3313.1476.

Seguinot, J., Rogozhina, I., Stroeven, A.P., Margold, M., and Kleman, J., 2016, Numerical simulations of the Cordilleran ice sheet through the last glacial cycle: The Cryosphere, v. 10, p. 639–664, doi:10.5194/tc-10-639-2016.

Shuster, D.L., Ehlers, T.A., Rusmore, M.E., and Farley, K.A., 2005, Rapid glacial erosion at 1.8 Ma revealed by He-4/He-3 thermochronometry: Science, v. 310, p. 1668–1670, doi:10.1126/science.1118519.

Smith, L.N., 2017, Repeated sedimentation and exposure of glacial Lake Missoula sediments: A lake-level history at Garden Gulch, Montana, USA: Quaternary Science Reviews, v. 155, p. 114–126, doi:10.1016/j.quascirev.2016.11.018.

Smith, L.N., Sohbati, R., Buylaert, J.-P., Lian, O.B., Murray, A., and Jain, M., 2018, Timing of lake-level changes for a deep last-glacial Lake Missoula: optical dating of the Garden Gulch area, Montana, USA: Quaternary Science Reviews, v. 183, p. 23–35, doi:10.1016/j.quascirev.2018.01.009.

Spooner, I.S., Osborn, G.D., Barendregt, R.W., and Irving, E., 1995, A record of Early Pleistocene glaciation on the Mount Edziza Plateau, northwestern British Columbia: Canadian Journal of Earth Sciences, v. 32, p. 2046–2056, doi:10.1139/e95-158.

Stoffel, K., Joseph, N., Waggoner, S., Gulick, S., Korosec, M., and Bunning, B., 1991, Geologic map of Washington-Northeast quadrant: Washington Division of Geology and Earth Resources:, https://www.dnr.wa.gov/Publications/ger_gm39_geol_map_ne_wa_250k.pdf.

Stumpf, A.J., Broster, B.E., and Levson, V.M., 2000, Multiphase flow of the late Wisconsinan Cordilleran ice sheet in western Canada: Geological Society of America Bulletin, v. 112, p. 1850–1863, doi:10.1130/0016-7606(2000)112<1850:MFOTLW>2.0.CO;2.

Sweeney, M.R., Gaylord, D.R., and Busacca, A.J., 2007, Evolution of Eureka Flat: A dust-producing engine of the Palouse loess, USA: Quaternary International, v. 162, p. 76–96, doi:10.1016/j.quaint.2006.10.034.

Waitt, R.B., 1985, Case for periodic, colossal jökulhlaups from Pleistocene glacial Lake Missoula: GSA Bulletin, v. 96, p. 1271–1286, doi:10.1130/0016-7606(1985)96<1271:CFPCJF>2.0.CO;2.

Waitt, R.B., 1984, Periodic jökulhlaups from Pleistocene glacial Lake Missoula—New evidence from varved sediment in northern Idaho and Washington: Quaternary Research, v. 22, p. 46–58, doi:10.1016/0033-5894(84)90005-X.

Waitt, R.B., 2017, Pleistocene glaciers, lakes, and floods in north-central Washington State, *in* From the Puget Lowland to East of the Cascade Range—Geologic Excursions in the Pacific Northwest. Geological Society of America Field Guide, v. 49, p. 175–205, doi:10.1130/fld049.

Waitt, R.B., Atwater, B.F., Lehnigk, K., Larsen, I.J., Bjornstad, B.N., Hanson, M.A., and O'Connor, J.E., 2021, Upper Grand Coulee: New views of a Channeled Scabland megafloods enigma, *in* Booth, A.M. and Grunder, A.L. eds., From terranes to terrains: Geologic field guides on the construction and destruction of the Pacific Northwest, Geological Society of America Field Guide 62, 56 p., https://doi.org/10.1130/2021.0062(07).

Waitt, R.B., and Thorson, R.M., 1983, The Cordilleran ice sheet in Washington, Idaho, and Montana, *in* Porter, S.C. ed., Late-Quaternary environments of the United States.

Vol.1, Minneapolis, University of Minnesota Press, Late-Quaternary environments of the United States, p. 53–70.

Wang, Y., Zou, Y., Henrickson, K., Wang, Y., Tang, J., and Park, B.-J., 2017, Google Earth elevation data extraction and accuracy assessment for transportation applications: PloS one, v. 12, p. e0175756, doi:10.1371/journal.pone.0175756.

Westgate, J.A., and Evans, M.E., 1978, Compositional variability of Glacier Peak tephra and its stratigraphic significance: Canadian Journal of Earth Sciences, v. 15, p. 1554–1567, doi:10.1139/e78-161.

APPENDIX 1-A1: NORMALIZED FLOWLINE DISTANCES

To create a quantitative framework for comparing surface exposure ages to each other, I drew Okanogan lobe flowlines for each glacial sample. These flowlines begin at the north tip of the Omak Plateau, intersect each sample site, and end at the maximum extent of Okanogan lobe glaciation. I drew flowlines parallel to drumlins and perpendicular to moraine crests. The relative position of each sample on its flowline is a "normalized flowline distance" that ranges from 0 at the north tip of the Omak plateau to 1 at the maximum extent of glaciation.

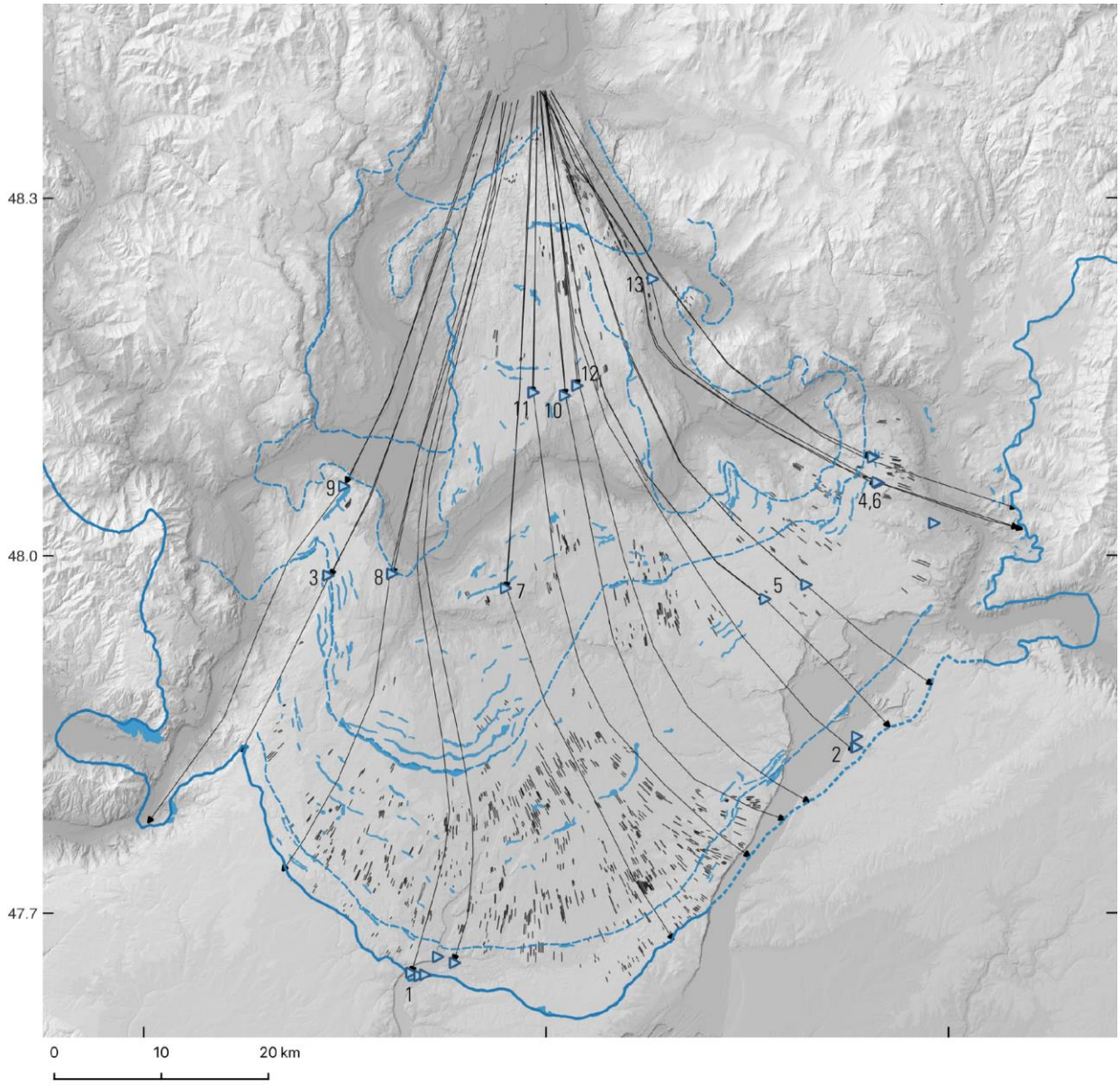

Figure 1-A1: Flowline normalization for plotting exposure ages. Map showing the position of surface exposure samples on glacially transported erratics of the Okanogan lobe (blue triangles) relative to glacial geomorphology (blue lines = recessional moraine crests, black lines = flutes and drumlins). Dashed blue lines are intermediate positions of the Okanogan lobe margin, drawn parallel to recessional moraine crests. Black arrows are interpretations of ice flow at the glacial maximum, drawn from the north tip of the Omak plateau, parallel to drumlins, through sample locations, and perpendicular to the ice margin at the maximum extent of glaciation. Arrows are used to calculate a normalized flowline distance for each sample, which ranges from 0 at the north tip of the Omak plateau, to 1 at the glacial maximum.

APPENDIX 1-A2: TIMING OF EPHRATA FAN FORMATION AND LAKE LEWIS RHYTHMITE DEPOSITION

Rhythmically bedded silts and sands (rhythmites) that accumulated in the temporary Lake Lewis of Quincy and Pasco basins likely correlate to the gravel of the Ephrata fan. However, OSL and radiocarbon dating of Lake Lewis suggest that the rhythmites accumulated between ~18 to ~15 ka (Last and Rittenour, 2021), before exposure of most boulders on the Ephrata fan from ~16 to ~14 ka. This offset is explainable by the inherent bias between surface exposure ages, which date the most recent event at a site, and ages from stratigraphic sections, which date events older than the most recent ones.

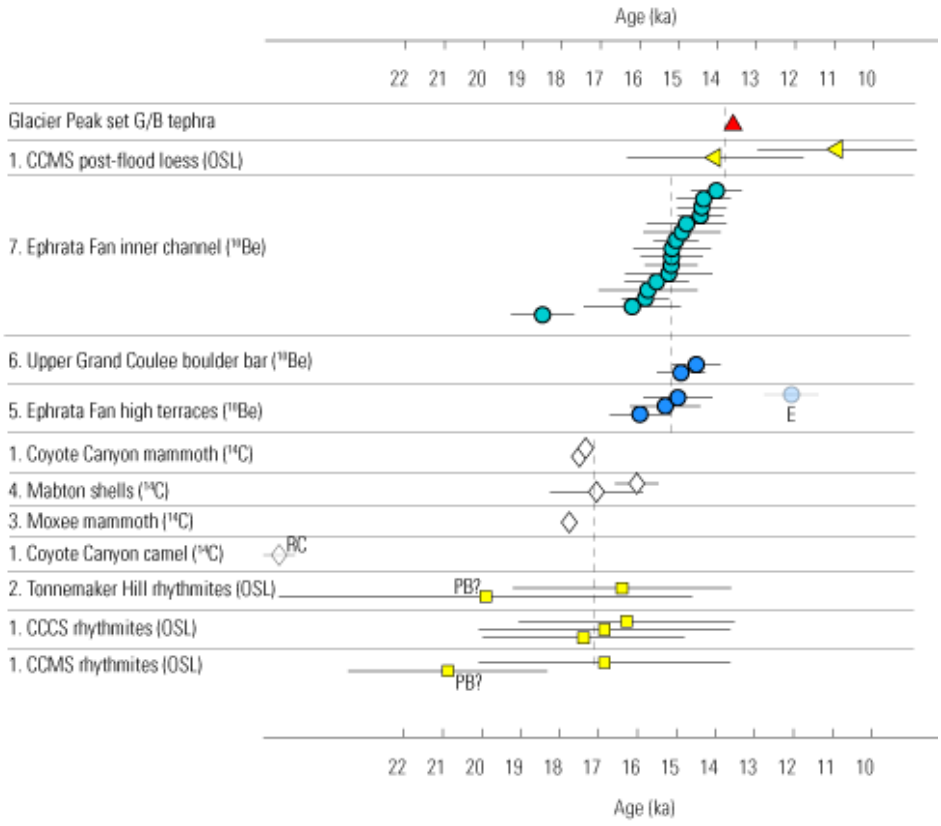

Figure 1-A2: Exposure ages of Ephrata fan compared to Missoula flood rhythmite geochronology. Relevant ages for history of Grand Coulee megafloods. Annotations indicate possible violations of dating assumptions (E = exhumed (boulder), RC = reworked clast, and PB = partial bleaching).

3. MISSOULA FLOODS VS. OKANOGAN LOBE SUBGLACIAL FLOODS AS THE SOURCE OF LAST-GLACIAL FLOODING IN MOSES COULEE

3.1 CHAPTER SUMMARY

Moses Coulee is an over-sized canyon in central Washington. Features in Moses Coulee clearly indicate that large glacial floods created the canyon system, but the water source for these floods is unclear. This study uses geomorphic mapping, geochronology, and field observations to investigate Moses Coulee megafloods, comparing the compatibility of geologic evidence with two scenarios for Moses Coulee megafloods: the lake Missoula flood scenario, in which Missoula floods, diverted by the Okanogan lobe, spilled into Moses Coulee, and the Okanogan lobe subglacial flood scenario, in which megafloods sourced from the Cordilleran Ice Sheet drained sub-glacially into Moses Coulee.

Moses Coulee is within the Channeled Scabland physiographic region of overfit, glacial flood-carved canyons in basalt, the formation of which has been linked to glacial lake Missoula. Thus, it is often presumed that lake Missoula was the source for Moses Coulee floods. However, the lack of obvious, channelized connectivity on the Waterville Plateau between the head of Moses Coulee and the Columbia River, the main drainage line for the Missoula floods, is an apparent discrepancy with the Missoula flood scenario for Moses Coulee floods. Missoula flood spillovers out of the Columbia valley eroded obvious channel systems leading into the Cheney-Palouse, Telford-Crab Creek, and Grand Coulee drainage tracts. In contrast, Moses Coulee lacks similar channels that connect to the Columbia River. It has been suggested that glaciation of the Waterville Plateau by the Okanogan lobe, after Moses Coulee floods, may have either eroded or

buried the channel system that previously linked Moses Coulee to the Columbia River, thus explaining the discrepancy.

However, the Waterville Plateau between the head of Moses Coulee and the Columbia River is heavily channelized, but not along the lower-elevation pathways that Missoula floods would have traveled. Instead, systems of bedrock channels on the Waterville plateau splay outward toward the former margin of the Okanogan lobe, and are aligned with drumlins and eskers, suggesting that the channels formed along subglacial drainage pathways that would have existed beneath the Okanogan lobe. This discrepancy suggests that further investigation of Moses Coulee megafloods is needed to resolve the apparent contradiction between the landscape upstream of Moses Coulee and the hypothesis that flooding of Moses Coulee occurred from Missoula floods.

Gravel in Moses Coulee flood bars ranges from boulder to pebble-sized having variable matrix content, and composed of clasts that are nearly 100% basaltic, fresh, and which vary from rounded to angular. Gravel textures in Moses Coulee include foreset-bedded boulder gravel, horizontally bedded, open-work cobble gravel, and boulder/cobble-rich diamict. The freshness of gravel clasts and the minor degree of soil development within gravel stratigraphies suggests that most exposed Moses Coulee gravel was deposited during the last-glacial episode of flooding, and that some bedrock erosion in or upstream from Moses Coulee likely occurred during the last-glacial episode of flooding to generate the fresh, angular clasts in some gravel. Confirming the interpretation that many flood gravels were emplaced in last-glacial floods, exposure ages from iceberg-rafted rocks in Moses Coulee, at elevations up to the highest recognized flood stage in Sagebrush basin, range from 28.1 ± 1.4 ka to 13.8 ± 0.7 ka (n=7), indicative of last-glacial

flooding. The exposure age population includes two outliers that violate external constraints, which limit Moses Coulee floods to between about 19 and 14 ka, leaving five plausible exposure ages that range from 15.5 ± 0.8 to 18.8 ± 1.0 ka. Older exposure ages occur at higher elevations suggest a trend of decreasing flood stage through time due to either lowering of the valley floor and/or decrease in incoming flood flows. The age range for Moses Coulee floods from ~15 to ~19 ka is broadly consistent with stratigraphy at Rock Island bar, which indicates at least four Moses Coulee megafloods occurred during the last glaciation and that those floods occurred after a pre-Okanogan lobe down-Columbia flood, but before cessation of Quincy Basin floods and before a late-glacial, post-Okanogan lobe down-Columbia flood. However, the exposure ages suggest a longer duration of flooding than indicated by the number of varves remaining in the Rock Island bar section. Based on this evidence, the interval over which last-glacial Moses Coulee floods occurred might have been as short as decades and as long as millennia.

A platy calcrete horizon at the base of a flood bar along Coyote Creek in Sagebrush basin provides a stratigraphic record in Moses Coulee prior to the last glaciation. This calcrete overlies a basaltic cobble gravel that may have been deposited in an ancient Moses Coulee glacial flood or in an ancient Coyote Creek flash flood. The origin of the gravel remains uncertain due to limited exposure, but crude gravel bedding that apparently dips up Coyote Creek favors the interpretation that the gravel formed in canyon-wide glacial flood. This gravel and the overlying calcrete hint that Moses Coulee megafloods may have occurred prior to the last glacial. U-series ages on the calcrete suggest that the gravel could be at least 220,000 years old, which might imply that megafloods in Moses Coulee occurred prior to the last glaciation, and prior to MIS 6 and 8.

To more fully understand the nature of channelized connectivity upstream of Moses Coulee, a detailed map of channels on the Waterville Plateau was generated from terrain and imagery analysis. This map reveals significant channelized connectivity on the Waterville Plateau between Moses Coulee and the Columbia River. However, the radial geometry of the channel network, its style of anabranching and elongation, and high-elevation, divide-crossing canyons within the network are inconsistent with channel formation in sub-aerial flows. The Waterville Plateau channels contrast with linear, anabranching networks of eastern Channeled Scabland tracts, but are similar to tunnel valley networks mapped beneath the former Laurentide and Fennoscandian ice sheets. The channels mostly do not follow surface slopes downhill, nor are they preferentially carved into the lowest crossings of hydrologic divides. The channel network on the Waterville Plateau shows little evidence of incision along the flow path that subaerial overflows from the Columbia River would have followed. The radial shape of the channel network, its alignment with drumlins and flutes, and its apparent disregard for surface slopes and low spill-over points is difficult to explain within a sub-aerial flow model but is consistent with channel formation from flows that were directed across subglacial hydro-potential gradients beneath the former Okanogan lobe.

Higher divides on the Waterville Plateau are breached by more prominent channels than lower divides, a pattern that is also difficult to explain with subaerially-routed meltwater. Divide overtopping by water results in the most erosive flows across the lowest divide crossings, and only minor flows and erosion across higher crossings. Overtopping of the Foster Creek basin into Moses Coulee would have begun with flow across two separate km-long stretches of low divide near Badger Wells and Chester Butte. This would have concentrated stream power there,

producing ever-deepening channels that would have progressively captured more flow, and set in motion a positive feedback that should have resulted in that reach of divide capturing much of the overflow with a deep canyon or broad area of channelized scabland, as occurred for Grand Coulee or the Cheney-Palouse Tract. However, it is the highest divides on the Waterville Plateau that host the biggest channels. These canyons, such as the ones near Mansfield, are up to 100's of meters across and up to 50 meters in depth. The channels on the Waterville Plateau breach pre-flood surfaces up to 780 m, above the highest level 750 m of flood-swollen glacial lake Columbia, and well above the divide elevations into the Grand Coulee, Cheney-Palouse, and Crab-Creek tracts that would have been activated had flood stage reached above 700 m on the Waterville Plateau. Thus, it is hard to explain how an over-topping process could explain the pattern of channelization on the Waterville Plateau.

Some scenarios that route Missoula floods into Moses Coulee require existence of a glacial Lake Columbia configuration with an arm in Foster Creek during the timeframe of large Missoula floods, i.e., early in the Okanogan lobe glaciation. However, reconnaissance stratigraphy along the Columbia River suggests that this glacial lake Columbia configuration may not have existed during the early phase of Okanogan lobe glaciation. The distribution of lake beds beneath till along the Columbia valley between Brewster and Grand Coulee suggests that the Okanogan glacier did not impound a stable and deep glacial Lake Columbia until its margin was upstream of Foster Creek. This suggests that the sub-aerial flow pathway into Moses Coulee might have been blocked by the time a sufficiently deep glacial lake Columbia came into existence.

Missoula floods in the Channeled Scabland often deposited distinctive rocks and sediment derived from western Montana and northern Idaho, including the distinctive Belt-Purcell argillite. This study examines provenance of flood-transported sediment in Moses Coulee, including ice-rafted erratics, in search of a lithologic connection to lake Missoula. Unique erratics in Moses Coulee include augen gneiss, megacrystic granite, and garnetiferous quartzite, matching metamorphic core complexes of northern Washington. There is no clear evidence of any rocks in Moses Coulee that derive from the low-grade metasediments of western Montana. Notably absent from the cataloged Moses Coulee erratics is Belt-Purcell argillite. While the assemblage of rocks in Moses Coulee can be explained by a Missoula flood scenario, it is unclear why a Missoula flood into Moses Coulee flood would lack the distinctive argillite found in other Missoula deposits, and why a Missoula flood into Moses Coulee would become so enriched in icebergs containing clasts from north Washington highlands.

The analysis of channels upstream of Moses Coulee, the Columbia valley stratigraphy, the timing of floods, and the erratic assemblages do not prove a source of Moses Coulee floods. However, the evidence seems most consistent with an alternative to the widely accepted scenario that Moses Coulee flooded from Missoula floods. Instead, Moses Coulee may have mainly flooded from glacial lake outburst floods that originated within the Okanogan drainage, and which flowed sub-glacially to the margin of the Okanogan lobe in the Moses Coulee basin.

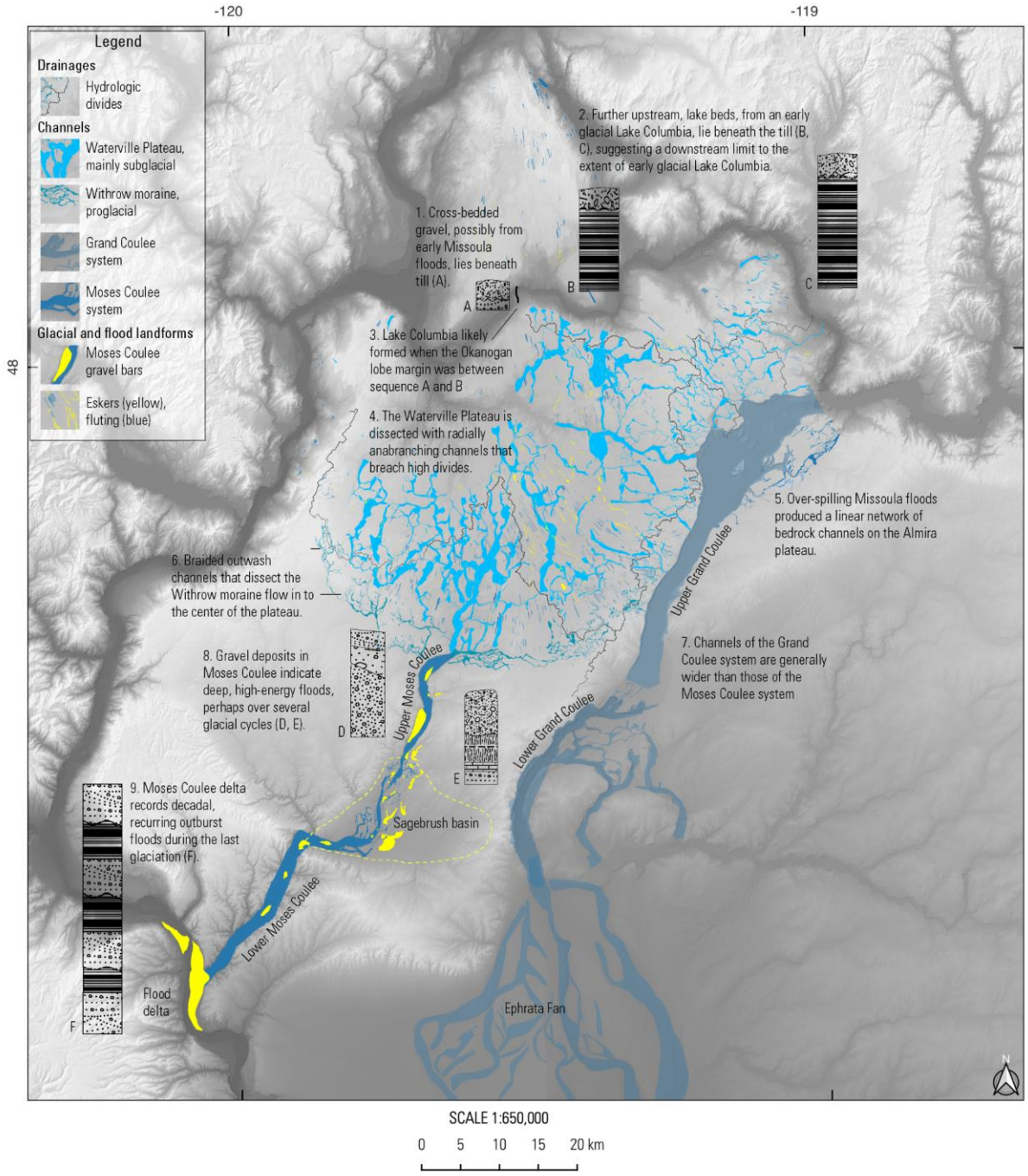

Figure 3-1: Glacial drainage routes and gravel deposition on the Waterville Plateau mapped from digital terrain models, satellite/air photos, and field observations. Also pictured are six simplified stratigraphic sections labeled A-F relevant to Moses Coulee floods.

3.2 METHODS

3.2.1 Field observations

I visited Moses Coulee and the Channeled Scabland on many separate field excursions between 2016 and 2022. I used hand-written notes, digital photography, and GPS to catalog crystalline erratics, to observe natural exposures of sediment, and to observe soil and bedrock surfaces. I occasionally dug small soil pits and used a shovel and brush to clean exposures. Reconnaissance stratigraphy of Rock Island delta and of pre-Okanogan lobe sediment along the Columbia River was completed over two days in June 2022.

3.2.2 Geomorphology

I mapped over-fit channels, eskers, and gravel bars primarily using terrain-enhanced imagery and the USGS 10-m DEM in Google Earth over 9 months from late 2021 through mid 2022. I manually drew individual polygons around the edges of landforms, resulting in KML files with dozens to hundreds of polygons for each class of landform.

I identified over-fit channels on the Waterville Plateau as those that are wider and deeper than modern streams, that lack dendritic tributaries typical of mature stream networks, that often connect to other overfit channels in anabranching networks, and that may cut across hydrologic divides. In practice, application of these criteria is subjective. Additionally, most channels are likely palimpsests, eroded by multiple generations of proglacial and subglacial meltwater. Given the likely multiple influences on channel formation, I did not attempt to classify channels by their presumed genetic origin, other than separating braided, outwash channels cut into sediment that dissect the Withrow moraine from the rest of the channels on the Waterville Plateau. The

map of channels presented here is an unreviewed, first attempt to delineate the channel network. Some mapped channels may be spurious or partly misdrawn, and many channels were not included in the map due to a lack of mapping time. Despite these shortcomings, the map is intended to capture the overall geometry of channelization on the Waterville Plateau, and the addition or subtraction of individual channels from the map is unlikely to change the overall picture.

3.2.3 Geochronology

This study uses surface exposure dating of flood-transported boulders to date last-glacial megafloods in Moses Coulee and uses uranium-series dating of soil carbonate to constrain the timing of more ancient fluvial events. Some nuances of surface exposure dating in the Channeled Scabland are reviewed in Chapter 1 of this thesis.

3.2.3.1 U-series dating

I sampled a calcrete soil horizon in the field using a flathead screwdriver and a hammer to break off fragments into labeled plastic bags. At University of Washington, I used a Dremel Stylo+ (2050-15) tool with a 1-mm tungsten carbide cutter to obtain powders for U/Th screening and isotope determination, targeting the range of calcrete textures present among the samples to obtain a sense of the uranium and thorium isotope compositions present in the varied textures within the calcrete. During sampling of 1-2 mm spots, surface carbonate was discarded, and interior material collected into glass vials. The drill bit was cleaned in deionized water, dilute hydrochloric acid, and isopropanol between samples. Powders were analyzed for U and Th

isotope composition using a Nu Plasma II-ES MC-ICP-MS at the McGee Lab at MIT by Adam Jost and ages calculated by David McGee.

3.2.3.2 Surface exposure dating

We obtained rock samples from the tops of boulders and cobbles in Moses Coulee with the aid of a hammer drill and rock-splitting wedges. At University of Washington, rock samples were crushed and processed into clean quartz, which was then dissolved and chemically processed into beryllium powder for isotopic analysis. Beryllium isotope ratios were measured at Lawrence Livermore National Laboratories, and ages calculated using the CRONUS v3 calculator. Exposure ages were calculated using LSD scaling, calibrated to UW measurements of Promontory Point wave-cut quartzite, presumed first exposed in the Bonneville Flood at 18,300 ± 300 years (Lifton et al., 2015).

3.3 Timing and discharge of Moses Coulee megafloods

Gravel exposures in Moses Coulee indicate varied, high-energy flow conditions during floods that deposited the gravels. Bedded, sorted gravels likely were deposited under tractive transport in steady flows, while bouldery diamicts likely were deposited in subaqueous debris flows during the same floods. The bars in Moses Coulee contain no stratigraphic evidence of more than one megaflood during the last glaciation and no rhythmic, slackwater deposits have been found in tributaries of Moses Coulee. However, stratigraphy in Rock Island bar, located at the outlet of Moses Coulee, suggests at least four separate Moses Coulee floods during the last glaciation, with inter-flood periods from years to decades based on counts of varves between flood beds.

Surface exposure dates on crystalline, ice-rafted erratics in Moses Coulee range from 28.1 ± 1.4 ka to 13.8 ± 0.7 ka (n=7). Comparison with external age constraints makes clear that one of these exposure ages is too old due to isotope inheritance, while another is probably too young due to exhumation or erosion. The five samples that give plausible ages range from 15.5 ± 0.8 to 18.8 ± 1.0 ka. Nominally this suggests that Moses Coulee floods occurred within a ~4,000-year timespan between ~19 and ~15 ka, longer than the many decades of time implied by varve counts between basaltic gravels in Rock Island delta. However, the clear effects of isotope inheritance and erosion or exhumation on two out of seven samples indicate that unconstrained, bidirectional error may affect all Moses Coulee samples, and therefore that the apparent 4,000-year range of time in which Moses Coulee floods occurred may be dilated by geologic error.

A hint of pre-last glacial flooding may be preserved in Moses Coulee. A cobble gravel in the Coyote Creek tributary of Moses Coulee lies beneath a platy calcrete soil. Preliminary U-series dating of the calcrete gave scattered results all of which may be biased old by uranium loss, though samples with denser, cleaner calcite returned ages from 100,000 to 200,000 years, suggesting that the calcrete likely pre-dates both the last glaciation, and the penultimate glaciation. The gravel beneath the calcrete may be organized into clinoforms that dip up Coyote Creek, and imbrication in the gravel may also indicate flow up Coyote Creek, suggesting that the gravel formed in a pre-last glacial Moses Coulee flood rather than a Coyote Creek flash flood.

The prevalence of angular basalt clasts in some gravel deposits suggests limited transport time and distance for these basalt clasts. The freshness and angularity of flood-transported gravel implies short duration of floods, a small number of floods, efficient evacuation of gravel from Moses Coulee during floods, and/or ongoing bedrock erosion during the last glacial floods.

3.3.1 Upper Moses Coulee gravel bars

Convex, elongate gravel mounds in Moses Coulee are best explained as bars that accumulated during large, down-coulee floods (Bretz, 1928, p. 673-675). Most bars have nearly flat tops that steepen along well-defined edges (Fig. 3-2, 3-3). Bars are typically elongated in the direction of paleo-flood flow, and located in areas downstream of bedrock obstacles, and/or downstream of channel constrictions where confined flows expanded, eddies may have developed, and/or flow velocities dropped. Deposits range in thickness from 5 to 50 m, and range in length from 10's to 1,000's of meters. The gravel in them consists almost entirely of basalt, with only the occasional fragment of non-basaltic rock. The freshness of almost all exposed gravel in Moses Coulee and lack of soil development on most gravel exposures indicates that most gravel in Moses Coulee was deposited during the last-glacial episode of floods from around 19 to 15 ka, though one bar along Coyote Creek has an old calcrete soil horizon on top of a gravel layer at the base of the bar, indicating a history of gravel deposition and bar formation that spans multiple glacial cycles.

Figure 3-2: Photographs of selected flood-gravel bars of Moses Coulee. Black arrows indicate inferred flow directions at time of bar deposition. (A) Expansion bar at mouth of Coyote Creek with fore-set gravel beds dipping down Coyote Creek and towards the inner channel of Moses Coulee. (B) Eddy bar along the old Hwy 2 in Sulphur Springs Canyon. (C, D) View of same bar along Coyote Creek showing wavy contact between uppermost gravel and underlying loess, and white, calcrete horizon at base of bar.

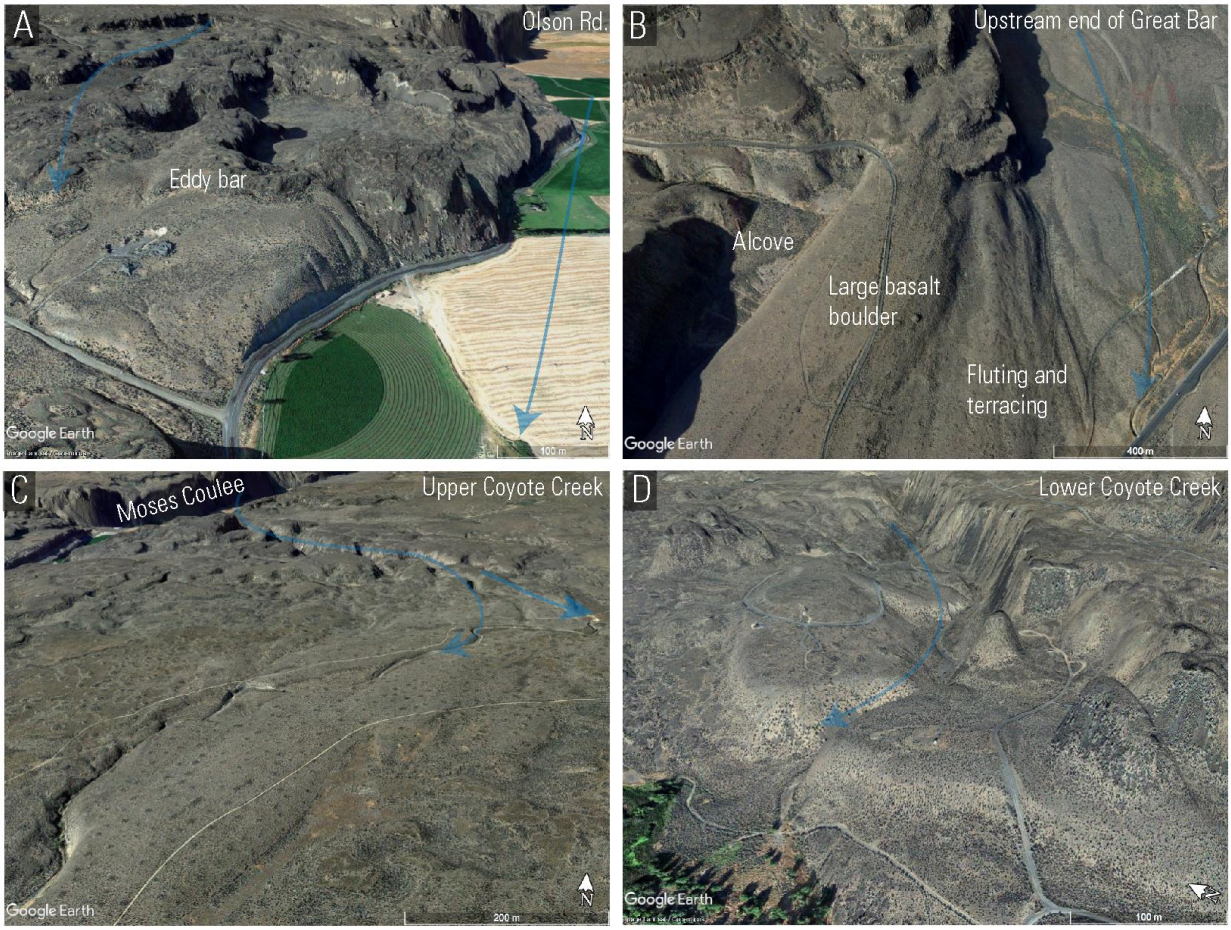

Figure 3-3: Bars of Moses Coulee viewed in Google Earth with 3x terrain exaggeration. (A) Pendant/eddy bar at intersection of Coulee Meadows Rd. and Olson Rd. (B) Upstream end of Great Bar in upper Moses Coulee north of Hwy 2. (C) Set of low relief, streamlined bars along Coyote Creek. (D) Expansion bars and terraced gravels at mouth of Coyote Creek.

High-water marks

Top surfaces of flood bars, flood-scoured bedrock surfaces, and ice-rafted erratics all must have been deposited below a flood surface, and thus provide minimum elevations of flood stage. The distribution of these depositional high-water marks suggests that Moses Coulee floods were 100's of meters deep in upper Moses Coulee and then shallowed downstream as flows expanded into Sagebrush basin (Figure 3-4).

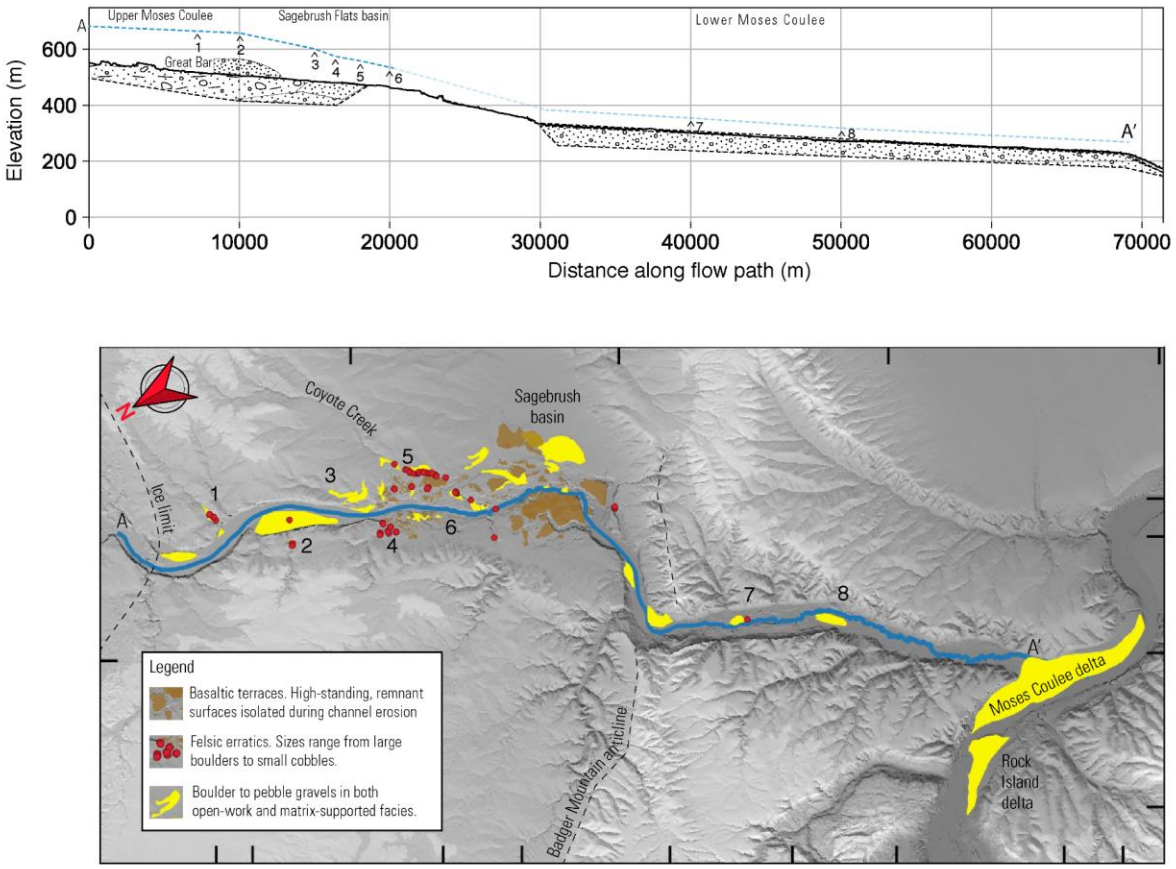

Figure 3-4: Reconstructed minimum flood profile based on elevations of gravel bar tops and felsic erratics along flow path through Moses Coulee. Sediment composition and depth to bedrock in upper Moses Coulee from well log analysis (Swope, 2007) and depth to bedrock in lower Moses Coulee from two seismic profiles (Hanson, 1970).

3.3.2 The Great Bar

A 4 km-long, 50 m-thick gravel bar in upper Moses Coulee consists mainly of cobble and boulder gravel. The bar accumulated downstream of an abrupt canyon widening and was built on a ~100 m-thick sediment fill of cobbles, gravel, and sand (Swope, 2007, Fig. 7; Fig. 3-3B). The nearly flat, broadly convex, top surface of the elongate landform dips gently downstream along most of its length, fringed with more-steeply dipping edges. The boulder-studded, loess mound-

dotted surface is fluted and terraced along the upstream half of the bar (Fig. 3-3B) and cut with modern alluvial distributary channels that emanate from Armor Draw near the middle of the bar.

Slumps and cut banks along these Armor Draw outflow channels, recently active, reveal variable bar composition consisting of foreset-bedded bouldery gravel, horizontally bedded cobble gravel, and bouldery, sandy diamict.

An exposure of boulder-gravel in the bar is organized into a single, fining-upward sequence of clinoforms (Fig. 3-5A), suggesting bar growth via accumulation of dipping gravel beds at the edge of a growing bar (Baker, 1973, p. 36). The largest boulders at the base of the stacked clinoforms are up to 2 m in diameter, while those near the top are closer to 0.5 m, suggesting a decrease in flow competency as the stack accumulated. Boulders typically have smooth surfaces characteristic of fluvial abrasion, and many are broken with sharp, jagged to conchoidal fractures indicative of rock-to-rock collisions (Fig. 3-5A, 3-26C). Long-axes of clasts are preferentially oriented along bedding planes (Fig. 3-5A), indicative of boulders rolling and sliding along slip faces. The foreset-bedding and clast orientation fabrics indicate bar accumulation in a process of tractive bedload transport along the top of the bar and deposition in the flow separation zone at the edge of the bar (O'Connor, 1993, p. 48-49). The eastward dip direction of the clinoforms indicates bar growth towards the center of the channel. The apparent cross-coulee flow indicated by the foreset dip directions might relate to an eddy that formed in the abrupt flow expansion zone downstream of the canyon widening where the bar accumulated, and/or vortices in down-coulee flow.

Further towards the eastern limit of the bar and the center of the channel, another exposure reveals well-sorted, open-work cobble gravel, pebble gravel, (Fig. 5C) and sand-cobble

diamict (Fig. 3-5D). The clast-supported, matrix-poor cobble gravel consists of horizontal beds of sub-rounded cobbles. The overlying diamict consists of small to large cobbles of sub-rounded basalt, suspended in a matrix of fine sand with minor silt. Long axes of clasts near the base of the diamict are preferentially oriented along the bedding plane between the diamict and the underlying cobble gravel (Fig. 3-5B) which dips gently eastward and appears wavy (Fig. 3-5B). The diamict transitions upwards into a matrix-rich cobble gravel (Fig. 3-5B).

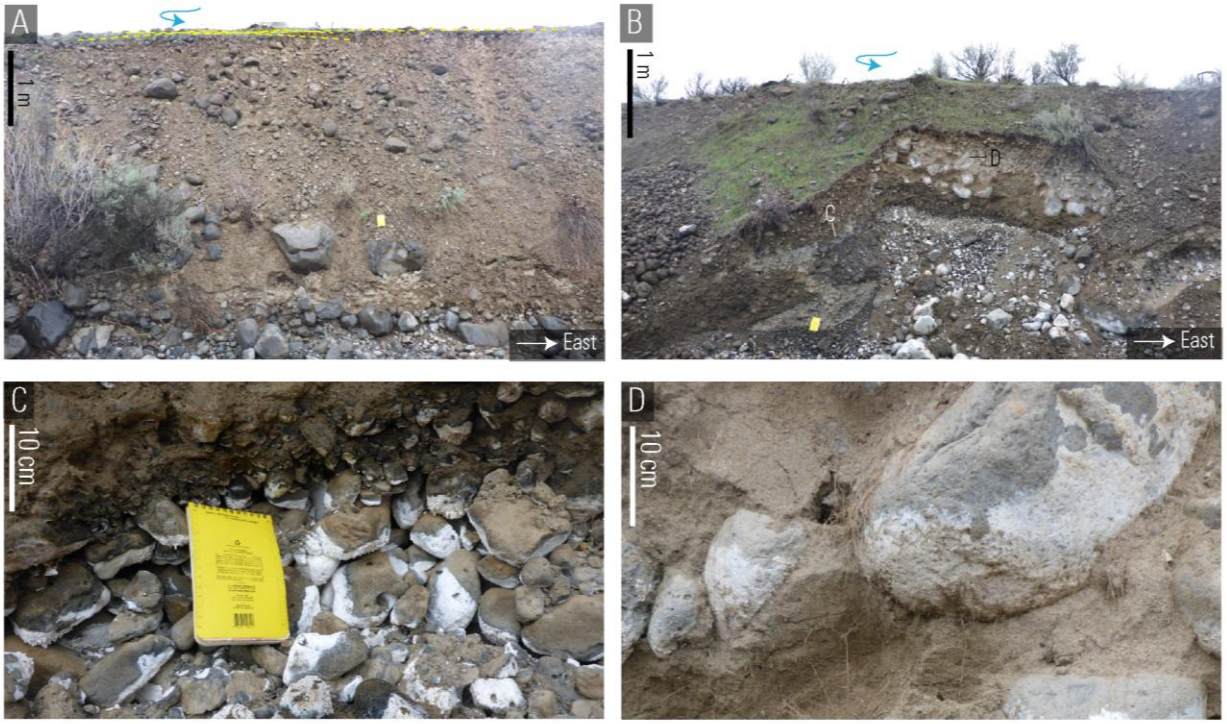

Figure 3-5: Gravel facies of Great Bar in upper Moses Coulee. (A) Fining- upward boulder to cobble gravel with foreset beds dipping towards the floor of Moses Coulee. (B) East of A; open-work cobble gravel interbedded with sand-cobble diamict (C) Detail of cobble gravel; clasts coated with soil carbonate (D) Diamict consisting of fine sand and cobbles.

Deposition of the open-work gravel required sorting of gravel by size and continued flow entrainment of fines during deposition of the gravel, preventing in-filling of the pore space with

sediment finer than cobbles (Maizels, 1993, p. 308). This suggests that pebbles and finer sediment were in suspension during the flow that deposited the cobble gravel. Additionally, had the flow waned before the diamict accumulated on top of the open-work gravel, fines might have fallen out of suspension and infilled the gravel. The nearly total absence of fines from the open-work gravel suggests that the diamict above the gravel was likely deposited in the same flood as the gravel, before the flow weakened enough to drop suspended sediment.

The diamict itself may have been a subaqueous debris flow based on its fabric and clast attributes. The pattern of bed-parallel clast alignment near the bottom of the diamict with decreasing horizontal alignment upwards (Fig. 3-5B) is typical for subaqueous debris flows due to shear stresses at the base of the flows (Collinson and Thompson, p. 118). The fine sand matrix in this diamict is similar to the fine sand present between Jameson and Grimes Lake (Swope, 2007, Fig. 3-6), suggesting that the sandy debris flow in the Great Bar could have obtained its matrix from sediment present upstream, and/or that both deposits received sand from the same source. The high degree of rounding of clasts in the diamict suggests that the debris flow only entrained flood-worked cobbles, and hints that the debris flow might have been generated at the base of the flood rather than from a valley wall or tributary, as the latter scenario might have introduced angular clasts.

3.3.3 Bars along Coyote Creek

Several kilometers downstream from the Great Bar, the confined Upper Moses Coulee expands into Sagebrush basin (Fig. 3-1). Here, the single canyon of upper Moses Coulee continues into Sagebrush basin as an inner channel that is flanked on both sides by higher, bedrock terraces cut with networks of anastamosing channels (Fig. 3-6). The orientation of these

channels and the streamlined bedrock residuals between them indicates that the confined flows in the upper canyon splayed radially as they entered Sagebrush basin. To the west of the inner canyon, the channel network trends SSW and is elongated sub-parallel to the trend of the inner canyon (Fig. 3-6). To the east of the inner channel, the channel network trends SE, orthogonal to the inner channel (Fig. 3-6).

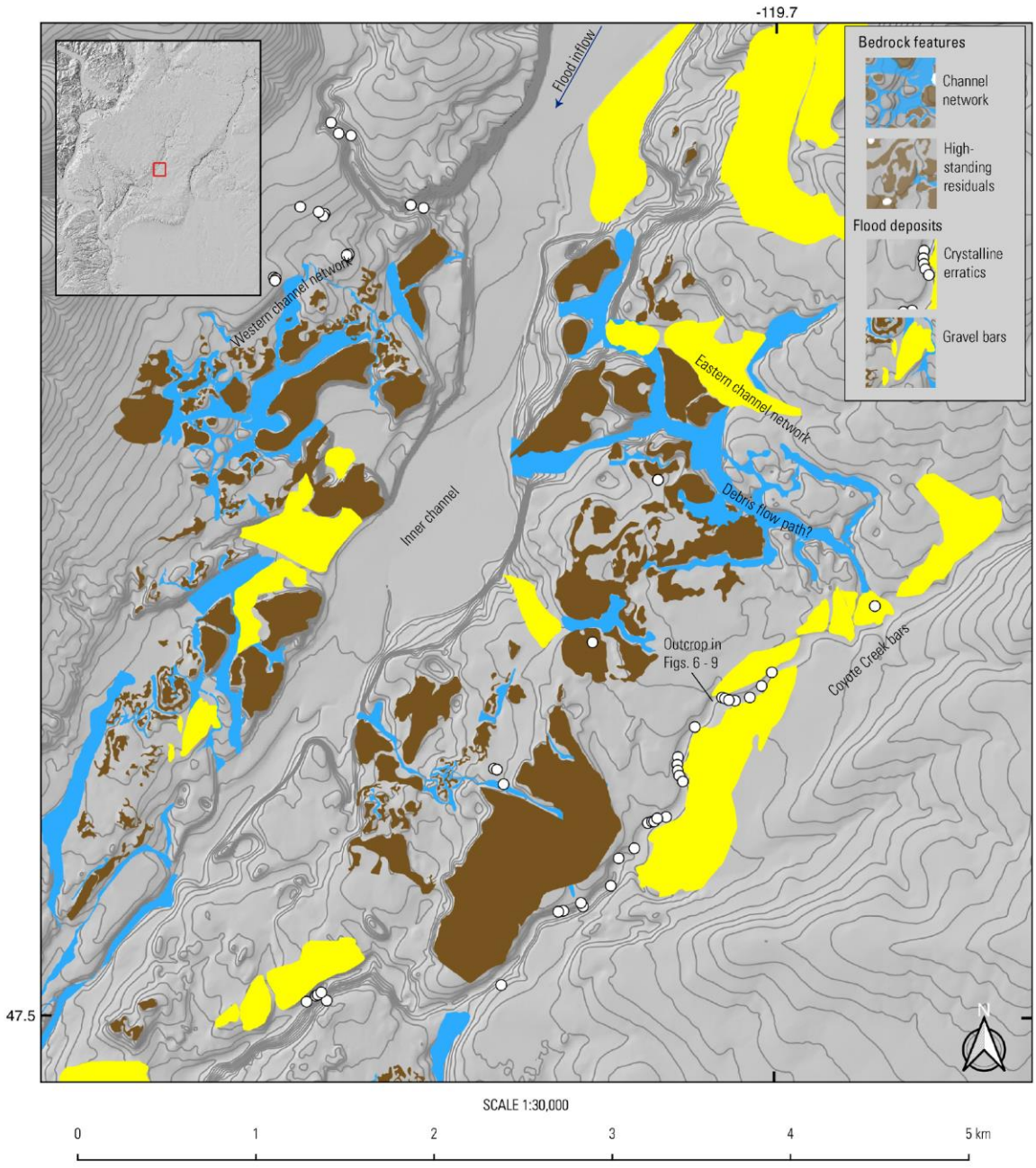

Figure 3-6: Flood geomorphic and gravel bar map across transition zone between upper Moses Coulee and Sagebrush basin.

The eastern channel network of upper Sagebrush basin drains into Coyote Creek. Here there is a fan-shaped gravel deposit and set of elongate, gravel bars that line the sides of Coyote Creek (Figs. 3-2C, 3-2D, 3-3C, 3-6; Hanson, 1970, p. 45). An outcrop at the downstream end of one of these bars consists of a last-glacial flood gravel overlying massive silt, a calcrete horizon,

and a cobble gravel. This sequence rests directly on a bedrock surface that dips eastward up Coyote Creek. The general stratigraphy here is (1) around 1 m of open-work, rounded, basaltic, cobble gravel coated in calcite, grading into (2) < 0.5 m of platy calcrete that caps and encases the gravel, grading into (3) 1-2 m of massive silt, and sharply transitioning into (4) 3-4 m of diamict and gravel (Figs. 3-7, 3-8, 3-9).

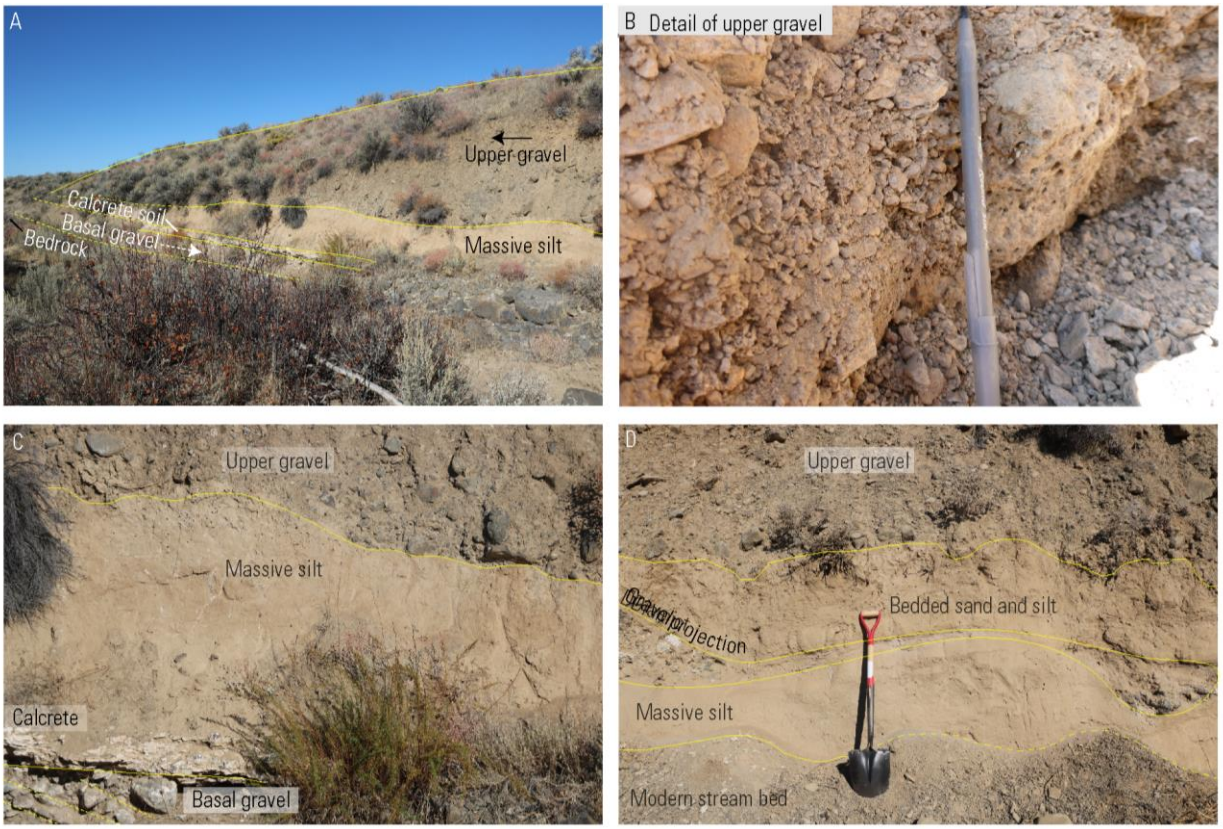

Figure 3-7: Exposure at downstream end of Coyote Creek bar at 47.5162, -119.7042. (A) View showing stratigraphy of old gravel, calcrete soil horizon, massive silt, and last-glacial flood gravel with broadly scoured sharp contact at base. (B) Detail of upper gravel where excavated, showing angular basalt pebbles and sub-rounded cobbles. (C) Detail showing stratigraphy of old gravel, calcrete, silt, and last-glacial flood gravel. (D) Detail to right/upstream of A/C, showing gravel projection structure.

The 3-4-meter-thick gravel at the top of the section consists of angular to sub-rounded, basaltic, pebbles, cobbles, and boulders in a silty matrix and/or open-work facies. While the exposed surface looks like a matrix-supported diamict (Fig. 3-7C), digging into the outcrop reveals clast-supported, angular pebble and cobble gravel (Fig. 3-7B). However, a significant

excavation of the bar was not completed, so the internal architecture and facies remain unknown. Comparison with the "Great Bar" in upper Moses Coulee suggests that the Coyote Creek bars may consist of a variety of gravel and diamict facies.

The predominant shape of gravel clasts in the uppermost flood gravel is angular (Fig. 3-7B). This angularity of some of the clasts in the Coyote Creek flood gravel indicates limited transport distance of the clasts. One explanation for this angularity is that the gravel was deposited during or shortly after bedrock erosion upstream. The bar is downstream from the SE-trending, eastern channel network of upper Sagebrush basin (Fig.3- 6), suggesting that these channels may have been eroding at the same time as the upper gravel in the Coyote Creek bar was accumulating.

The basal contact between the upper gravel and the underlying massive silt is sharp, horizontal, and wavy (Fig. 3-7A), similar in appearance to the broad, erosive scour typical of the lower contacts of subaqueous debris flows (Collinson and Thompson, Fig. 7.14, p. 118). There is no obvious grading in the uppermost gravel. Elongate basalt clasts within the gravel may be preferentially oriented along a near-horizontal axis, also typical of subaqueous debris flows (Collinson and Thompson, Fig. 7.14, p. 118).

A narrow strand of gravel, diamict, and sand projects from the main gravel and appears injected into the silt (Fig. 3-8A). The strand varies laterally in grain size and thickness. In places it consists of pods of unsorted, randomly arranged cobbles in a fine-grained matrix and in other places it thins and fines to bedded, coarse sand (Fig. 3-8C). The clusters of cobbles include higher concentration of jasper (?) and mudstone (?) clasts than the main gravel body (Fig. 3-8D) and one cluster contains a large clast of poorly indurated, white volcanic ash. The preservation of

the fragile ash clast, which would have easily crumbled to pieces in a single collision, hints that the gravel clusters could be pods that traveled in ice blocks (Carling et al., 2009, Plate 37C). The basal contact between the gravel strand and the underlying silt is sharp and wavy. Between the top of the gravel strand and the main gravel body is a zone of thickly bedded silt, with bedding defined by sub-horizontal, resistant lines and, in some cases, color changes from brown to tan (Fig. 3-8B). The upper contact between this bedded silt and the overlying, main gravel body is sharp.

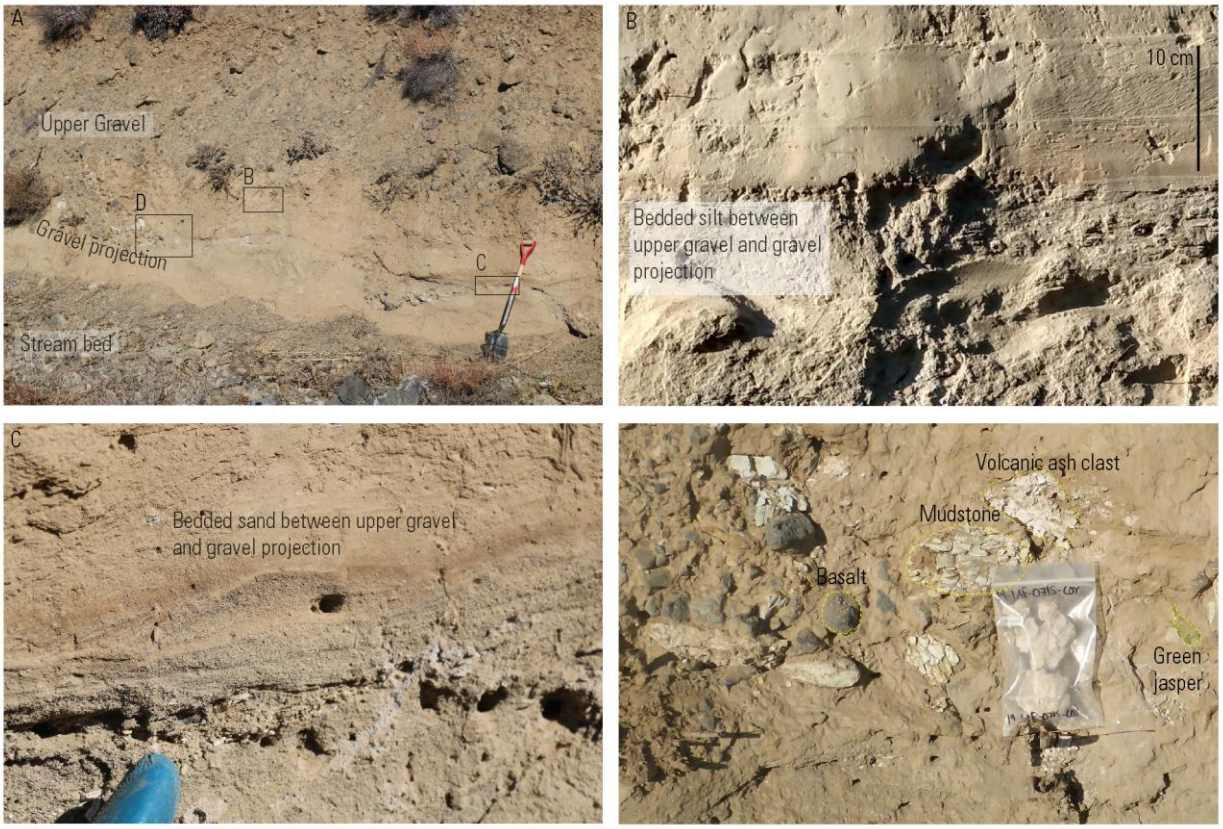

Figure 3-8: Details of projection structure in Coyote Creek bar. (A) Stratigraphic overview showing strand of gravel projecting from main gravel body. (B) Bedded silt at top of fine sediment between gravel projection and main gravel body. (C) Bedded and cross-bedded granules and sand along thinner extent of gravel projection. (D) Gravel pod in projection with higher proportion of non-basalt clasts than main gravel body.

This gravel strand and bedded sand and silt could represent older and smaller flows than the flow which left behind the upper gravel. However, there is no obvious erosive contact between the main gravel body and the gravel strand where the two intersect. Instead, the strand appears to be a continuous extension from the main gravel body. The connectivity suggests that both formed during the same event.

The bedded sand and bedded silt between the gravel strand and the overlying gravel body could be a large rip-up clast or an intraclast that originally accumulated upstream and was then transported as a clast in a debris flow. Sand or silt intraclasts in diamicts often have bedding planes that are tilted relative to the fabric of the diamict (Menzies, 1990, p. 189) and diamicts that contain intraclasts often contain more than one intraclast (Menzies, 1990, p. 190). It would be unusual for an energetic flood to entrain only one rip-up clast and to maintain the horizontal orientation of that clast during transport. The Coyote Creek diamict appears to contain one intraclast, and the bedding within that possible intraclast is oriented parallel to the internal fabric, erosive contacts, and bed orientation of the diamict. The conformity between silt and sand bedding and diamict fabric may indicate that the bedded sand and silt formed in the midst of debris flow pulses, when flow conditions changed such that sand and silt were deposited from suspension.

3.3.3.1 Possible pre-last glacial megaflood

At the base of the Coyote Creek bar exposure is a cobble gravel beneath a 0.5 m-thick calcrete horizon (Fig. 3-7C). This sub-rounded gravel consists entirely of basalt. The gravel clasts are coated with calcite which occurs as veins on the outside of clasts or as rough pendants

on the base of clasts (Fig. 3-8D). Clasts in the basal gravel range from small cobbles (Fig. 3-8D) to granules (Fig. 3-8B). The gravel appears crudely stratified into upstream-dipping beds (Fig. 3-8A, 3-8C), though the existence of these dipping beds is subjective. These upstream-dipping beds, if real, suggest that the gravel may have been deposited in a pre-last glacial Moses Coulee flood that flowed up or across Coyote Creek. Within the gravel, elongate clasts tend to lean in an upstream direction and there is a tendency for such clasts to be arranged in upstream-leaning stacks (Fig. 3-8C, yellow shading), suggestive of imbrication in flows up or across Coyote Creek.

An alternative interpretation is that the gravel accumulated in a Coyote Creek flash flood. Open-work cobble gravel consisting of angular to rounded basalt clasts occurs in terraces along Pine Canyon where Pine Canyon flows into the western side of Sagebrush basin in Moses Coulee, well above the limit of last-glacial megafloods. These Pine Canyon gravels must have accumulated in floods down Pine Canyon from rain and/or snowmelt. Similar flood flows may have descended Coyote Creek during past rain or rain on snow events. Thus, it is the architecture of upvalley-dipping fore-sets and upvalley-imbrication, rather than the grain size, that are the key criteria for inferring whether the old Coyote Creek gravel is from a glacial megaflood or a rainfall-induced flash flood. The absence of granite or quartzite and the absence of glacially striated rocks in the old gravel is not a significant determinant of whether the old gravel formed in a glacial megaflood, as last-glacial flood gravels in Moses Coulee also typically lack erratics and striated clasts, instead typically consisting entirely of water-worked basalt (Fig. 3-5C, 3-7B).

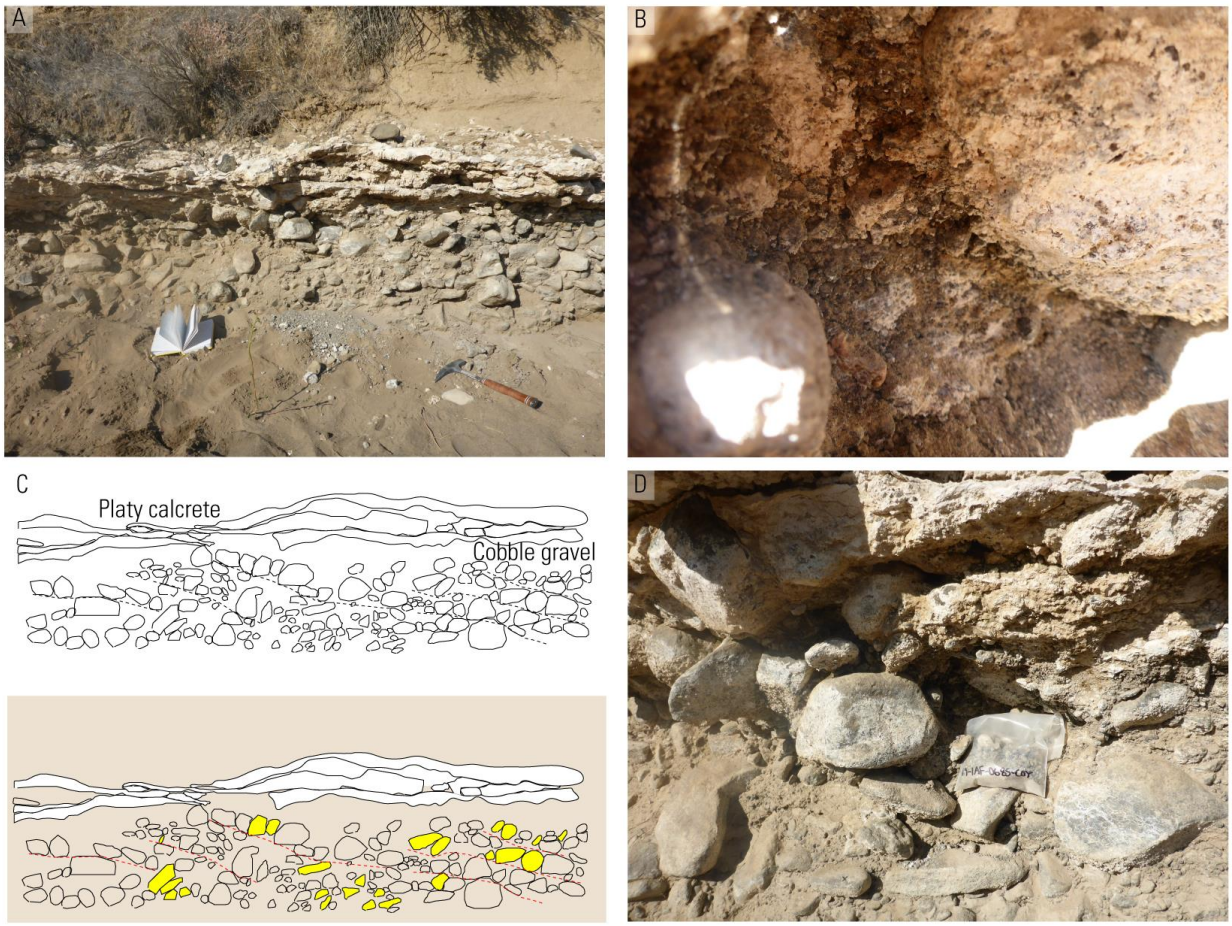

Figure 3-9: Details of cobble gravel beneath calcrete horizon in Coyote Creek bar. (A) Cobble gravel beneath calcrete horizon. (B) Basalt granules near top of cobble gravel bed. (C) Sketch of cobble gravel clasts. Dashed lines indicate possible bedding planes, and yellow in-filling indicates imbricated clasts. (D) Calcite veins and pendants on cobbles in old gravel.

The old cobble gravel, whatever its origin, must be older than the calcrete horizon above the gravel. Thus, the age of the calcrete horizon is a minimum for the age of the gravel deposition. The calcrete horizon has a platy appearance and is around 0.5 m thick (Fig. 3-9A) Fine-scale textures present in the calcrete include porous drip structures (Fig. 3-10A), botryoidal mounds (Fig. 3-10B), finely laminated calcite and opal (?) (Fig. 3-10C), breccia with a calcite matrix and calcite and basalt clasts (Fig. 3-10C), and folded layers (Fig. 3-10D). Some of the

calcrete contains floating sand, silt, and pebbles (Fig. 3-10D), while other zones consist mainly of clean calcite (Fig. 3-9C). The platy appearance, significant thickness, and diverse textures in this calcrete are characteristic of well-developed calcrete soils that likely require much more than 20,000 years to form in the Columbia basin, suggesting that the calcrete pre-dates the last glacial episode of Moses Coulee megafloods. Textural comparison with less-developed soil carbonate formations in Sand Hills Coulee that are 8,000 to 30,000 years old (Lechler et al, 2018, Fig. 2) suggests that the Coyote Creek calcrete is much older.

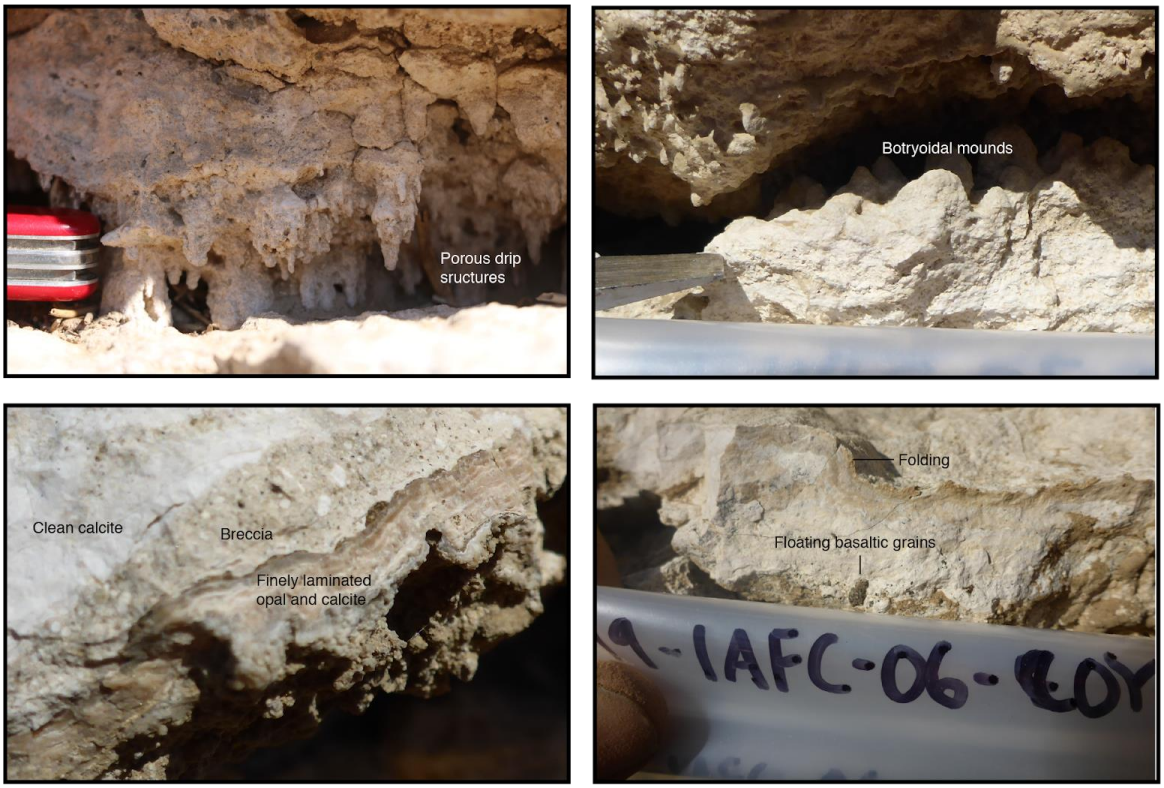

Figure 3-10: Details of calcrete horizon at base of Coyote Creek bar. (A) Drip structures with holes indicating leaching (81 ± 2 ka) (B) Botryoidal mounds (3.9 ± 0.3 ka) (C) Laminated opal and calcite overlain with calcite breccia (120 ± 6 ka), overlain by clean, dense calcite (217 ± 3 ka). (D) Floating basaltic grains in calcite matrix, with apparently folded brown calcite layer at top of horizon.

U-series analysis of calcrete of varying textures from the deposit returned scattered results, with apparent ages ranging from 3.9 ± 0.4 ka to 217 ± 3 ka, and two samples undatable with ($^{230}Th/^{238}U$) activity ratios well above 1, indicative of uranium leaching (Table 3-2). Textural evidence for leaching and re-precipitation (Fig. 3-10A, 3-10B), and these age data both suggest a complex history of calcite formation, leaching, and re-precipitation. The samples with clear evidence of uranium loss have less dense textures compared to samples without clear evidence of uranium loss, which have denser textures. Therefore, while nominal U-series ages on the calcrete that range from 3.9 ± 0.4 ka to 217 ± 3 ka should be treated with caution until the ages can be replicated, samples with dense or crystalline textures may give a more accurate sense of the age of calcrete formation. Two ages on denser, cleaner calcrete zones are 120 ± 6 ka and 217 ± 3 ka. The oldest age of 217 ± 3 ka comes from a zone of dense, clean calcite with no textural evidence of leaching. If this age is accurate and unbiased by uranium loss, it suggests that the calcrete and underlying gravel may have formed more than 200,000 years ago. This would suggest that the last episode of Moses Coulee megafloods was not during the penultimate glaciation of MIS 6 or the previous MIS 8 glacial, but during an earlier glacial interval.

Table 3-1: U-series ages on calcrete that overlies cobble gravel near base of Coyote Creek bar**.**

Sample ID	Sample texture	Analysis notes	^{238}U (ng/g)	^{232}Th (pg/g)	$\delta^{234}U$ (per mil)	($^{230}Th/^{238}U$) activity	Age (yr. BP) (corrected)	± (2σ)
1 02-COY-A	Powdery, botryoidal	Low yield	21,315	508,864	48	0.04	3,929	352
2 01-COY-B	Mini stalactite		1,822	280,516	92	0.6	81,340	2,343
3 02-COY-B	Powdery, porous		1,649	486,382	120	0.71	98,232	4,512
4 04-COY-B	Laminated silica and calcite	Residual solids	2,387	852,777	51	0.74	119,761	6,275
5 04-COY-A	Dense, white		1,245	89,959	129	1.01	217,196	2,730
6 03-COY-A	Powdery	Likely U loss	992	11,987	454	3.32	N/A	
7 06-COY-A	Flakey, tan-colored	Likely U loss	2,054	128,054	246	1.82	N/A	

3.3.4 Timing of last-glacial Moses Coulee floods

Exposed gravel deposits in Moses Coulee show little evidence of multiple floods during the last glaciation. In contrast, stratigraphy at the delta that built outward from the mouth of Moses Coulee indicates multiple large floods from Moses Coulee during the last glaciation (Fig. 3-11). The absolute timing of these last-glacial floods is not directly determinable from gravel strata in the delta, though varves between gravel beds, if interpreted as annual, provide a minimum estimate of the total duration over which floods occurred (Waitt, 1985, p. 1276). This stratigraphy, combined with new exposure ages, indicates that multiple floods occurred in Moses Coulee between around 19 to 15 ka. However, it remains unclear whether the flooding occurred within several decades to centuries, as indicated by varve counts in Rock Island bar, or whether the flooding spanned millennia as suggested by the exposure ages. The exposure ages likely provide an overestimate of the flooding interval due to geologic error, while the varves likely provide an underestimate of the flooding interval, due to erosion of varves by subsequent floods (Fig. 3-12A).

3.3.4.1 Stratigraphy of delta at outlet of Moses Coulee

A prominent terrace that fills ⅔ the width of the Columbia valley at the mouth of Moses (Figs. 3-1, 3-4, 3-11, 3-12) contains beds of angular, basaltic gravel (Bretz, 1930, p. 392-393), organized into up-valley dipping fore-sets and imbrication fabric reflecting flow up the Columbia River and away from Moses Coulee (Bretz, 1930, p. 396). These characteristics indicate that these basaltic gravel beds accumulated in outflows from Moses Coulee outburst floods into the Columbia River (Bretz, 1930, p. 396; Hanson, 1970, p. 70).

The stratigraphy of this delta was originally described as a lowermost granite-basalt gravel containing 10-20% granite, a transitional gravel with less than 10-20% granite and containing clasts of peat and clay, and an uppermost pure-basalt gravel (Hanson, 1970, p. 69-70).

More detailed observation upstream at Rock Island delta, once part of a continuous fill with Moses Coulee delta, revealed rhythmic repetition of basaltic gravel beds, each of which fine upward into silt, and some of which are interbedded with varved clays (Waitt, 1985, p. 1275-1276). Four separate basaltic gravels, each separated from the other by a silty cap and by 0 to 37 varves, implied four separate floods through Moses Coulee (Waitt, 1985, p. 1275). Varves, if interpreted as yearly, provided a minimum estimate of recurrence interval between floods. Inter-gravel varves were counted as 0 above the uppermost two beds, 3 above the second lowest bed, and 37 above the lowest bed, though erosive contacts between gravel and varved clays showed that flood recurrence intervals estimated from varves would only provide a minimum recurrence time between Moses Coulee floods (Waitt, 1985, p. 1275). The sequence of varves and basalt gravels is conformably overlain by 11 meters of rhythmically bedded sand and silt, interpreted as back-flows from the Quincy Basin into the Columbia River (Waitt, 1985, p. 1275). This, finally, is overlain by a granite and metamorphic clast-rich boulder gravel, the surface of which is organized into transverse gravel dunes oriented perpendicular to the Columbia (Waitt, 1985, p. 1276). The entire sequence represents an early down-Columbia flood (Hanson, 1970, p. 70), at least four Moses Coulee floods, repetitive Quincy Basin floods that back-flooded up the Columbia River, and a final down-Columbia outburst flood (Waitt, 1985, p. 1276).

Reconnaissance stratigraphy of the Rock Island deposit in summer 2022 confirmed and complicated previous observations. Slumping of the embankment had obscured the lower ⅔ of

the section, covering basaltic gravel bed 1 that outcropped in the 1970's as seen in a black and white field photo (Waitt, 1985, Fig. 9). Working along the upper ~⅓ of the section, Brian Atwater and I observed three fining upwards packages of gravel, sand, and silt, each capped with varved clays (Fig. 3-11; 3-12). We observed laterally variable erosion of varves atop each package (Fig. 3-12A), resulting in no varves preserved in some places and tens of varves preserved elsewhere above the same gravel bed. While Waitt (1985) observed no varves above the two highest basalt gravel packages, we observed up to tens of varves above each of the two highest basalt gravel packages. Laterally variable erosion of varves and changes in exposure due to slumping likely explain this discrepancy between observations. The new observations of varves higher in the section than previously recognized suggests that there were originally varves between all gravels, but that those varves have been completely eroded in places. If the varves are annual, this suggests that multiple years elapsed between each Moses Coulee flood recorded in Rock Island delta, not just between the first two floods as originally interpreted (Waitt, 1985, p. 1275).

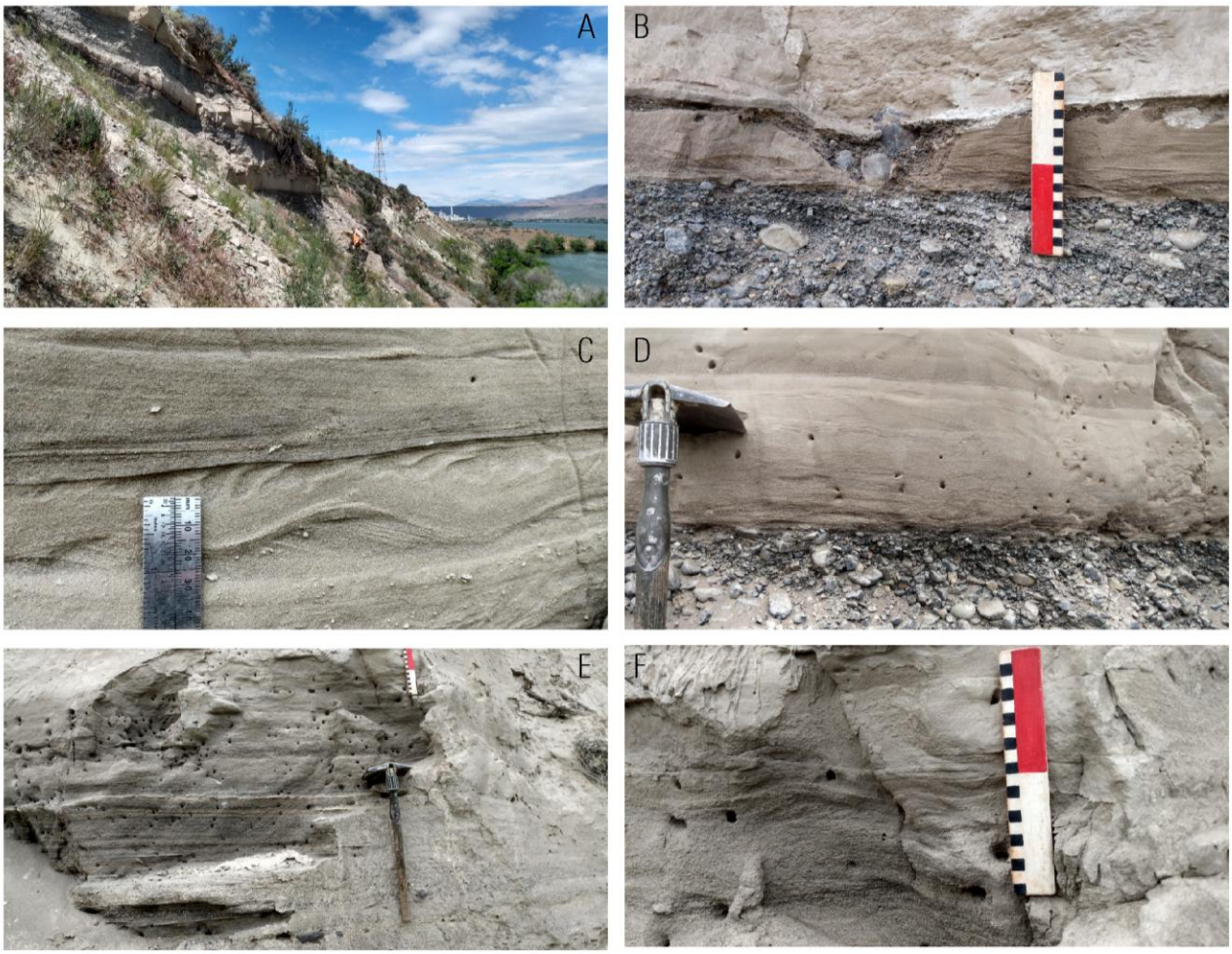

Figure 3-11: Exposures of Rock Island delta at outlet of Moses Coulee. (A) Three dark bands in outcrop are basaltic gravel-to-silt flood beds, each capped with varves. (B) Gravel clinoforms dip upstream (to right). Second gravel layer eroded into bedded sand suggests changing flow conditions and multiple high-energy pulses in a single flood. (C) Upvalley-dipping sand clinoforms and flame structures beneath horizontally bedded sand indicative of rapid deposition on wet sediment. (D) Typical Moses Coulee bed consisting of basaltic gravel that abruptly transitions to bedded sand fining upward into bedded silt. (E) Plane-bedded sand at base of 2022 exposure (~⅔ of the way above base of section). (F) Downvalley-dipping sand clinoforms at top of plane-bedded sand shown in (E).

Figure 3-12: Varves of Rock Island delta. (A) Erosive contact between cobble gravel and varves. (B) Details of varves above gravel near top of section (C) Typical fining upward sequence of cobble gravel to silt transitioning into varves.

The position of the three basaltic gravel packages that we observed is similar to beds 2, 3, and 4 of Waitt (1985) and thus we likely observed the same gravels as Waitt (1985). However, bed 1 of Waitt (1985) was covered during our visit in 2022, located tens of meters below the lowest exposure of basalt gravel that was visible in 2022. Below the lowest basalt gravel package visible in 2022, but above the lowest basalt gravel observed by Waitt (1985), we observed a package of plane-bedded sand of mixed lithology that transitions upwards into sand structured into down-valley dipping clinoforms (Fig. 3-11E, 3-11F). The sand fines upward into silt and is capped by a few pairs of varved clay. This sand package is apparently between bed 1 and bed 2 of Waitt (1985) and was thus deposited in between two Moses Coulee floods or in the waning

stage of a Moses Coulee flood. The plane-bedded sand with down-valley dipping sand clinoforms seems to reflect flows down an open Columbia River, though it could also reflect sloshing in a lake upstream of the Moses Coulee delta sediment dam. The varves atop the package indicate that down-valley flow was followed by re-establishment of a low-energy, lake environment.

3.3.4.2 Exposure ages

^{10}Be ages from iceberg-rafted boulders in central Moses Coulee range from 28.1 ± 1.4 ka to 13.8 ± 0.7 ka (n=7; Table 3-2). These ages come from cobbles and boulders on or within sandy silt deposits that typically contain clusters of crystalline erratics. We interpret these deposits as remnants from melted icebergs that arrived in megafloods.

The exposure ages come from samples that span the elevation range of flood-impacted terrain. The highest-elevation sample in the group, 19-IAF-091-MOS, is located at 570 m, ~95 meters above the sediment-filled inner channel of Moses Coulee, and on a terrace above scabland topography. The exposure age for this sample was 18.8 ± 1 ka, possibly reflecting a deep flood early in the last glacial episode of flooding.

However, the oldest of the ages is 28.1 ± 1.4 ka, inconsistent with evidence that the CIS did not exist at that time (Clague, 2009, Fig. C72). This anomalous quartzite cobble was likely pre-exposed before being eroded by the CIS and transported into Moses Coulee. This suggests that other erratics in Moses Coulee could also be biased old due to inheritance.

The youngest exposure age of 13.8 ± 0.7 ka is also inconsistent with regional geologic history, as the Okanogan lobe margin was to the north of the Columbia River by 14 ka (this study, Chapter 1), and the presence of Glacier Peak Set G/B tephra throughout Moses Coulee

and on the glaciated Waterville Plateau indicates that glacial floods and Waterville Plateau glaciation had ended by 13.5 ± 0.2 ka. The boulder with the anomalously young age of 13.8 ± 0.7 ka was embedded in a deposit of sandy silt with a top surface 18 cm above the soil. A plausible explanation for the young age is that post-glacial winnowing by wind and water removed tens of centimeters of sand and silt that initially covered the rock, resulting in a period of attenuated cosmic ray flux and an exposure age younger than the depositional age.

Table 3-2: Exposure ages flood-transported boulders and cobbles in Moses Coulee.

Sample	Latitude	Longitude	Altitude (m)	Sample substrate	Exposure age (ka)	Error (2σ)
1 095-MOS	47.52711	-119.7088	557	Erratic-rich silty sand, flat.	13.8	0.7
2 090-MOS	47.54043	-119.73371	565	Erratic-rich silty sand, slope.	15.5	0.8
3 104-MOS	47.48475	-119.77719	511	Erratic-rich pavement over silty sand, flat.	16.1	0.8
4 092-MOS	47.51173	-119.72022	530	Erratic-rich silty sand, flat.	16.3	0.7
5 094-MOS	47.51891	-119.71362	543	Erratic-rich pavement over silty sand, flat	17.4	0.8
6 091-MOS	47.53722	-119.73732	570	Embedded in erratic-bearing gravel, flat.	18.8	1
7 093-MOS	47.51891	-119.71362	543	Erratic-rich pavement over silty sand, flat	28.1	1.4

Figure 3-13: Photographs of six dated cobbles and boulders from Moses Coulee dated using the ^{10}Be method.

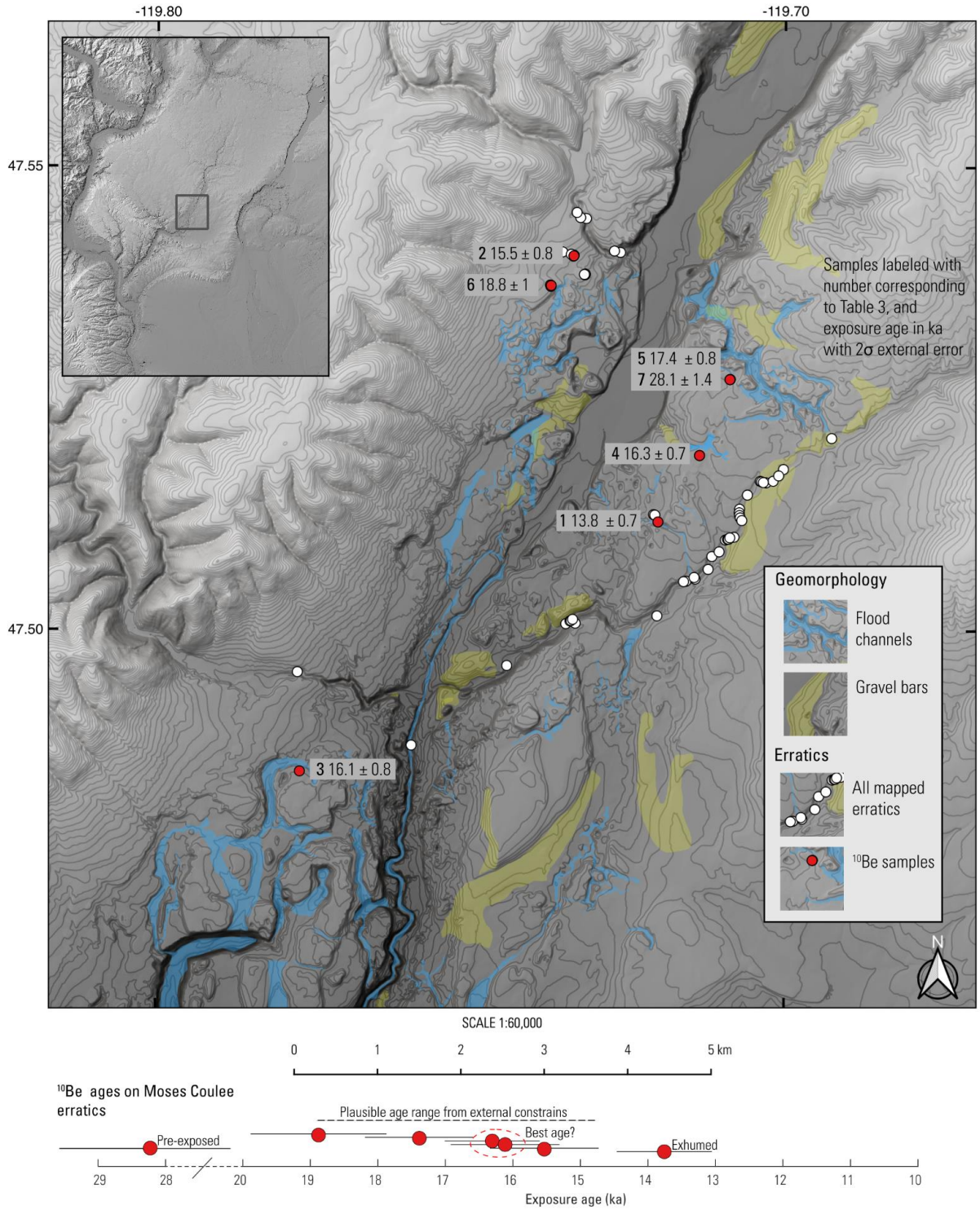

Figure 3-14: Locations of Moses Coulee surface exposure dating samples.

A pair of two samples on opposite sides of the inner channel near the upstream end of Sagebrush basin suggests that the age from one of the two samples is wrong, either due to inheritance, exhumation, or erosion. Sample 19-IAF-094-MOS (5 in Fig. 3-13)), a cobble located at 543 m, gave an age of 17.4 ± 0.8 ka, whereas sample 19-IAF-095-MOS (2 in Fig. 3-13), a boulder at 565 m, gave an age of 15.5 ± 0.8 ka. If a flood had inundated this reach of Moses Coulee to 565 m at 15.5 ± 0.8 ka it would have likely inundated the lower sample site to a depth of at least 22 meters, likely producing a strong enough flow to sweep away the cobble. Yet, the exposure age for that cobble suggests that it has been there since 17.4 ± 0.7 ka. One explanation for this apparent discrepancy is that the higher-elevation sample doesn't directly date a megaflood but dates the time of boulder exhumation from megaflood sediment. This explanation is motivated by the observation that the higher-elevation, apparently younger sample was embedded in sandy silt (Fig. 3-14) and located on a slope (Fig. 3-14), while the lower-elevation, apparently older sample, was perched on a rocky pavement on a flat surface (Figs. 3-13, 3-14). Erosion by slope wash is more likely to have progressively exhumed the sample on the silty slope than the sample on the flat, rock pavement. Another explanation is that the lower-elevation rock returned an exposure age that is too old due to inherited isotopes. This is plausible because the population of seven samples contains one sample that is clearly pre-exposed, suggesting potential influence of pre-exposure on all samples in the population, though the obviously pre-exposed sample was a more resistant quartzite than 19-IAF-094-MOS, a granite. A third explanation for the discrepancy is that the water surface of a 15.5 ± 0.8 ka flood dropped so steeply between the more upstream 19-IAF-094-MOS (2 in Fig. 3-14) and the more downstream 19-IAF-090-MOS (5 in Fig. 14) that the lower-elevation sample was not inundated or moved.

Elevations of high-water indicators and flow dynamics of a confined flow expanding into Sagebrush basin do suggest that the water surface profile would have been steeper near these samples (Fig. 4), though the exact water surface slope is not clear.

Ignoring the clearly pre-exposed sample with an age of 28.1 ± 1.4 ka (7), the clearly exhumed rock with an age of 13.8 ± 0.7 ka (1), and the possibly exhumed rock with an age of 15.5 ± 0.8 ka (2), the four remaining samples date between 16.1 ± 0.8 ka and 18.8 ± 1.0 ka. Within this group of four, there is a consistent trend of younger ages at lower elevations (Table 3). The small number of samples provides little confidence in the apparent age-elevation trend. Additionally, it is difficult to see how any other exposure age-elevation trend would be preserved. Floods tend to move or bury rocks that they inundate, meaning that a flood-transported erratic from an older flood would typically not be preserved if subsequent floods occurred. However, if the age-elevation trend is meaningful, and Moses Coulee flood stage did lower throughout the last glaciation, this could be explained by deepening or widening of Moses Coulee channels, and/or by a decrease in water influx from the flood source(s). Prevalence of fresh, angular basalt gravel in flood bars suggests active channel erosion during the last glaciation, consistent with the idea that channel deepening or widening may have contributed to a lowering of flood stage through the last glacial episode of flooding.

3.4 Scenarios for Moses Coulee megafloods

While there exists a scientific consensus that Moses Coulee experienced megafloods, there is no universally accepted theory for the source of those floods. Geologists have developed two distinct scenarios for the source of Moses Coulee megafloods. Though the scenarios are not mutually exclusive nor are they the only possible explanation for Moses Coulee floods, they are

a helpful starting point for analyzing how floods drained into Moses Coulee. The first, the Missoula flood spillover scenario, posits that Moses Coulee floods occurred when Missoula floods diverted by the Okanogan lobe spilled into Moses Coulee (Hanson, 1970, Fig. 20; Waitt, 2021). The second, the Okanogan lobe subglacial outburst flood scenario, posits that Moses Coulee floods occurred when subglacial meltwater from the Okanogan lobe drained directly into the Moses Coulee basin (Lesemann and Brennand, 2009).

3.4.1 The Missoula flood spillover scenarios

The Missoula flood spillover scenarios posit that the Okanogan lobe, blocking the Columbia River north of the Waterville Plateau, diverted Missoula floods from the Columbia River into Moses Coulee. In this family of scenarios, Missoula floods flow into a glacial Lake Columbia impounded by an incipient Okanogan lobe and swell the lake level, resulting in over-spills across the lowest divides along the southern shores of glacial lake Columbia. The pathways of spillovers depend on the elevations of spillways and/or impoundments across them, with floodwaters preferentially draining through lower and open spillways. Many of these spillways likely deepened and widened during the last glaciation, and possibly after Moses Coulee floods, but the extent and timing of erosion of key spillways remains unclear, and thus it remains unclear what the elevations of key spillways were at the time of last-glacial Moses Coulee floods. Additionally, glacial isostatic adjustment in response to the Cordilleran Ice Sheet load resulted in changes to absolute elevations and relative displacements between spillways (Pico et al., 2022).

The spillover scenarios for Moses Coulee flooding all require intermediate stages of Okanogan lobe glaciation, such that the Okanogan lobe is thick and extensive enough to block the Columbia River north of the Waterville Plateau, preventing Missoula floods from draining

through the Columbia mainstem, but not so extensive that it blocks flow into Moses Coulee (Hanson, 1970, p. 83).

Secondly, and most critical for routing Missoula flood water into Moses Coulee, upper Grand Coulee must have not existed in its present form to route Missoula floods into Moses Coulee (Hanson, 1970, p. 79). This requirement stems from the flood-routing implications of modern Grand Coulee. With a floor at ~470 m, depth of 200 to 250 m, cross-sectional area of 3-10 km, and position upstream of Moses Coulee, Grand Coulee is a low and large conduit upstream of Moses Coulee. Modern Grand Coulee would drain most Missoula floodwater into Quincy Basin at a point upstream from Moses Coulee, resulting in a peak flood stage too low to inundate the Waterville Plateau and thus too low to send significant flows into Moses Coulee (Hanson, 1970, p. 79; Denlinger et al., 2021, Fig. 8, Scenario 3B).

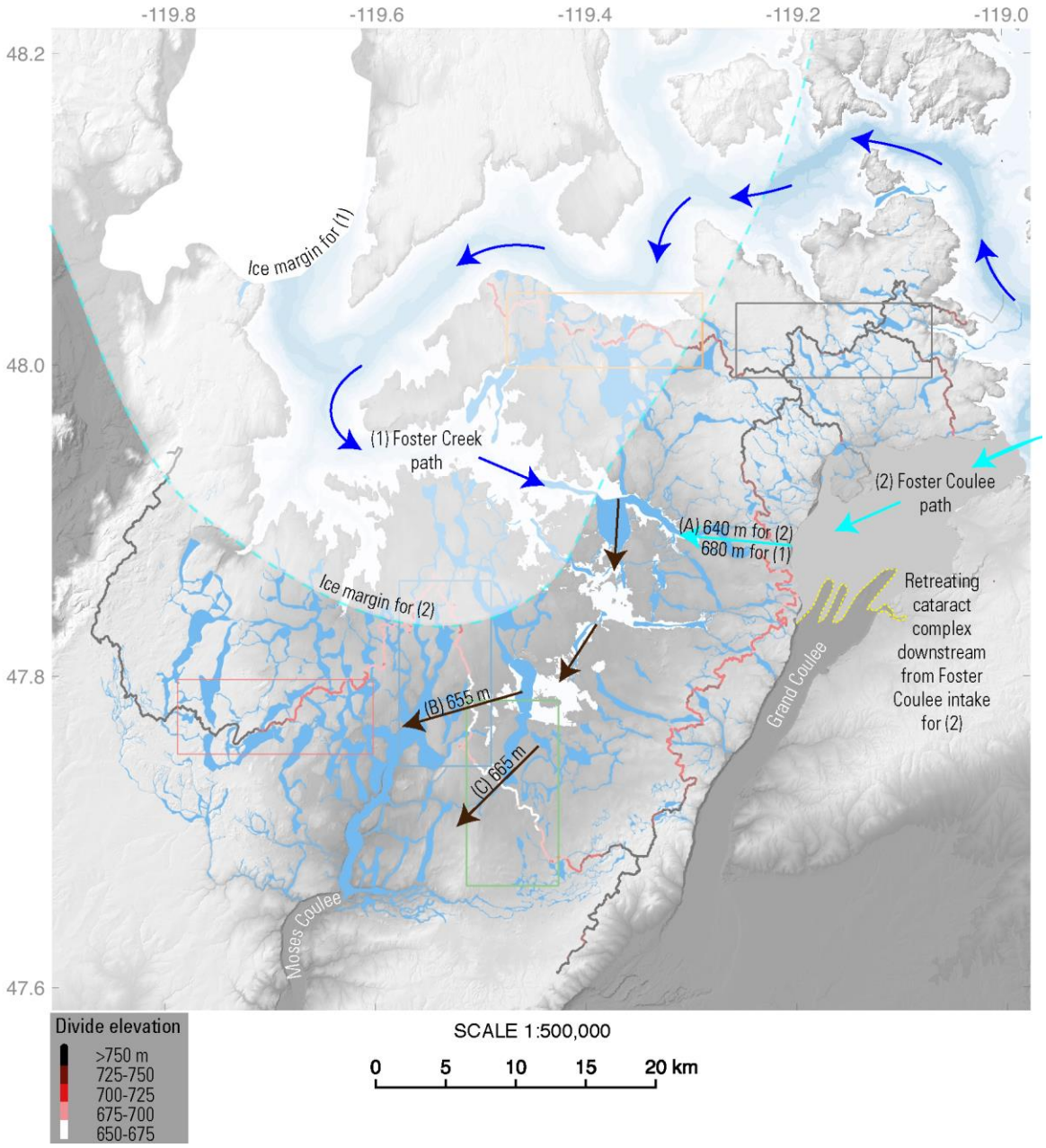

Figure 3-15: Map of two spillover scenarios for routing large surface floods into Moses Coulee. Base map shows two possible ice extents of the Okanogan lobe, and a glacial lake Columbia (color-coded by depth from blue deeps to white shallows) that is impounded by rock in upper Grand Coulee and by an incipient Okanogan lobe (labeled "Ice margin for (1)"), resulting in spillover across the divides (B) and (C) into Moses Coulee, assuming that divide (A) of upper Foster Coulee is not yet cut to its modern 640 m elevation, which would instead route water eastwards back into Grand Coulee.

With Grand Coulee restored to the elevation of the surrounding uplands (680 to 700 m), and with the Okanogan lobe across the Columbia River, there are two low-elevation pathways that Missoula floods could have taken into Moses Coulee: the up-Foster Creek path (Fig. 3-15, scenario (1)), and the down Foster Coulee path (Fig 3-15, scenario (2)).

The up-Foster Creek path sends Missoula flood water into a glacial lake Columbia with an arm that fills the Foster Creek basin and fills the Foster Creek basin with water until spillover commences across one or both of the low divides to the east of Moses Coulee. This scenario requires an Okanogan lobe margin that is both downstream of the mouth of Foster Creek, but thick and extensive enough to create an ice dam across the Columbia River in order to pond glacial lake Columbia. This scenario also requires that upper Grand Coulee remain uneroded and filled in with rock, as the modern Grand Coulee would result in too much water lost to Quincy Basin, and a flood stage too low in the Foster Creek basin to overspill into Moses Coulee. Additionally, this scenario requires that upper Foster Coulee remain uneroded and filled in with rock. This requirement about Foster Coulee is imposed because the modern elevation of the floor of Foster Coulee at the divide between Foster Creek and Grand Coulee is 640 m, about 15 m lower than the lowest 655-meter divide into Moses Coulee. With the modern 640 m divide in upper Foster Coulee, rising water levels in a Foster Creek arm of glacial lake Columbia would spill out through Foster Coulee into Grand Coulee, rather than across the higher 655 m divide into Moses Coulee. But, with upper Foster Coulee and Grand Coulee restored to the heights of their surrounding uplands, and the Okanogan lobe securely blocking the Columbia River downstream of Foster Creek, the outflow of glacial lake Columbia would be through its Foster Creek arm and over a 655-meter divide near Badger Wells, with overspill entering into Moses

Coulee (Waitt, 2021, p. 376). When flood-swollen, the depth of outflow across this divide could have reached around 50 meters before water from glacial lake Columbia began spilling across the Telford Crab-Creek or Grand Coulee divides.

Restoration of upper Foster Coulee to the height of surrounding uplands is however less favorable for the down Foster Coulee path into Moses Coulee. The down Foster Coulee scenario routes glacial lake Columbia spillover across a pre-upper Grand Coulee upland or through a partially open Grand Coulee, into upper Foster Coulee, south out of Foster Coulee due to downstream ice blockage, and finally across the 655 m divide (B) into Moses Coulee. The higher the divide in upper Foster Coulee, the less water is able to travel along this pathway, thus a modern Foster Coulee configuration is most favorable for this pathway. However, an even less developed Grand Coulee configuration is required for this pathway. The position of the inferred retreating cataract complex in upper Grand Coulee must be downstream (south) of the intake to Foster Coulee. Once the cataract complex had retreated to the north of the Foster Coulee intake, the flood surface at the Foster Coulee intake would have dropped, likely below the height needed to route water into Foster Coulee.

Table 3-3: Two overland scenarios for routing Missoula floods into Moses Coulee and required geometries of Grand Coulee, Foster Coulee, and the Okanogan lobe for each scenario.

Overland pathway into Moses Coulee	**Condition of upper Grand Coulee**	**Condition of upper Foster Coulee**	**Condition of Okanogan lobe**	**Level of glacial lake Columbia**
Up Foster Creek	Uneroded, position of the retreating cataract complex irrelevant	Uneroded, to block outflow into Grand Coulee	Margin downstream of Foster Creek mouth, but ice thick and extensive enough to totally block Columbia River.	655 m, controlled by divide (B) between Foster Creek and Moses Coulee
Down Foster Coulee	Uneroded, retreating cataract complex preferably to the south of upper Foster Coulee intake	Preferably eroded, allowing more water to drain onto the Waterville Plateau	Ice securely blocking the Columbia River, but margin to the west of low elevation drainage path between Foster Coulee divides (B) and (C).	700 m? Controlled by the Grand Coulee divide between the Columbia River and Quincy Basin

3.4.2 The subglacial flood scenario

The subglacial flood scenario posits that Moses Coulee flooded in subglacial outbursts from the Okanogan lobe (Fig. 3-16; Lesemann and Brennand, 2009, p. 2439). A viable possibility for generating outburst floods during maximal Okanogan lobe glaciation is subglacial volcanism. Tuyas, flat-topped volcanoes that form under ice, are widespread throughout areas glaciated by the Cordilleran Ice Sheet, including beneath ice and meltwater source areas that fed the Okanogan lobe. The Wells-Gray tuya field to the east of the Fraser Plateau erupted basaltic tuyas during the last glaciation (Hickson et al., 1995). Meltwater from Wells-Gray eruptions

would have routed through the Thomson Valley, into the Okanogan Valley, and drained to the margin of the Okanogan lobe (Lesemann and Brennand, 2009, Fig. 1).

The largest glacial outburst floods in recorded history occurred as a result of subglacial volcanic eruptions. The 1918 Katla caldera eruption in Iceland resulted in an outburst flood with a maximum flow rate of 3×10^5 m^3/s (Tómasson, 1996, p. 249, p. 254) and the Holocene eruption of Kverkfjo¨ll released discharges up to 2×10^5 m^3/s (Carrivick, 2006, p., 191). These values are similar to Moses Coulee floods modeled with the threshold shear stress model for bedrock erosion, which predicts peak discharges of around 4 to 6×10^5 m^3/s (Larsen and Lamb, 2016, Fig. 3), but likely too low to explain inundation depths in Moses Coulee with modern topography or with the inner channel filled.

The simplest version of the subglacial flood scenario is that floods in Moses Coulee occurred when the southern margin of the Okanogan lobe was in the Moses Coulee basin. Under this ice configuration, subglacial water sourced from throughout the Okanogan drainage basin would travel across hydro-potential gradients beneath the Okanogan lobe and emerge from the Okanogan lobe into the Moses Coulee basin (Lesemann and Brennand, 2009, p. 2439). Depending on the ice extent and ice thicknesses, water may also have emerged from the Okanogan lobe into the Columbia River, Grand Coulee, or Foster Creek basins. The subglacial water routing and ultimate destination of Okanogan lobe meltwater would have depended on the geometry of the Okanogan lobe. The geometry most favorable to sending water into Moses Coulee would have been the near-maximum Okanogan lobe configuration, with ice in the Columbia valley west of the Waterville Plateau creating a zone of high hydro-potential that blocked water from draining to the ice margin in the Columbia valley between Chelan and

Brewster, and an ice margin in the Moses Coulee basin allowing floodwater to enter Moses Coulee without crossing any divides sub-aerially.

If subglacial floods occurred when the Okanogan lobe margin was to the north of the Foster Creek-Moses Coulee divide, water would have emerged from the glacier into the Foster Creek basin, and like in the overland scenario, water could only enter Moses Coulee when upper Foster Coulee and upper Grand Coulee remained uncut. If upper Foster Coulee and upper Grand Coulee were open, subglacial water entering the Foster Creek basin would flow into Grand Coulee through upper Foster Coulee.

Like the overland scenario, the subglacial flood scenario requires that Moses Coulee floods occurred after the Okanogan lobe had advanced across the Columbia River, though the two scenarios predict that Moses Coulee floods occurred at different extents of Okanogan lobe glaciation. The subglacial scenario posits that the biggest Moses Coulee floods occurred when the Okanogan lobe was in the Moses Coulee basin and near its maximum extent, while the overland scenario disallow a configuration this extensive because ice blocks overland flow into Moses Coulee.

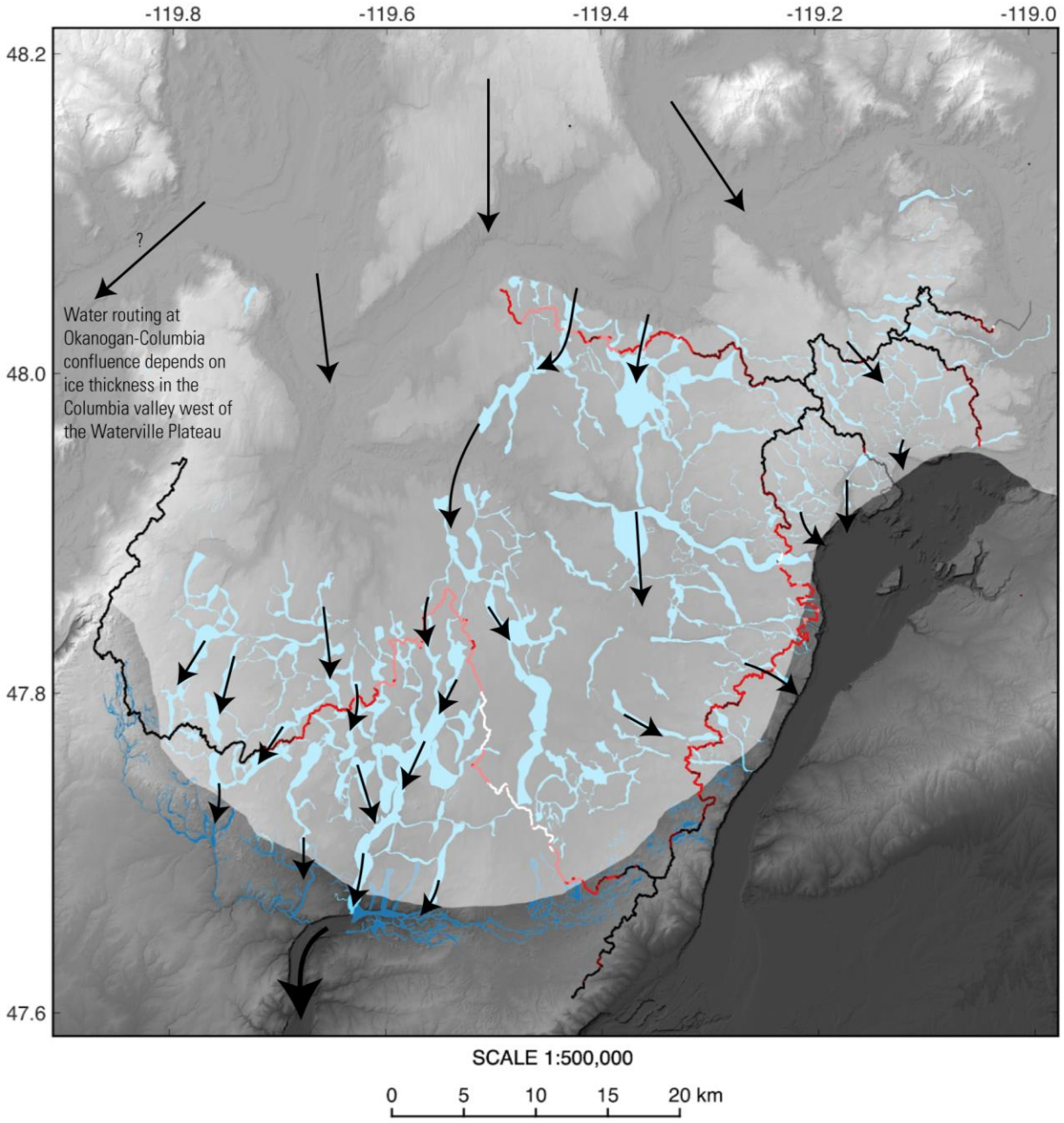

Figure 3-16: Map view of subglacial flood hypothesis, showing mapped valley network on the Waterville Plateau (in light blue), possible ice extent (opaque white) at time of large subglacial floods into Moses Coulee, and position and elevation of hydrologic divides on Waterville Plateau (white to red to black lines). Flows through the western Mansfield channels would have drained into Moses Coulee, while flows through eastern Wilson Butte channels would have drained into Grand Coulee. Smaller, braided channels that dissect the Withrow moraine (highlighted in blue) and follow surface slope gradients are interpreted as ice-marginal channels formed from pro-glacial meltwater.

3.5 GEOLOGIC EVIDENCE PERTAINING TO MOSES COULEE FLOOD SOURCE

3.5.1 Sedimentary record in the Columbia valley between Foster Creek and Grand Coulee

In the up-Foster Creek scenario, a version of glacial lake Columbia would have formed when the Okanogan lobe was just beginning to advance into the Columbia valley, with a margin downstream of Foster Creek. In the most optimal scenario for routing water into Moses Coulee, the Okanogan lobe ice dam formed downstream of Foster Creek *and* was thick enough to maintain a lake level at 660 m (Fig. 3-15). While such an ice margin during advance is consistent with glaciological intuition and with most observations, sedimentary sequences along the Columbia valley suggest that the early Okanogan lobe was thin and its ice dam susceptible to failure. This would have resulted in a lower maximum lake level while the pathway up Foster Creek was open and would have made it harder for water to fill the Foster Creek basin and overtop the divide into Moses Coulee.

Stratigraphies in the Columbia Valley suggest that a stable glacial Lake Columbia might not have formed until the Okanogan lobe ice margin was upstream from Foster Creek and might imply that the early Okanogan lobe ice dam was unstable. A stratigraphy at RM 554, upstream from the site of initial ice damming, suggests a history of down-valley floods in a river that was at least temporarily open prior to site glaciation (Fig. 3-17A), while stratigraphies further up-valley indicate that a stable pro-glacial lake receiving periodic floods existed before those sites were glaciated (Fig. 3-17B, 3-17C). The most downstream observation of lake beds beneath till is near RM 570 (Hibbert, 1985, p. 97; this study, Fig. 3-17B), 25 miles upstream of the Foster Creek mouth at RM 545. Downstream of RM 570, thinner pre-till sediment consists mainly of gravel, sand, and silt, with down-valley dipping clinoforms indicating flow down-valley (Fig. 3-

18A). This pattern suggests that the Columbia River may have initially flowed around or under a thickening and advancing Okanogan lobe that was still too thin to raise the glacial Lake Columbia water level above the critical threshold of Grand Coulee needed to maintain lake stability. In this scenario, an incipient glacial Lake Columbia would have intermittently formed and then drained out through its ice dam. This hypothesized period of lake instability might have coincided with the ice margin configuration necessary for routing floods through Foster Creek.

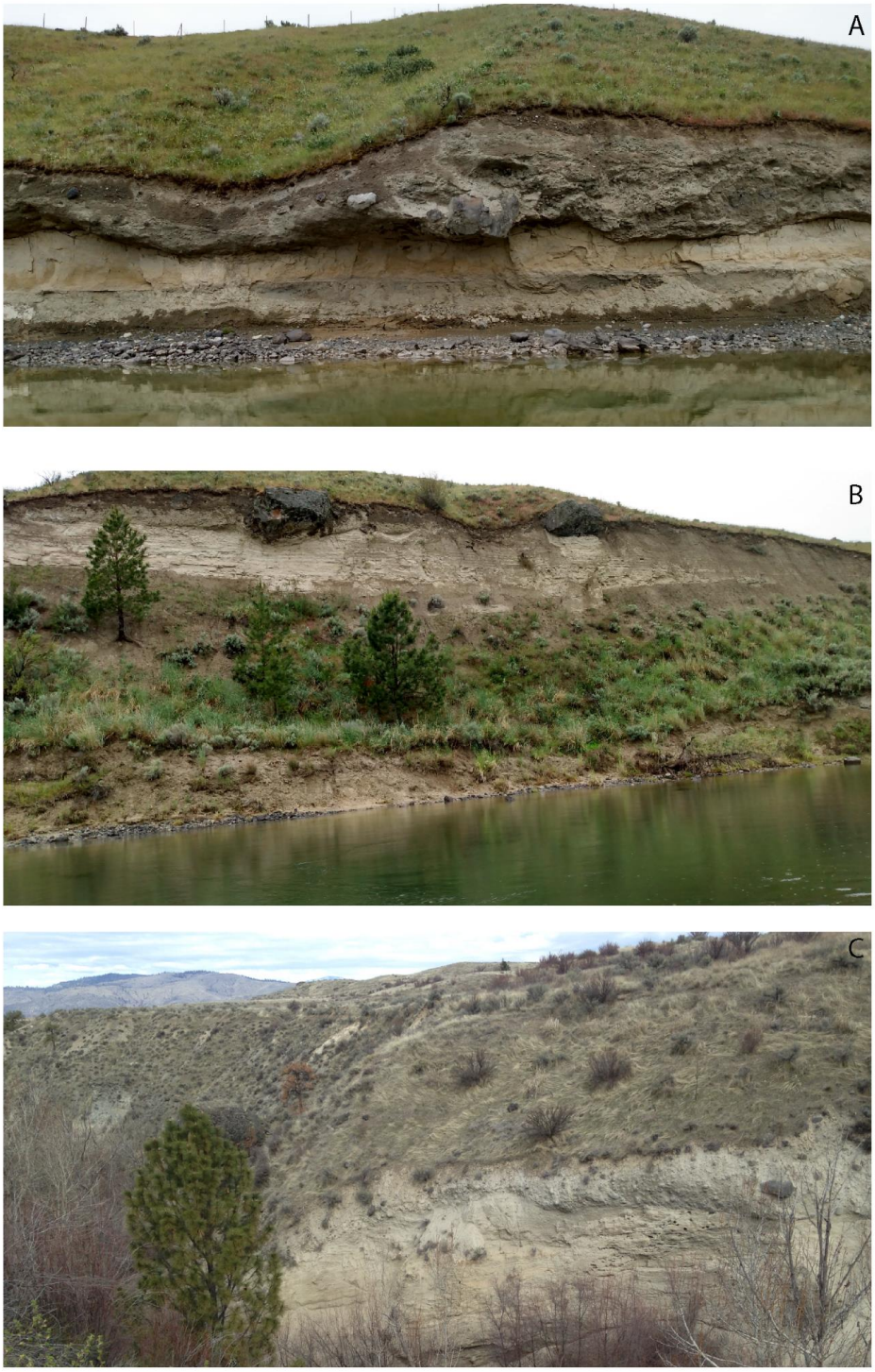

Figure 3-17: Three till-capped exposures along the Columbia River. (A) Down-valley Missoula (?) flood bed beneath till at Eagle Rapids section (RM 554) (B) Lake sediment interbedded with Missoula flood layers beneath till at Granite Rapids section (RM 570). (C) Lake sediment interbedded with Missoula flood layers beneath till in Kaiser Canyon (RM 585).

An outcrop at 48.0772, -119.5099 near RM 554 exposes a sequence of bedded gravel, sand, and silt underneath till (Fig. 3-17A). Pebble-sand clinoforms dip westward, down the Columbia River (Fig. 3-18A). Above this flood-deposited gravel, sand, and silt is a boulder-cobble diamict with a gray clay matrix, likely glacial till. The contact between the two units is flat to wavy (Fig. 3-17A).

The flood-deposited gravel overlies deformed sand and silt clasts (Fig. 3-18). Flame structures indicate that the silt was injected upwards into the gravel via loading and dewatering, suggesting that the underlying silt was wet at the time of gravel deposition. This may imply that the gravel-depositing flood ran into a lake, or onto otherwise wet silt, but that the flood destabilized the lake, resulting in the through-going flows indicated by the bedded gravel.

Early versions of glacial Lake Columbia would have likely been too shallow to overtop the entrance to Grand Coulee, provided the Okanogan glacier was not higher than the Grand Coulee divide. Early glacial Lake Columbia may have been an unstable, ice-dammed lake that breached its ice dam and released floods. Floods from this hypothesized version of glacial Lake Columbia could have resulted from either a gradual lake level rise as a result of steady inflows or from a sudden influx of water during Missoula or other floods.

The absence of thick lake beds beneath till at the RM 554 site, in contrast to sites upstream, suggests that a deep, stable lake may not have existed along this reach of the Columbia before site glaciation. While it is possible that glaciation and floods into an early glacial Lake Columbia could have eroded lake beds that once existed at the site, lake beds are well preserved beneath till at two sites upstream, suggesting that the advance of the Okanogan lobe over slippery lake beds was not particularly erosive of the lake sediment.

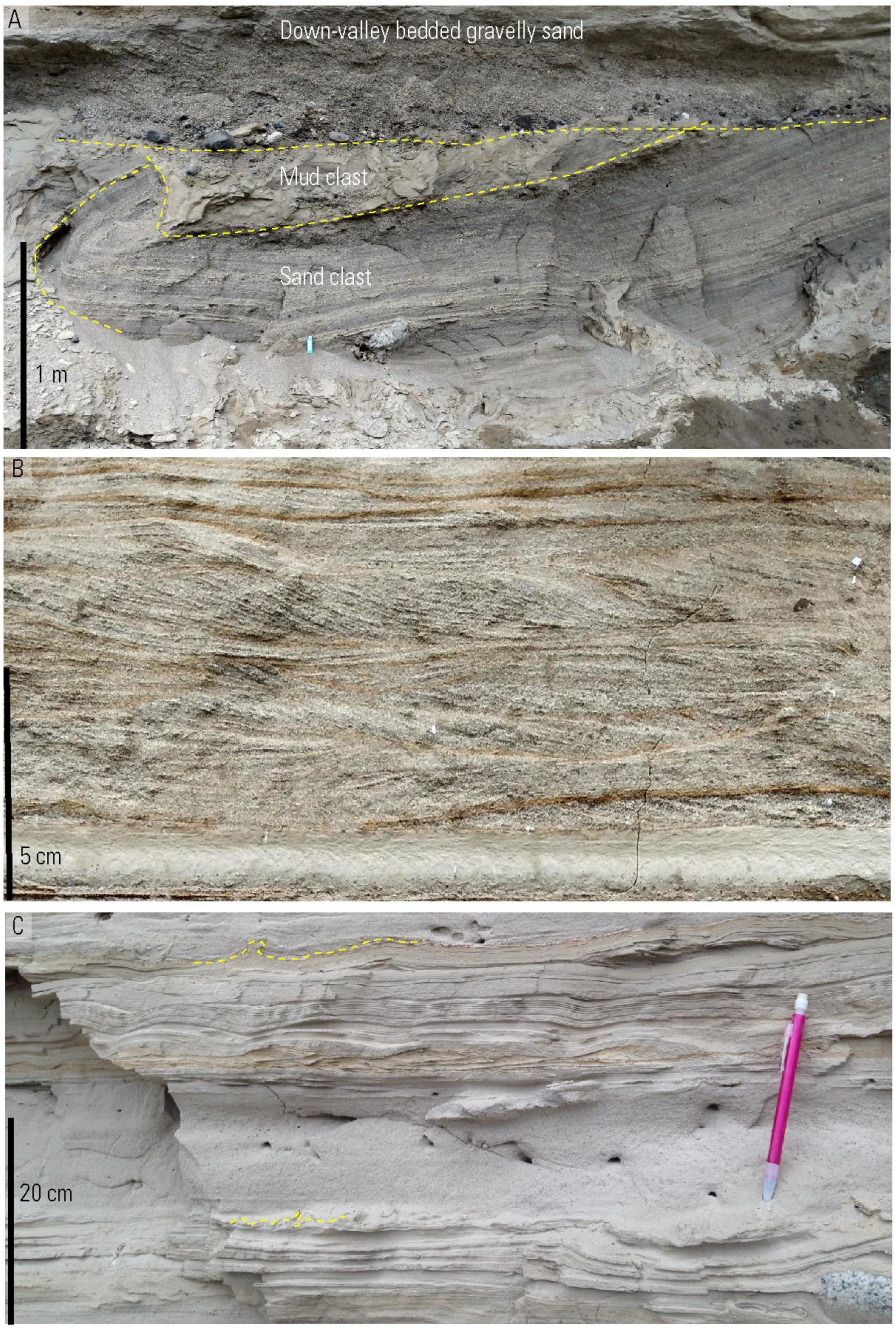

Figure 3-18: Comparison of pre-till flood beds exposed along the Columbia valley. Note variable thicknesses shown by scale bars to the left of images. Letters correspond to exposures in Fig. 3-17 and locations in Fig. 3-19 (A) Deformed mud and sand overlain by cross-bedded pebbly sand (RM 554), deposited in wet environment; beneath till (Fig. 3-17A). (B) Cross-bedded sand, interbedded with lake sediment (not pictured); beneath till (Fig. 3-17B). (C) Massive and cross-bedded sand, flame structures (outlined in yellow), and granitic dropstone (at bottom right of image), interbedded with lake sediment; beneath till (Fig. 3-17C).

Further upstream, a section at 48.1036, -119.2716, near RM 570 and near the former Granite Rapids, consists of lake beds beneath till (Fig. 3-17B). The lake beds are finely laminated, though not in a rhythmic style typical of varves. Interbedded with the lake beds are massive silts and cross-bedded sands (Fig. 3-17B), similar to Missoula flood beds in the Sanpoil valley. The lake beds at the RM 570 site suggest that an early, stable glacial lake Columbia existed at the site prior to glaciation of the site by the Okanogan lobe. Similarly, interbedded varves, cross-bedded to massive sands, and massive silts are present beneath till in Kaiser Canyon (Atwater, 1987, p. 196-197; Figs. 3-17C, 3-18C) and near Grand Coulee (Flint and Irwin, 1939, p. 666).

Together, these sequences suggest that the initial incursion of the Okanogan lobe into the Columbia valley may not have consistently dammed the river. The sequences can be explained by a scenario in which water flowed around or under the ice while the ice margin progressively advanced and thickened in the Columbia valley (Fig. 3-19), until thickening sufficiently to establish a stable lake.

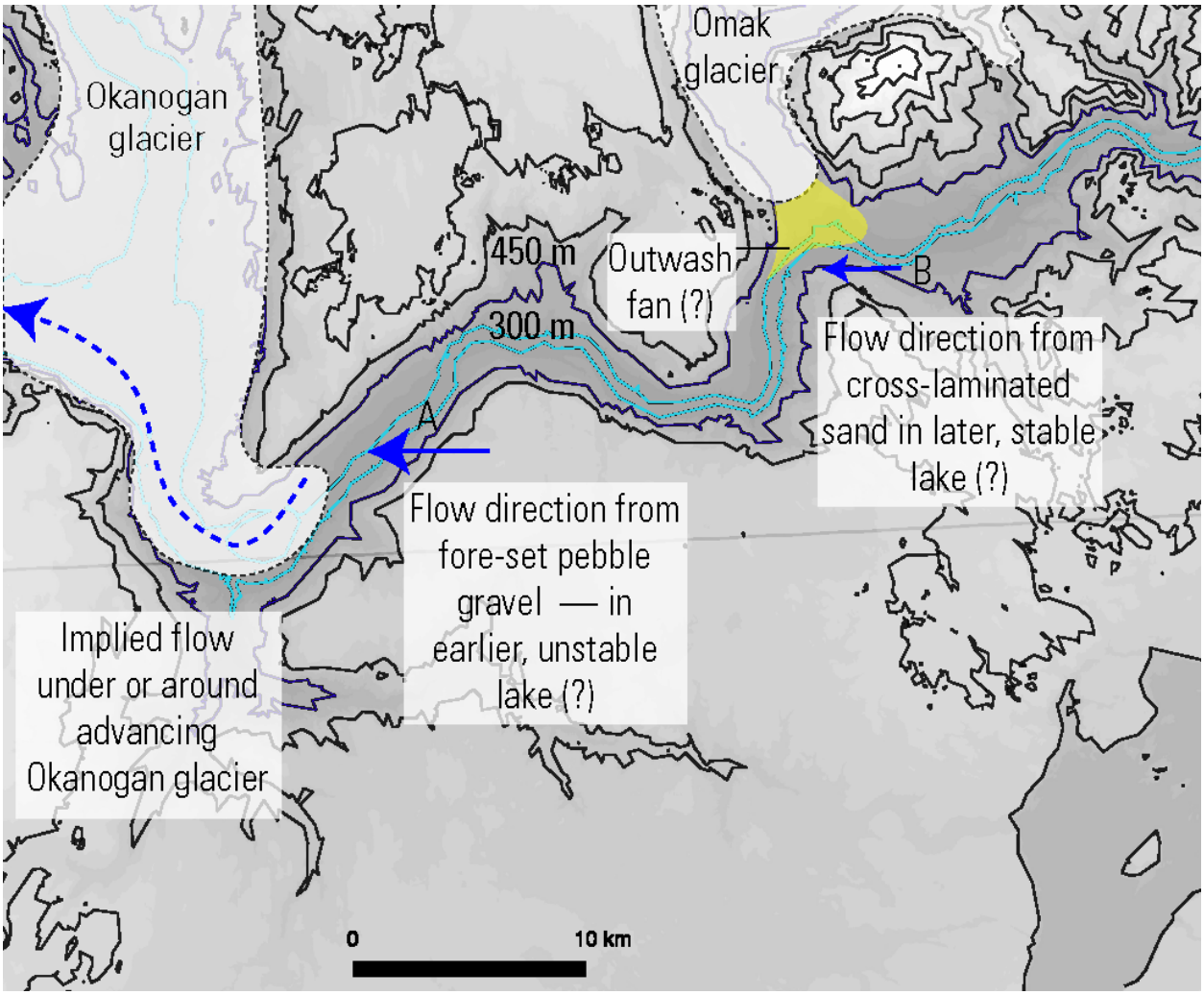

Figure 3-19: Possible early glacial configuration of advancing Okanogan and Omak glaciers, and unstable glacial Lake Columbia. Pre-glaciation flood flow directions in the Columbia valley from fore-set bedded gravel (A) and cross-laminated sand (B) beneath till. Cyan and dark blue contours at 300 and 450 m show possible early lake levels.

Modern observations of glacier-river systems indicate an interplay of diversion and/or impoundment of rivers by glacial ice with fluvial erosion of ice and bedrock. Systems in the Coast Range of the Alaska panhandle exhibit river erosion of an ice margin (Childs Glacier, Fig. 3-20A), formation of a proglacial lake through which the river flows (Alsek River and Lowell Glacier, Fig. 3-20C), and river erosion of a bedrock canyon in front of the glacier, isolating the river from the glacier below the level of the glacier (Tweedsmuir Glacier and Turnback Canyon,

Fig. 3-20D). In the Karakoram range of Kashmir, the Shaksgam River flows under the Singhi Glacier, despite the Singhi Glacier extending to the opposite valley wall (Fig. 3-20B). Surges of the Lowell Glacier have dammed the Alsek River in the past, resulting in a lake that was up to 200 meters deep before draining (Clague and Rampton, 1982). It is likely that similar processes as observed in modern systems also occurred when the Okanogan lobe first advanced in the Columbia valley during the last glaciation, suggesting that the Okanogan lobe may have initially struggled to dam the Columbia River as water eroded the ice margin, carving pathways under or around the ice (Flint and Irwin, 1939, p. 671).

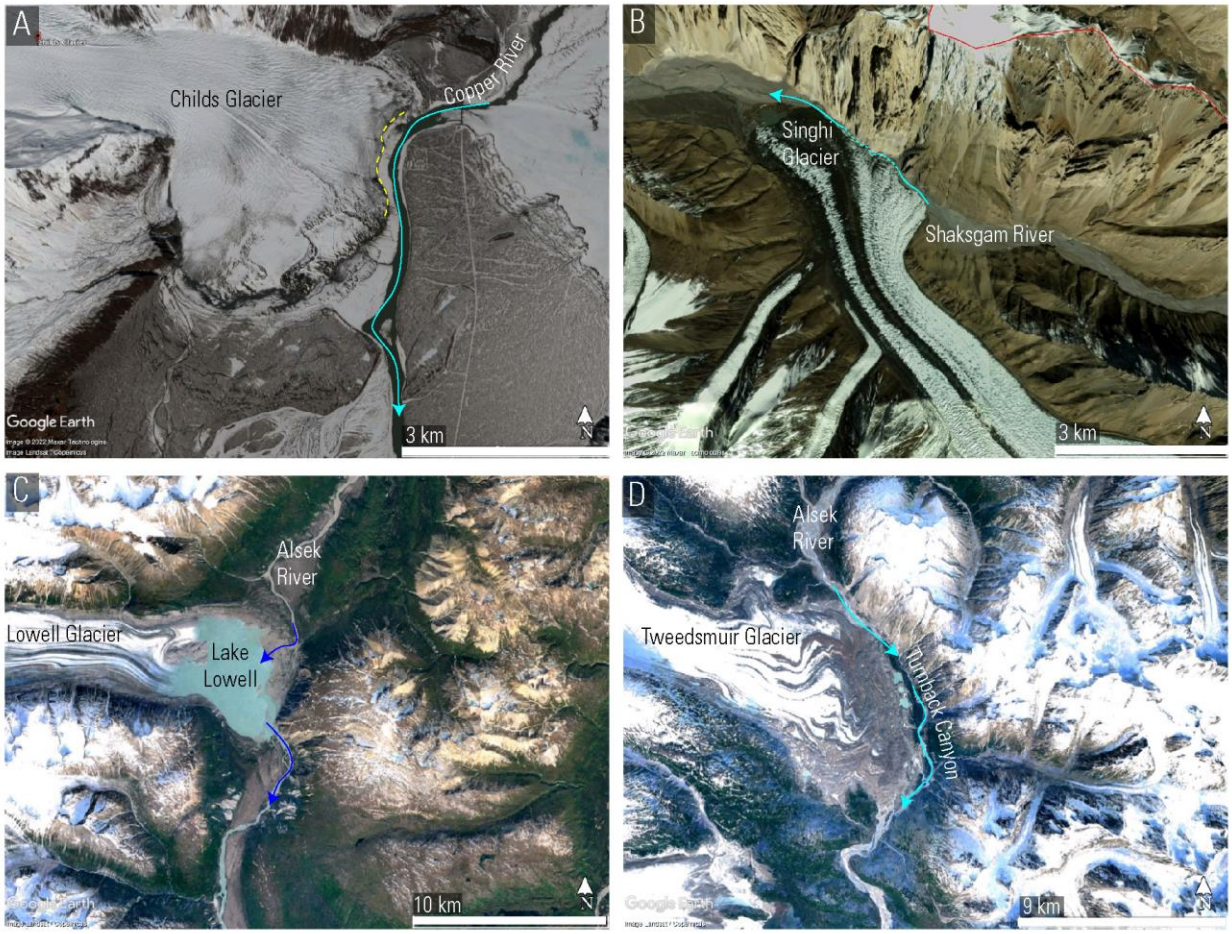

Figure 3-20: Modern examples of glacial incursions into river valleys. (A) Copper River eroding cut bank (yellow line) on Childs Glacier (B) Shaksgam River flowing under Singhi Glacier (C) Alsek River flowing through proglacial Lowell Lake, in front of Lowell Glacier. (D) Alsek River flowing through Tumwater Canyon, below Tweedsmuir Glacier.

3.5.2 Elevations of divide-crossing channels on the Waterville Plateau

Channels on the Waterville Plateau cross hydrologic divides across a wide range of elevations on the Waterville Plateau. The most prominent, deepest, and widest bedrock channels cross divides between 700 and 800 m, while divide-crossing channels between 650 and 700 m are more subtle than those at higher elevations. The observed pattern of divide-crossing channelization on the Waterville Plateau is opposite the pattern predicted by the spillover hypothesis, which implies that the deepest and most erosive flows would have been across the

lowest divide crossings, and thus that the most prominent channel systems should have formed perpendicular to the lowest divide crossings near Badger Wells and Chester Butte. Instead, channels across those lowest divide crossings are more obscure and minor than channels across much higher divides.

Moses Coulee megafloods must have first flowed across the hydrological divide that separates the Foster Creek and Moses Coulee basins. The precise position of the Foster Creek-Moses Coulee divide that floods must have crossed is somewhat ambiguous because the Waterville Plateau has low slopes and many internally drained basins. However, the general position of the divide is visually traceable from contours on topographic maps (Waitt, 2021, Fig. 2) and calculable from standard hydrological algorithms in GIS software (Fig. 3-21).

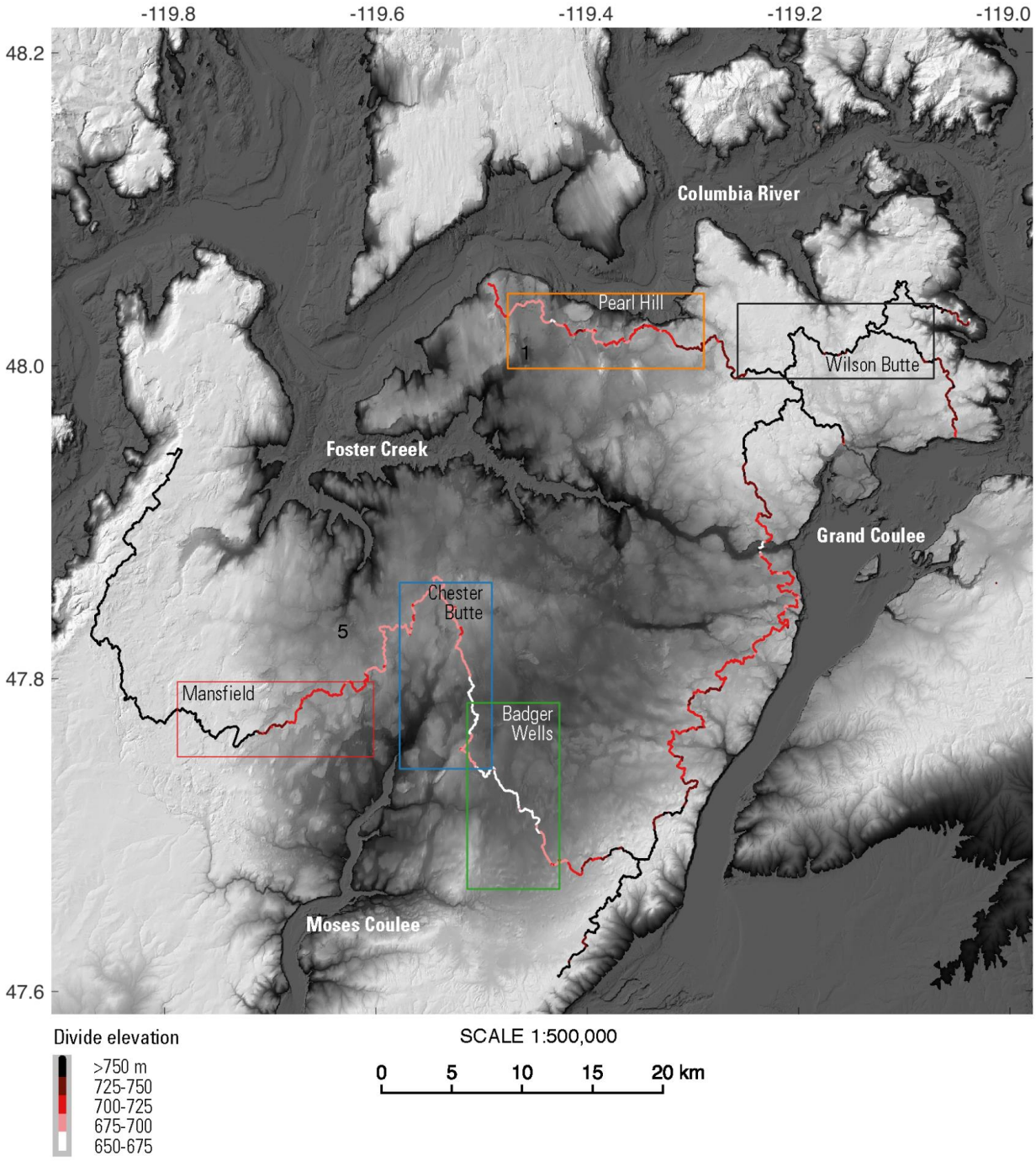

Figure 3-21: Topography, and divides on the Waterville Plateau. NED (National Elevation Dataset) 10-m topography black at 600 m to white at 750 m. Drainage divides color-coded by elevation. Five areas of divide-crossing channels highlighted by boxes of different colors and shown in greater detail in figures 22 and 23.

The shape of the Moses Coulee-Foster Creek divide likely reflects underlying tectonic structure as well as competing headward erosion from the Foster Creek and Moses Coulee systems. That the central stretch of the divide impinges northward into the Foster Creek basin (Fig. 3-21), forming a V-shape that opens southward towards Moses Coulee, is likely the result of headward erosion from Moses Coulee having extended its basin northward into the Foster Creek basin and capturing drainage area formerly part of the Foster Creek basin. This headward erosion extends north, not east towards the lowest point in the divide crossing. The shape of the hydrologic divide itself hints that main flows into Moses Coulee originated from the north, not from the lowest divide crossings to the east.

The lowest divide crossings into Moses Coulee are to its east, where two stretches of divide, each multiple km in length, are at elevations between 650 and 675 m (Figs. 3-21, 3-22). A low point on the Badger Wells divide at 653 m is the first place that water would spill out of the Foster Creek basin and into the Moses Coulee basin in the spillover scenario (Waitt, 2021, p. 375, Figs. 3-15, 3-21, 3-22). Had huge floods spilled across this divide sub-aerially, deeper flows over this lowest divide should have preferentially eroded channels here. This might have initiated a positive feedback between channel incision and ever-increasing flow capture, as likely occurred for divide crossings leading into the Cheney-Palouse and Telford-Crab Creek tracts.

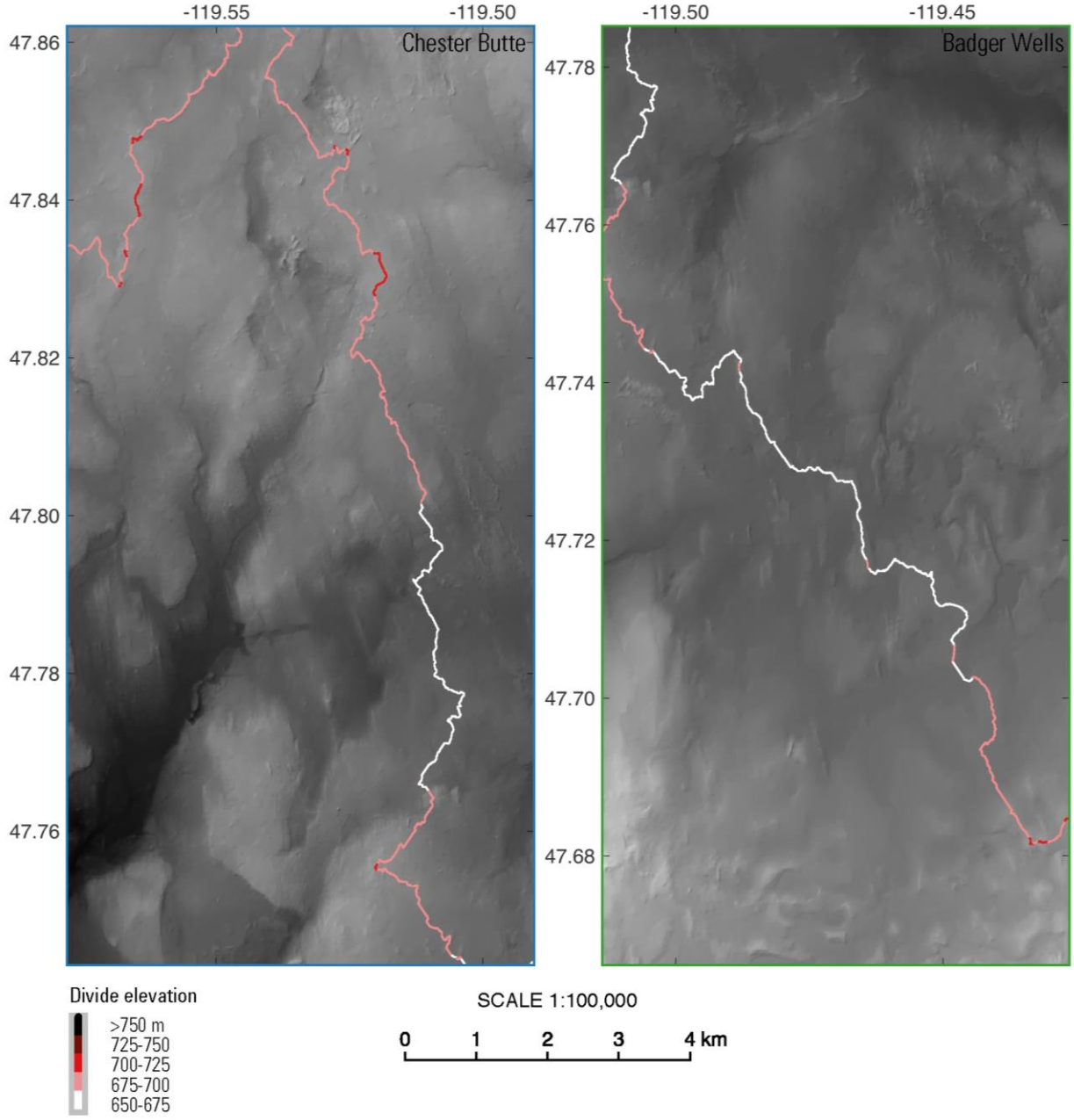

Figure 3-22: Topography and divide location across lowest divide crossings from Foster Creek basin into Moses Coulee basin, near Chester Butte and Badger Wells. While subtle channels cross these 650 to 675 meter divides, the most prominent direction of channelization is perpendicular to divides.

However, the most prominent divide crossing channels that enter into the Moses Coulee basin are on the north and west side of Moses Coulee, at higher elevations than the lowest crossings near Badger Wells and Chester Butte. The Mansfield channels (Hanson, 1970, p. 52-54) breach pre-channel surfaces 75 to 100 m above the Badger Wells divide (Figs. 3-21, 3-23A, 3-24, 3-25). One of the main coulees of the Mansfield channels has a sinuous planform and a strath terrace along its west wall, indicating a fluvial origin for this coulee (Fig. 3-25). This channel breaches a basalt surface with a top at 740 to 750 m. Floodwater must have therefore risen above 750 m to carve this and other channels, assuming no pre-existing valley breached the high basalt surfaces. This is a water level 97 m higher than the 653 m lowest divide crossing near Badger Wells, and significantly higher than modeled in scenario 3B of Denlinger et al. (2021). It is therefore difficult to explain the Mansfield channels with an overspilling Missoula flood. Additionally, it is difficult to explain formation of the Mansfield channels with proglacial meltwater scenarios (Waitt, 2021, p. 379), as the channels cross the hydrologic divide. Proglacial meltwater would have followed surface slopes downhill, so would be unlikely to erode divide-crossing channels, unless the Okanogan lobe maintained a stable margin directly on or near the divide. Yet thin, recessional moraines indicate that the Okanogan lobe only briefly stabilized at any one position during its retreat phase, and there is no particular reason or evidence that the Okanogan lobe would have stabilized on the divide during its advance phase.

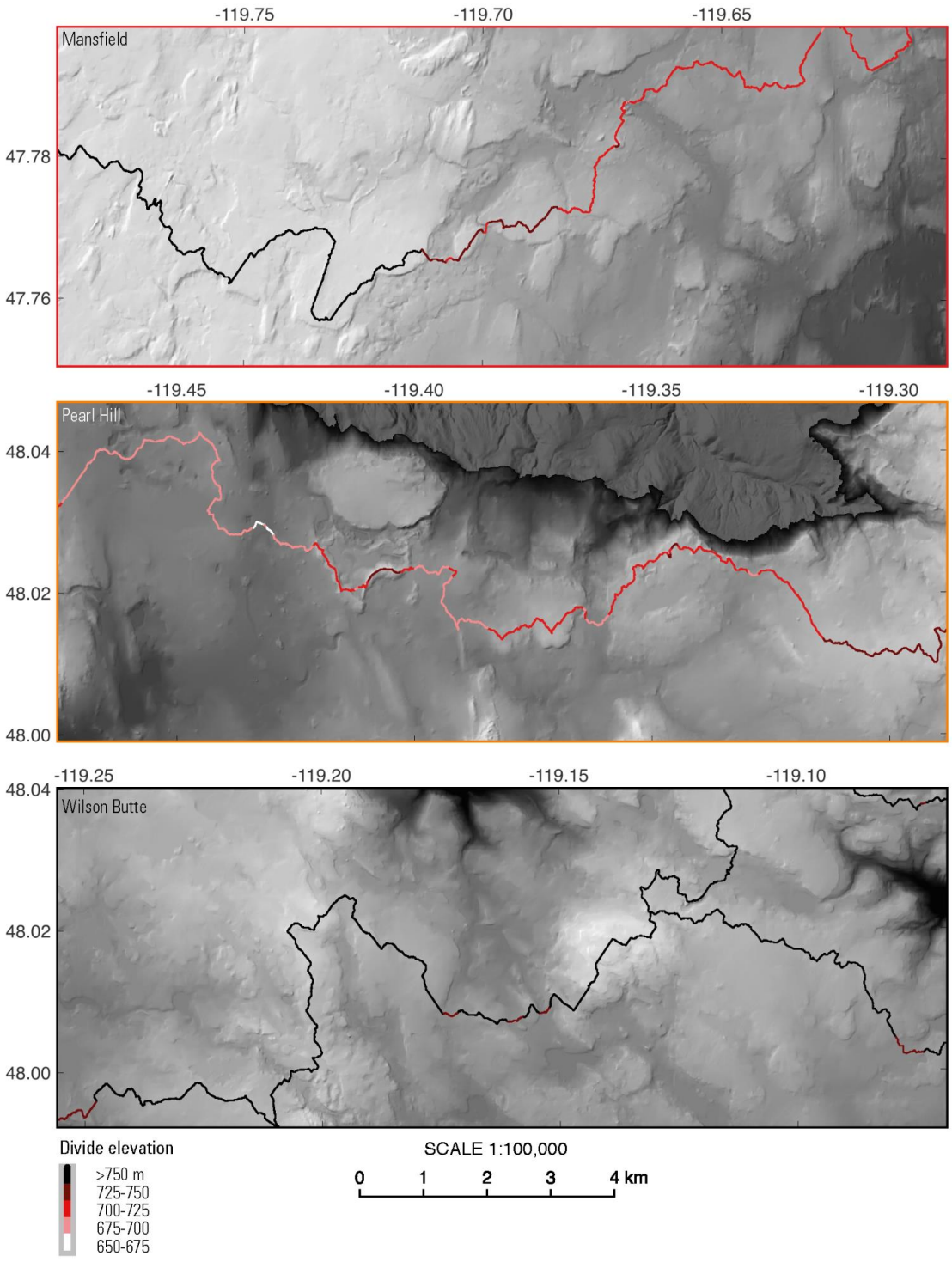

Figure 3-23: Topography and hydrologic divides across high divide crossings on the Waterville Plateau. Prominent channels near Mansfield, Pearl Hill, and Wilson Butte cross pre-channel divides between 700 and >750 m.

Figure 3-24: View north from the Moses Coulee basin into the Foster Creek basin through a segment of one of the Mansfield channels. This terraced, basaltic coulee, 500 meters wide and at least 40 m in depth, cuts through a pre-channel surface from 740 to 750 m.

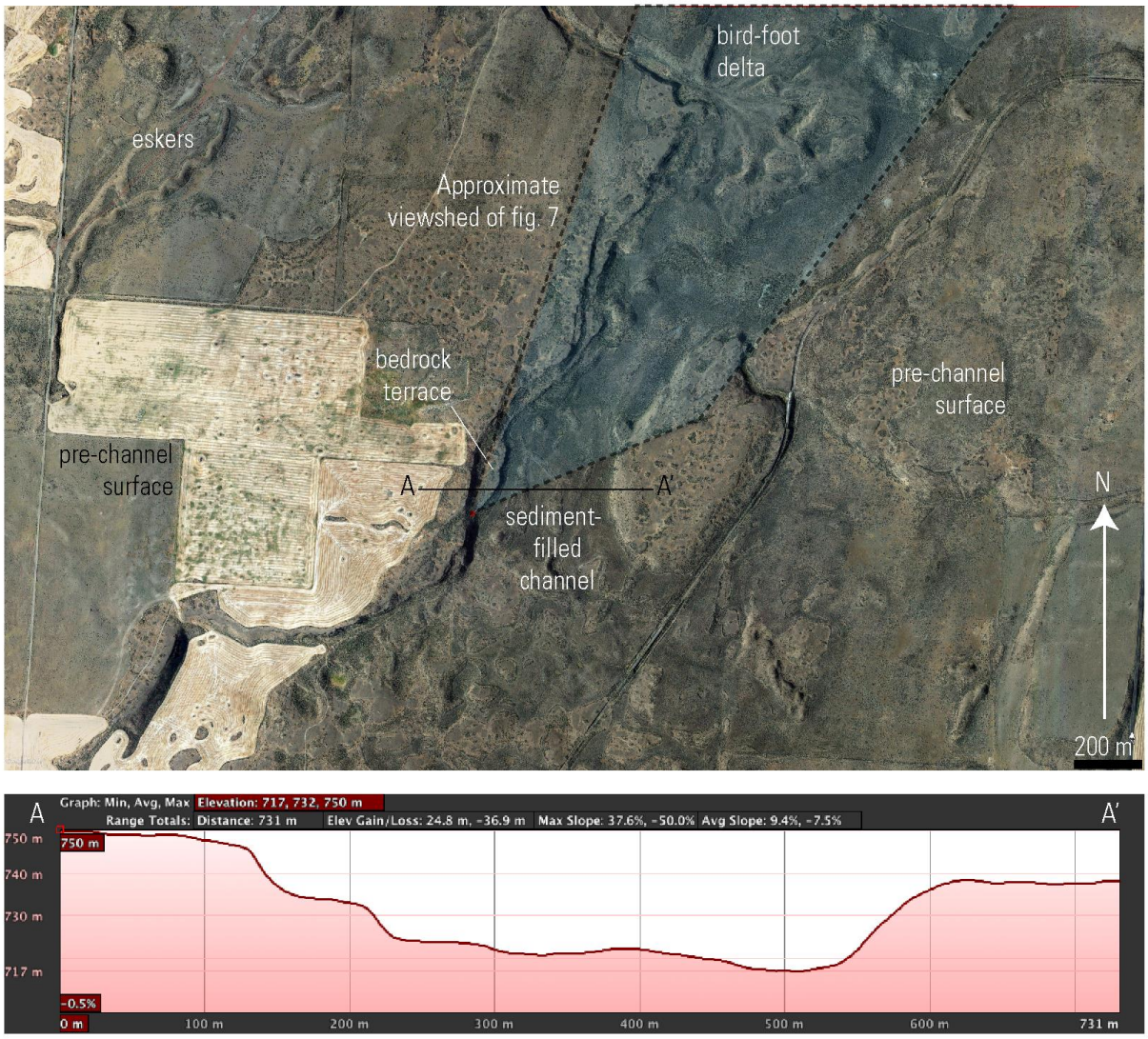

Figure 3-25: Satellite image and cross-sectional profile of basaltic coulee SW of Mansfield.

Two areas of divide-crossing channels on the northern Waterville Plateau further illustrate that water flows on the plateau crossed divides irrespective of surface elevation. The Pearl Hill channels consist of several km-wide basaltic coulees that dissect the Columbia River-Foster Creek divide at 725 to 750 m (Fig. 3-23B). The Wilson Butte channels are even higher. Here a system of bedrock channels crosses the divide between the Columbia River and Grand Coulee at elevations from 750 to 790 m (Fig. 3-23C).

Even with the most favorable possible scenario for spillover into Moses Coulee, in which upper Grand and Foster Coulees are filled, and the Okanogan lobe is blocking the Columbia west of Foster Creek, it is difficult to see how a flood-swollen lake Columbia could have risen high enough to deeply overtop the pre-channel surfaces that were breached to carve the divide-crossing channels near Mansfield, Pearl Hill, and Wilson Butte. Elevations of ice-rafted boulders along the shores of glacial lake Columbia do indicate that lake Columbia briefly reached stages of ~750 m when swollen with flood water (Atwater, 1986, Fig. 2), but this highest lake Columbia stage would have produced only minor overflows over the high divides near Mansfield and Pearl Hill and would have been too low to produce any overflow over the breached divides near Wilson Butte. Additionally, glacial lake Columbia stratigraphy suggests that the high stage of lake Columbia occurred only briefly, and when the Okanogan lobe was near or at its maximum extent (Atwater, 1986, p. 34, Fig. 3-17). If this inference is correct, then the high divides on the Waterville Plateau would have been beneath the Okanogan lobe at the only time when lake Columbia would have been high enough to possibly overtop them. These discrepancies suggest that a different model is required to explain the high divide-crossing channels on the Waterville Plateau.

The analysis of divide-crossing channels is complicated by changes to the divide elevation since channel erosion due to post-glacial isostatic adjustment and tectonic movement. Glacial isostatic deformation from the Okanogan lobe would have changed the absolute elevations of the critical Foster Creek-Moses Coulee divide, but relative displacements between locations on Foster Creek-Moses Coulee divide would been less pronounced than relative changes between divides along an E-W transect, because the Okanogan lobe advanced towards

the middle and at a nearly right angle to the Foster Creek-Moses Coulee divide, likely resulting in similar displacements at similar times along the whole divide.

Post-glacial tectonic displacement on the Waterville Plateau is likely too small to have distorted the elevations of divide-crossing channels significantly since the last glaciation but could have been a significant factor in deforming the divide-crossing channels if they formed during pre-MIS 2 glaciations.

3.5.3 Overall geometry of the Waterville Plateau channel network

A map of overfit channels on the Waterville Plateau provides context to interpret channels that cross high divides on the Waterville Plateau. This map describes an anabranching channel network that radiates outward from the northern rim of the plateau towards the former ice margin (Fig. 3-26). Previous mapping of the channel network was accurate, but only delineated a subset of the channels (Hanson, 1970, Fig. 4). The form of the more-fully delineated network is similar to tunnel valley systems that formed beneath the Saginaw lobe of the Laurentide ice sheet (Fisher et al., 2005, Fig. 6) and beneath the Fennoscandian ice sheet in the North German Lowlands (Stackebrandt, 2009, Fig. 2; Meyer, 1983, Fig. 1).

The channel network on the Waterville Plateau is aligned and elongated parallel to with drumlins, flutes, and eskers, and orthogonally to former ice margins (Fig. 3-26). The network flows freely across divides at all elevations with no evidence of preferential incision at lower elevations (Figs. 3-21 to 3-25).

Though the anabranching and radial form of the network suggests that channelization occurred in a subglacial environment beneath a lobe-shaped piedmont glacier, channels would have also received pro-glacial meltwater flows during intermediate stages of glaciation and

might have also received spillover flows from flood-swollen glacial lake Columbia. These other flows could have also contributed to channel formation. However, the anabranching nature of the network, the radial pattern of elongation and orientation, and the lack of relationship to surface slope suggest that the channels primarily eroded in the subglacial environment. In contrast, the geometric character of proglacial channels is illustrated by the channels that dissect the Withrow moraine complex. These channels, delineated in dark blue in Fig. 3-26, have a braided geometry, are not as broad as the subglacial channels, and they follow surface slope toward the center of the bowl-shaped Waterville Plateau.

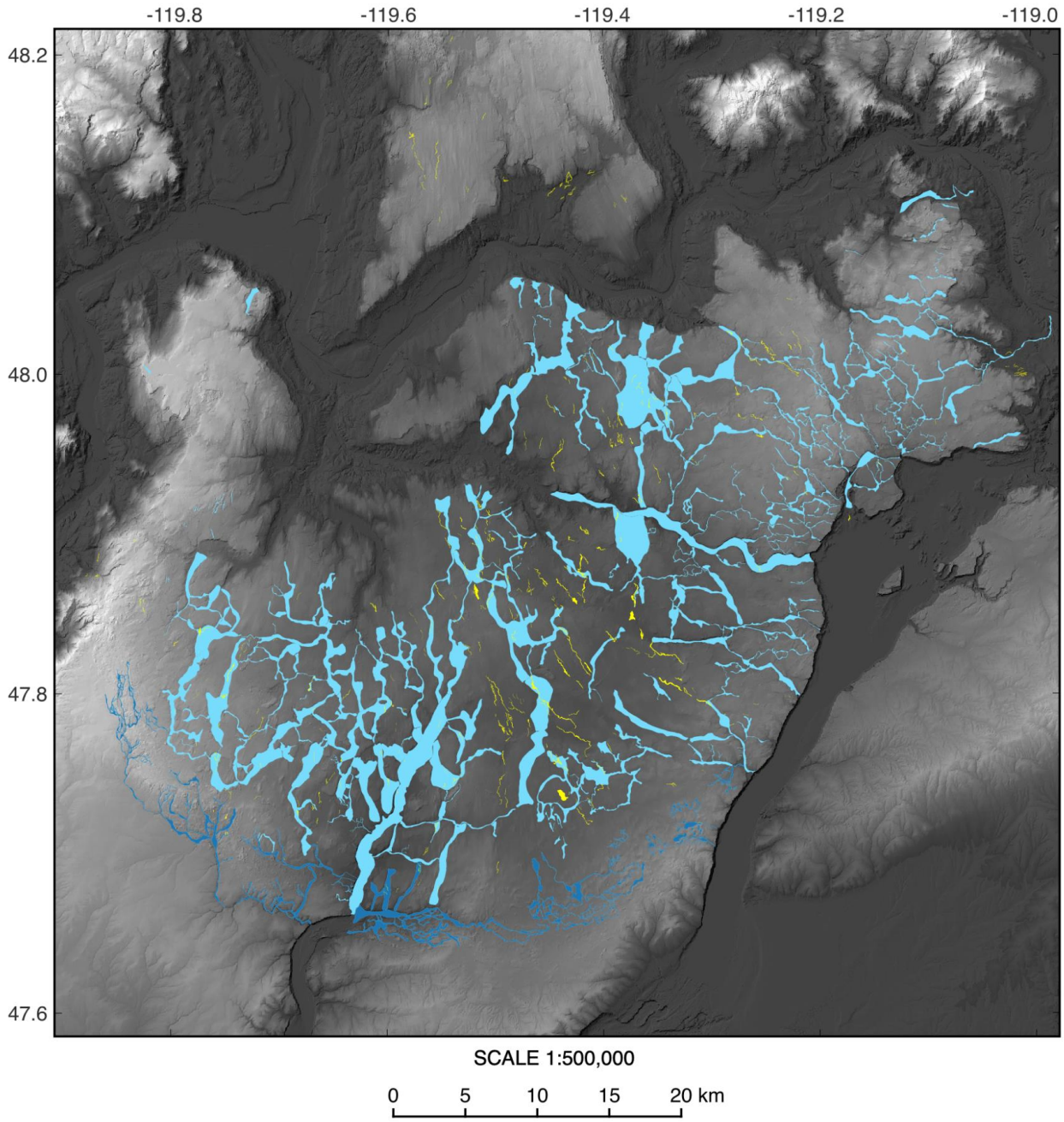

Figure 3-26: Map of overfit channels and valleys (blues) on the Waterville Plateau overlain with eskers (yellow), mapped from terrain-enhanced satellite imagery in Google Earth and 10 m resolution USGS National Elevation Dataset. Light blue shows valleys interpreted primarily as subglacial tunnel valley network, and darker blue shows channels interpreted mainly as glacial outwash. Tunnel valleys would have also carried glacial outwash during ice recession, but their geometry and size is inconsistent with formation under pro-glacial flows.

Comparison between the geometry of the Telford-Crab Creek and Cheney-Palouse channel networks with the Waterville Plateau channel network illustrates substantial differences in network geometry (Fig. 3-27). The two channel networks in the eastern Channeled Scabland are generally linear, with network elongation along single SW-NE axes. There, floodwater spilled across divides at the northern edge of the Columbia basin, followed pre-flood slopes that dipped to the SW, enlarged existing valleys, and breached minor divides between them to form the anabranching channel network clearly visible on the modern landscape (Bretz et al., 1956, p. 959). In contrast to the linear, single-axis elongation of the Cheney-Palouse and Telford-Crab Creek networks, the Waterville Plateau network is elongated along multiple axes that radiate outward from the northern edge of the Waterville Plateau. On the western side of the plateau, network elongation is mainly along a north-trending axis. However, network elongation progressively rotates eastward on the Waterville Plateau, eventually aligning with a northwest-trending axis on the eastern part of the Waterville Plateau. Had the channel network formed from overland flow, the implied topography of the pre-channel Waterville Plateau would be a dome structure centered over East Foster Creek.

The Channeled Scabland networks in the Telford-Crab Creek and Cheney-Palouse systems are generally broader than the Waterville Plateau channels. Spillover floods there produced a smaller number of broader coulees than exist in the Waterville Plateau network, which has a larger number of narrower channels.

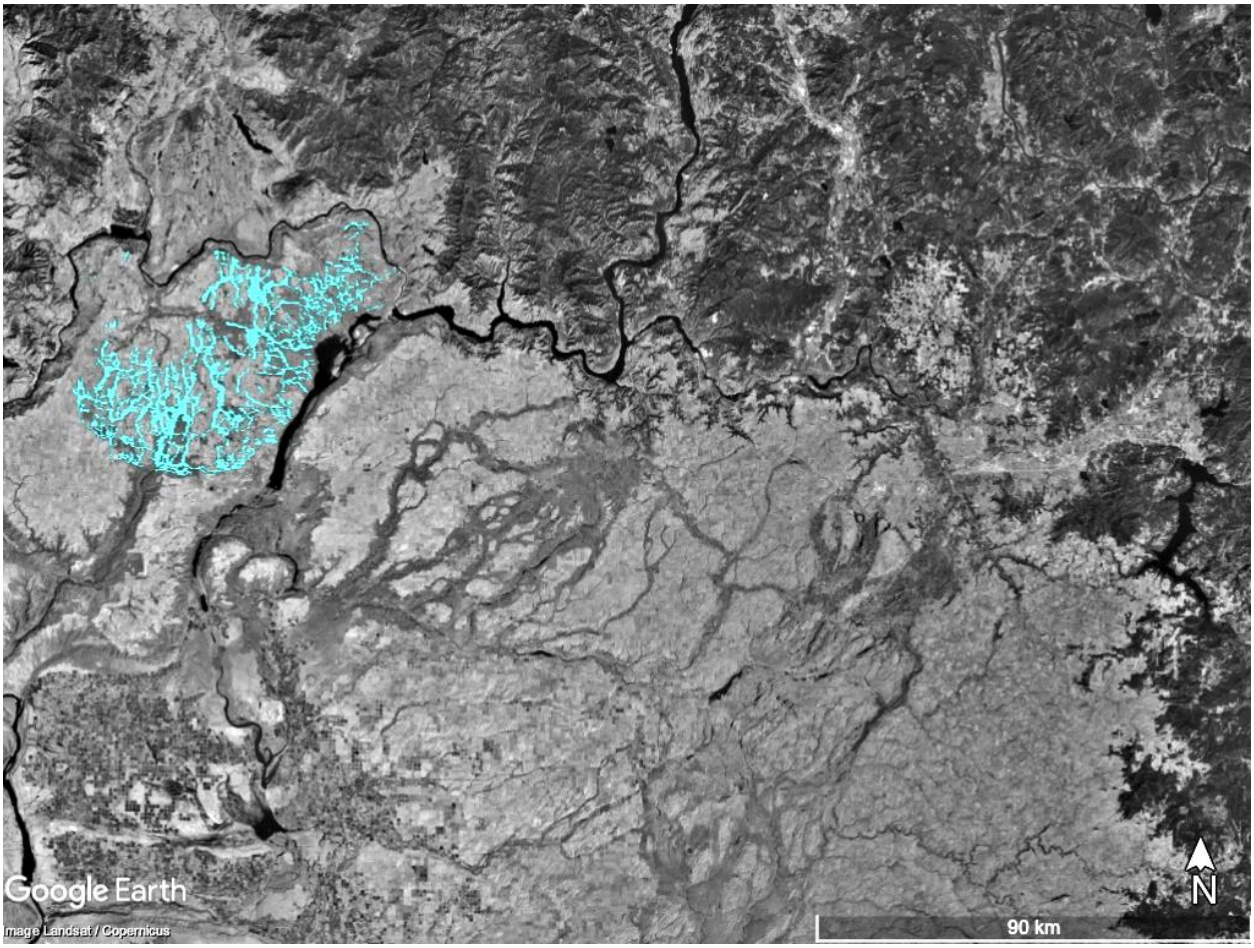

Figure 3-27: Satellite image of Channeled Scabland overlain with Waterville Plateau channel network drawn with heavy outlines to enhance visibility at this map scale (some actual channel widths are smaller than depicted here). Comparison between the Waterville Plateau channel network with the Telford-Crab Creek and Cheney-Palouse networks suggests that the eastern networks formed under overland flows directed along surface slopes, while the Waterville Plateau network formed under subglacial flows directed along subglacial hydropotential beneath the Okanogan lobe.

3.5.4 Lithologies of ice-rafted erratics in Moses Coulee

Some flood-transported erratics in Moses Coulee match metamorphic core complexes of northern Washington but none are obvious matches to low-grade metasedimentary rock of the Belt-Purcell Supergroup. The provenance of these erratics may be more consistent with the Okanogan lobe subglacial flood scenario than with the Missoula flood overspill scenario, but

iceberg-transport scenarios within either model for Moses Coulee flooding could explain the observed patterns.

Granitic and metamorphic rocks within Moses Coulee and downstream from the Withrow moraine must have been transported by floods as they are downstream from the direct influence of glacial ice and are within basalt-floored basins. Many of the felsic erratics in Moses Coulee were likely transported in flood-borne ice blocks or bergs, not as bedload or suspended load in floods. This interpretation is based on the prevalence of sub-angular shapes among Moses Coulee erratics, on the grouping of crystalline erratics in clusters in or on thin deposits of silty sand, on the preservation of glacial striations on a few erratics, and on the positions of erratics on top of gravels instead of within them (Hanson, 1970, p. 93). Sub-angular shapes of many erratics and glacial striations on some erratics would have been difficult to preserve in bedload or suspended load transport because fluvial transport rounds and abrades. Clusters of felsic cobbles, pebbles, and sand in Moses Coulee are similar to bergmounds and difficult to explain through a process other than ice bergs or blocks.

Table 3-4: Lithologies of erratics in Moses Coulee, Rattlesnake Mountain (Bjornstad, 2014), Gingko Petrified Forest (Karlson, 2006), and Willamette Valley (Minervini et al., 2003).

Rock type	Moses Coulee (n)	% of total	Rattlesnake Mountain (n)	% of total	Gingko Petrified Forest (n)	% of total	Willamette Valley (n)	% of total
Granitic	49	60%	1636	80%	269	80%	69	62%
Quartzite	23	28%	155	8%	26	8%	13	12%
Diorite	4	5%	112	5%	22	7%	3	3%
Argillite	**0**	**0%**	**89**	**4%**	**0**	**0%**	**2**	**2%**
Basalt	N/A	0%	73	0%	0	0%	0	0%
Gneiss	6	7%	25	1%	12	4%	7	6%
Schist	0	0%	21	1%	0	0%	4	4%
Gabbro	0	0%	7	0%	0	0%	2	2%
Other	0	0%	14	1%	8	2%	12	11%
Total	82	100%	2132	100%	337	100%	112	100%

Figure 3-28: Surface features of flood-transported rocks in Moses Coulee. Rocks in A and B have surface features indicative of glacial transport, while rocks in C and B have surface features indicative of flood transport as bedload or suspended load where rocks experienced energetic collisions. (A) Quartzite pebble with glacial striations and chatter marks, found at 47.50530, -119.716114 on a gravelly slope along Coyote Creek. (B) Basalt boulder with linear scratches. (C) Boulder gravel in Pine Canyon flood gravel with percussion marks. (D) Boulder gravel in Great Bar with percussion marks and jagged fractures.

Modern glacial lake outburst floods typically generate large numbers of ice blocks as a result of subglacial tunnel collapse (Sugden et al., 1985, Fig. 5), and/or via fluvial undercutting and subsequent ice cliff collapse along glacier margins eroded by floodwaters (Sugden et al., 1985, Fig. 6). Ice blocks are transported downstream both in flotation and as rolling bedload

(Russel, 1993, p. 1095) and eventually become stranded in areas of low flow depths, such as on deltas and on outwash plains (Russel, 1993, Fig. 4a).

In Moses Coulee, erratics that were apparently transported in ice blocks or in icebergs are distributed semi-randomly across the landscape, with larger apparent concentrations in side valleys. It is more common to find crystalline erratics in Moses Coulee on top of surfaces rather than within gravel bodies (Hanson 1970, p. 93). A relatively high abundance of erratics apparently occurs just downstream and to the west of the transition from upper Moses Coulee into Sagebrush basin (Figs. 3-4, 3-13), a zone where flood stage dropped rapidly downstream due to flow expansion from the confined upper coulee into Sagebrush basin. Large numbers of erratics also occur along the thalweg of Coyote Creek (Figs. 3-4, 3-13). If these erratics were transported in deep-keeled bergs, it is possible that iceberg keels became trapped in flows across Coyote Creek. If the erratics were transported in smaller, equidimensional ice blocks, it is not clear why they would concentrate in Coyote Creek, though post-flood winnowing of finer sediment by ephemeral Holocene rainfall and snowmelt floods may have preferentially exposed erratics in side valleys.

Figure 3-29: Granitic and gneissic erratics with oriented feldspar megacrysts in Coyote Creek, Moses Coulee. (A) Tabular, sub-angular boulder of porphyritic granite on bedrock-floored reach of Coyote Creek at 47.51601, -119.703440. (B) Sub-rounded small boulder of porphyritic granite. (C) Small, sub-angular boulder of augen gneiss perched on stream gravel of Coyote Creek at 47.51598, -119.702990. (D) Sub-rounded boulder of augen gneiss.

Figure 3-30: Inside of rounded, garnet-bearing quartzite cobble found on sediment-coated bedrock terrace in Sagebrush Flat basin. Sand-sized garnet and unknown gray-black mineral cluster in center-left of exposed face. A thin, orange weathering rim mantles the rock.

Lithologies of Moses Coulee erratics provide clues about the source of the Moses Coulee floods. Unique erratics in Moses Coulee are a better match to high-grade metamorphic core complexes of northern Washington than to low-grade metasediments of western Montana and southern Alberta.

Sub-angular boulders of augen gneiss (Fig. 3-29) and megacrystic granite are present in Coyote Creek, a tributary of Moses Coulee that was inundated by flood flows across and down Coyote Creek. A proximal source of augen gneiss and megacrystic granite is the Okanogan dome

(Hansen, 1983, Fig. 3). Ice flow lines into Moses Coulee would have crossed the Okanogan dome, potentially eroding bedrock from it and transporting that rock into the Moses Coulee basin. The augen gneiss in Moses Coulee has distinctive boudins and imbricate feldspar megacrysts (Fig. 23-9), as does Okanogan dome bedrock (Hansen, 1983, Fig. 8; p. 23).

When broken open, some Moses Coulee quartzites contain sand-sized garnet (Fig. 3-30). Though garnet-grade metamorphic rocks occur in the Lake Missoula basin (Cressman, 1989, p. 7), garnet is rare in Belt-Purcell and Windermere Supergroups, which experienced only low-grade regional metamorphism (Cressman, 1989, p. 11). In contrast, high-grade metamorphic rocks are common in north-central Washington, including in the Okanogan and Kettle domes, areas that experienced much higher grades of regional metamorphism than did the Belt or Windermere Supergroups. Quartzite containing potassium feldspar, muscovite, garnet, sillimanite, and/or tourmaline, has been noted in the Tenas Mary Creek metamorphic unit of the Kettle Dome at T 40 N, R 32 E & 33 E (Orr, 1985, Table 1, Map A) and quartzite within a unit of sillimanite-grade metamorphic rocks is noted in the Hall Creek orthogneiss and paragneiss unit in the northern Kettle Dome (Atwater and Fleck, 1984, p. 6). Tenas Mary Creek unit rocks also purportedly outcrop in the NE Okanogan dome (Cheney, 1980, Fig. 3), potentially a plausible source of garnet-bearing quartzite upstream of Moses Coulee, though it is not clear from available maps and publications whether a garnet-bearing quartzite occurs in the Tenas Mary Creek rocks within the NE Okanogan dome. At the glacial maximum, ice flowing over the Kettle Dome would have likely flowed into the Sanpoil lobe (Clague, 2009, Fig. C72d), though flowlines during earlier phases of CIS glaciation when a Rocky Mountain ice divide drove regional ice flow to the SW might have transported sediment from the Kettle Dome into the

Okanogan drainage (Clague, 2009, Fig. C72c). It is not clear whether ice flowing over the NE Okanogan Dome would have drained into the Okanogan lobe or Sanpoil lobe as paleo-flowlines in the mountainous topography of the Okanogan Dome are not obvious.

Given this context, there are several possibilities for how garnet-bearing quartzites entered Moses Coulee. A possibility within the overland flood paradigm is that ice flowing over the Kettle Dome entrained garnet-bearing quartzites and delivered them to calving fronts of the Sanpoil or Columbia River lobes, supplying icebergs with garnetiferous quartzite into glacial Lake Columbia. A Missoula flood into Lake Columbia might have additionally eroded and undercut the ice margin of the Columbia River and Okanogan lobes, resulting in ice block generation due to ice cliff collapse. Floodwaters might have swept those icebergs into Moses Coulee. One of the challenges with this scenario is that dropstones deposits are relatively rare in glacial Lake Columbia sediment, suggesting that icebergs were not particularly common in the lake. A second challenge is that icebergs would have had to remain in flotation as the floodwater crossed the divide into Moses Coulee, a difficult zone for iceberg transport where low flow depths might have grounded any deep-keeled icebergs.

A possibility within the subglacial flood paradigm is that ice flow over the NE Okanogan Dome entrained garnet-bearing quartzites and brought those rocks to the margin of the Okanogan lobe upstream of Moses Coulee. A subglacial flood emerging from the ice margin might have then calved icebergs into the outgoing flood as a result of subglacial tunnel collapse or due to undercutting of the Okanogan lobe ice margin by pro-glacial flood water, supplying quartzite-bearing icebergs directly into Moses Coulee floods. The challenge with this scenario is that there are no mapped occurrences of garnetiferous quartzite in the Okanogan Dome.

Belt-Purcell argillite is a tracer for Lake Missoula floods. It is a distinctive argillite with a reddish-purple color, banded texture, and delicate sedimentary features like mud-cracks, rain drops, and ripple marks. Of the 2112 erratics counted at the Rattlesnake Mountain bergmound site, 89, or 4% of the total, were classified as argillite and linked to glacial Lake Missoula (Bjornstad, 2014). I have not yet found any Belt-Purcell argillite in Moses Coulee.

3.6 Late-glacial Okanogan outburst floods

There are gravel dunes on terraces in the Okanogan valley (Fig 3-31, site 1; Cooley, 2022;) and in the Omak trench (Fig 3-31, site 2; Hibbert, 1986, p. 106) that indicate large sub-aerial floods descended these valleys during deglaciation. Cobbles on the surface of the gravel dunes in the Omak trench are around one foot in diameter (Hibbert, 1986, p. 106). The ripple chords (crest-to-crest distance) of both the Omak trench and Okanogan valley dune sets are similar. Both dune sets have chord lengths consistently between 50 to 75 meters (Fig. 3-31, Fig. 3-32). These distances are in the first to second quartile of chord-lengths in other Scabland settings (Baker, 1973, Table 2, Fig. 53). The Okanogan valley dunes have dune heights of around 2 m (Fig. 3-32A), while the Omak trench dunes have dune heights of around 1 m (Fig. 3-32B). These heights are minima because loess accumulation in swales can subdue apparent dune heights (Baker, 1973, p. 54).

Gravel dunes in wide channels are indicative of large, subaerial floods. Therefore, these dunes, located on sites that were glaciated by the Okanogan lobe, must have formed after the ice had retreated to their north. Both sites likely became ice-free between around 14 to 13 ka (this study, chapter 2). At that time, proglacial lakes astride the still-glaciated Okanogan valley were

releasing outburst floods (Stewart and Allard, 2017, p. 39). These flows would have drained to the margin of the Okanogan glacier, which was progressively thinning and retreating northward.

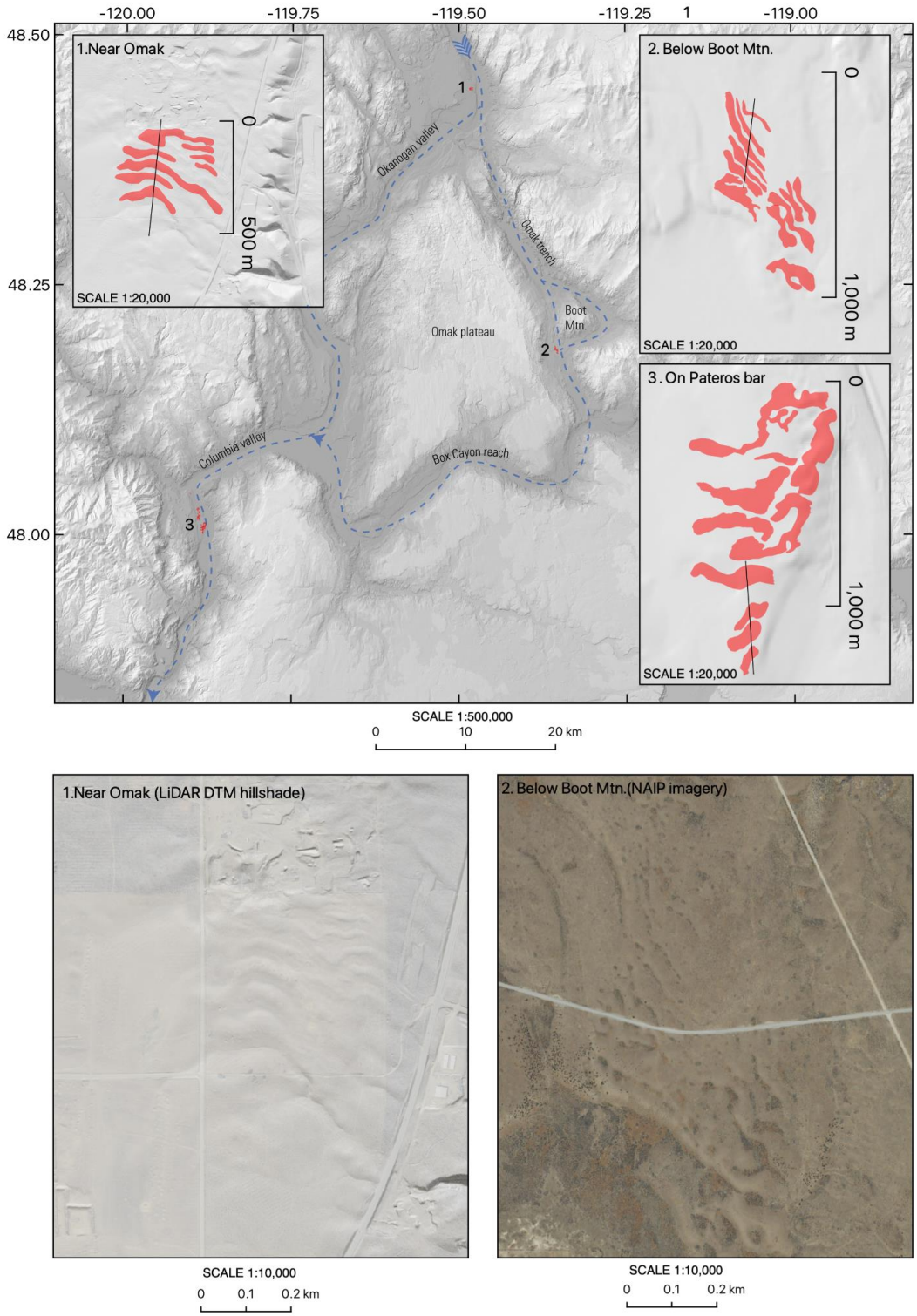

Figure 3-31: Gravel dunes in the Okanogan valley near Omak (1), Omak trench near Boot Mtn. (2), and Columbia valley near Pateros (3).

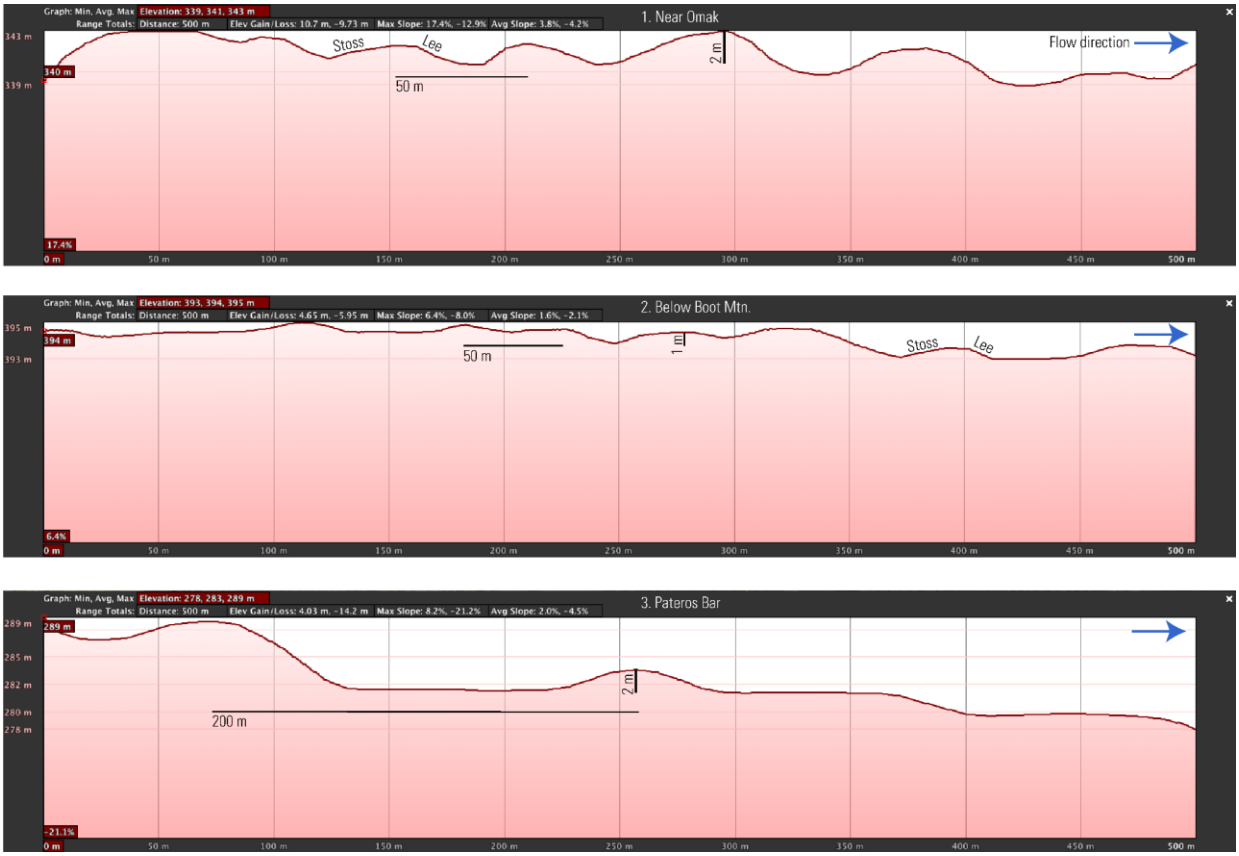

Figure 3-32: Cross-dune profiles of dune sets shown in Fig. Profiles along black lines in Fig. 3-31.

The two dune sets may have formed sequentially or in the same flood. The Okanogan lobe bifurcated into Omak and Okanogan sub-lobes during deglaciation, and ice likely lingered in the Omak and Okanogan valleys after the plateaus had deglaciated (this study, Chapter 1). The gravel dunes in the Omak trench (Fig. 3-31, site 2) may have formed first, while there was an ice margin in the Omak trench upstream of or adjacent to Boot Mtn., and the dune-bearing site in the Okanogan valley was beneath ice (Fig. 3-31, site 1). Alternatively, the dunes may have formed in

the same flood that simultaneously inundated the Okanogan and Omak valleys, and which was released when the Okanogan lobe margin was to the north of site 1 in Fig. 3-31.

The gravel dunes below Boot Mtn. and near Omak indicate large, late-glacial outburst floods from the Okanogan. These dunes must have formed while the Okanogan ice margin was to their north, so they cannot correlate to Moses Coulee floods, which only occurred when the ice margin was further south. Nonetheless they indicate that large outburst floods drained through the Okanogan valley during the last glacial period and generally highlight the flood-producing potential of the Okanogan sector of the Cordilleran Ice sheet.

3.7 Conclusions

This study confirms that megafloods drained through Moses Coulee during the last glaciation, and highlights problems with the hypothesis that those floods were Missoula floods.

The style of Moses Coulee megafloods is inferred from gravel deposits in upper Moses Coulee and Sagebrush basin. A mixture of clast-supported and matrix-supported gravel indicates that both steady, clear-water flows, and subaqueous debris flows occurred during floods.

Calcrete over possible megaflood gravel at the base of a Coyote Creek bar also suggests a longer history of megafloods in Moses Coulee, with U-series ages on the calcrete hinting that megaflooding in Moses Coulee may have skipped several glacial cycles. This generally implies that the Channeled Scabland formed over multiple glacial periods, but that flooding did not occur during every glacial period.

The study then reviews two hypotheses for how megafloods routed into Moses Coulee and examines whether the evidence in and upstream from Moses Coulee is more consistent with either the Missoula flood hypothesis, or with the Okanogan subglacial flood hypothesis.

Firstly, reconnaissance stratigraphy along the Columbia River between Brewster and Grand Coulee suggests a downstream limit to pre-Okanogan lobe glacial lake Columbia sediment. Obvious lake beds beneath till occur at RM 570 and RM 585, but not at RM 554. The pattern of flood gravel beneath till closer to the Okanogan confluence and lake beds beneath till further upstream suggests that the Okanogan lobe may have advanced and thickened in the Columbia valley, but with a margin that was continually eroded by the Columbia River. When the Okanogan lobe finally filled the valley to the point that the Columbia River was blocked in a stable fashion, even when swollen with a Missoula flood, the ice margin may have been well upstream of Foster Creek. If this history is correct, it implies that early glacial Lake Columbia never had a deep arm in Foster Creek and that it might have been unable to rise high enough to send water across the 655 m spillway across the Badger Wells divide into Moses Coulee.

Between Moses Coulee and the Columbia River, the pattern of channelization across the Badger Wells and other divides into Moses Coulee is inconsistent with formation under sub-aerial flows across the lowest spillways, but indicative of sub-glacial flows directed by subglacial pressure gradients. In particular, an analysis of channels that cross the hydrologic divide between Foster Creek and Moses Coulee shows that the deepest, widest, and most prominent divide-crossing channels are cut along some of the highest elevations on the divide, not across the lowest spillways. Sub-aerial spillover should have produced only minor channels at higher elevations near Mansfield, and deeper channels at lower elevations near Badger Wells. The fact that the opposite pattern exists on the landscape is inconsistent with sub-aerial flows across the Foster Creek-Moses Coulee divide.

Two points of context help to make sense of the pattern of high-altitude channelization across the Foster Creek-Moses Coulee divide. Firstly, divide-crossing channels on the Columbia River-Foster Creek divide and on the Columbia River-Grand Coulee divide cross their respective divides at elevations up to 780 m, above the highest ice-rafted erratics that mark the flood-swollen 750 m level of glacial lake Columbia. These highest, divide-crossing channels indicate that sub-aerial flows alone cannot explain the pattern of channelization on the Waterville Plateau.

Secondly, the overall geometry of the channel network on the Waterville Plateau is radial and anabranching, similar to the geometries of tunnel valley networks beneath the former Laurentide and Fennoscandian ice sheets, and distinct from the linear, elongate geometries of the eastern Channeled Scabland, spillover systems.

The combination of more prominent channels across higher divides and the geometric style of the channel system suggests that the predominant meltwater flows across the Waterville Plateau were subglacial rather than subaerial.

In Moses Coulee, a new catalog of 82 photographed and geo-referenced crystalline erratics shows that many Moses Coulee erratics arrived in ice bergs or blocks carried by floods. Distinctive megacrystic granite, augen gneiss, and garnetiferous quartzite in Moses Coulee match metamorphic core complexes in northern Washington, suggesting that the icebergs derived from the Okanogan lobe or the Columbia River lobe. The presence of icebergs from one or both of these glaciers is consistent with both the Missoula flood and the Okanogan subglacial flood scenarios. The catalog of Moses Coulee erratics lacks any clasts of Belt-Purcell argillite, a tracer for Lake Missoula floods found in other comparable catalogs of erratics in the Channeled

Scabland, suggesting a difference in initial iceberg assemblage for the Moses Coulee floods, and/or a filtering process in that selectively removed certain icebergs.

This study suggests that a new formulation of the Missoula flood spillover hypothesis may be necessary to explain large, last-glacial floods in Moses Coulee, or that a version of the Okanogan lobe subglacial flood hypothesis might better match the evidence.

3.8 References

Atwater, B.F., 1986, Pleistocene glacial-lake deposits of the Sanpoil River valley, northeastern Washington: U.S. Geological Survey Bulletin 1661, 39 p., doi:10.3133/b1661.

Atwater, B.F., 1987, Status of glacial Lake Columbia during the last floods from glacial Lake Missoula: Quaternary Research, v. 27, p. 182–201, doi:10.1016/0033-5894(87)90076-7.

Atwater, B.F., and Fleck, R.J., 1984, Preliminary geologic map of the Colville Indian Reservation, Ferry and Okanogan Counties, Washington: USGS Open-File Report 84–389, doi:10.3133/ofr84389.

Baker, V.R., 1973, Paleohydrology and Sedimentology of Lake Missoula Flooding in Eastern Washington:, doi:10.1130/SPE144.

Bjornstad, B.N., 2014, Ice-rafted erratics and bergmounds from Pleistocene outburst floods, Rattlesnake Mountain, Washington, USA: E&G Quaternary Science Journal, v. 63, p. 44–59, doi:10.3285/eg.63.1.03.

Bretz, J.H., 1928, Bars of channeled scabland: Bulletin of the Geological Society of America, v. 39, p. 643–701, doi:10.1130/GSAB-39-643.

Bretz, J.H., 1930, Valley deposits immediately west of the channeled scabland: Journal of Geology, v. 38, p. 385–422, doi:10.1086/623737.

Bretz, J.H., Smith, H.T.U., and Neff, G.E., 1956, Channeled Scabland of Washington - New Data and Interpretations: Geological Society of America Bulletin, v. 67, p. 957–1049, doi:10.1130/0016-7606(1956)67[957:csownd]2.0.co;2.

Carling, P.A., Martini, P.I., Herget, J., Borodavko, P., and Parnachov, S., 2009, Megaflood sedimentary valley fill: Altai Mountains, Siberia, in Megaflooding on Earth and Mars, p. 243–264.

Carrivick, J.L., 2006, Application of 2D hydrodynamic modelling to high-magnitude outburst floods: An example from Kverkfjöll, Iceland: Journal of Hydrology, v. 321, p. 187–199, doi:10.1016/j.jhydrol.2005.07.042.

Cheney, E.S., 1980, Kettle dome and related structures of northeastern Washington, in Max D. Crittenden, P.J.C., George Herbert Davis, George Hamilton Davis ed., Cordilleran Metamorphic Core complexes, Geologic Society of America, p. 463–484.

Clague, J.J., 2009, Cordilleran ice sheet: Encyclopedia of Paleoclimatology and Ancient Environments, p. 206–211, doi:10.1007/978-1-4020-4411-3_49.

Clague, J.J., and Rampton, V., 1982, Neoglacial Lake Alsek: Canadian Journal of Earth Sciences, v. 19, p. 94–117, doi:10.1139/e82-008.

Collinson, J.D., and Thompson, D.B., 1982, Sedimentary Structures: London, UK, George Allen & Unwin (Publishers) Ltd.

Cooley, S., 2022, Giant Current Ripples at Omak, WA:, https://www.skyecooley.com/single-post/2020/07/01/giant-current-ripples-at-omak-wa.

Cressman, E.R., 1989, Reconnaissance stratigraphy of the Prichard Formation (Middle Proterozoic) and the early development of the Belt Basin, Washington, Idaho, and

Montana: United States Geological Survey, Professional Paper, Medium: X; Size: Pages: 1-80 2009-12-17 p., https://www.osti.gov/biblio/6034271.

Denlinger, R.P., George, D.L., Cannon, C.M., O'Connor, J.E., and Waitt, R.B., 2021, Diverse cataclysmic floods from Pleistocene glacial Lake Missoula: Untangling the Quaternary Period: A Legacy of Stephen C. Porter, v. 548, p. 333, doi:10.1130/2021.2548(17).

Fisher, T.G., Jol, H.M., and Boudreau, A.M., 2005, Saginaw Lobe tunnel channels (Laurentide Ice Sheet) and their significance in south-central Michigan, USA: Quaternary Science Reviews, v. 24, p. 2375–2391, doi:10.1016/j.quascirev.2004.11.019.

Flint, R.F., and Irwin, W.H., 1939, Glacial geology of Grand Coulee Dam, Washington: Bulletin of the Geological Society of America, v. 50, p. 661–680, doi:10.1130/GSAB-50-661.

Hansen, V.L., 1983, Kinematic interpretation of mylonitic rocks in Okanogan dome north-central Washington and implications for dome evolution [Master of Science]: University of Montana, https://scholarworks.umt.edu/etd/7442?utm_source=scholarworks.umt.edu%2Fetd%2F7442&utm_medium=PDF&utm_campaign=PDFCoverPages.

Hanson, L.G., 1970, The origin and development of Moses Coulee and other scabland features on the Waterville Plateau, Washington: University of Washington, https://www.proquest.com/openview/d1f4ec1ed1e7958503c42e788b365f59/1?pq-origsite=gscholar&cbl=18750&diss=y.

Hibbert, D.M., 1986, Quaternary Geology and the History of the Landscape along the Columbia between Chief Joseph and Grand Coulee Dams, in Campbell, S.K. ed., Summary of

Results, Chief Joseph Dam Cultural Resources Project, Washington, https://apps.dtic.mil/sti/pdfs/ADA166700.pdf.

Hickson, C.J., Moore, J.G., Calk, L., and Metcalfe, P., 1995, Intraglacial volcanism in the Wells Gray-Clearwater volcanic field, east-central British Columbia, Canada: Canadian Journal of Earth Sciences, v. 32, p. 509–509, doi:10.1139/e96-039.

Karlson, R.C., 2006, Investigation of Ice Age Flood Geomorphology and Stratigraphy in Ginkgo Petrified Forest State Park, Washington: Implications for Park Interpretation [Master of Science]: Central Washington University, https://www.cwu.edu/geography/sites/cts.cwu.edu.geography/files/Karlson_Thesis.pdf.

Larsen, I.J., and Lamb, M.P., 2016, Progressive incision of the Channeled Scablands by outburst floods: v. 538, p. 229–232, doi:10.1038/nature19817.

Lechler, A.R., Huntington, K.W., Breecker, D.O., Sweeney, M.R., and Schauer, A.J., 2018, Loess–paleosol carbonate clumped isotope record of late Pleistocene–Holocene climate change in the Palouse region, Washington State, USA: Quaternary Research, v. 90, p. 331–347, doi:10.1017/qua.2018.47.

Lesemann, J.E., and Brennand, T.A., 2009, Regional reconstruction of subglacial hydrology and glaciodynamic behaviour along the southern margin of the Cordilleran Ice Sheet in British Columbia, Canada and northern Washington State, USA: Quaternary Science Reviews, v. 28, p. 2420–2444, doi:10.1016/j.quascirev.2009.04.019.

Lifton, N., Caffee, M., Finkel, R., Marrero, S., Nishiizumi, K., Phillips, F.M., Goehring, B., Gosse, J., Stone, J., and Schaefer, J., 2015, In situ cosmogenic nuclide production rate

calibration for the CRONUS-Earth project from Lake Bonneville, Utah, shoreline features: Quaternary Geochronology, v. 26, p. 56–69, doi:10.1016/j.quageo.2014.11.002.

Menzies, J., 1990, Sand intraclasts within a diamicton mélange, southern Niagara Peninsula, Ontario, Canada: Journal of Quaternary Science, v. 5, p. 189–206, doi:10.1002/jqs.3390050303.

Meyer, K.-D., 1983, Zur Anlage der Urstromtäler in Niedersachsen: Zeitschrift für Geomorphologie, p. 147–160, doi:10.1127/zfg/27/1983/147.

Minervini, J., O'Connor, J., and Wells, R., 2003, Inundation map, ice-rafted erratics, and deposits of Late Pleistocene Missoula floods in the Portland Basin and Willamette Valley, Oregon and Washington: USGS Open-File Report, doi:10.3133/ofr2003408.

O'Connor, J.E., 1993, Hydrology, hydraulics, and geomorphology of the Bonneville flood: Geological Society of America Special Papers, v. 274, https://books.google.com/books?id=LTUCAQAAQBAJ&pg=PA3&source=gbs_selected_pages&cad=3#v=onepage&q&f=false.

Orr, K.E., 1985, Structural features along the margins of the Okanogan and Kettle domes, northeastern Washington and southern British Columbia [PhD]: University of Washington.

Pico, T., David, S.R., Larsen, I.J., Mix, A.C., Lehnigk, K., and Lamb, M.P., 2022, Glacial isostatic adjustment directed incision of the Channeled Scabland by Ice Age megafloods: Proceedings of the National Academy of Sciences, v. 119, p. e2109502119, doi:10.1073/pnas.2109502119.

Russell, A.J., 1993, Obstacle marks produced by flow around stranded ice blocks during a glacier outburst flood (jökulhlaup) in west Greenland: Sedimentology, v. 40, p. 1091–1111, doi:10.1111/j.1365-3091.1993.tb01381.x.

Stackebrandt, W., 2009, Subglacial channels of Northern Germany - a brief review: Zeitschrift Der Deutschen Gesellschaft Fur Geowissenschaften, v. 1603, p. 203–210, doi:10.1127/1860-1804/2009/0160-0203.

Stewart, M., and Allard, R., 2017, North Okanagan aquifer mapping and geologic modelling: Summary of results and 3D interpretation: Government of British Columbia Water Science Series, WSS2017-03, Victoria BC, https://a100.gov.bc.ca/pub/acat/documents/r54472/WSS2017-03_N_Okanagan_1532284399084_2278704448.pdf.

Sugden, D.E., Clapperton, C.M., and Knight, P.G., 1985, A jökulhlaup near Søndre Strømfjord, West Greenland, and some effects on the ice-sheet margin: Journal of Glaciology, v. 31, p. 366–368, doi:10.3189/S0022143000006729.

Swope, S., and Group, P.G., 2007, Jameson Lake and Moses Coulee Flood Mitigation Hydrogeologic Assessment:, https://apps.ecology.wa.gov/publications/SummaryPages/1203320.html.

Tómasson, H., 1996, The jökulhlaup from Katla in 1918: Annals of Glaciology, v. 22, p. 249–254, doi:10.3189/1996AoG22-1-249-254.

Waitt, R.B., 1985, Case for periodic, colossal jökulhlaups from Pleistocene glacial Lake Missoula: Geological Society of America Bulletin, v. 96, p. 1271–1286, doi:10.1130/0016-7606(1985)96%3C1271:CFPCJF%3E2.0.CO;2.

Waitt, R.B., 2021, Roads less travelled by—Pleistocene piracy in Washington's northwestern Channeled Scabland, in Waitt, B., R., Thackray, D., G., Gillespie, and R., A. eds., Untangling the Quaternary Period—A Legacy of Stephen C. Porter, doi:10.1130/2021.2548(18).